Best available copy

[redacted]

Reassigned
73N70937
Jan 1979

*Gb 6-1,6-97

FACILITY FORM 602

~~X65 64330~~	~~X65 84350~~
(ACCESSION NUMBER)	(THRU)
257	5A
(PAGES)	(CODE)
TMX 51728	
(NASA CR OR TMX OR AD NUMBER)	(CATEGORY)

COMPILATION OF PAPERS PRESENTED TO MEETING ON SPACE VEHICLE LANDING AND RECOVERY RESEARCH AND TECHNOLOGY

NASA Headquarters

July 10-11, 1962

[redacted]

[redacted]

[redacted]

AGENDA

MEETING ON SPACE VEHICLE LANDING AND RECOVERY

RESEARCH AND TECHNOLOGY

NASA Headquarters
July 10-11, 1962
9:00 A.M. EDT

I. July 10, 1962 - Opening Remarks - J. E. Greene- Headquarters

II. Presentation of Program Summaries from the Centers

Parachute Recovery Systems Design and Development Efforts Expended on MERCURY-REDSTONE Booster and SATURN S-1 Stage - Barraza, R. M. - MSFC X65-84331

Application of Paragliders to S-1 Booster Recovery for C-1 and C-2 Class Vehicles - Mc Nair, L. L. - MSFC X65-84332

Recovery of Orbital Stages - Fellenz, D. W. - MSFC X65-84333

A Review of Launch Vehicle Recovery Studies - Spears, L. T.- MSFC X65-84334

A Review of the Space Vehicle Landing and Recovery Research at Ames - Cook, W. L. - ARC X65-84335

Survey of FRC Recovery Research - Drake, H. M. - FRC X65-84336

Manned Paraglider Flight Tests - Horton, V. W. - FRC X65-84337

Gemini Landing and Recovery Systems - Rose, R. - MSC X65-84338

Presentation to NASA Headquarters

~~Apollo and Future Spacecraft Requirements and~~ Landing and impact Systems ~~Concepts~~ - Kiker, J. W. - MSC X65-84339

III. July 11, 1962 - Continuation of Program Summaries

JPL Requirements for Spacecraft Landing and Recovery - X65-84340
Pounder, T., Framan, E., and Brayshaw, J. - JPL

Langley Research Efforts on Recovery Systems - X65-84341
Neihouse, A. I. - LRC

* Summary of Static Aerodynamic Characteristics of Parawings - X65-84342
Sleeman, W. C., Croom, D. R., and Naeseth, R. L. - LRC

* Dynamic Stability and Control Characteristics of Parawings - X65-84343
Johnson, J. L., and Hassell, Jr., J. L. - LRC

Deployment Techniques of a Parawing Used as a Recovery Device for Manned Reentry Vehicles and Large Boosters - X65-84344
Burk, S. M. - LRC

* An Analytical Investigation of Landing Flare Maneuvers of a Parawing-Capsule Configuration - Anglin, E. L. - LRC X65-84345

Paraglider Loads, Aeroelasticity and Materials - Taylor, R.T. and Mc Nulty, J. F. - LRC X65-84346

Rotary-Type Recovery Systems - Libbey, C. E. - LRC X65-84347

Parachute Performance at Supersonic Speeds - Charczenko, N. - X65-84348
LRC

Aerodynamic Drag and Stability Characteristics of Solid and Inflatable Decelerator Devices at Supersonic Speeds - X65-84349
Mc Shera, J. T. - LRC

The Problems of the Energy Dissipation Systems in Spacecraft Recovery - Fisher, L. J. - LRC X65-84350

MEETING ON SPACE VEHICLE LANDING AND

RECOVERY RESEARCH AND TECHNOLOGY

NASA Headquarters

July 10-11, 1962

SUMMARY OF MEETING

A meeting on Space Vehicle Landing and Recovery was held on July 10-11, 1962 at NASA Headquarters. The Centers were asked to participate in this meeting in accordance with their interest, activities, and requirements in the subject area. Primary emphasis was directed toward parachutes, parachute-rocket systems, paragliders, and lifting rotor concepts applicable to both booster and spacecraft landing and recovery.

The meeting was devoted to presentation of completed, current, and planned programs on landing and recovery research and technology within the Centers. A major part of the papers presented at the meeting dealt with paraglider research and development efforts. MSFC presented a comprehensive review of their in-house and out-of-house studies of booster recovery utilizing both parachute and paraglider concepts. Performance penalties, operational considerations, and economic trade-offs that could be expected with booster recovery were also discussed. Ames reported on their wind-tunnel studies of steerable and clustered parachutes and on their tests of a half-scale Gemini paraglider landing system. Those present at the meeting were impressed with the FRC program results showing glide performance, approach, and landing capabilities of a manned paraglider. The FRC program utilized a high wing loading, low L/D vehicle with unpowered flights from altitudes up to 2500 feet. Langley presented a number of papers dealing primarily with their research efforts on design, performance, and deployment of rigid and inflatable paragliders. Experimental results from a supersonic decelerator program in the UPWT were also shown. In addition, some qualitative results of lifting rotor studies in the spin tunnel at Langley were also discussed. The Manned Spacecraft Center outlined their requirements and supporting efforts in research and development of the Gemini and Apollo landing systems. Much of their experimental work on Gemini has been carried out in Ames and Langley facilities. This work was reported by the Center involved. JPL discussed their planetary program by outlining mission criteria, restraints, and landing and recovery requirements for entry capsules

[redacted]

in alien atmospheres. They stressed that JPL expects to do very little in-house development of landing systems, but will depend heavily on the other NASA Centers and industry.

The Centers were asked to provide copies of their papers to Headquarters for subsequent inclusion in a meeting summarization to be distributed to the Centers. These papers are reproduced in this document in the order listed in the attached agenda.

SPACE VEHICLE LANDING AND RECOVERY RESEARCH AND TECHNOLOGY MEETING
July 10-11, 1962

ATTENDEES

Anglin, E. L.	LRC
Barraza, R. M.	MSFC
Brayshaw, Jr., J. M.	JPL
Brewer, J.	Hqs. OART
Burk, S. M.	LRC
Carr, R. E.	Wallops
Champine, R. A.	LRC
Charczenko, N.	LRC
Colonna, R. A.	MSC
Cook, W. L.	ARC
Croom, D. R.	LRC
De Meritte, F. J.	Hqs. OART
Drake, H. M.	FRC
Esenwein, G. F.	OSMF
Fellenz, D. W.	MSFC
Fisher, L. J.	LRC
Framan, E. P.	JPL
Frandsen, N. P.	OMSF
Greene, J. E.	Hqs. OART
Horton, V. M.	FRC
Johnson, J. L.	LRC
Kelly, H. N.	LRC
Kiker, J. W.	MSC
Koons, W. E.	MSC
Libbey, C. E.	LRC
Lofton, L. K.	LRC
May, R. W.	Hqs. OART
Martin, J.	Hqs. RA
Mayer, N. J.	Hqs. OART
Mc Nair, L. L.	MSFC
Mc Shera, J. T.	LRC
Miller, W. E.	OMSF
Naeseth, R. L.	LRC
Neihouse, A. I.	LRC
Pearson, Jr., E. O.	Hqs. OART
Pounder, T.	JPL
Remson, O. J.	OMSF
Rogallo, F. M.	LRC
Rose, R. G.	MSC
Rosche, M. G.	Hqs. OART
Salmassy, O. K.	OMSF
Sleeman, Jr., W. C.	LRC
Shantz, I.	OMSF
Spears, L. T.	MSFC
Spiegel, J. M.	JPL
Taylor, R. T.	LRC
Whitten, J. B.	LRC
Wilbur, S. W.	Hqs. RA

[redacted]

X65 84331

Presentation Title:	Parachute Recovery Systems Design and Development Efforts Expended on MERCURY-REDSTONE Booster And SATURN S-1 Stage
Presented by:	Rodolfo M. Barraza Propulsion and Vehicle Engineering Division George C. Marshall Space Flight Center Huntsville, Alabama
Place of Presentation:	NASA Headquarters 1512 H Street, N. W. Washington, D.C.
Date of Presentation:	July 10, 1962

PARACHUTE RECOVERY SYSTEMS DESIGN AND DEVELOPMENT EFFORTS EXPENDED ON MERCURY-REDSTONE BOOSTER AND SATURN S-1 STAGE

I. INTRODUCTION

The George C. Marshall Space Flight Center's (MSFC) presentation will be given in four steps. The four presentations will cover separate but related areas of effort expended by the MSFC.

I will give a rundown on the early research and development of two parachute recovery systems - one being for the MERCURY-REDSTONE booster, the other being the SATURN S-1 stage. I will also give a short rundown on two other related programs done parallel with the recovery system developments - these being the MERCURY-REDSTONE booster retrieval exercises and the salt water immersion of the H-1 engine.

Mr. Lewis McNair will summarize the Rogallo Flexible Wing feasibility studies for the first stage recovery on the C-1 and C-2 SATURN programs.

Mr. Dietrich Fellenz will give a short review of study results, both in-house and out-of-house, on recovery of an upper stage from orbit employing a Rogallo Flexible Wing.

Mr. Luke Spears will cover the parametric studies that the MSFC has underway now and planned. He will outline performance penalties, operational considerations, and economic trade-offs. Mr. Spears will also summarize the future effort on Booster Recovery by the MSFC.

II. RECOVERY PROGRAM

The Recovery Project Office, Propulsion and Vehicle Engineering Division, MSFC, has been conducting studies on first stage recovery

since February, 1959. Some feasibility studies were conducted as early as June 11, 1958, by the Future Projects Office, MSFC.

Two contracts for the design and development of a recovery system for the SATURN C-1 booster and the MERCURY-REDSTONE booster, respectively, have been supervised by the Recovery Project Office. The two recovery systems employed the same basic technique since the requirements outlined for both of the contractors stated that the system be highly reliable and simple, avoiding in so far as possible, the use of techniques and/or components which would require extensive development. Also, a major requirement imposed on the contractors was that the system be designed such that it would not interfere with, or compromise the vehicle design. With the above requirements and limitations, the only recovery system conceivable was one employing parachutes.

Following the basic requirements that the booster recovery system be highly reliable, simple, and avoiding in so far as possible the use of techniques and/or components requiring extensive development work, a brief outline of the MSFC's approach in determining the initial design of the recovery system for SATURN C-1 S-1 stage is as follows:

1. Approaches that were considered.

Various approaches to the recovery problem were considered in view of the foregoing requirements and limitations. The approaches were generated by variations of the following parameters:

a. Booster cutoff conditions: velocity, altitude, and angle.

b. Booster re-entry: structural loads and temperature capabilities.

c. Booster attitude: either broadside or end-on, during re-entry and impact.

d. Terminal recovery parachute: type, size, and number.

e. Terminal decelerating rocket: thrust, burning time, and number.

2. Having given careful consideration to the above mentioned parameters, it was decided that the simplest and quickest approach for initial deceleration would be by ribbon parachute. Dive brakes were undesirable for reasons of required size and complexity. The use of retro-rockets for initial deceleration, in addition to being inefficient weight wise, would require close attitude control of booster in order to align thrust vector with the velocity vector. Use of parachutes for initial deceleration required only quasi-stability of the booster permitting angles of yaw up to ninety degrees at parachute deployment.

3. After the initial deceleration by the ribbon parachute, further deceleration of the booster to water entry velocity could be accomplished by the following: (1) parachutes, (2) retro-rockets, or (3) combination of parachutes and retro-rockets.

Making the proper selection required consideration of reliability, simplicity, weight, volume, and cost of each alternative. The use of only retro-rockets would mean that the stabilization of the booster with the initial parachute would be ineffective at lower velocities, and the thrust and velocity vector would not be aligned so as to provide predictable deceleration. The use of only parachutes to accomplish recovery appeared

very attractive at first glance; but because of booster weight such as the SATURN, the water impact velocity would be too high. Also, the complexity of a parachute system would increase and the reliability would decrease as the parachutes increased in size and number. The conclusions were that neither the retro-rocket system nor the parachute system was capable of performing the terminal deceleration phase by themselves.

With the above observation, it was decided that the most efficient deceleration system would be to combine the use of a few parachutes for the high velocities, and other means, such as retro-rockets for the lower velocities.

The immediate advantages of the combination system over the system using the retro-rockets only were (1) booster attitude stabilized by parachutes during retro-rocket firing, and (2) reduced weight and cost. The combination system advantages over the system using only parachutes were (1) greatly reduced complexity, (2) increased reliability, (3) reduced weight, and (4) reduced parachute stowage volume requirement.

The booster attitude at water impact was considered for both the end-on and horizontal positions. The horizontal position presented the following problems: (1) placement of retro-rockets, (2) the possibility of impacting on top of a wave with the center section, and (3) the possible misfiring of retro-rockets, thus, providing an unpredictable attitude at water impact. It was therefore decided that the end-on position would have a definite advantage, and the booster was far more capable of standing

heavy loads in the end-on position than the horizontal. As a result, the method and sequencing of the system selected was (1) initial deceleration by ribbon parachute, (2) terminal deceleration by parachutes and retro-rockets, and (3) end-on attitude at water impact.

The control system (sequencing system) was not finalized at the termination of the studies, but the method of initiating the operation of the system would most probably have been to use either a barometric switch, deceleration switch, or the control timer on the booster, or any combination of the three to have given greater reliability.

After having made some preliminary investigations and selecting the recovery system design approach as outlined above, a contractor proposal was accepted and funded by MSFC in February, 1959.

The recovery system consisted of a deceleration system and a control system that provided for recovery of the booster from the ocean. The deceleration system consisted of parachutes which deployed after re-entry, and a retro-rocket system which decelerated the booster to a safe velocity for water impact. The control system consisted of the devices which determined the initiation of the recovery events. This system located the parachutes and control unit in a cylindrical shaped container at the top of the stage and the retro-rockets on the periphery of the tail structure.

During the course of the recovery system development, preliminary investigations indicated that the ability of the SATURN booster structure to withstand re-entry and impact loads was marginal, but acceptable, since no reuse of components was planned. A damaged booster was acceptable provided the booster would float so as to allow retrieval.

As the development program progressed, changes in the vehicle configurations and in the cutoff conditions were made. This necessitated further investigations into the ability of the booster structure to withstand re-entry and impact loads. After careful evaluation, it was concluded that the booster could not reasonably be expected to survive re-entry without the incorporation into the recovery system of special means to stabilize the booster attitude prior to re-entry and during re-entry.

Studies made of the additional recovery system requirements and the various design constraints, imposed as a result of the specific nature of the SATURN vehicle, led to the adoption of a recovery system concept incorporating the following features:

1. Spatial attitude control of the booster from separation to the start of re-entry by means of vernier rockets, which were to be located near the forward end of the booster. This system incorporated its own independent stable reference system and the necessary associated hardware.

2. During the free space portion of the flight, an inflatable drag device initially housed within the recovery package was to be inflated and deployed so that it would help stabilize the booster and augment its aerodynamic drag during the re-entry period with a resultant reduction in the peak aerodynamic loads on critical areas.

3. The terminal portion of the recovery was to be accomplished by the original system which deployed a 57-foot-diameter first stage parachute; the first stage parachute in turn would deploy a cluster of

three 108-foot-diameter parachutes which decelerated the booster to a terminal velocity of 100 ft/sec. A series of landing rockets were to be ignited to reduce the booster water entry velocity to theoretically zero.

To accommodate the modification, two design layouts were proposed. Figure 1 shows the proposed layout of components which would have required modifications to the existing front I-beam structure. Figure 2 shows the layout which required minimum modifications to existing structure by providing a wafer or spacer for installation of the attitude control system and sub-systems. This allowed more time to test and qualify the complete recovery system by requiring a later delivery date for installation.

Figures 3 through 9 give typical cutoff conditions investigated and illustrate the sequence of events of the revised recovery system.

With the proposed incorporation of the above mentioned features, additional funds were requested by the contractor. The overall SATURN program at the time was having funding problems; and since recovery was not a primary mission, the booster recovery program was postponed to later vehicles in order to make funds available for other necessary flight hardware required on early flights.

The MERCURY-REDSTONE Recovery Program was an outgrowth of a feasibility study initiated by the Future Projects Office of this Center. In June, 1958, a feasibility study contract on booster recovery was initiated by the Future Projects Design Branch (presently Advanced Flight Systems Branch), Propulsion and Vehicle Engineering Division, with Aeronautical Equipment Research Corporation, a Division of M. Steinthal and Company, Inc.

During the time this study was being conducted, the MERCURY Program came into existence. The Future Projects Branch having supervision over the study contract, requested, received, evaluated, and accepted the contractor's proposal on a recovery system applicable to the MERCURY-REDSTONE booster. After acceptance of the proposal, the technical supervision was transferred to the Recovery Project Office. The basic scope of work covered design and development, bench testing of components, aerial testing of parachutes and overall system, finalization of design and drawings, and finally fabrication and delivery of five systems.

The recovery package (Figure 10) is a self-contained unit. It is installed in the booster by joining two mating structural rings, one an integral part of the booster, the other a part of the recovery system structure. Installation of the package is accomplished by bolt attachments through the mating rings, and attachment of the power supply and telemetry network plugs. All components of the recovery system are installed in the package prior to installation on the booster.

Parachute recovery is accomplished in the order shown in Figures 11 through 14. The first-stage parachute is deployed in a reefed condition to limit the possible bending moment on the booster within its structural capability. When sufficient time to orient the booster in a vertical tail-down attitude has passed, the parachute is disreffed to allow greater deceleration. When the first stage parachute has brought the booster below a 5000-foot altitude, and has been deployed for more than 15 seconds, the rate of descent will be in the range of 300 to 350 feet per second, and

within the design capability of the final recovery parachutes. At that time the first-stage parachute will be disconnected, and acting as a pilot parachute will then extract and deploy the final recovery parachutes. The final recovery parachutes will deploy reefed to limit the load on the booster, and progressively open through a second step of reefing to their full size. When the final parachutes are fully deployed, terminal velocity at sea level is approximately 40 feet per second.

During the time the contract was in effect, the recovery system conceptual design was established, and fabrication of three systems initiated (one of which is approximately 95% complete). The other two are approximately 40% completed. The drop test program, although difficulties were encountered in the first drops, was progressing satisfactorily at termination of contract. Several times during the development, changes to the recovery system had to be made to guarantee no interference or compromises to the primary mission of the booster. The final design, both mechanically and electrically, was approved by the Manned Spacecraft Center (MSC) and the MSFC.

The end of the program came when contractor and funding problems were encountered. The MSFC was unable to obtain additional funds to complete the development program and delivery of flight hardware.

A major problem in the water recovery program for the MERCURY-REDSTONE booster is the determination of possible damage sustained upon water impact, the angle of flotation, and the depth of submersion. The solution to the problem was of great interest as the solution of these unknown factors

determined the method for safing and retrieval employed in floating the booster into the recovery vessel. The tests were conducted at Madkin Mountain quarry, Redstone Arsenal, with a booster approximately four years old, i.e., the REDSTONE RS-33, which was used by the Army as a back-up in the REDSTONE program and also as a troop training missile at the Ordnance Guided Missile School. RS-33 was altered in weight and configuration so as to simulate MERCURY-REDSTONE booster retrieval conditions.

In parallel to the impact and flotation tests, the proper procedures were established for safing the booster prior to floating aboard the recovery vessel. During the performance of this exercise, handling procedures were also studied and later applied during the rehearsals in the Atlantic Ocean.

Results obtained from prior investigations indicated that the use of an LSD as a recovery vessel was the most practical method of recovering a MERCURY-REDSTONE booster. A two-day training exercise was conducted, about 50 miles out at sea from Norfolk, Virginia, to ascertain the capabilities of the LSD and to provide training for the underwater demolition team and LSD crew.

Special recovery equipment was used by the UDT in preparing the booster for towing aboard ship and for receiving and securing the booster to the saddles.

Prior to bringing the booster aboard the LSD, the saddles in which it was to be set were positioned and anchored in the ship's well. The

saddles were used and were placed 36 feet 4 inches apart along the ship's centerline. The rear skid was placed 19.5 feet from the stern gate allowing about 10 feet of working area between the tail of the booster and the stern gate. Since six connecting points were established on the booster for handling purposes, six 175-foot-long lines were made up, with quick fastening snaps, and numbered for identification.

There were four retrieval exercises conducted. Figures 15 through 19 illustrate the position of the saddles in the well of the LSD and operational procedure in towing the booster into the well of the LSD and placed on the saddles.

The primary objective of this first retrieval attempt was to check out the proposed handling procedures. As the first step, the booster, swimmers and their rubber boat, and the towing crew aboard the LCVP were launched. The LSD drained the well and moved away several thousand yards. The swimmers then approached the booster and went through the safing procedures without any difficulty, and also installed the handling connections.

After the safing operation was completed the booster was taken in tow by the LCVP and positioned astern the LSD which was maintaining a constant heading into the sea. The LSD was ballasted so as to have 8 feet of water in the well at the stern gate sill. The LCVP continued towing until its bow was over the LSD stern gate, then reversed, disconnected its tow line, and moved off to the port side and stood by. Swimmers with lines from the LSD attached lines to prescribed connections on the booster, and the booster was positioned over saddles. Once the booster was positioned, deballasting of the well proceeded until booster rested firmly on saddles. After the

well was drained, the booster and recovery equipment were checked for damage.

The second operation omitted the safing procedure, but went through with towing booster out and back into LSD with the LSD maintaining a heading of 2 to 3 knots into the waves. The third operation was very similar to the second. A change on the tiedown location of the nylon restraining slings was made.

The final operation was a complete simulated recovery. The booster was set free and all personnel stayed aboard the LSD. The LSD deballasted and steamed off ten miles from booster. At ten miles the booster was held on surface radar while the P2V tracked it 50 miles from 1500 feet.

Once the tracking exercises were over, the LSD started toward the booster. Ballasting of LSD and preloading of LCVP were performed while enroute. When the LSD was approximately 1000 yards from booster, the LCVP was launched and proceeded to the booster. Upon arriving at the booster, the swimmers went through the safing operation; the booster was taken in tow, and brought into the well of LSD and positioned as before.

Sea water immersion tests were conducted on a Rocketdyne H-1 engine in order to evaluate the corrosive effects of sea-water recovery on the engine and to define the procedures necessary to restore the engine for flight service. This program involved a series of tests in which the H-1 engine was immersed in sea water for given periods of time, followed by various post treatments designed to minimize the corrosive effect of sea water. The engine was then disassembled, evaluated for corrosion damage, reassembled, and test fired.

"Page missing from available version"

f. Hot fired short duration and full duration (150 sec.).

2. Second test - June 1961

a. Immersed H-1 engine to a depth of 10 feet for one hour, half submerged for three hours, and on the surface for three hours.

b. Waited twelve hours before purging, and applying minimum preservatives.

c. Upon arrival at the MSFC, it was dismantled, inspected, cleaned, replaced damaged parts and assembled.

d. Hot fired short duration and full duration.

3. Third test immersion in August 1961 - Hot fired in March 1962

a. Dropped H-1 engine into water to simulate water entry conditions, immersed it, held it half submerged, and on the surface for a total of nine hours.

b. Washed it with fresh water, no preservative compounds were used.

c. Upon arrival at the MSFC, it was dismantled, inspected, and partially cleaned, and left in storage.

d. Six months later the engine was assembled and hot fired, short duration and full duration.

The two reasons for delay on the third test are as follows:

1. The Test Division was over loaded with work.

2. The first two tests were so successful that the Recovery Project Office had difficulty justifying the manhours required to complete the hot firings, especially since the engine was dismantled, and the components looked as good as the previous two times.

In order to establish an approximate cost factor, a log was kept of the procedures, reconditioning manhours, materials, and an itemized list of replaced engine parts. The cost to recover and recondition the H-1 engine was approximately 5% of the cost of a new one.

In closing, it should be stated that the selection of the recovery systems employing parachutes was primarily brought about by the requirements and limitations previously stated, and possibly early availability. Also, the MSFC saw no need in duplicating study efforts by other government agencies that were investigating the economics and feasibility of other recovery system concepts. Aware that the studies were giving varying results, the MSFC preferred to develop a simple recovery system capable of recovering the SATURN S-1 stage and actually recover the first flight vehicles. Having actual post-flight hardware on hand would provide factual data and define precisely the economics, feasibility, and practicability of booster recovery. This would be accomplished without having to develop a new recovery technique. However, during the parachute recovery system development program on both the SATURN and MERCURY-REDSTONE vehicle programs, funding problems were encountered; and in both cases, the first program to be canceled was recovery.

Between the termination of the SATURN parachute recovery system and parallel with the H-1 salt water exercise, several proposals with different recovery system concepts were received and reviewed by the MSFC. Among these proposals were two similar techniques utilizing the Rogallo Flexible Wing concept. Approximately six months after termination of SATURN recovery

program, funds were again made available. At this time, the concept that looked the most promising was the Rogallo Wing; and a decision was made to investigate the feasibility of the Rogallo Wing to recover a SATURN S-1 stage of the C-1 or C-2 program. Mr. McNair will present the result of the studies.

Rodolfo M. Barraza

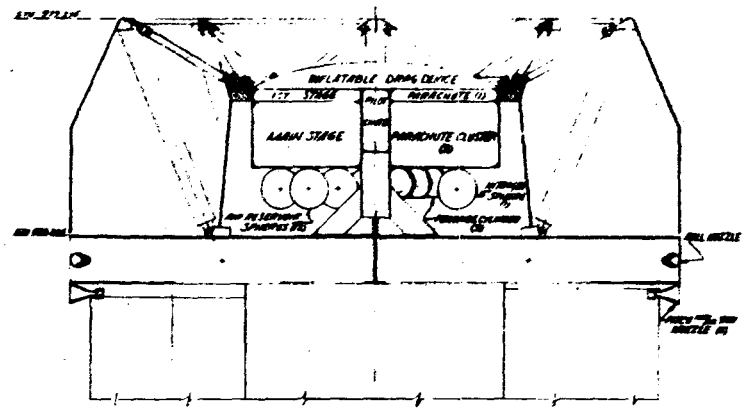

SECTION LOOKING OUTBOARD

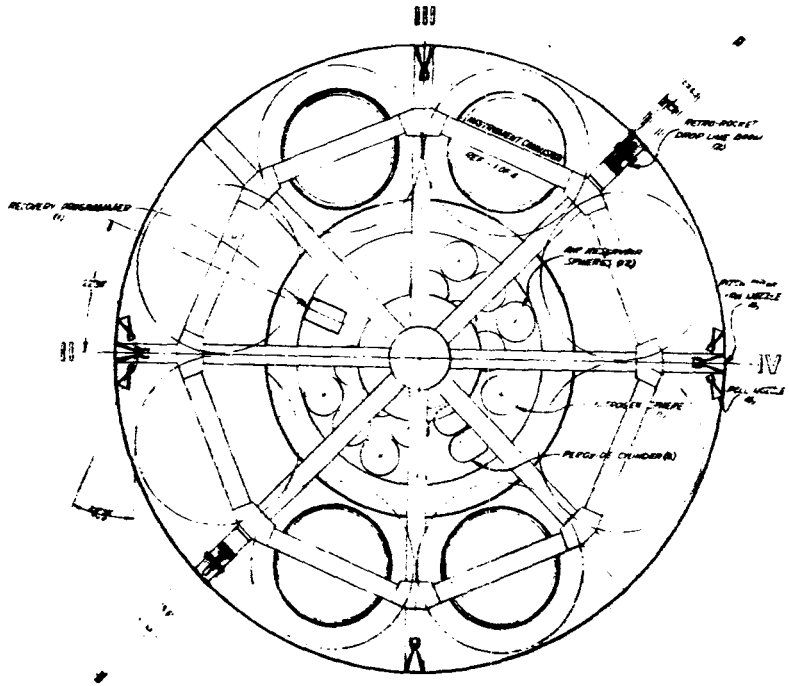

PLAN VIEW LOOKING FORWARD

Fig. 1

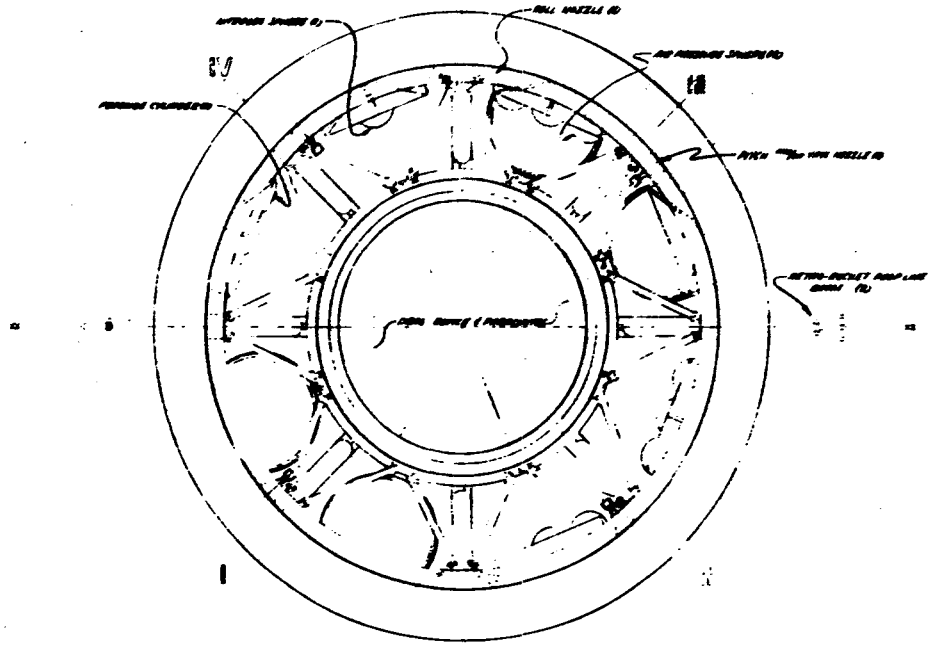

PLAN VIEW LOOKING AFT

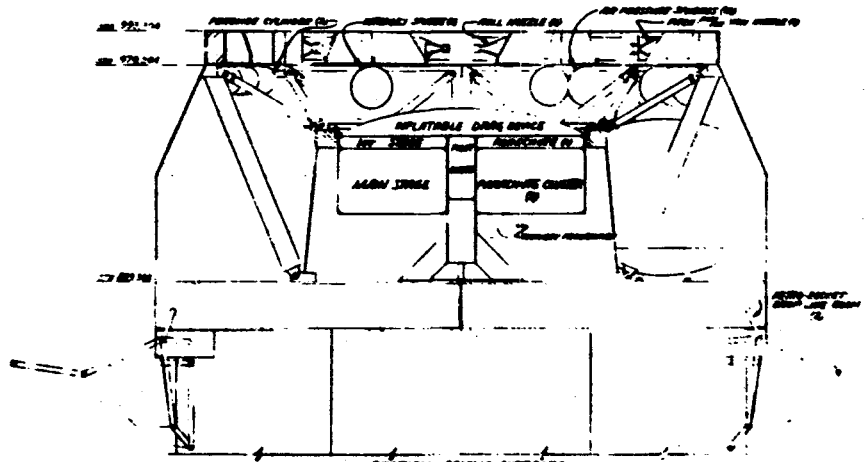

SECTION LOOKING OUTBOARD

Fig. 2

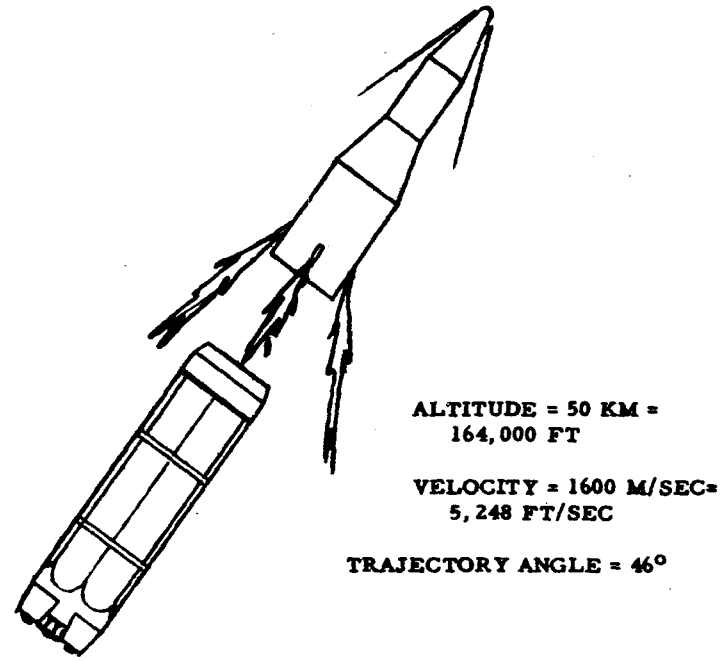

SECOND STAGE SEPARATION

FIG. 1

Fig. 3

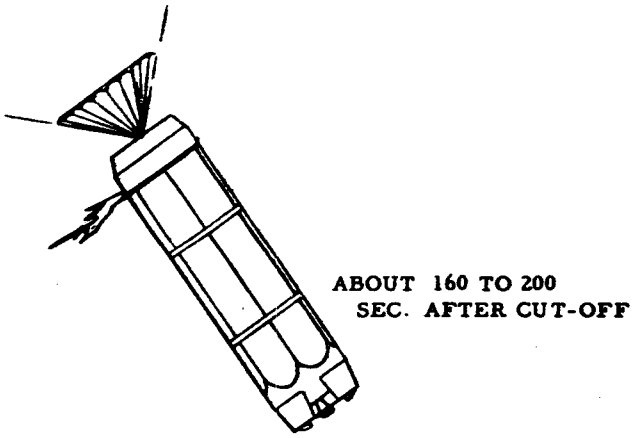

DRAG DEVICE INFLATING CLOSE TO BOOSTER AND
ATTITUDE CONTROL JETS TRIMMING ATTITUDE OF BOOSTER

FIG 3

Fig. 4

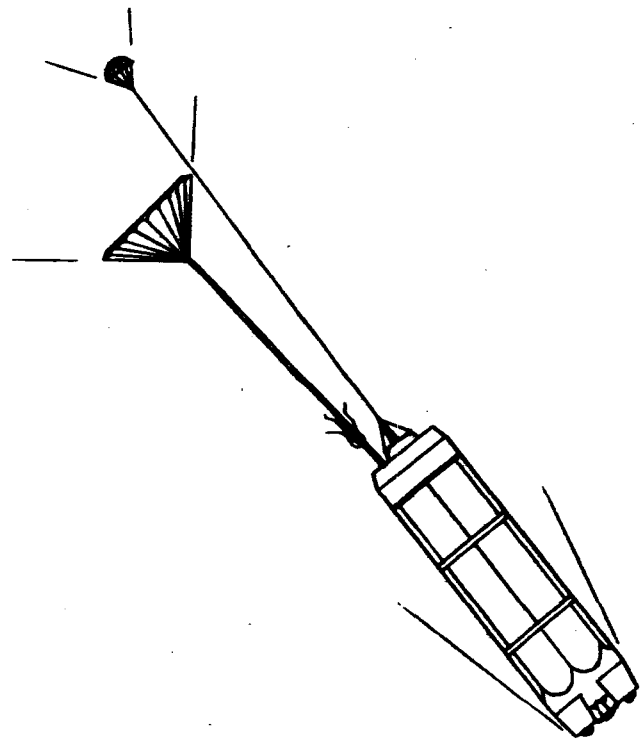

MAJOR NUMBER OF DRAG DEVICE LINES CUT LOOSE TO ALLOW PARACHUTE DEPLOYMENT OPERATION. DRAG DEVICE RETAINED OFF CENTER AND PILOT PARACHUTE DEPLOYED. PILOT PARACHUTE WILL EXTRACT FIRST STAGE PARACHUTE IN REEFED CONDITION.

FIG. 5

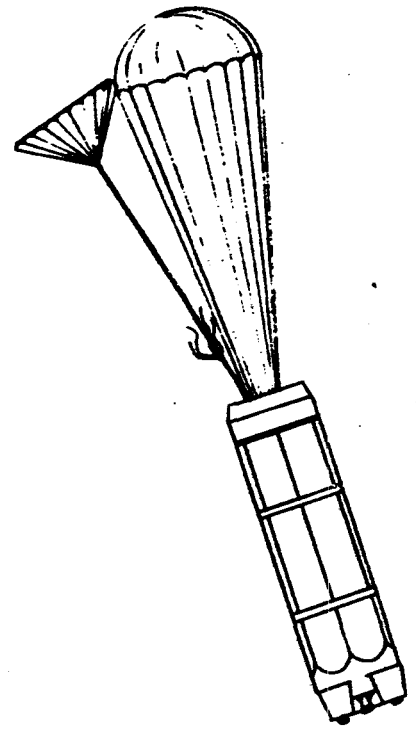

FIRST STAGE PARACHUTE
DISREEFED AND FULLY INFLATED.

FIG. 6

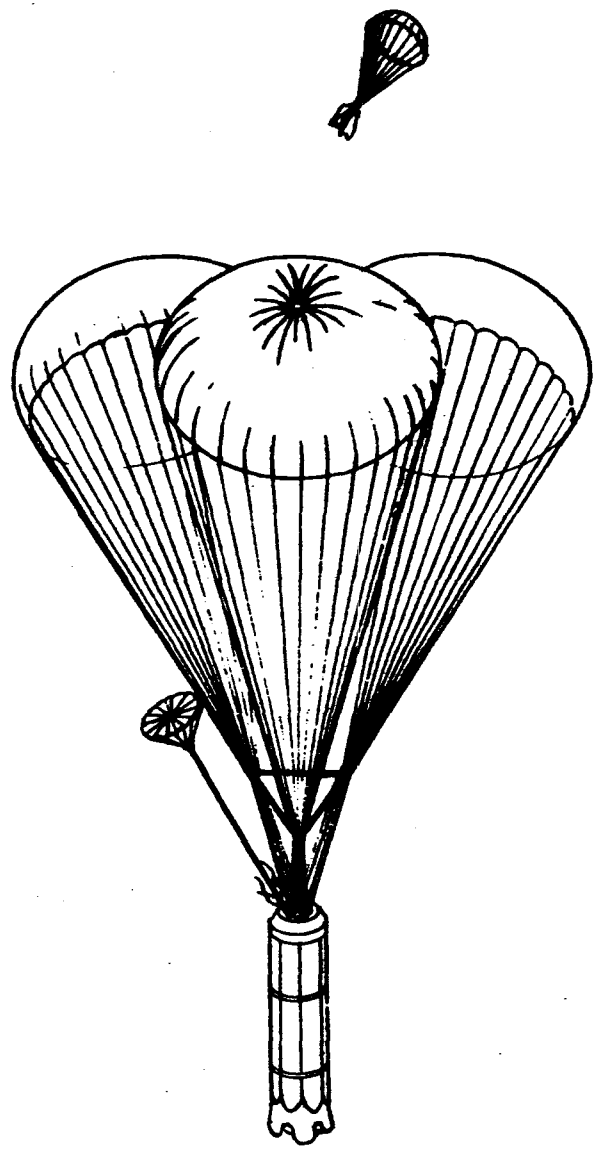

FIRST STAGE PARACHUTE LOOPS SEVERED AND
MAIN STAGE PARACHUTES DEPLOYED.
DRAG DEVICE RETAINED TO FUNCTION
AS BACK-UP FLOTATION SYSTEM.

FIG. 7

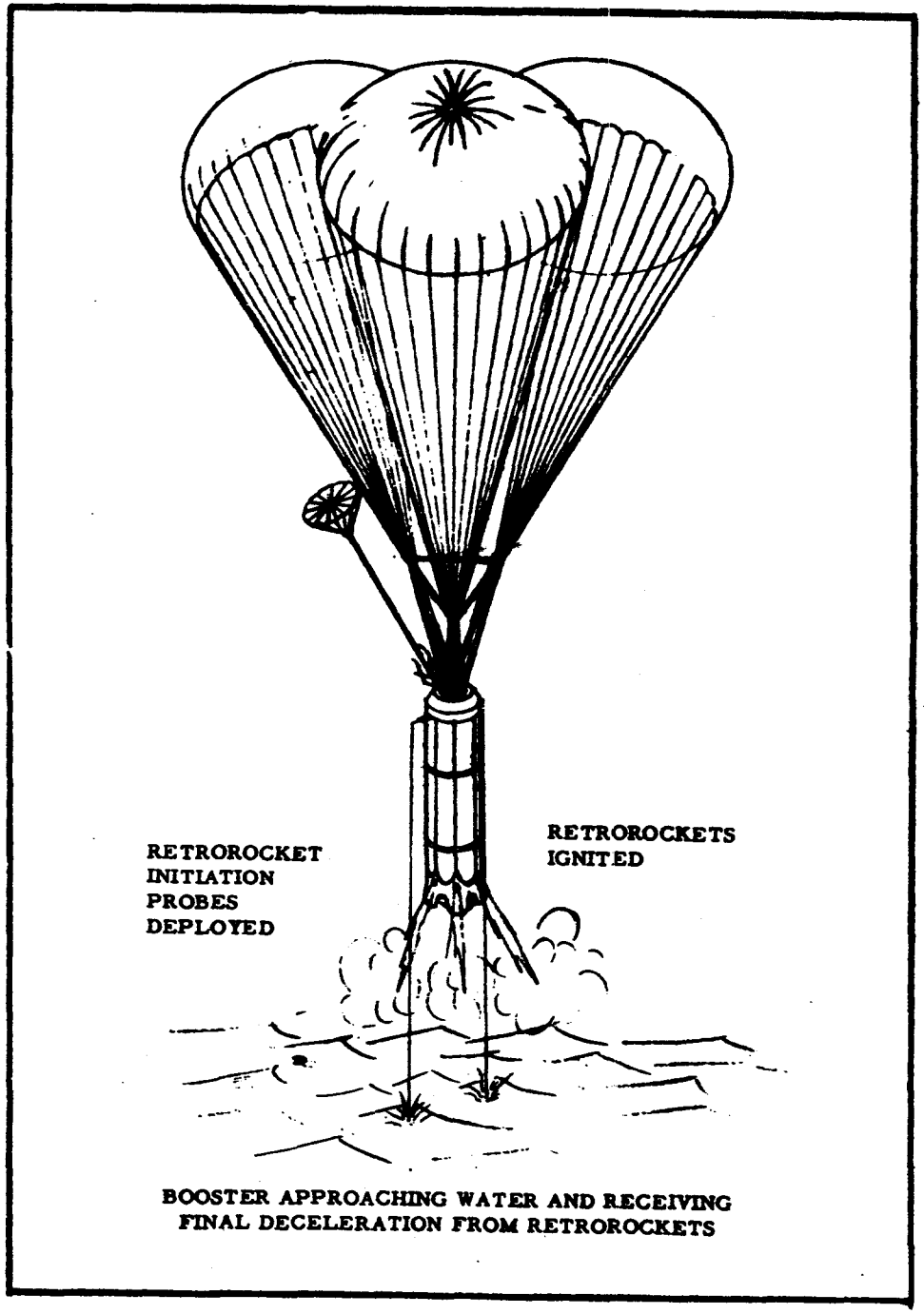
RETROROCKET
INITIATION
PROBES
DEPLOYED
RETROROCKETS
IGNITED
BOOSTER APPROACHING WATER AND RECEIVING
FINAL DECELERATION FROM RETROROCKETS

FIG. 8

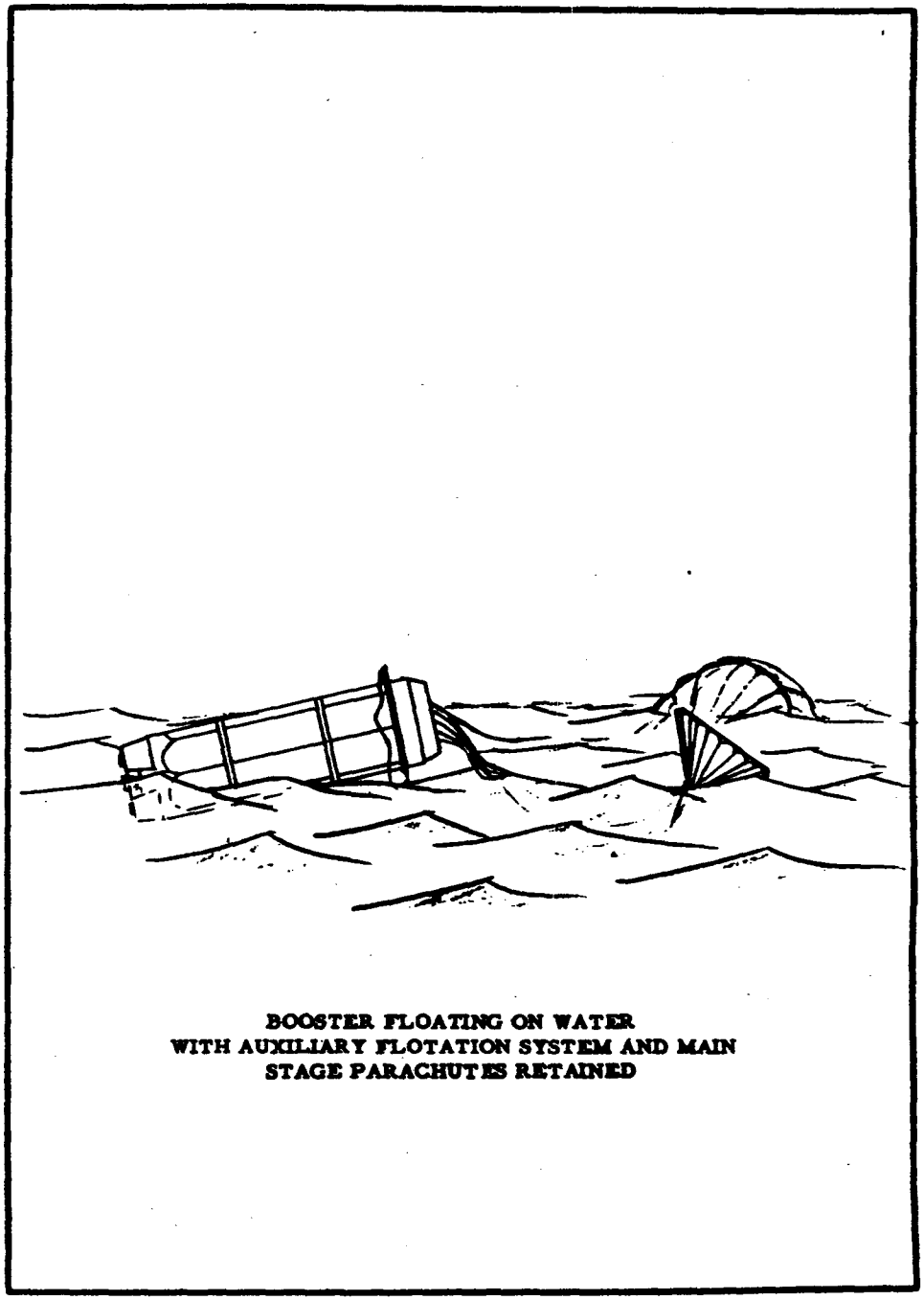

BOOSTER FLOATING ON WATER
WITH AUXILIARY FLOTATION SYSTEM AND MAIN
STAGE PARACHUTES RETAINED

FIG. 9

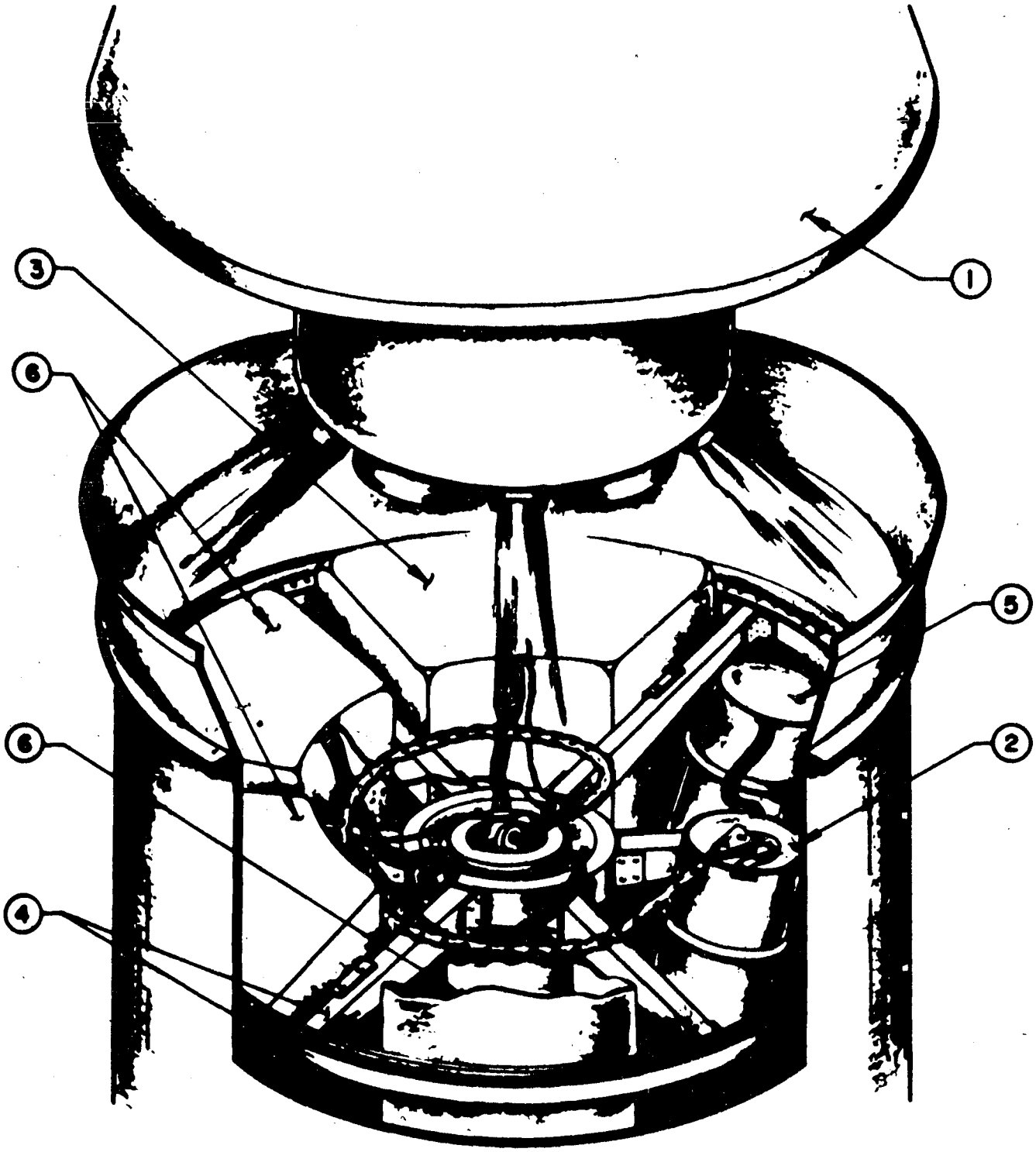

1. CAPSULE
2. RISER MORTAR
3. MAIN PARACHUTE RISERS
4. RECOVERY PACKAGE STRUCTURE
5. DECELERATION PRCHT. MORTAR.
6. FINAL RECOVERY PARACHUTES

BOOSTER RECOVERY PACKAGE

(HEAT PROTECTION COVER NOT SHOWN FOR CLARITY)

GE 112-16-5th

S.R. Fig. 10 50

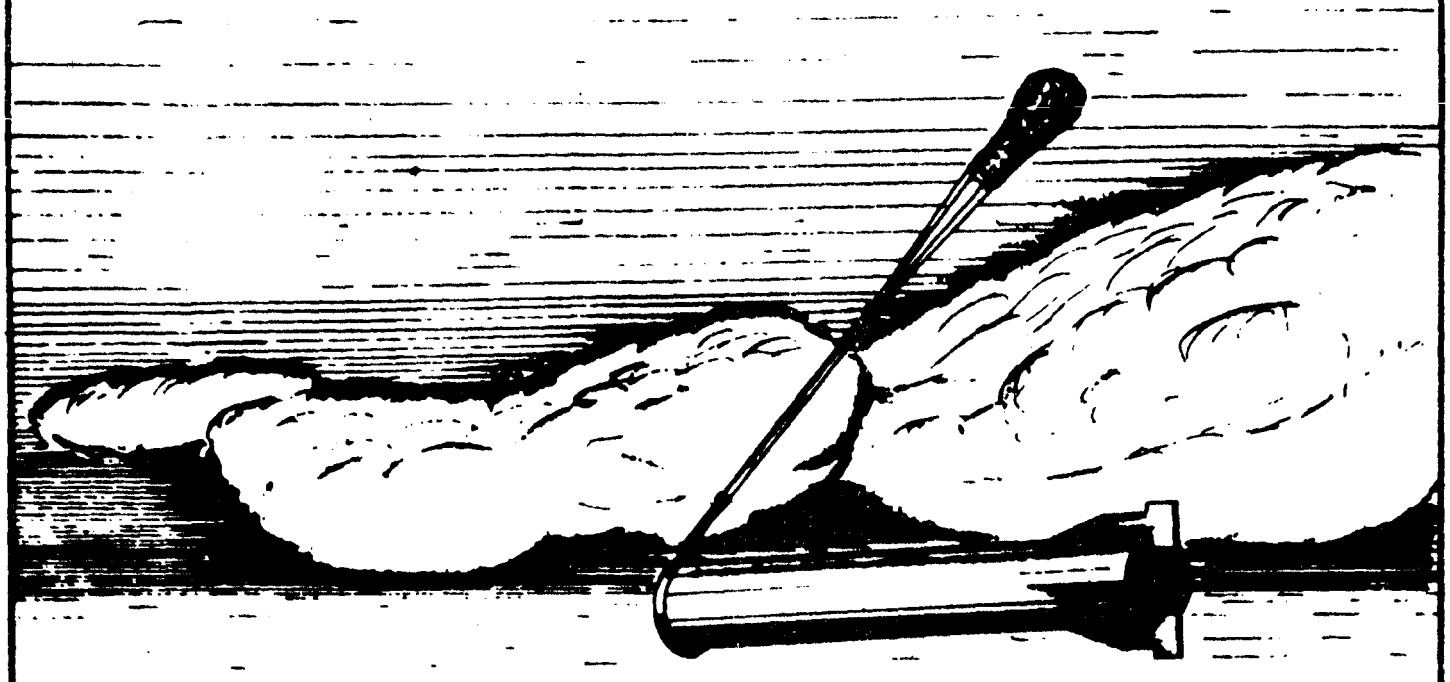

INITIATION OF RECOVERY

DEPLOYMENT OF DECELERATION PARACHUTE

Fig. 11

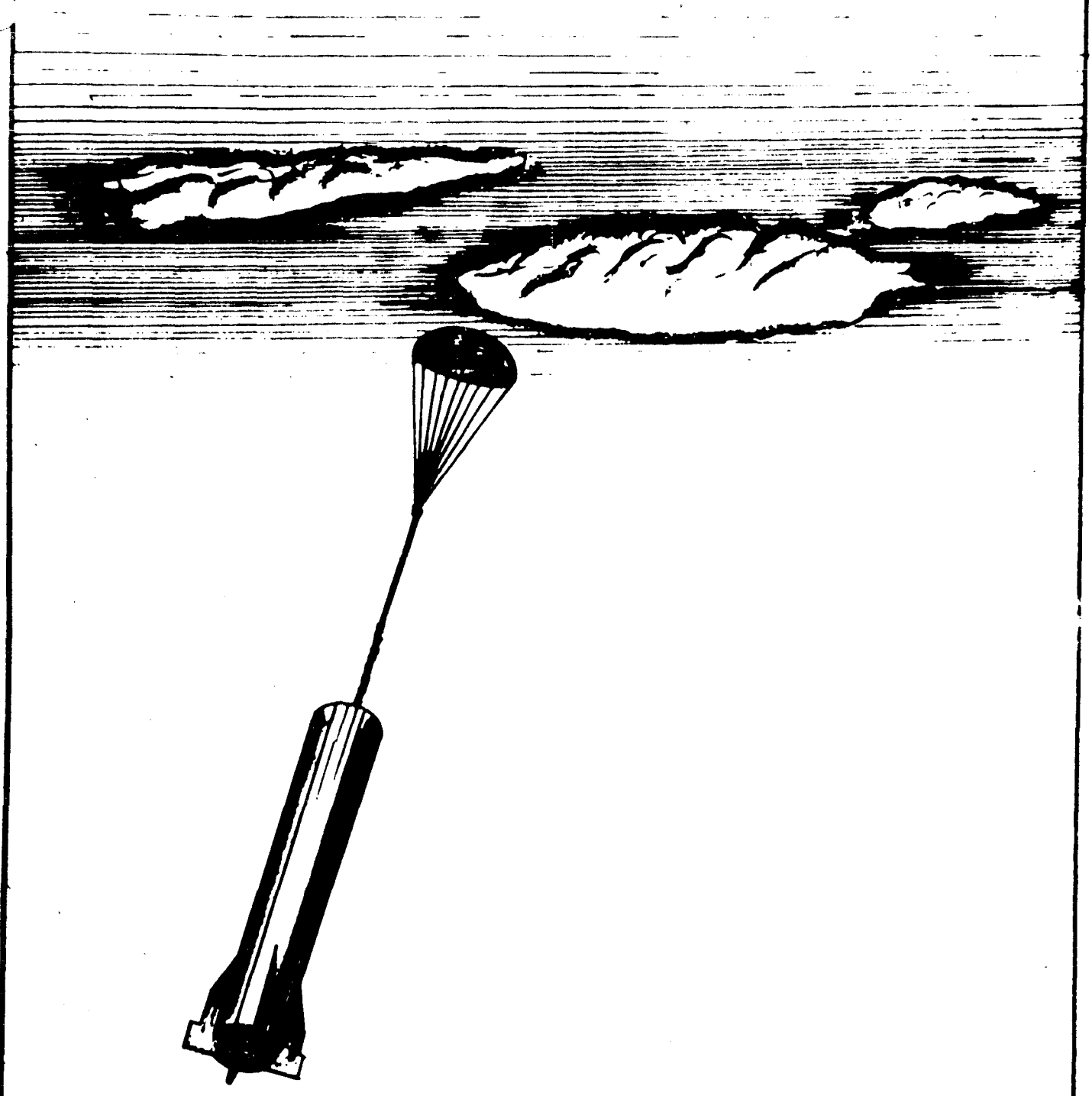

DECELERATION PARACHUTE DISREEFED

Fig. 12

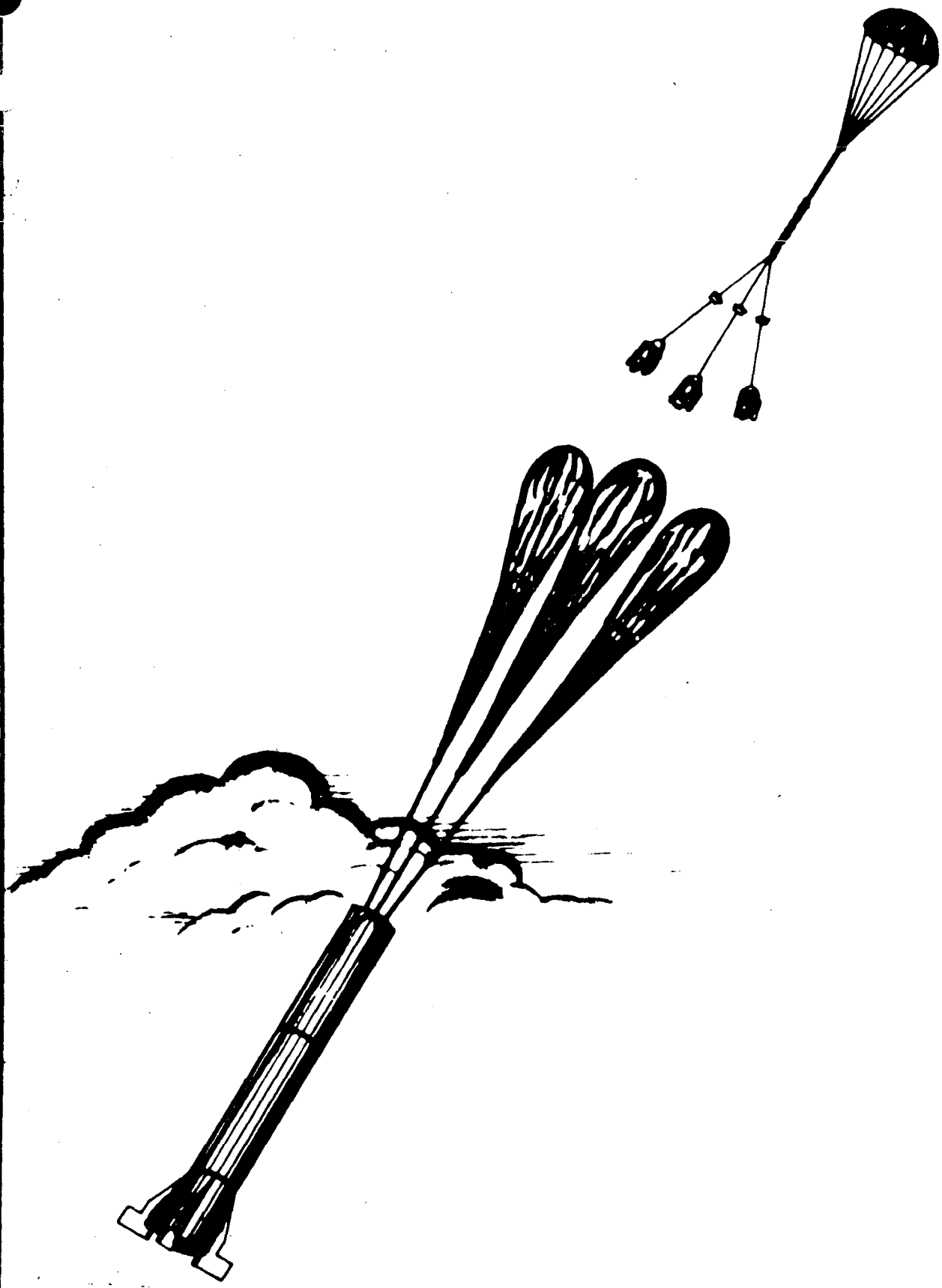

DISCONNECT OF DECELERATION PARACHUTE
DEPLOYMENT OF FINAL RECOVERY PARACHUTES

Fig. 13

GE 27-16-60 11 MAR 60

SPACE RECOVERY SYSTEMS INC.

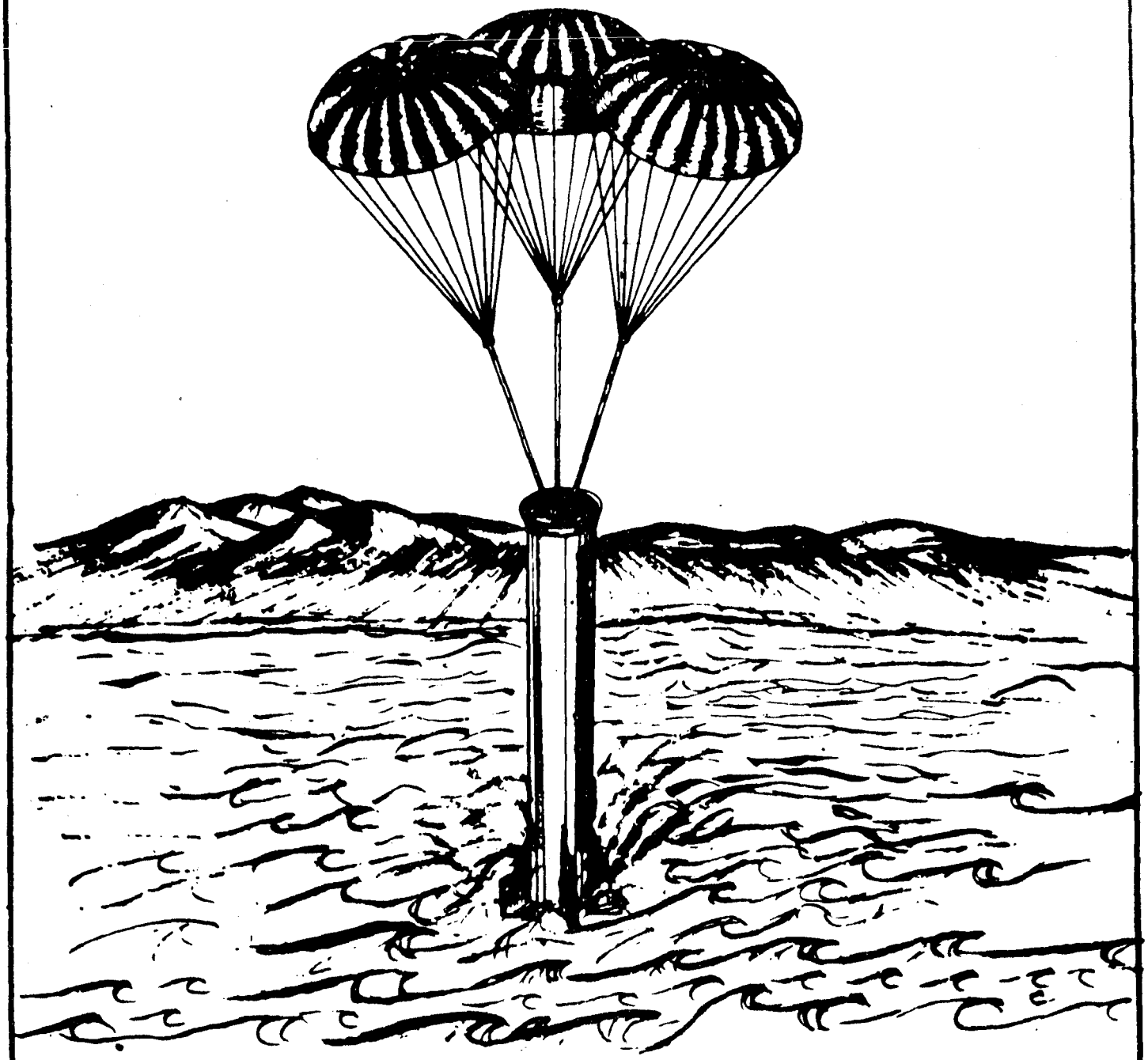

WATER IMPACT

Fig. 14

GE27-17-60 11 MAR 60

SPACE RECOVERY SYSTEMS INC.

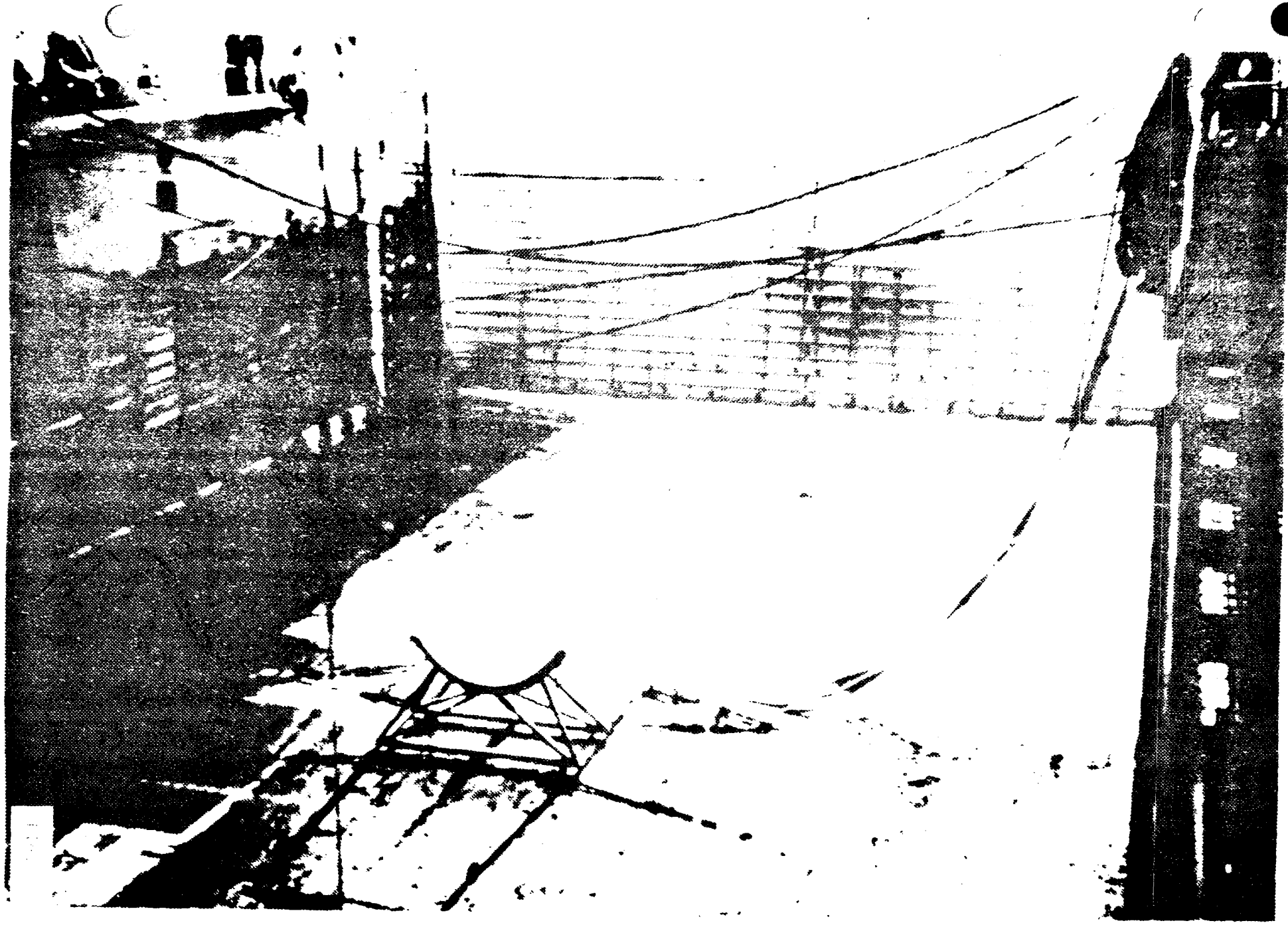

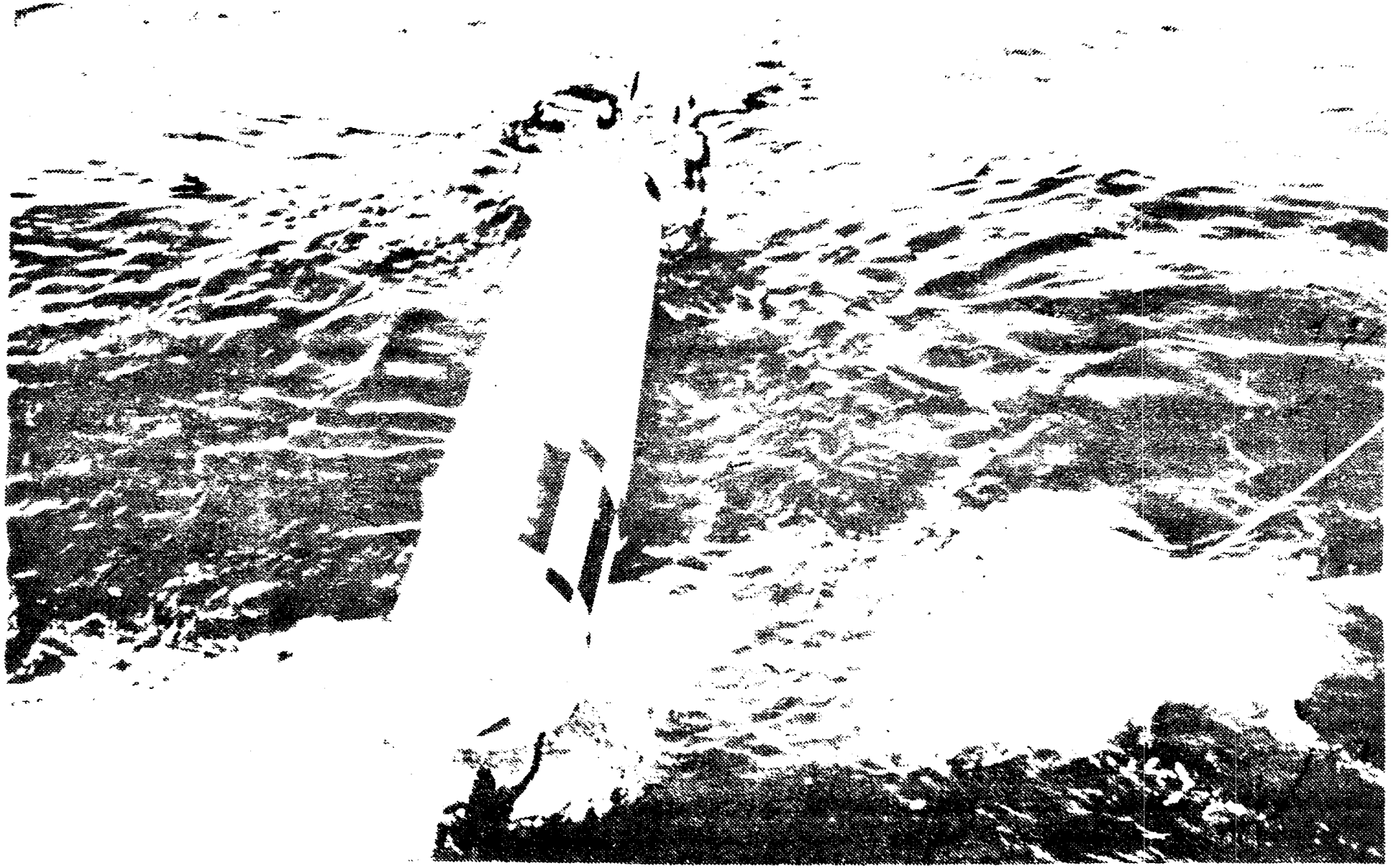

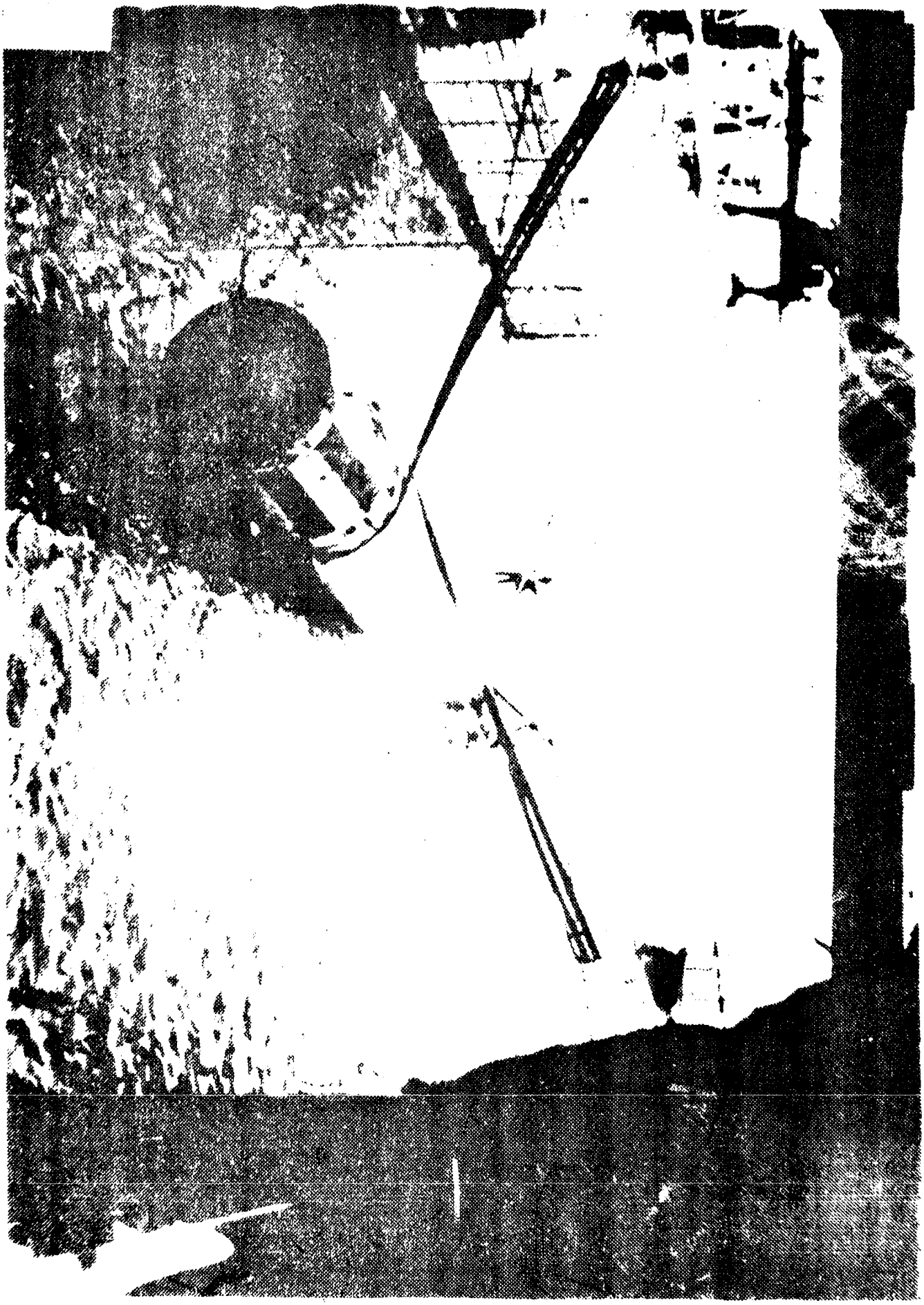

X65 84332

[redacted]

Presentation Title:	Application of Paragliders to S-1 Booster Recovery for C-1 and C-2 Class Vehicles
Presented By:	Lewis L. McNair Marshall Space Flight Center Aeroballistics Division
Place of Presentation:	NASA Headquarters 1512 H Street, N.W. Washington, D.C.
Time of Presentation:	July 10, 1962

TITLE: Application of Paragliders to S-1 Booster Recovery for C-1 and C-2 Class Vehicles

This presentation will be a summary of the results of a feasibility study to investigate the "Rogollo Flex Wing" for use in dry landing booster recoveries. Feasibility studies were initiated concurrently with North American Aviation, Inc. and Ryan Aeronautical Co. in January of 1960 and terminated in August of 1960. Main emphasis was placed on the "Rogollo Flex Wing" or paraglider as applied to the recovery of the S-1 stage of the C-1 and C-2 class Saturn vehicles.

The program objective (slide #1) was to demonstrate the technical and economical feasibility of the paraglider for S-1 stage dry land recovery. Dry land recovery was a basic ground rule that was imposed at the time of this study, because of the low confidence level of the reuseability of materials recovered from salt water. This restraint may not necessarily be imposed on future recovery techniques. Salt water tests of propulsion units are proving to be much less obstructive to engine materials than at first expected.

The development of the flex wing represents a major advancement in the field of aerodynamic structure providing an extremely lightweight, aerodynamic lifting surface. Langley Research Center had prior to this study demonstrated the feasibility of the paraglider concept both in the wind tunnels and flight tests. Also, Ryan Aeronautical Co. had designed and built a manned utility vehicle incorporating the "Flex Wing" principle. The experience and test data derived at Langley and at Ryan, and the obvious structural weight and packaging advantages,

suggested this concept as a highly desirable solution for the recovery of larger boosters.

The program study scope (slide #2) may be divided into four phases. (1) Preliminary design of the recovery system. This phase includes the parametric analysis necessary to define the wing geometry, and sufficient detail study of general characteristics to insure booster and wing compatibility for control during main fly back time and landing phase. (2) Method of attachment with minimum modification to booster. Since the S-1 stage at this time had been almost completely designed, extreme care had to be placed on the packaging of the wing within reasonable boundaries of the stage such as not to impose adverse aerodynamic and structural problems during flight. Special emphasis was placed on attachment of wing design to booster to insure adequate control during fly back and landing phase. (3) Complete operational and cost analysis. It is probably clear to everyone that the addition of a booster recovery system to a space vehicle program requires additional functions otherwise not needed if expendable boosters are employed. Typical of such functions are the recovery package operations of installation, checkout, and booster refurbishment after recovery. Other functions, such as transportation of boosters from the manufacturing site to the launch site, would be changed to the extent that such operations are required to support a given launch frequency. Cost analysis will very much depend on the operational sequence. These items will later

be covered. (4) Detailed research and development. A R&D program would definitely be recommended for the C-2 type vehicle, but as of today (1962) the C-2 vehicle is not in the NASA overall program.

The S-1 booster physical characteristics are given on slide #3. The booster not including interstage has an overall length of 66 feet and a diameter of 257 inches. The booster cutoff weight is 120,866 pounds which includes about 15,000 pounds of residual fuels. The center of gravity at cutoff of booster is slightly toward the rear of the booster. For the case of fuel residuals at bottom of tanks, the CG would be at station 331 and for fuel residuals at top of tanks the CG would be at station 344. Stations are referenced from engine or base end of booster.

The configuration selected by Ryan and its mode of attachment to the booster is shown on slide #4. The wing is 100 feet long for the keel and leading edges with a wing area of 7,070 square feet, and a wing loading of 15 pounds/feet^2. The wing has a flat planform sweep-back angle of 45 degrees and inflated in flight to a sweep angle of 50 degrees. The wing membrane material may be either fabric or foil gage material depending upon the temperature requirements. The keel and leading edges would be of rigid aircraft structure design - rivited sheet metal construction.

A spreader bar located at approximately the 58 per cent keel and leading edge stations for minimum bending, is of tubular construction

and deploys the leading edges to the desired sweep angle. Fixed cables attach the wing to the control bar and operating cables attach the control bar to the booster. The cables from the control bar to the booster allow for both pitch and roll control.

The booster cutoff velocity versus altitude is given on slide #5 for the various missions for both the C-1 and C-2 type vehicles. The various missions are escape, low orbit satellite, re-entry and Dyna-Soar. In comparing, one can see that the C-1 burn out velocities and altitudes are by a factor of three to four times as great as the C-2 values. It turns out, as we will see later, that these C-1 cutoff conditions are detrimental for flying back to land. The high altitudes coupled with the high velocities also produce excessive temperatures on the booster.

The anticipated C-2 sequenced mission profile is shown on slide #7 (similar for C-1 mission profile). Down range, lateral range, and altitude corresponding to the time of flight and associated event of flight are given.

The recovery system necessary for dry landing must permit scheduled energy dissipation under all boost missions and expected environmental conditions. Shortly after first stage burn out, a chute, approximately 36 feet in diameter, is deployed for stabilization (pitch and slide slip) and energy dissipation. The wing is deployed about 15 to 20 seconds after burn-out of first stage and the large chute is then ejected

immediately. (This time period of 20 seconds permits a reasonable range of wing sizes to be deployed at lift coefficients up to C_L maximum and to maintain tolerable deployment loads). Shortly thereafter, a preset 30 degree bank angle command is initiated and a 180 degree turn is performed. The 180 degree turn indicates a desire to return to or near the original launch site. Fly back to the flare position is then made with a near $\frac{L}{D}$ maximum condition. The existing energy at the flare position is then used for execution of the final landing phase.

The C-1 glide or fly back to land capability for various winds and no wind conditions is given on slide #6. The range or impact footprints is given for an azimuth 110 degrees East of North. From a range safety viewpoint, this is about as far south as firings would be allowed. The wind magnitudes given as 97% and 95% probability levels are defined as values that will not be exceeded during the worst month of the year (March) at and surrounding area of Cape Canaveral not more than 3 and 5 percent, respectively.

The wing loading was 4.0 pounds/feet^2 which was determined mostly from loads and heating viewpoint.

The two outer circles show impact points for the vehicle flying with a tail wind, which indicates for these assumptions the booster would have a possibility of landing on some of the down range islands. Unfortunately, we cannot live under the assumptions of always being assisted by winds to gain more range; it is just as likely that the

booster would be flying under head wind conditions which would confine the impact points to the inner most two circles. The middle circle shows the impact points for glide under no wind conditions.

The important thing to be gained from this slide is that no guarantee can be made for dry landing for the C-1 type booster. Since dry landing was a ground rule of this study, the idea of recovering the C-1 type booster will be dropped at this point and the remainder of this discussion will concentrate on the recovery of the booster for the C-2 type vehicle.

The effect of wing loading on range is shown on slide #8. Two representative extreme cutoff conditions were chosen, namely, the re-entry test mission and the Dyna-Soar mission. The effects of winds both head and tail for the 97% probability of occurrence along with the no wind case are shown. Since tolerable loads and temperatures did not prove to be exceeded during flight, the wing loading was chosen on the basis of achievable range. Thus, as indicated by slide, the wing loading is chosen to be 15 lbs/ft^2.

With this wing loading, the C-2 fly back capability is given on slide #9. The assumed firing azimuth of 45 degrees East of North was chosen only for convenience. The most adverse case, the Dyna-Soar Mission, was chosen for demonstration of fly back capability. Here, as in the C-1 case, the range impact areas are shown for the various wind and no wind conditions. This points out that it is possible to return to the vicinity of Cape Canaveral for all considered

environmental conditions with the exception of the 97% probability head wind which is slightly marginal.

At this point, it is noteworthy to point out that this range capability is achieved only with the $\frac{L}{D}$ values obtained from the wing with rigid leading edges. The $\frac{L}{D}$ values obtained from the inflatable leading edge wing are somewhat smaller and will not return the vehicle to the Cape.

Slide #10 shows main advantages and disadvantages of the rigid leading edge wing and the inflatable leading edge wing. The rigid leading edge wing provides a maximum $\frac{L}{D}$ of 3.85; whereas, the inflatable leading edge only produces a maximum $\frac{L}{D}$ of 2.5. This difference in $\frac{L}{D}$ is sufficient to render no dry landing capability for the inflatable leading edge wing, whereas, the rigid leading edge wing provides sufficient range for all cases except the Dyna-Soar Case (highly improbable).

The structure weight of total system for the rigid leading edge is estimated to be about 8% of recovered weight. The inflatable leading edge wing combined with system structure is estimated to be between 6 and 8% of recovered weight. These weight estimates are given by the Ryan Aeronautical Company. North American Aviation weight estimates of the different constructed wings are about twice as great. This, of course, is a significant difference in results of the companies.

Deployment may be made at high q values with the rigid leading edge wing; whereas, the inflatable rigid leading edge is thought to

require low q deployments. For best use of energy dissipation, it appears necessary for fly back to Cape missions to have early deployment and turn around after first stage cutoff.

Slide #11 shows a more detail view of the Ryan selected rigid leading edge wing configuration attached to the booster. Since the proposed glide technique of recovery employs no auxiliary aerodynamic or jet reaction controls, very careful attention has to be given to the manner of booster suspension from the wing.

An aft end view of booster and wing combination is shown on the left hand side of the slide. The cables leading from the strong points of booster (both front and aft end) to the control bar are movable and are for pitch and roll control. Control is accomplished by properly controlling the total mass center of the system. The array of cables leading from control bar to the leading edges and keel are held fixed.

The right hand side of slide shows a side view of wing attached to booster. Longitudinal wing position and angle of incidence depend on the required booster angle of attack for various trimmed flight conditions or the pitch attitude desired for landing. For maximum range, the booster should fly with a near zero angle of attack. It is possible to fly with adequate stability at a wing angle of attack (α_w) up to 20 degrees, which corresponds to just above $\frac{L}{D}$ maximum. A greater α_w value usually results in a radical pitch up as a result of normal transient conditions encountered during the trajectory.

During the flyback portion of the trajectory, wing incidence is commanded by the ground operator to keep the vehicle along the desired flight path. Phugoid motion will occur at nearly constant angle of attack but the automatic trimming system will damp out the phugoid mode, while preventing variations of wing angle of attack to angles not consistent with $\frac{L}{D}$ maximum.

The system as shown here may be considered completely rigid, thus eliminating requirements for interrelated booster dynamics with respect to the wing.

The actual flight path during flare will be determined to some extent by the variable vehicle configuration and variable inflight conditions upon initiation of the flare maneuver. The flare command system is not designed to establish a fixed flight path during flare, but rather a specifically commanded sink rate as a function of altitude. This method results in an appropriate utilization of the energy available during flare. In general, this means that systems with excess energy perform longer, slower flares to dissipate energy as a result of drag. Systems with less or minimum energy will initiate flare automatically at an altitude at which the system is capable of a successful flare. Conceptually, the control commands during flare are computed by a ground-based computer and transmitted to the wing control system by radio link. The ground base computer utilizes altitude and range information to compute the error equation.

A typical example of the system performance during flare is given

on slide #12. The simulated system performance is measured against the commanded sink rate. Touchdown was accomplished with less than 5 ft/sec vertical velocity. The final landing gear design is based on landing skis with conventional energy absorbing oleo struts.

Since the subjects of control, flare, and landing requirements for the paraglider system is going to be covered in later talks by Langley Research Center, I will not dwell further on these subjects.

A schematic diagram of the rigid wing packaging attachment to booster and deployment sequence is given on slide #13. The rigid wing is packaged between a single lox and fuel tank. Next to the wing between adjoining fuel and lox tanks, the keel and control bars are housed. In the nested position, the wing, fairing door, and control bar will be attached to the booster at approximate stations 187 and 771. There will be clips welded to the tanks to accommodate straps across the wing to minimize deflection and vibration. Clips will also be added to accommodate cables crossing over tanks from the control bar to wing.

Cartridge ejection separates the package from the booster. This ejection mechanism is attached to the top leg of the forward spider and will operate on tracks. An ejection hammer strikes the folded aft end of the keel, imparting a rotational moment. A second lip on the ejection hammer then strikes the wing apex. This system is sequenced in such a manner as to impart translational and rotational energy to the keel to insure positive separation and unfolding of the

100 foot keel, Ejection of the undeployed wing also causes, by cable attachment, control bar separation from the booster. Cable tension, within the wing and control bar, causes spreader bar action which forces both wing and control bar in their operating geometry.

It may at this point be well to point out that very little is known of deployment characteristics of such a wing for high dynamic pressures.

The main steps of the booster re-use cycle are shown on slide #14. The addition of a booster recovery system to a space vehicle program requires additional functions otherwise not needed if expendable boosters are employed. Typical of such functions are the recovery package operations of installation, checkout, and booster refurbishment after recovery. Other functions, such as transportation of boosters from the manufacturing site to the launch site, would be changed to the extent that such operations are required to support a given launch frequency.

The installation and checkout of recovery package would be done on pad at launch or within the near area depending upon installation requirements. Transportation from landing site to refurbishment site would probably be done by large trucks with special equipment for transporting boosters. Then, after refurbishment is complete, the boosters may either go to storage or back to the launch site for further action.

All of the steps in the re-use cycle have definite inputs to the cost analysis of such a program.

A booster program savings versus average launch per booster is

shown on slide #15. The program cost without recovery for a launch rate of 12 per year for a 12 year period was estimated at 1.3 billion dollars. The parameter E is defined as the ratio of refurbishment cost to original cost of booster. E was chosen to be .2, .4, and .6 respectively. This graph was based on recovery mission reliability of 60% and an average payload of 40,000 lbs. to low orbit. (C-2 configuration)

A most probable range relative to number of launches per booster is from 2.4 to 3.7. These limits are based on the flex wing recovery system reliability analysis, which is converted from probability of booster re-use to launches per booster. The minimum point, and most conservative, within the probable range (2.4 launches per booster and a 60% of booster cost allowance for refurbishment) indicates a total program savings of 185 million dollars; while the maximum point and most liberal (3.7 launches per booster and a 20% of booster cost allowance for refurbishing) shows a total program savings of 644 million dollars.

The last slide, #16, gives a summary of conclusions and recommendations. The conclusions are as follows:

(1) Boosters for C-2 type vehicles may be recovered on dry land (Cape area) by application of paragliders.

(2) Packaging of the wing system could be done within contours of C-2 booster.

(3) A general package type recovery system could be installed on booster. This implies almost no modification to booster structure.

TITLE: Application of Paragliders to S-1 Booster Recovery for C-1 and C-2 Class Vehicles

(4) Recovery system weight is about 8% of recovered weight.

(5) Sink speeds of 5 ft/sec or less are possible to obtain during flare and landing.

The recommendations at the time of study (1960) were to start immediately on a program of development which included hardware testing, etc. Unfortunately, the C-2 type vehicle is now not in the plans of NASA launch vehicles; thus, no development plans are in progress.

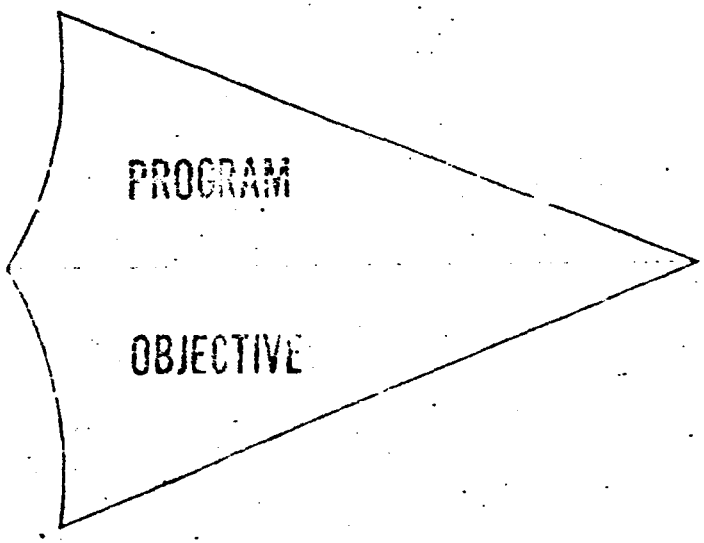

TECHNICAL AND ECONOMICAL FEASIBILITY OF THE RUGALLO "FLEX WING" FOR SATURN S-1 BOOSTER DRY LAND RECOVERY

Fig. 1

1. PRELIMINARY DESIGN OF RECOVERY SYSTEM
2. METHOD OF ATTACHMENT WITH MINIMUM MODIFICATION TO BOOSTER
3. COMPLETE OPERATIONAL & COST ANALYSIS
4. DETAILED RESEARCH & DEVELOPMENT PROGRAM

PROGRAM SCOPE

Fig. 2

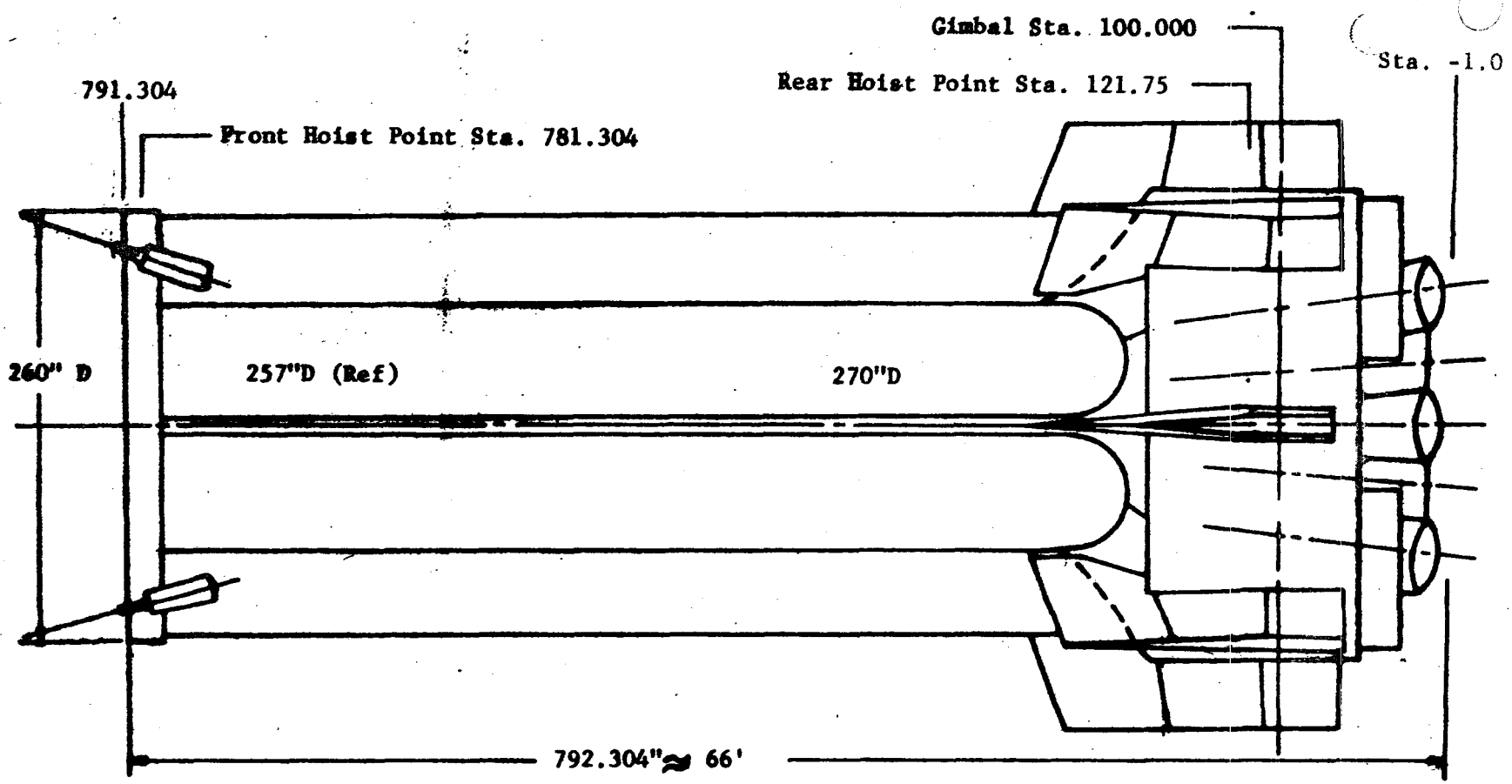

C-2 VEHICLE, S-1 STAGE PRELIMINARY MASS CHARACTERISTICS

	Weight (lb)	C.G. Sta.	Moment of Pitch	Inertia Roll
Dry Booster (Including Fins)	88,000	307	217,168	15,808
A. Front Hoist Point Load	25,785	781.304		
B. Rear Hoist Point Load	62,215	121.750		
Dry Booster with S-1/S-11 Inter. Sect. Retro Rockets, & Recovery Package	106,000	344	284,331	22,099
Booster at Separation (Separation Sta. 868.304)				
Case 1. With Residual at Bottom of Tanks	120,866	331	303,897	24,598
Case 2. With Residual at Top of Tank	120,866	344	318,812	24,598

Fig. 3

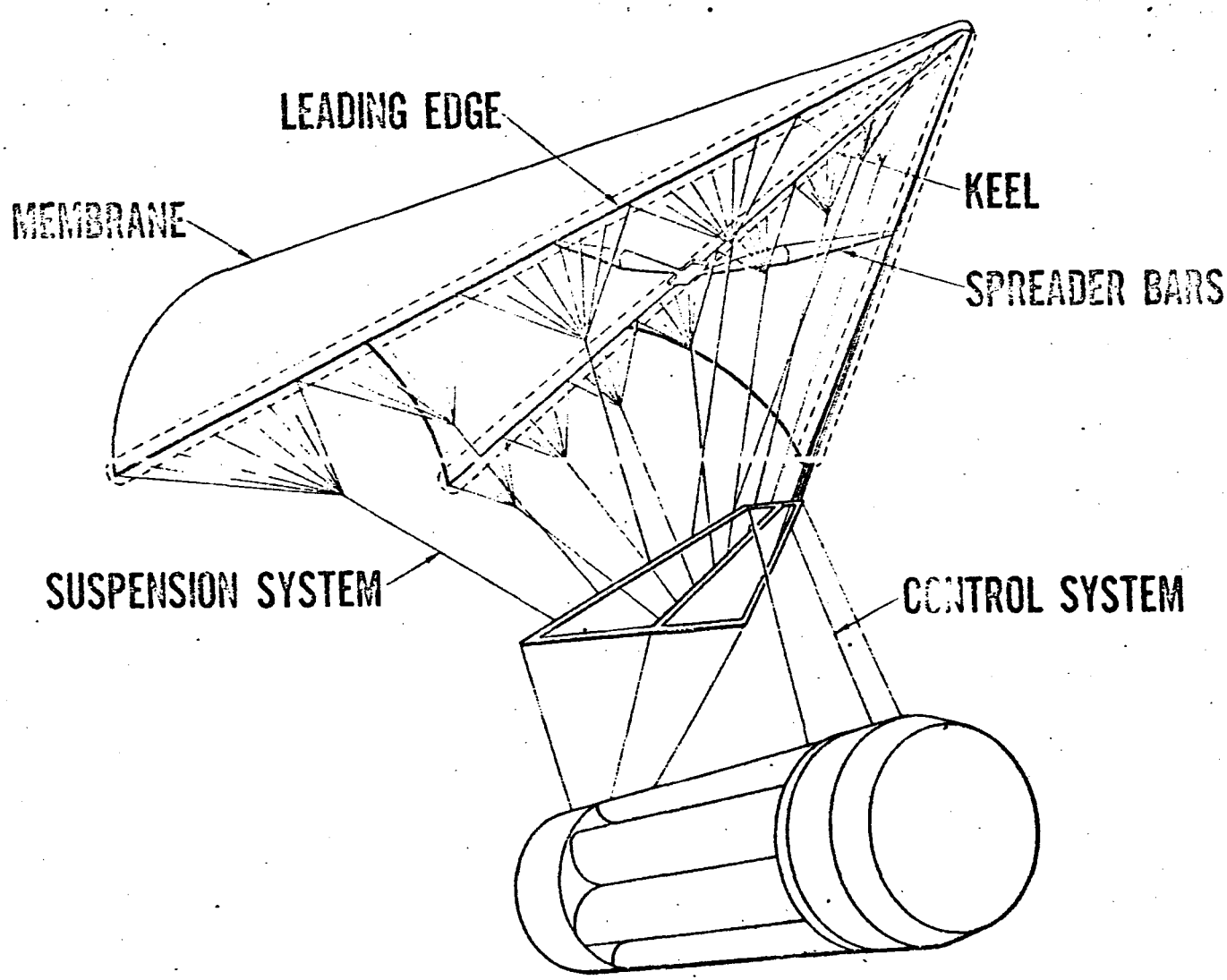

FLEX WING CHARACTERISTICS

Fig. 4

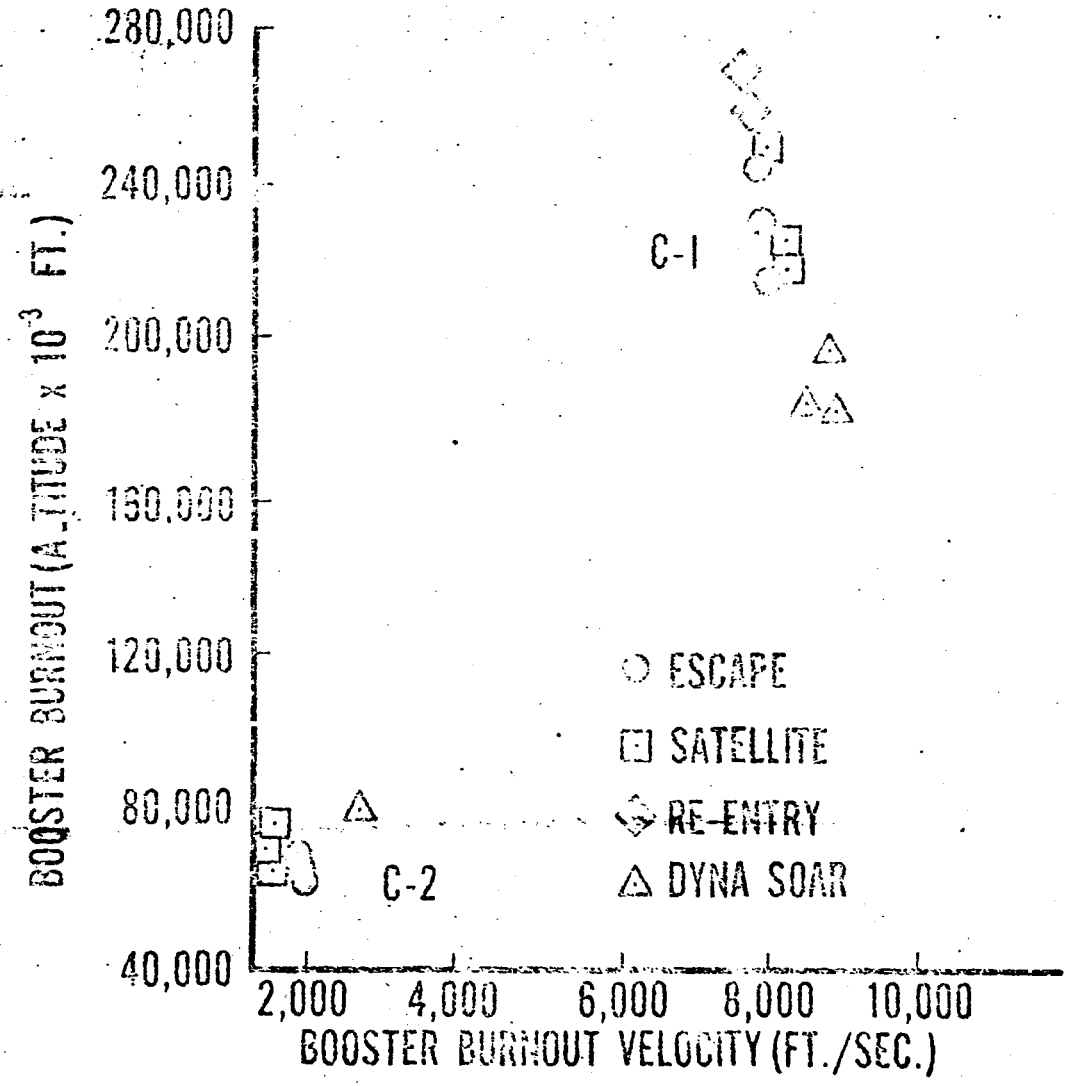

BOOSTER BURNOUT STUDY CONDITIONS

Fig. 5

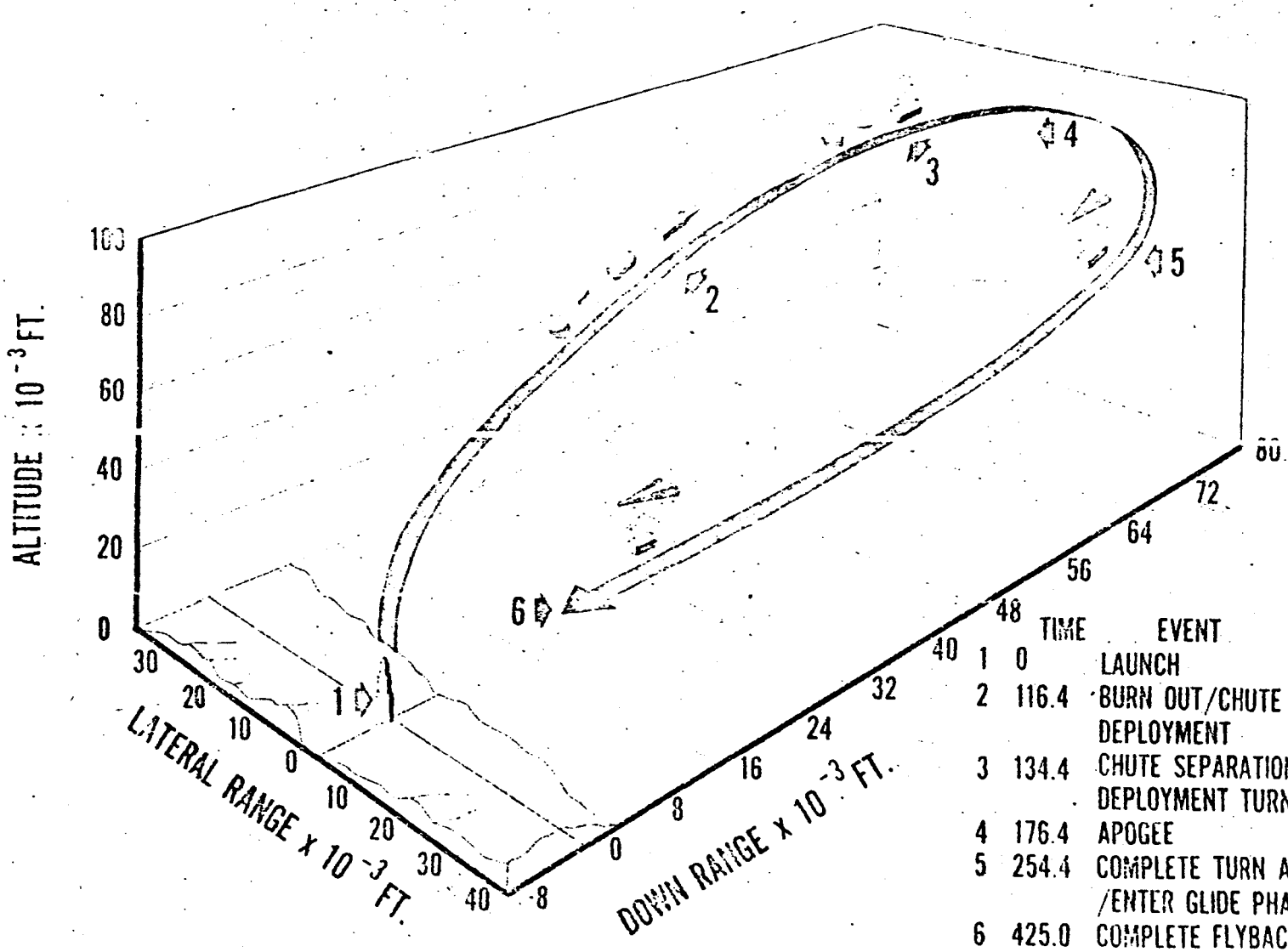

	TIME	EVENT
1	0	LAUNCH
2	116.4	BURN OUT/CHUTE DEPLOYMENT
3	134.4	CHUTE SEPARATION /WING DEPLOYMENT TURN EXECUTION
4	176.4	APOGEE
5	254.4	COMPLETE TURN AROUND /ENTER GLIDE PHASE
6	425.0	COMPLETE FLYBACK USE REMAINING ALTITUDE FOR EXECUTION OF LANDING PHASE

C-2 MISSION PROFILE

FIG. 6

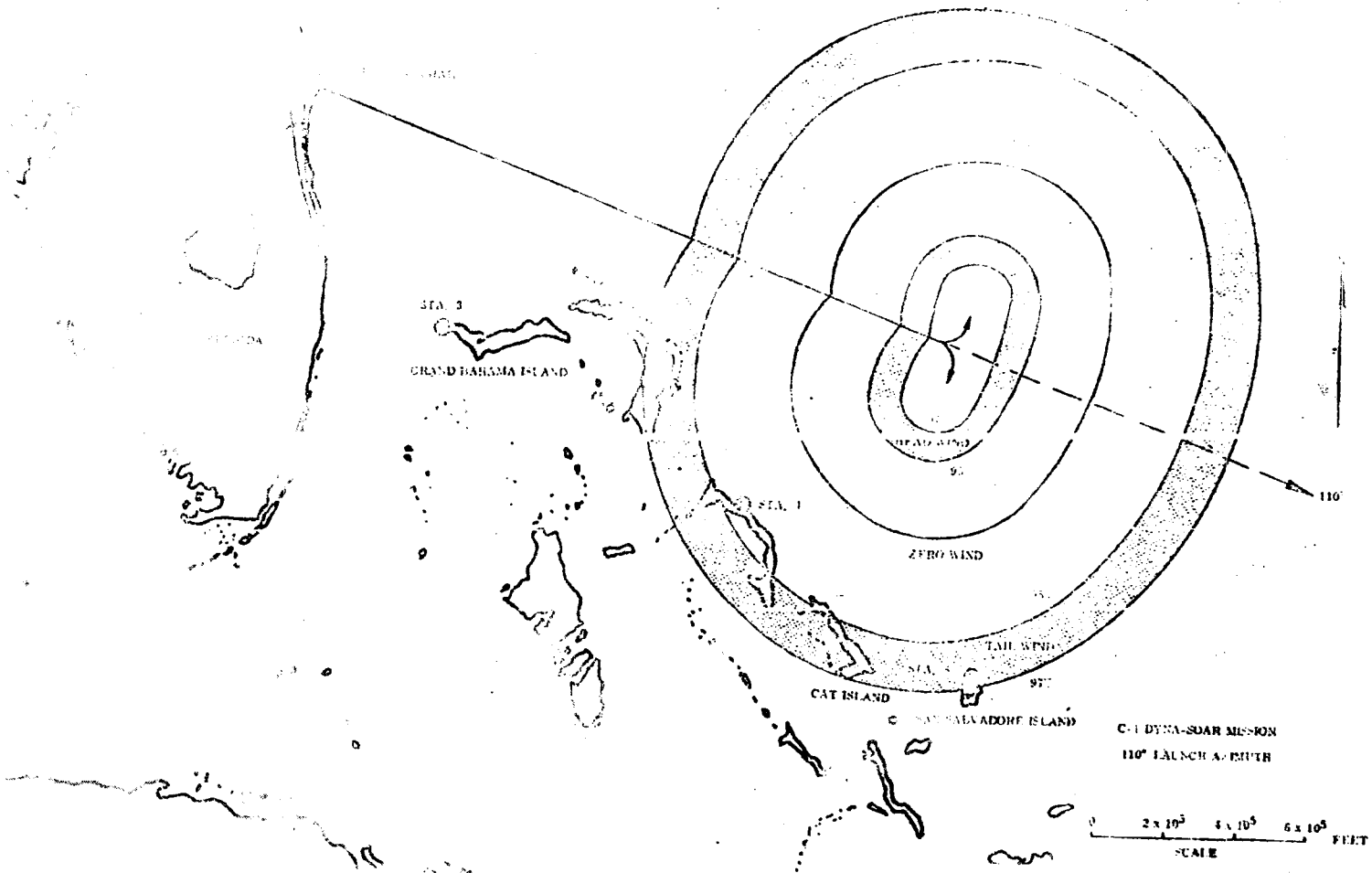

GLIDE CAPABILITY

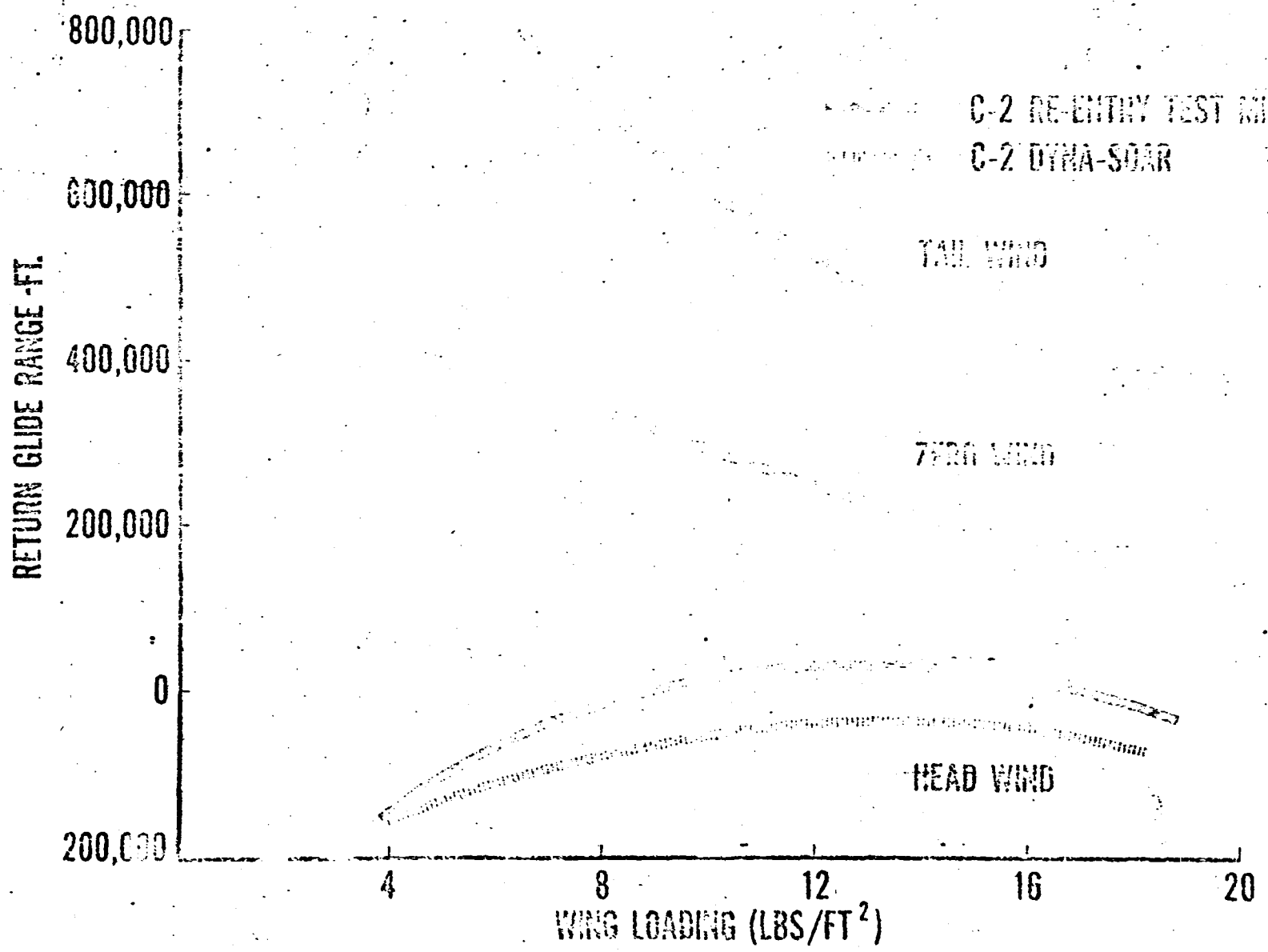

GLIDE RANGE VS WING LOADING

FIG. 8

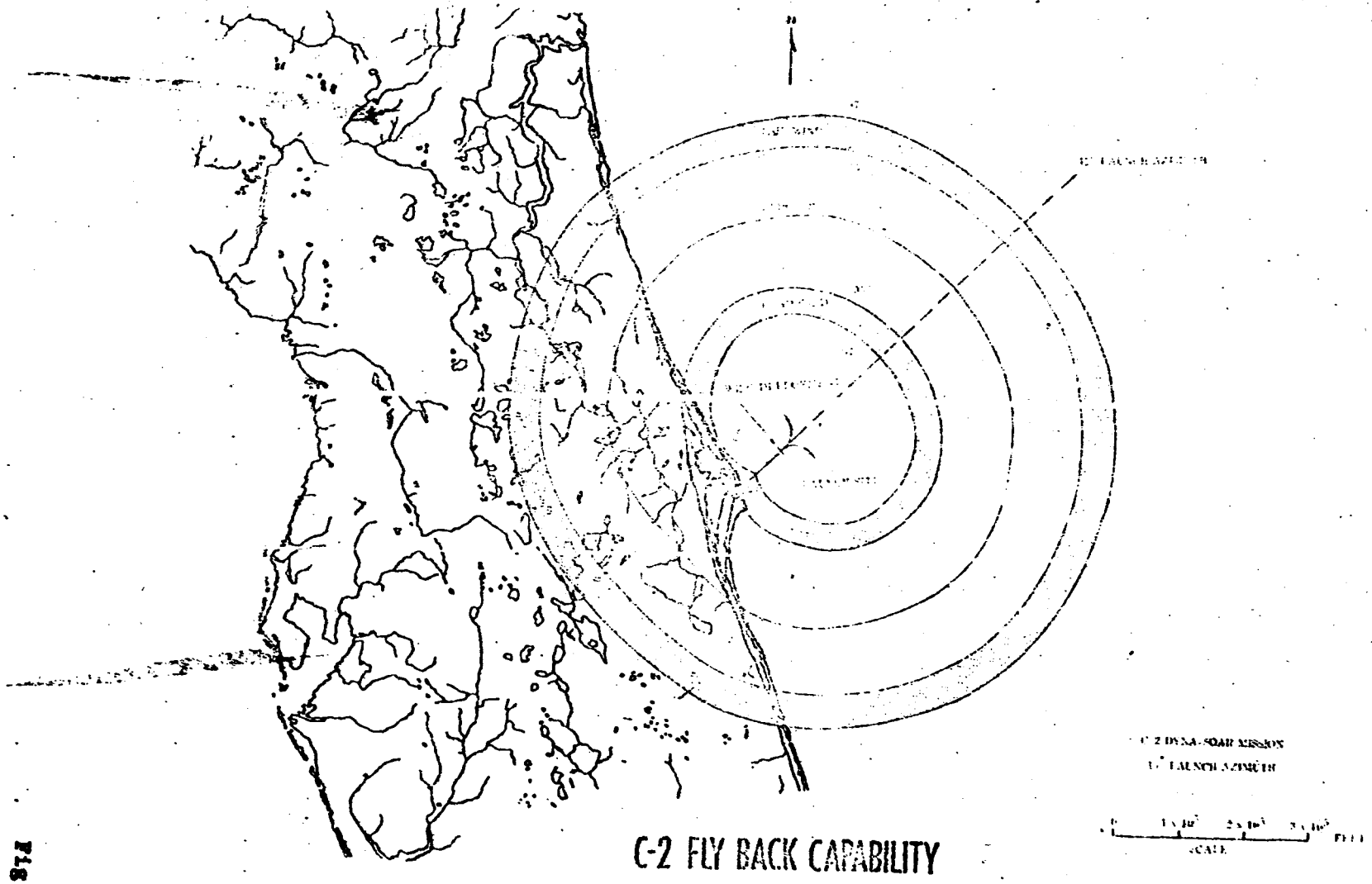

C-2 FLY BACK CAPABILITY

FIG. 9

	RIGID LE	INFLATABLE LE
MAXIMUM GLIDE	L/D = 3.85	L/D = 2.5
	[illegible] LANDING CAPABILITY FOR [illegible] - 2 MISSIONS [illegible] - SOAR	NO DRY LANDING CAPABILITY
STRUCTURE WEIGHT	8% RECOVERED WEIGHT	6% TO 8% RECOVERED WT.
PACKAGING	MORE DIFFICULT	COMPARATIVELY SIMPLE
DEPLOYMENT	HIGH "G" DEPLOYMENT CAPABILITY	LOW "G" DEPLOYMENT CAPABILITY

REQUIRED FOR MISSION

RIGID LEADING EDGE
VS
INFLATABLE LEADING EDGE

Fig. 10

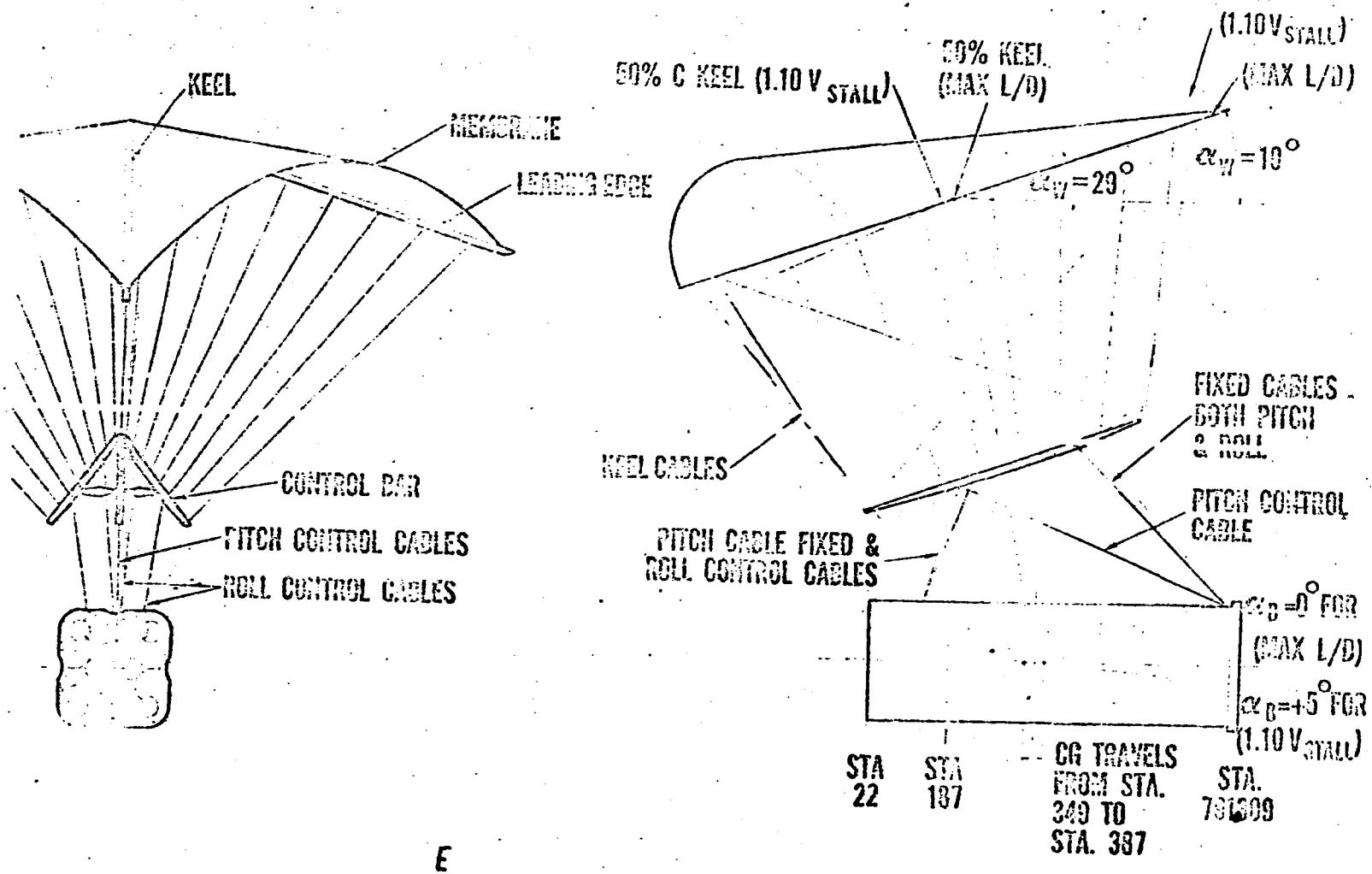

[illegible] LEADING EDGE DESIGN CONFIGURATION

Fig. 11

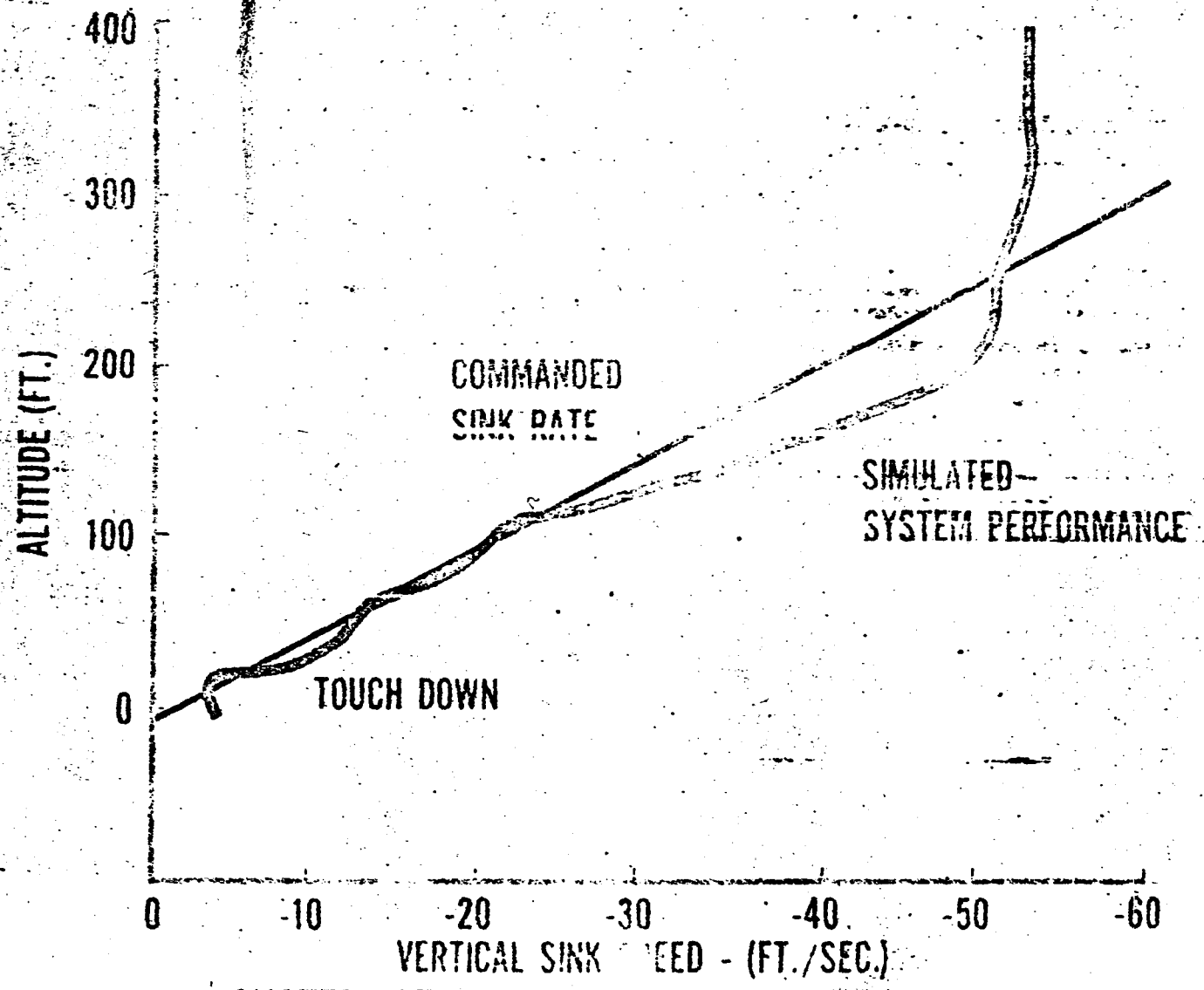

SYSTEM PERFORMANCE DURING FLARE

Fig. 12

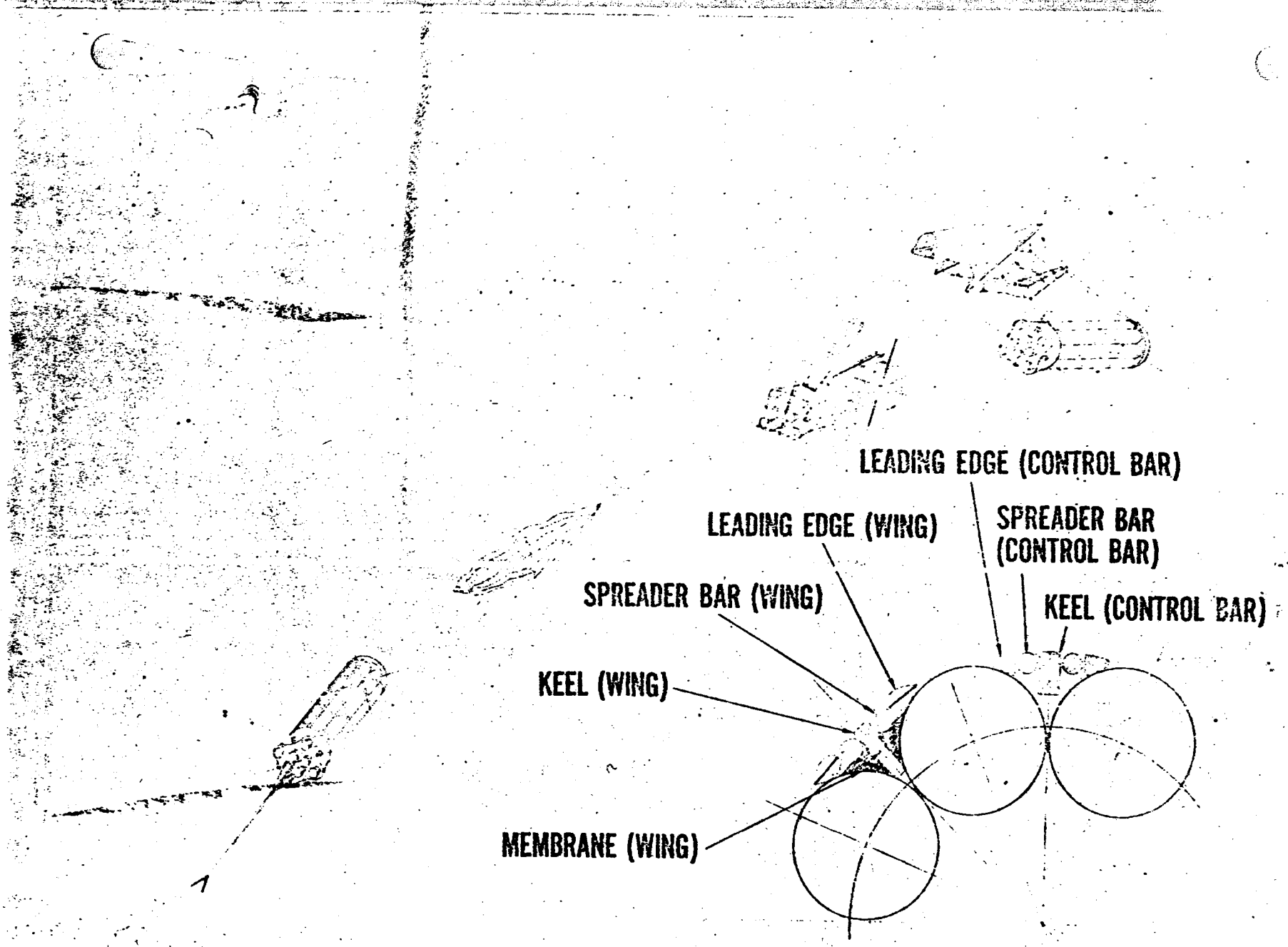

PACKAGING & DEPLOYMENT

Fig. 13

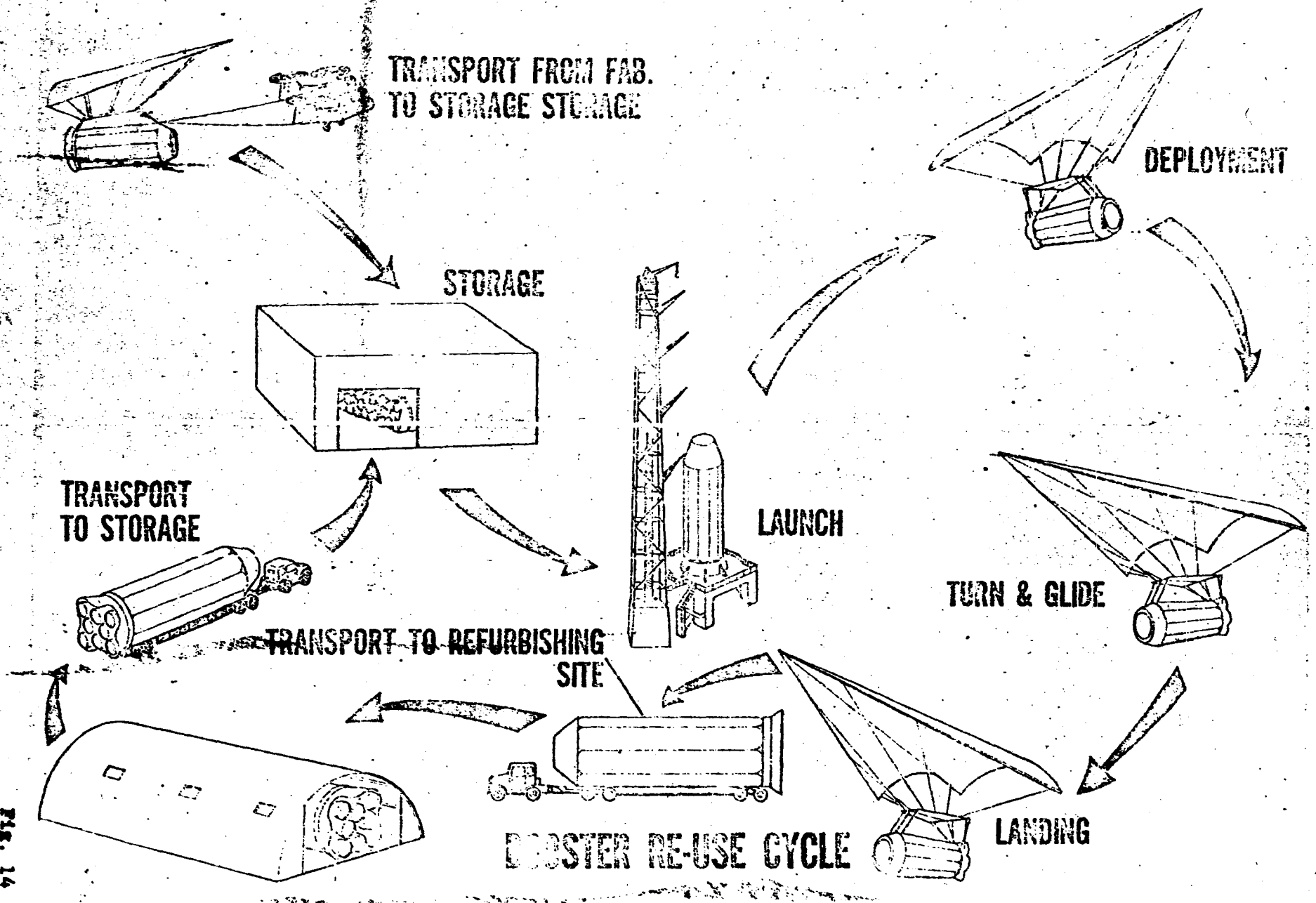
TRANSPORT FROM FAB.
TO STORAGE STORAGE
STORAGE
DEPLOYMENT
LAUNCH
TRANSPORT
TO STORAGE
TURN & GLIDE
TRANSPORT TO REFURBISHING
SITE
LANDING
BOOSTER RE-USE CYCLE

FIG. 14

PROGRAM COST WITHOUT RECOVERY = 1.3 BILLION
PROGRAM DURATION 12 YRS.
LAUNCH RATE 12 YRS.

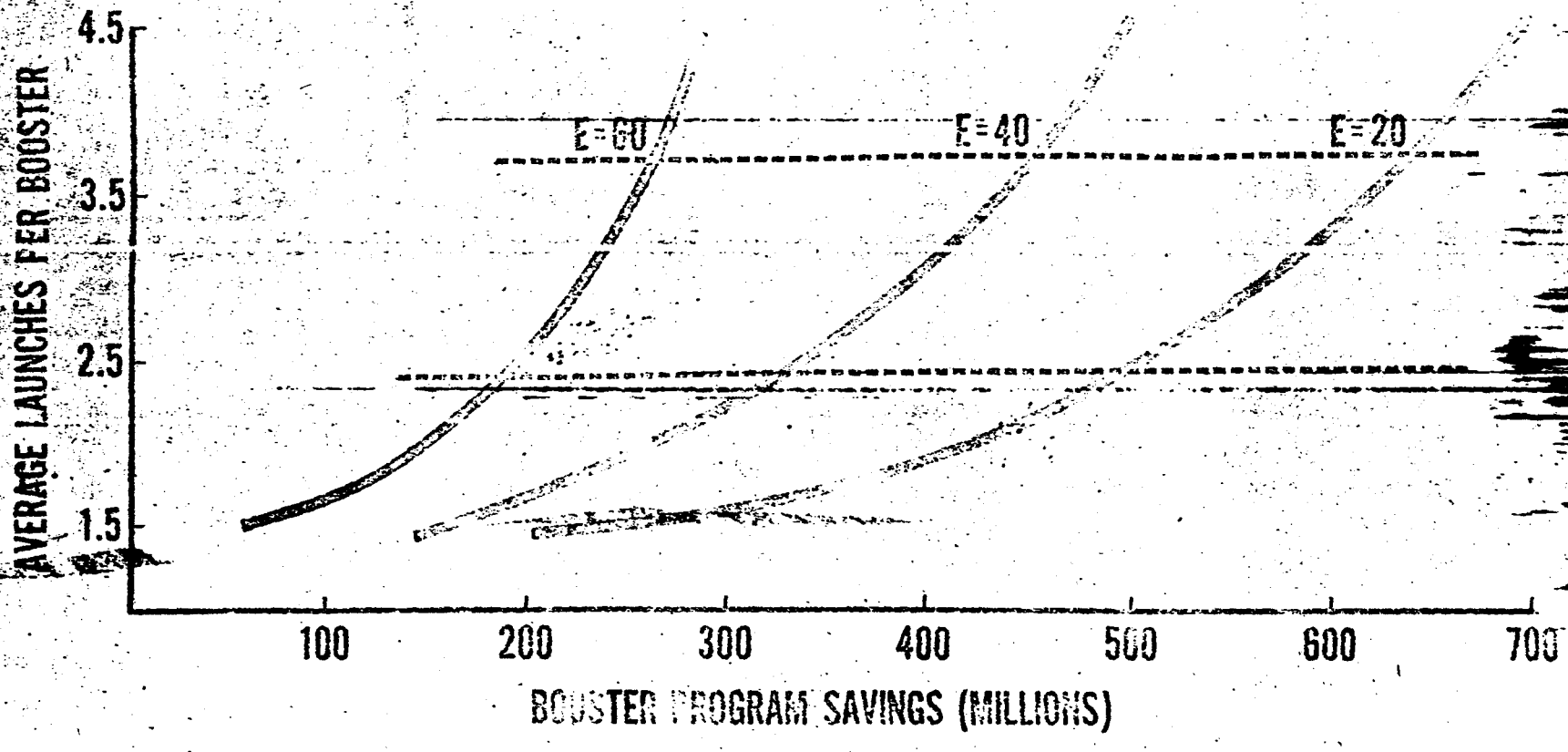

AVERAGE LAUNCHES PER BOOSTER vs BOOSTER PROGRAM SAVINGS

FIG. 15

CONCLUSIONS

1. C - 2 DRY LAND RECOVERIES ARE POSSIBILITIES
2. PACKAGING WITHIN C - 2 CONTOURS IS POSSIBLE
3. PACKAGE "TYPE" RECOVERY SYSTEM INSTALLATION IS POSSIBLE
4. RECOVERY SYSTEM WEIGHT EQUALS 8% OF RECOVERED WEIGHT
5. SINK SPEEDS EQUAL TO 5FT./SEC. OR LESS ARE POSSIBLE

RECOMMENDATIONS

1. PROGRAM DEVELOPMENT

FIG. 16

X65 84333

RECOVERY OF ORBITAL STAGES

By

Dietrich W. Fellenz*

[redacted]

The reasons to be interested in the recovery of a stage that reaches orbital injection conditions (usually a second stage) are basically the same as for the recovery any other piece of space hardware:

1. Post-flight inspection affords the detection of design shortcomings and a better evaluation of the actual environment of the component (loads, heat input etc.).

2. Reduction of cost per pound of payload in orbit due to re-use of hardware.

3. Operational advantages of positive disposal of hardware and if possible return to the refurbishment and launch site.

While post flight inspection is always desirable from an engineers point of view in order to advance the state of the art, it looks like that the development of a recovery system can only be sold on the basis of points 2 or 3 above.

To prove the desirability of recovery on a cost basis alone would require that all developmental and operational costs referred to the reduced payload in orbit would come out cheaper than in the case of an expendable reference vehicle. Studies performed or contracted by MSFC in this area showed that this point could be proven for first stages assuming the present state of the art. The discussion of cross-over points, of course, is influenced very strongly by the basic cost assumptions. At the present time, it seems, that no cost reductions can be derived from second stage recovery.

The third and by no means less important aspect is the operational. It can be expected that the volume of launch operations in support of

*Advanced Flight Systems Branch, Propulsion and Vehicle Engineering Division, Marshall Space Flight Center

orbital operations, lunar and planetary missions will continue to grow and will reach dimensions where the controlled disposal of all spent space hardware will become mandatory. Taking an expendable vehicle with such a "disposal" system and its reduced performance as reference, it might prove that full recovery and return of all stages can become economical. The requirements for recovery forces will grow proportionally to the volume of the launch operations. It is obvious that the capability to return to the launch base has to be more and more incorporated in the vehicle. This would in turn speed up the refurbishment and increase the overall flexibility of the operation.

That means that the first stage requires sufficient propulsion for fly-back, and that the second stage glides back to the launch site after one or more revolutions around the earth and subsequent aerodynamic re-entry.

To study the sensitivity of various parameters of recovery the Marshall Space Flight Center sponsored three industry study contracts (NAS 8-1513/1514/1515) on the subject "Study of a Two to Three Million Pound Thrust Launch Vehicle". The basic mission was defined as two-stage to 307 N. M. orbit. Recovery was to be considered for both stages. Fig. 1 shows a typical mission profile.

An evaluation of the final reports of the three studies with respect to structural weight increases due to recovery was made and the results are shown in Fig. 2. The parameter shown is the weight of the recovery system in percent of the structural weight of the expendable reference vehicle, based on equal propellant ratio, i.e., on equal ideal velocity increment of recoverable and expendable stage. The data generated by the different companies scatter considerably. This is partly due to the different assumptions with respect to structural efficiency as indicated by the structure ratio of the expendable reference vehicle shown in Fig. 3, partly due to the relative novelty of a

particular recovery mode. We expect to be able to smooth out some of the scatter in these data after a presently going study of fixed wing recovery systems* has been evaluated. In order to get a better feel for the performance penalty associated with orbital stage recovery by paraglider a conceptual design study was performed at MSFC, the results of which will be discussed later in some detail.

In the case of a two stage to orbit configuration we find that there is a payload decrease of about 1 lb per 5 lbs increase in first stage structure weight and a payload decrease of 1 lb per 1 lb increase in second stage structure weight.

In addition to that the increase in second stage structure weight due to recovery is considerably higher than that for first stage recovery. This is mostly so because of the more severe re-entry environment and the much longer glide and exposure times requiring heavier thermal protection.

This explains why second stage recovery is so expensive in terms of payload. Fig. 4 shows the effect of second stage recovery on the payload of a two stage to 307 N. M. orbit configuration with an initial weight of $2.4 \cdot 10^6$ lb and $3 \cdot 10^6$ lb thrust. First stage LOX/RP; Second Stage LOX/LH_2. The ascent trajectories utilized intermediate parking orbits and Hohmann transfer up to 307 N. M. altitude. The recovery factor, as defined by NAA, see Fig. 4 for equation, represents the ratio between the stage structure weight factors of the recoverable and the expendable reference vehicles. The figure shows on its left side for $K_2 = 1.0$, which means no weight added for second stage recovery, the payload performance of the corresponding lower stage (again with or without recovery) carrying an expendable second stage.

Some of the scatter in the payloads shown can be explained by different staging orbit altitudes and different "kicker systems" to

*Conceptual Design Study of Ten Ton Reusable Orbital Carrier Vehicle NAS 8-2687/5037.

perform the transfer maneuver up to the target orbit. The recovery modes suggested for study in the "2-3 Million Pound Thrust Launch Vehicle Study" were "Paraglider" or "Fixed Wing". The lightest of these modes of course is the Paraglider, although, as you saw from Fig. 2, this sytem can amount to a sizable weight penalty. Increasing second stage recovery factor K_2 means heavier and more sophisticated recovery systems, usually associated with extended cruise capability.

I would now like to present some details on our parametric design study of the application of a paraglider to the recovery of an orbital stage.

The paraglider concept looked attractive to us because of its light weight, the simplicity of the system, the possibility to stowe it away in a fairly small volume along the stage which would not penalize the vehicle configuration during ascent, and the inherent stability of the paraglider configuration.

With respect to the mission we assumed that the payload shall be delivered in a 307 N. M. orbit using a two-stage plus "kicker-stage" arrangement. The second stage burns out at low altitude at a velocity equal to the local orbital velocity plus the velocity increment for Hohmann transfer up to 307 N. M. Then it was assumed that the empty stage plus payload were injected into orbit. After waiting in orbit the orbital stage was brought to re-enter with a zero altitude virtual perigee, corresponding in this case to a flight path angle of 92 deg at 400,000 ft altitude.

Starting from this condition we investigated the influence of paraglider wing loading and deployment altitude on the thermal protection requirements and the overall structural weight of the paraglider package. The characteristics of the stage were those of an early version of a Saturn second stage.

The wing loadings considered were 1.25; 5; 10 lbs/ft^2. The deployment conditions investigated were 400,000 ft altitude; maximum dynamic pressure, and finally Mach 5.

Upon entry into the sensible atmosphere a drag device would be deployed to stabilize the stage. This drag device would be retained after deployment of the parawing. The de-reefing of the wing was controlled to keep the normal acceleration of the stage below a certain limit. The following assumptions were made on the part of the paraglider system:

- The physical dimensions of the paraglider wing installations of different wing loadings are assumed to be geometrically similar;
- Keel length equals leading edge length for easy stowing;
- Wing leading edge sweep angle in fully deployed condition is $\varphi = 50°$
- C. G. location required to fly at subsonic L/D_{max} and 11% static margin is 0.65 $\bar{c}$ below wing leading edge, and 0.55 $\bar{c}$ behind leading edge of $\bar{c}$;
- The wing would be oriented at an angle of attack that yielded max. L/D for that particular wing/body combination; supersonic flow: $\alpha \approx 40°$; Subsonic flow: $\alpha \approx 25°$;
- The stage body is always oriented parallel to the flight path;
- The net structure weight of the stage, which is equal to the weight recovered was $W_n = 41,000$ lb;
- The basic structure weights of the paraglider packages were obtained by scaling with respect to wing loading;

W/S [lb/ft^2]	W_{5s}/W_n [%]
15	13
10	16
5	25
1.25	78

Assumes load factor $n = 6$

- In scaling of the structural weights from a 15 lb/ft^2 wing loading base point vehicle the following assumptions were made:

1. Wing structure weights scale proportional to wing area, i.e., inversely proportional to wing loading.

2. Cable weights scale inversely proportional to the square root of the wing loading under the assumption of a geometrically similar suspension system. (Only length affected. Loads and ϕ are same.)

3. Landing gear, control system and drogue body structural weights are roughly independent of wing loading.

We ran re-entry trajectories deploying wings of the different wing loadings at the different points along the trajectory. The results of these runs were fed into a thermodynamic analysis to determine the heat protection required. It was arbitrarily decided to use an ablative system. The basic stage structural material was changed from Aluminum 2014 to stainless steel.

The ablation material weights were then determined, added to the glider structural weight and referred to the net structural weight of the recovered stage. The results are shown in Fig. 5.

In this figure it is considered that in the cases of deployment at 400,000 ft altitude the maximum resultant load factor almost independently of wing loading was not higher than 3 g's, and that in the cases of deployment at q_{max} and Mach 5, the max. resultant load factor incurred was 10 and 9 g's respectively.* The weight of the glider was then adjusted assuming that the structural weight scales directly proportional to the load factor.

The main trend of the curves on Fig. 5 seems to indicate an advantage in going to higher wing loadings, i.e., smaller wings. Furthermore the curves would indicate a preference for deployment at 400,000 ft altitude. However, there is a design difficulty in that it is hardly conceivable how the suspension cables with a diameter of in the order of

---

* Normal load factor during deployment is kept at 6 g's

2 in. and an additional ablation coating of in the order of 1/2 in. could be stowed and then deployed within a split second without loosing the ablation coating. No such coating is required for the lower altitude deployments.

Therefore, our tentative conclusion at this time is to prefer to deploy the wing below Mach 5, preferably at subsonic speeds and to go to as high wing loadings as are compatible with the overall flight stability and glide capability to ensure safe automatic landings. We feel that even the application of a radiative cooling system for the case of deployment at 400,000 ft altitude would not change this preference. If the subsonic glide capability of a paraglider is not required, a very similar system can be based on a parachute. The resulting weight penalty would be very low but has to be bought at the expense of impact and retrieval problems.

At the present time it cannot be stated positively that orbital stage recovery will save costs, however it can be said that from the operational point of view it would be very attractive. Advances in the state of the art of recovery systems will reduce the weight penalty associated with reusability, and in general will tend to make orbital stage recovery also attractive from the economical aspect.

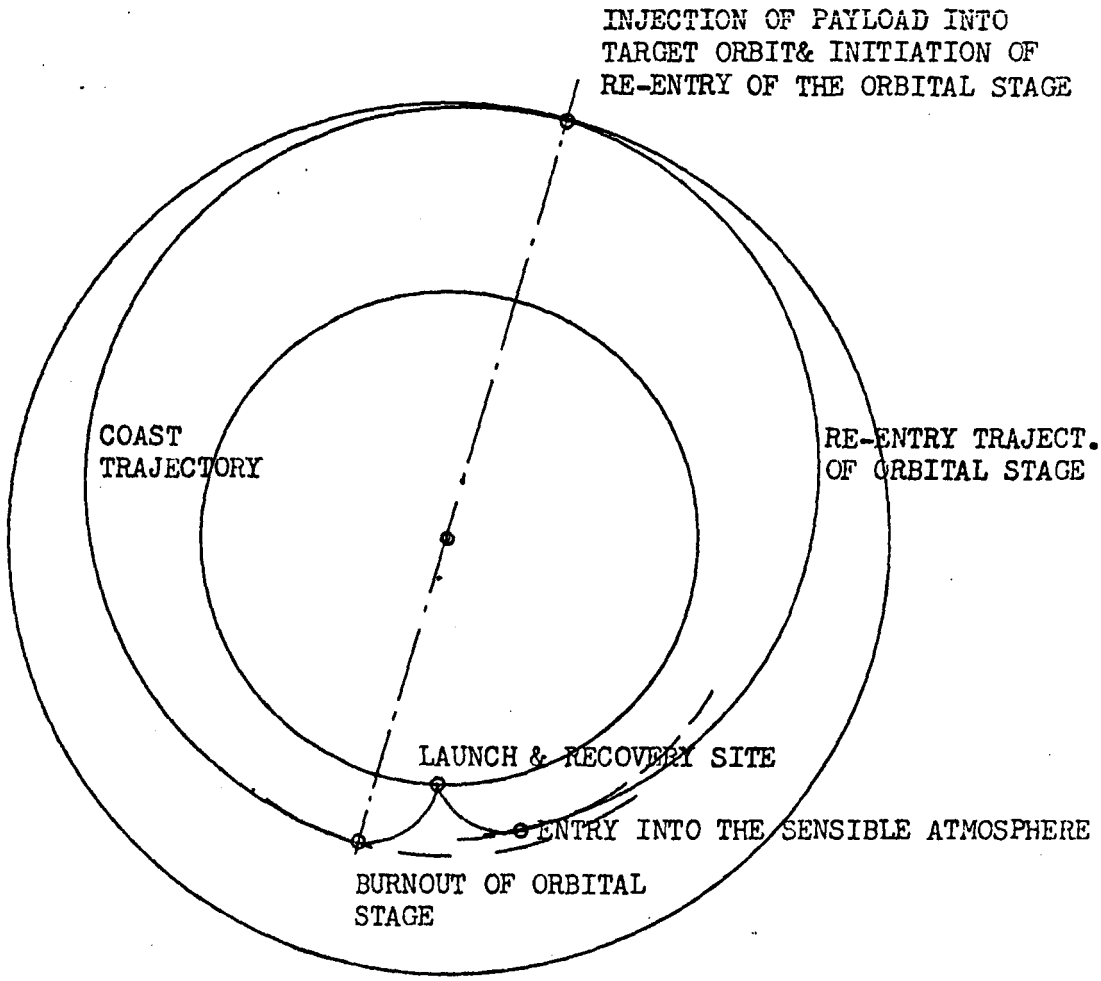

Fig.1 TYPICAL ORBITAL MISSION PROFILE INCLUDING RECOVERY OF THE ORBITAL STAGE IMMEDIATELY AFTER ONE REVOLUTION AROUND THE EARTH.

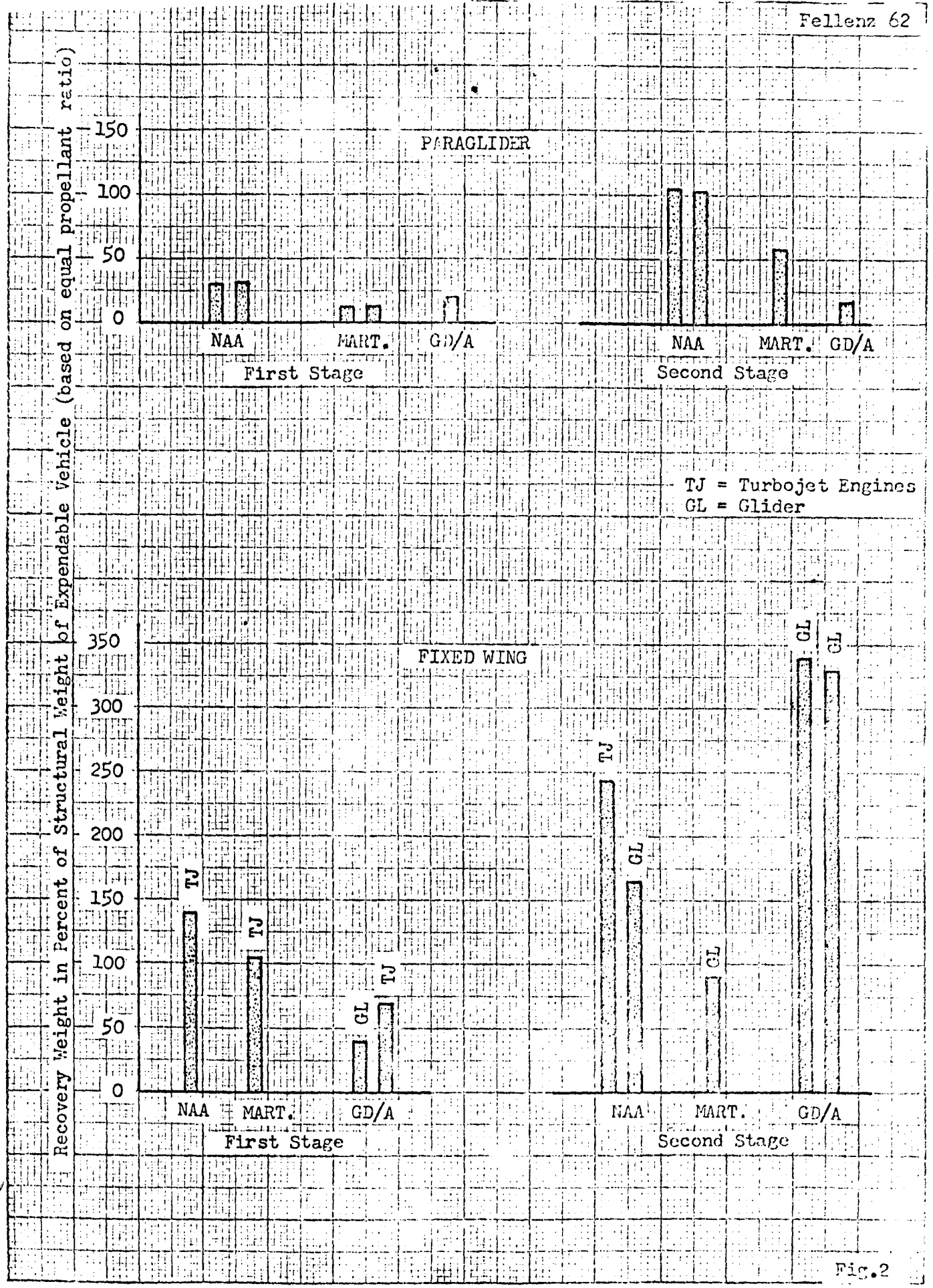
Recovery Weight in Percent of Structural Weight of Expendable Vehicle (based on equal propellant ratio)
PARAGLIDER
150
100
50
0
NAA
MART.
GD/A
First Stage
NAA
MART.
GD/A
Second Stage
TJ = Turbojet Engines
GL = Glider
FIXED WING
350
300
250
200
150
100
50
0
TJ
TJ
GL
TJ
TJ
GL
GL
GL
GL
NAA
MART.
GD/A
First Stage
NAA
MART.
GD/A
Second Stage

Fig.2

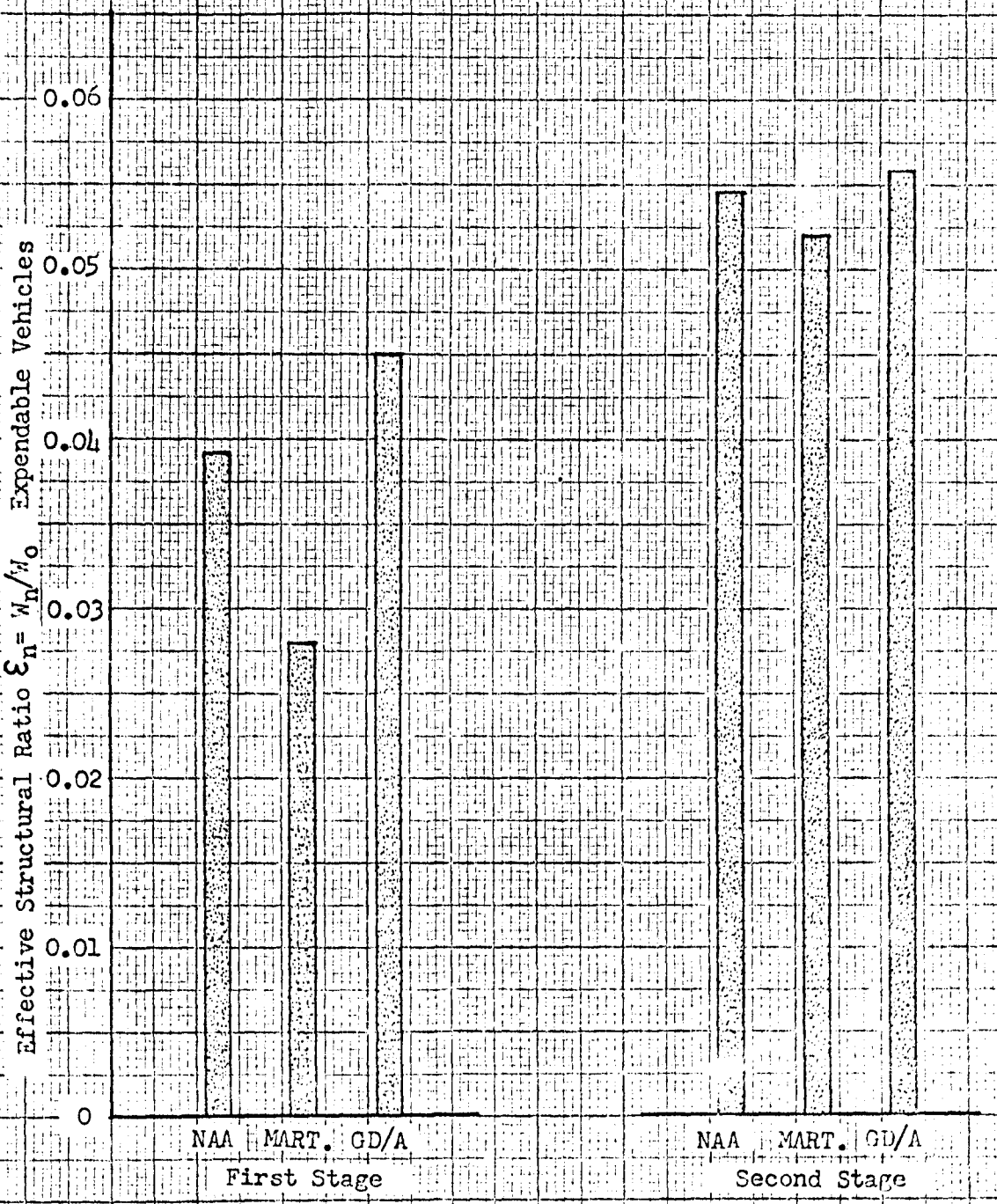
Effective Structural Ratio $\varepsilon_n = W_n/W_o$ Expendable Vehicles
0.06
0.05
0.04
0.03
0.02
0.01
0
NAA
MART.
GD/A
First Stage
NAA
MART.
GD/A
Second Stage

Fig.3

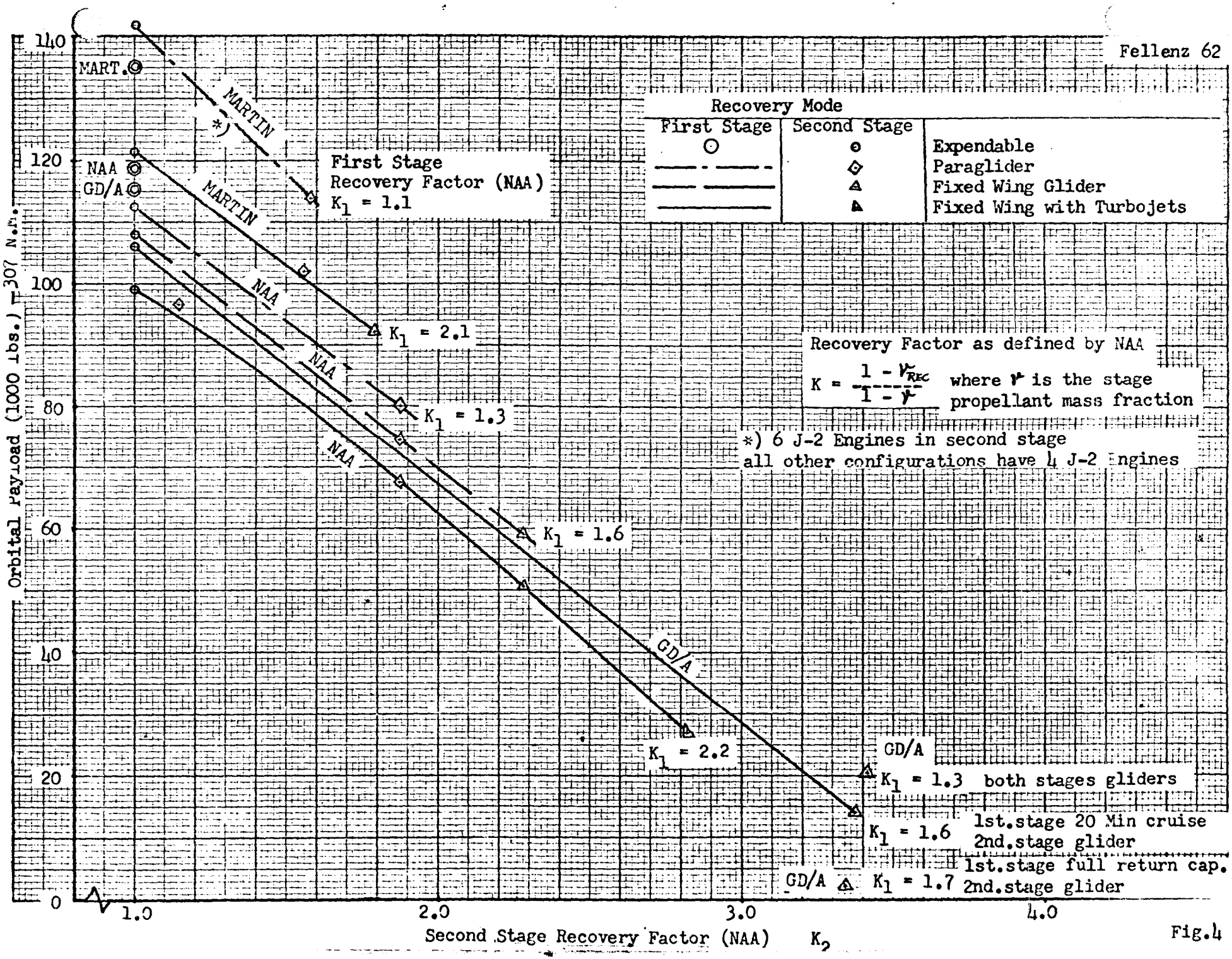
Orbital Payload (1000 lbs.) ≡ 307 N.M.
140
120
100
80
60
40
20
0
1.0
2.0
3.0
4.0
Second Stage Recovery Factor (NAA) K_2
MART.
NAA
GD/A
MARTIN *)
MARTIN
NAA
NAA
NAA
GD/A
First Stage
Recovery Factor (NAA)
K_1 = 1.1
K_1 = 2.1
K_1 = 1.3
K_1 = 1.6
K_1 = 2.2
Recovery Mode
First Stage
Second Stage
Expendable
Paraglider
Fixed Wing Glider
Fixed Wing with Turbojets
Recovery Factor as defined by NAA
$K = \frac{1 - \nu_{REC}}{1 - \nu}$ where ν is the stage propellant mass fraction
*) 6 J-2 Engines in second stage
all other configurations have 4 J-2 Engines
GD/A
K_1 = 1.3 both stages gliders
K_1 = 1.6 1st.stage 20 Min cruise 2nd.stage glider
1st.stage full return cap.
GD/A K_1 = 1.7 2nd.stage glider

Fig.4

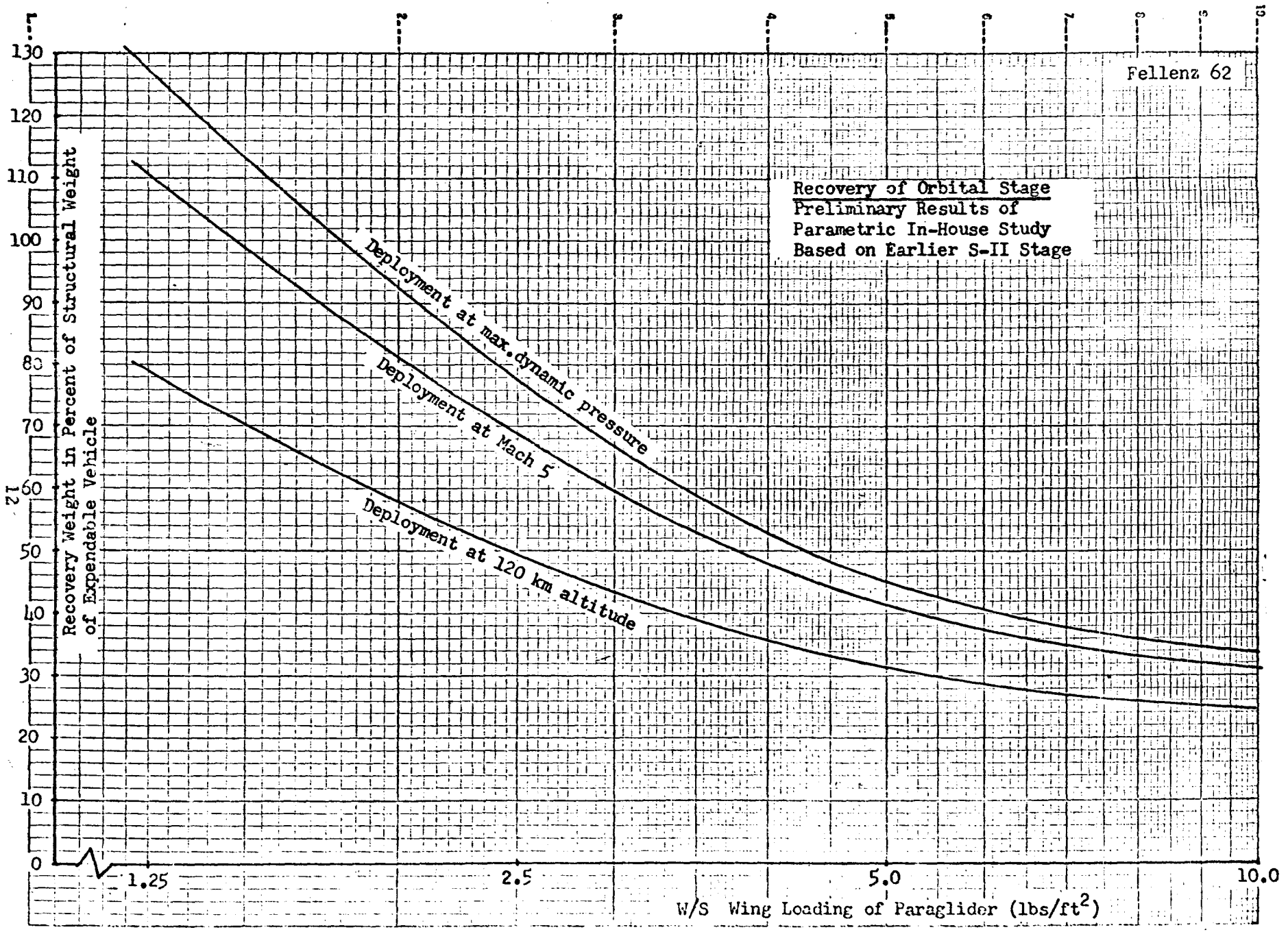
SEMI-LOGARITHMIC 358-51
KEUFFEL & ESSER CO.
1 CYCLE X 70 DIVISIONS
Fellenz 62
Recovery of Orbital Stage
Preliminary Results of
Parametric In-House Study
Based on Earlier S-II Stage
Deployment at max.dynamic pressure
Deployment at Mach 5
Deployment at 120 km altitude
Recovery Weight in Percent of Structural Weight
of Expendable Vehicle
130
120
110
100
90
80
70
60
50
40
30
20
10
0
1.25
2.5
5.0
10.0
W/S Wing Loading of Paraglider (lbs/ft²)

Fig.5

X65 84334

A REVIEW OF LAUNCH VEHICLE RECOVERY STUDIES

[redacted]

July, 1962

L. T Spears
Future Projects Office

GEORGE C. MARSHALL SPACE FLIGHT CENTER
HUNTSVILLE, ALABAMA

SUMMARY

As a part of a NASA-wide review of past and current work in the field of payload and launch vehicle recovery, this paper presents a summary of launch vehicle recovery studies conducted under sponsorship of the MSFC Future Projects Office. Previous study programs are reviewed, a current assessment of mission prospects and vehicle concepts is presented, and current MSFC studies in this area are outlined. Areas are suggested in which research and experimental work can hlep establish a foundation for future vehicle developments.

A REVIEW OF LAUNCH VEHICLE RECOVERY STUDIES

By L. T. Spears
MSFC Future Projects Office

INTRODUCTION

With our greatly expanded space program objectives, space launch vehicles will soon become a major new form of transportation. Launch vehicles to date, patterned after their ballistic missile predecessors, are characterized by "one-shot" operation in which the vehicles of highly refined design are discarded after a flight operating lifetime of only a few minutes. Recovery of expensive flight equipment, and the strong need for first hand flight test information, have prompted work for some time toward launch vehicle recovery; however, the difficulty of the task in some cases, but more often the over-riding priority of primary program objectives, have resulted in little concrete progress to date.

Interest and work toward booster recovery at MSFC date back to REDSTONE and JUPITER projects (as part of the Army Ballistic Missile Agency) in 1958/1959. Considerable work has continued since that time, as described in the MSFC papers given at this meeting. The three preceding papers have reviewed individual Marshall projects relating to launch vehicle recovery. This paper will present a summary of past and current MSFC work in this area, including a number of system studies, conducted under direction of the MSFC Future Projects Office. This material will be presented in the following arrangement:

(1) Summary of previous launch vehicle studies, and recovery methods considered.

Summary

POTENTIAL BENEFITS of RECOVERY

- POST FLIGHT EXAMINATIONS
- RE-USE OF FLIGHT-PROVEN HARDWARE
- COST REDUCTION
- AVOID EXPENDED BOOSTER FALL-OUT
- ABORT CAPABILITY

(2) A brief discussion of recovery implications, and comparisons of recovery methods.

(3) A current assessment of mission prospects and vehicle concepts.

(4) An outline of current reusable vehicle studies at MSFC, and suggestions for complementary research and experimental work.

POTENTIAL BENEFITS OF RECOVERY

It might be helpful to begin with a review of the potential benefits of launch vehicle recovery, some of which are listed in table 1. Most booster recovery studies have been begun with the incentive of reducing costs. As these studies progressed, however, there has been an increasing recognition that the operational benefits of vehicle reuse will likely be more important than costs, particularily for the high traffic rate transportation of passengers and cargo between earth and orbit.

The reuse of vehicles which have operated successfully on previous flights is believed to be of advantage, compared to the use of completely new equipment on each flight. Post-flight examinations of actual flight hardware should allow quicker diagnosis and correction of early design deficiencies than with limited telemetry data, and a faster growth to design maturity in the development phase. Growth to higher reliability levels can also be expected through repeated flight checkouts and design refinements.

The extent of range safety problems will depend on actual launch rates encountered, and upon future desires or necessity to relax restrictions in launch site location and launch azimuth. In any of these circumstances, the problem of expended booster fallout will be alleviated

PREVIOUS RECOVERY STUDIES

- REDSTONE/JUPITER 1958/59
- SATURN S-I PARACHUTE & PARAGLIDER 1959/60
- ECONOMICAL BOOST SYSTEM STUDIES 1959
- RECOVERABLE BOOSTER STUDIES (AIR FORCE) 1959/60
- 2-3 MILLION LB. THRUST BOOSTER STUDIES 1960/61

RECOVERY METHODS CONSIDERED

- DECELERATION

DRAG	LIFTING
BALLISTIC BODY	FIXED WINGS
DRAG BRAKES	FLEXIBLE WINGS
PARACHUTE	ROTARY WINGS
BALLOON	

- MANUEVER & LANDING

VERTICAL DESCENT	HORIZONTAL LANDING
BALLOON FLOATATION	FIXED WINGS
RETRO-ROCKETS	FLEXIBLE WINGS
TURBO-JETS	
ROTARY WINGS	

by their recovery.

Abort capability will be important to launch vehicle life as well as range safety. In fact, some data from aircraft experience indicate that abort capability, perhaps more than reductions in malfunction rates, is the key to extended vehicle life.

PREVIOUS RECOVERY STUDIES

The possibility for recovery of REDSTONE and JUPITER missiles prompted conceptual studies of recovery methods in 1958/1959, leading to design and fabrication of parachute recovery systems as described in the preceding papers. Other studies have followed, as indicated in table 2. The first two of these involved the addition of recovery systems to vehicles of existing design, whereas the latter three investigated vehicles of new design, incorporating a veriety of recovery concepts. The latter study produced comparative designs of recoverable and expendable vehicles in the SATURN C-3 class, concentrating on fixed wing or paraglider recovery of one or both stages.

The various recovery methods considered during these studies are tabulated in table 3. In all cases, aerodynamic drag and/or lift is the means for primary deceleration for the expended stage. A number of methods have been suggested for the maneuver to a selected landing site, cancellation of residual velocity, and for final touch-down. The simpler methods allow little or no deviation from the ballistic impact point for the expended stage. The glide capability inherent in fixed or flexible wings allows greater freedom in this respect; however, studies have shown

RECOVERY OPERATIONS CONSIDERATIONS

- WATER IMPACT
  - DEPLOYMENT OF RECOVERY FORCE
  - RETRIEVAL
  - TRANSPORT TO LAUNCH SITE
  - POSSIBLE IMPACT & WATER DAMAGE
- FIXED DOWN-RANGE LANDING SITES
  - LIMITS FLIGHT PATH SELECTION
  - TRANSPORT TO LAUNCH SITE
- RENDEZVOUS FOR RETURN
  - DEPLOYMENT OF SHIPS OR TOW AIRCRAFTS
  - RENDEZVOUS AND TIMING
  - TRANSPORT TO LAUNCH SITE
- POWERED CRUISE RETURN
  - MINIMUM RANGE EQUIPMENT AND OPERATIONS

Weight and Performance Penalties

LAUNCH VEHICLE RECOVERY

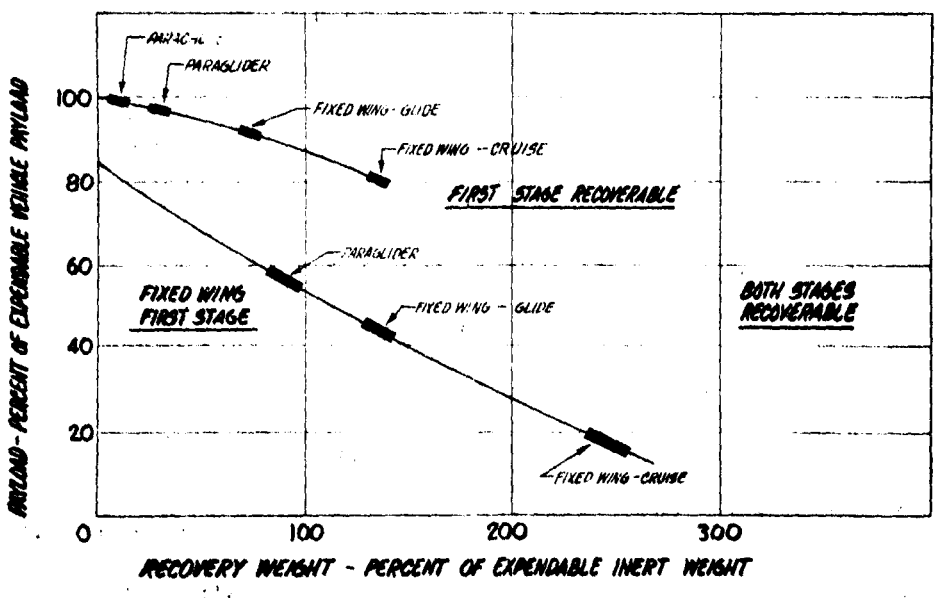

that favorably staged vehicles will require auxiliary propulsion (such as air-breathing engines) to allow the desired return of expended booster stages to the launch site.

Circumstances have not allowed investigation of all concepts in equal depth. Choices for particular applications have resulted in greatest depth of MSFC study in parachute systems, paraglider, and fixed wing vehicles.

SOME IMPLICATIONS OF RECOVERY

In studies investigating reusable vs expendable mode of operation and the relative merit of the different recovery concepts, many considerations of course come into play. Comparisons on the basis of three significant considerations are summarized in tables 4 and 5 and figures 1 and 2.

Table 4 compares recovery operations required for the simpler forms of recovery, involving down-range water landings, with the more extensive forms of recovery, which allow glide or cruise to a prepared landing site. Although probably acceptable for low launch rates, sea recovery operations (similar to Project Mercury experience) would become unwieldy for higher launch rates. Immediate return of boosters into the refurbish and check-out cycle at the launch site - avoiding water impact, down-range recovery operations, and transport back to the launch site - is considered an important factor in selection of recovery methods.

All known forms of recovery increase vehicle inert weight through addition of equipment and/or increased structural strength, resulting in payload penalty of some degree. Figure 1 shows penalties typical of various booster recovery methods; second stage recovery penalties, as discussed in the preceding paper, are shown for reference. In comparative

COST CONSIDERATIONS

- DIRECT OPERATING COSTS
  - BOOSTER PURCHASE PRICE
  - NO. OF USES PER BOOSTER
  - RECOVERY/RE-FURBISHMENT

- AMORTIZED COSTS
  - DEVELOPMENT
  - FACILITIES

COMPARATIVE COST ESTIMATES

2-3 MILLION POUND THRUST BOOSTER STUDY

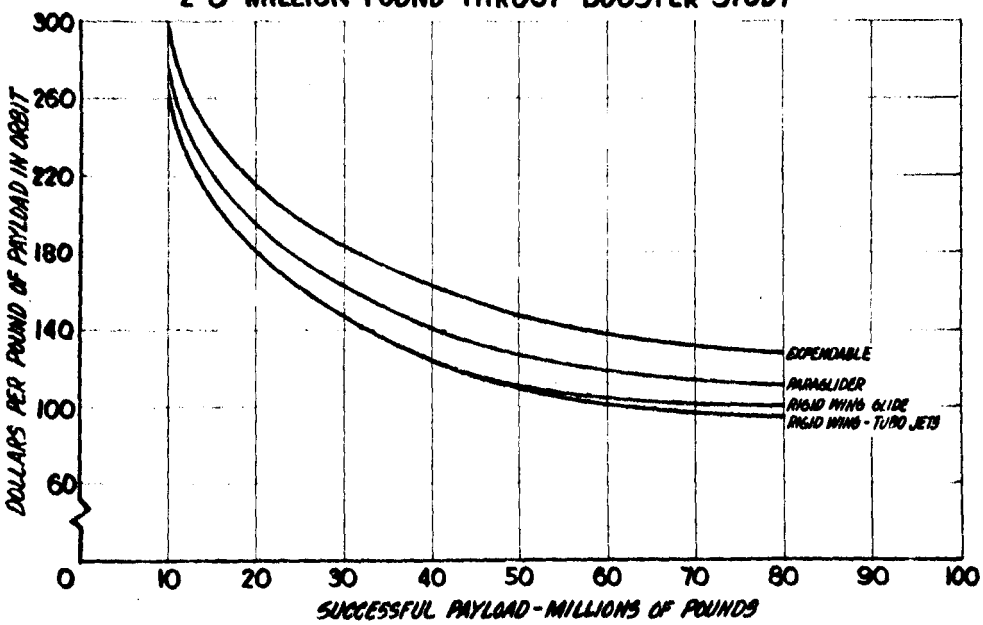

analyses, this performance decrement is reflected in costs through additional launches required to deliver equal (cumulative) pa loads, or increased booster size to provide performance equal to that of an expendable stage.

Primary factors determining the degree of cost benefit from booster reuse are shown in table 5. For the simpler recovery methods, booster reuse rate vs recovery/refurbish costs dominate, whereas increased booster purchase price and development costs become more prominent for reusable vehicles of advanced designs.

Analyses continue to show cost benefit for booster reuse, with the degree of benefit dependent upon variable estimates for some of the individual elements in which our experience is limited or lacking. Typical results of comparative costs estimates, based on studies of vehicles in the 2-3 million pound thrust class, are shown in figure 2.

CURRENT ASSESSMENT - MISSION PROSPECTS/VEHICLE CONCEPTS

Our immediate future space program objectives place primary emphasis on:

(1) Increased launch vehicle performance; i.e., capability to perform missions not previously possible.

(2) The need for this capability as early as possible.

Since recoverability would reduce payload capability and might require additional time for design and development, early introduction of recovery into major vehicle programs is not likely.

As in other technological evolutions, however, establishment of a new

MISSION PROSPECTS

- FOR IMMEDIATE FUTURE GOALS
  - MAXIMUM PERFORMANCE CAPABILITY
  - EARLIEST POSSIBLE AVAILABILITY
- NEXT PHASE OF SPACE ACTIVITY
  - MORE FREQUENT/ROUTINE TRIPS
  - IMPROVE OPERATIONS AND EFFICIENCY
  - PASSENGER FACTOR DOMINANT IN SOME SIZES

PRESENT STATUS - VEHICLE CONCEPTS

- HIGH TRAFFIC RATE/ PASSENGER - CARRYING CLASSES - FIXED WINGS WITH POWERED CRUISE

- LOWER LAUNCH RATE CLASSES - PURSUE WATER IMPACT, PARACHUTE, OTHERS

capability can be followed by concentration on improvement in operations and efficiency. The operating environment for the expected next phase of space activity emphasizes the potential for such improvements through the use of reusable launch vehicles. In contrast with the first phase, frequent and repetitive launchings will be required to support sustained operations in earth orbit and on the moon. Orbital space stations, both manned and unmanned, will require frequent visits for crew rotation, inspection of equipment, maintenance, and repairs. Particularly in some vehicle classes, the passenger-carrying function will place greater emphasis on reliability, safety, and abort capability. In general, this environment suggests a need and an approach similar to that of current air transportation.

At this point, fixed wing boosters seem the most promising choice for high traffic-rate, passenger-carrying classes. Equipped for powered cruise, this concept offers the best probability for recovery and reusability, with a minimum of recovery operations. Also significant with respect to the expected early establishment of orbital space stations, the concept requires only modest advances in technology, allowing timely availability. The simpler forms of recovery are probably more adaptable in the lower launch-rate classes. With no clear cut choice of recovery method apparent at this time, investigation of several methods - including water impact, parachute, and paraglider - should be pursued.

PRESENT MSFC STUDY EFFORTS

Payload Class	Studies
ATLAS/TITAN	RS-70 or SST TYPE LAUNCHER
SATURN C-1	REUSABLE 10 TON ORBITAL CARRIER
SATURN C3/C-5	50-100 TON REUSABLE VEHICLE STUDY
C-5/NOVA	POST-NOVA SERIES SEA-LAUNCH & RECOVERY

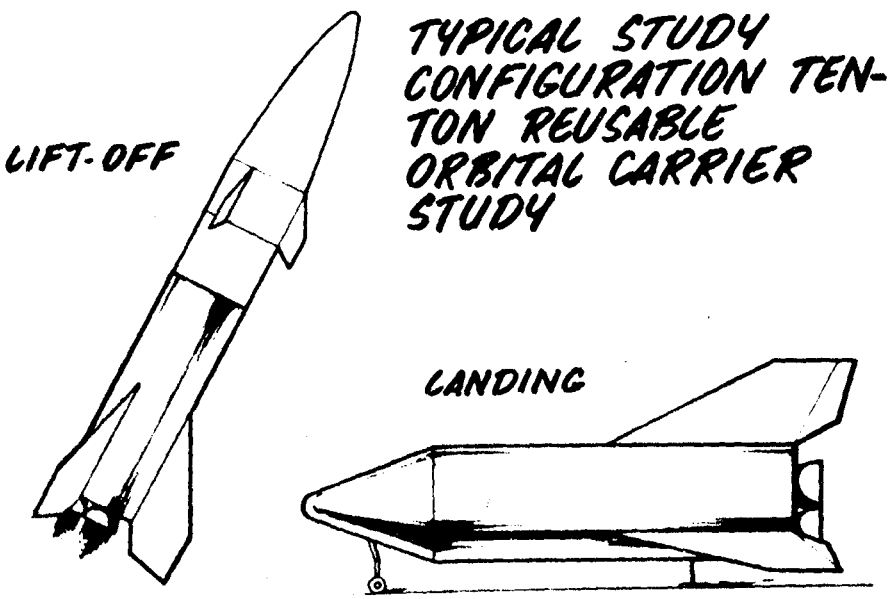

TYPICAL STUDY CONFIGURATION TEN-TON REUSABLE ORBITAL CARRIER STUDY

CURRENT MSFC STUDIES

Based upon this background and conclusions to date, Marshall-sponsored studies as shown in table 8 are now in progress* to help define the next generation launch vehicles.

Paraglider recovery of rocket vehicles in the 5-ton orbital payload class is to be studied, along with possible use of airplane-type boosters, adapted from RS-70 or supersonic transport design for air launching of rocket-powered upper stages.

The 10-Ton Orbital Carrier Study will concentrate on the job of passenger transportation between earth and orbit and, as such, is considered a probable first application for the fixed wing, "rocket airplane" concept. The 50-100 Ton Vehicle Study, on the other hand, is aimed toward a "space truck" cargo carrier concept as a successor to the current SATURN C-5, with a probable primary mission of sustained lunar operations support. The first phase of this study is investigating prospects for conversion of the C-5 into reusable configurations.

There are several study programs now active to determine vehicle configurations for payload capability greater than SATURN C-5; two are listed in which recovery/reuse are being considered. The first of these is conceived as a sea-launched, pressure-fed vehicle which can be recovered by water impact without requiring auxiliary recovery devices. Recovery concepts within the Post-NOVA studies include inflatable drag and flotation devices, integral lifting (glide) capability, etc.

* With exception of the 5-ton payload class study, which is planned as part of FY 63 program.

RESEARCH AREAS

- *STUDY/RESULTS LIMITED BY:*
  - *PRIOR EXPERIENCE*
  - *EXPERIMENTATION*

- *RESEARCH/EXPERIMENTATION NEEDED:*
  - *RECOVERY METHODS*
  - *TO ESTABLISH DEGREE OF REUSABILITY*
  - *DESIGN & FABRICATION FOR REUSABILITY*

RESEARCH & EXPERIMENTAL WORK

As in most advanced concept investigations, past experience in several aspects of vehicle recovery and reuse is very limited or lacking. However, with the date for initiation of second generation launch vehicle developments still a few years away, there is an opportunity to provide a preparatory foundation of research and experimental work in the areas indicated.

Recovery Methods

With the choice of recovery methods for the different vehicle classes not clearly defined at present, research work for a number of methods should continue. Considerable experience is being gained with parachute and paraglider. Fixed-wing data are being gained from X-15, X-20, and a limited amount of research work now in progress at the Langley Center. Although we have no specific recommendations for research in other methods at this time, studies now in progress may point out additional needs.

Degree of Reusability

The actual benefit of recovery, examinations, and reuse will remain somewhat intangible until we have gained actual recovery experience. The REDSTONE and SATURN S-I recovery programs would have provided this start had they reached fruition. A program of this nature is needed in the near future, possibly in the form of subscale test vehicles, but preferably through recovery of operational vehicles most closely approaching expected future vehicles.

Design For Reusability

Although the design of flight vehicles for reusability and long life has a strong background, rocket engines and related systems have been designed almost exclusively for one-time or short-time usage. A project has been proposed by MSFC, as a part of the FY 63 Launch Vehicle Technology Program, to explore the basic question: In what ways should the design and construction of rocket systems differ from present practice when reuse and extended operating life are intended?

With the combined contributions of studies, experimental work, and, hopefully, some operational recovery experience, the following can be accomplished:

(1) Reduce uncertainties in estimates as to recovery and reusability.

(2) Allow selections from alternative designs and procedures.

(3) Equip ourselves for rapid implementation of a reusable vehicle development at the time a decision is made to do so.

[redacted]

REVIEW OF THE SPACE VEHICLE LANDING AND RECOVERY RESEARCH AT AMES

by W. L. Cook

[redacted]

X65 34335

Introduction

A very limited effort has been directed at manned space vehicle recovery and landing systems at the Ames Research Center. In general, up to this time, most of the wind-tunnel test results have been directed at specific projects of the Manned Spacecraft Center such as the steerable parachute for the Apollo mission and the paraglider development for the Gemini mission. Some work has been done at small-scale of the variation of lifting reentry body shapes to give significant range in the earth's atmosphere and enable horizontal landing capability. In this regard, large-scale wind-tunnel studies are planned of a lifting reentry configuration with an inflatable afterbody and control system for glide and landing. The fourth system which Ames has done some work and plans to do more is in the use of lifting rotors, both rigid and flexible, for deceleration, glide and landing of manned space vehicles.

Discussion

Parachutes. - The tests in the development of the Apollo steerable parachute were conducted in the Ames 40- by 80-foot Wind Tunnel and were primarily directed at determining the extendable flap arrangements for the best lift-to-drag ratio and static stability. A short motion picture film shows how the studies were conducted with a single parachute having an extendable flap for glide path control. The motion picture film is a supplement of TN D-1334. In these studies the extendable flap span was varied from 7 gores to 13 gores and the flap chord was varied from 10 percent to 33 percent of the parachute diameter which resulted in maximum L/D varying from 0.4 to about 0.55. The static longitudinal and directional stability was also measured for a range of conditions of the extendable flaps. The control response characteristics of

letting out and pulling in the flap were measured which indicated that the control response would be instantaneous and the L/D ratios at dynamic conditions could be approximately 40 percent higher than at static conditions. The maximum value L/D ratio was controlled by the stall of the second skirt at the leading edge of the parachute, however, in this condition, the parachute remained very stable.

Wind-tunnel studies of multiple parachutes were also made which are shown in figures 1, 2 and 3. For the case of two side-by-side parachutes with extendable flaps the lift-to-drag ratio obtained was approximately the same as the single parachute of the order of 0.5, however, the dynamic stability was considerably poorer. For the triple parachute with a single pusher as shown in the next slide, the maximum L/D ratio was very low of the order of 0.1 to 0.3 depending on the number of parachutes utilizing extendable flaps for control. The low value of 0.1 was obtained with only the single pusher utilizing the controllable flap. For the case of the double pusher with a triple parachute system the L/D ratio obtained was the same as with the single parachute and the stability of the system appeared fairly good although some small oscillation did occur probably due to the inability to control the yaw.

Future studies are planned with multiple parachutes in the presence of bodies to determine the effect of a large wake on the stability and performance of a cluster system of parachutes.

Paragliders. - Wind-tunnel studies have recently been completed of a half-scale model of the Gemini paraglider landing system. Studies were made for the glide regime, pre-flare, and flare-to-landing as shown in figure 4. Line loads and the normal six component aerodynamic measurements were made for various conditions of pitch attitude, sideslip angle and control variations. Studies were also made in the U-shape first phase of deployment. Motion pictures were shown

to indicate the method used to obtain these results and also show tests where the lines were let out quite rapidly during the last stages of deployment just preceding paraglider gliding flight.

Lift-to-drag ratios of the order of 2.7 to 2.9 were obtained dependent on the configuration. Three-bolt rope settings of 4.1 percent, 8.2 percent and 12.3 percent were studied with the 8.2 percent giving slightly better values of lift-drag ratio than the others. The stability and control of the vehicle appears adequate for glide and landing with possible touchdown speeds of about 45 knots for the full-scale vehicle.

Deployment of the paraglider to the U-shape was attempted, but due to the inadequate tie-down and bolt-rope attachments on the paraglider, the deployment and the inflation of the keel and booms during this phase of the deployment could not be accomplished. The deployment studies are planned to be continued in the near future with improved design and inflation techniques. Several problem areas appear to exist during deployment such as, the length of inflation time and the effects of the body flow on the oscillations of the partially deployed paraglider.

Inflatable afterbody. - A number of wind-tunnel studies have been made of small-scale models at Ames of lifting-body reentry shapes. Some of the tests have been directed at numerous afterbody shapes with control surfaces on the M-1 vehicle for glide and landing as shown for one case in figure 5. At present plans are to conduct large-scale tests of an M-1L configuration with an inflatable afterbody and control surfaces that would be deployed at high subsonic speeds. From the small-scale tests, it appears the maximum lift-to-drag ratios of the order of 4.0 can be obtained and landings with horizontal velocities of the order of 120 knots on runways would be required with a lifting-body type of configuration. Dependent on the success obtained, the

deployment of inflatable afterbodies and control surfaces and their ability to carry the loads and give the required lift-drag ratios and stability and control, further studies would be pursued with inflatable systems applied to obtain low aspect-ratio wing shapes on the lifting body reentry configuration. Deployment of the afterbody at a supersonic Mach number of the order of 2.5 is being considered as well to provide glide ranges of the order of 150 miles.

Lifting rotor. - It is planned at present to conduct wind-tunnel tests of large-scale lifting rotor system for deceleration, glide and landing of a manned space vehicle. Two stages, the deceleration and glide phases are illustrated in figure 6. The intention at present is to conduct studies at deployment and deceleration phases at subsonic speeds where the dynamic pressures at high altitudes are of the same order as can be obtained in the Wind tunnel. During the deceleration, the rotor blades will be operating in the stalled blade state to give high-drag at subsonic tip speeds. The drag forces for deceleration should be controllable thus eliminating high deployment loads and enabling control of the rotor loads and oscillating stresses. Wind-tunnel studies will also be made in the autorative glide state with cyclic control to enable trim at higher lift-to-drag ratios than possible by simply tilting the rotor axis. It is anticipated that lift-to-drag ratios of the order 5 to 6 can be obtained with rotor systems.

During landing, figure 7, the horizontal and vertical velocity components can be made to be essentially zero by conducting a cyclic and collective flare as done by helicopters in autorotative landings. The other method is to conduct a collective flare from a vertical descent configuration. The effect of higher disc loading of this type of rotor system can be offset by tip weights so that flares can be accomplished with little or no vertical velocity at touchdown.

A number of problem areas can exist which should be studies, among these are deployment, operation in the stalled blade state, high rotor tip speeds, flare and landing with high disc loading rotors. Consideration is being given to conducting studies at supersonic speed to determine the effectiveness of a highly coned rotor as a deceleration device to enable autorotative glide to be started at high altitudes and thus enable extensive increases in the useable range.

FIGURE 1.- SIDE BY SIDE

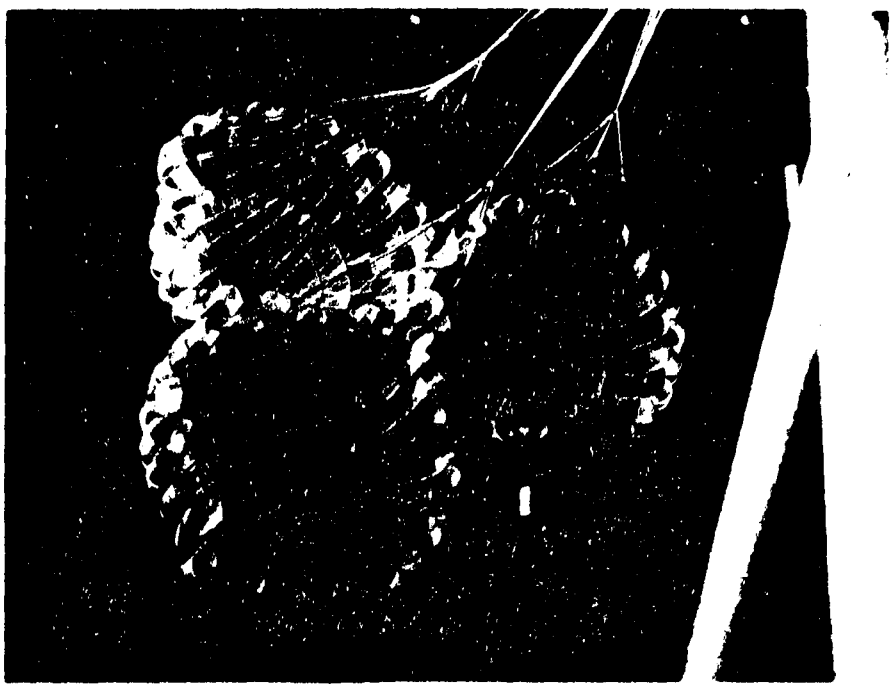

FIGURE 2.- SINGLE PUSHER

A-29455-2

NATIONAL AERONAUTICS AND SPACE ADMINISTRATION
AMES RESEARCH CENTER, MOFFETT FIELD, CALIFORNIA

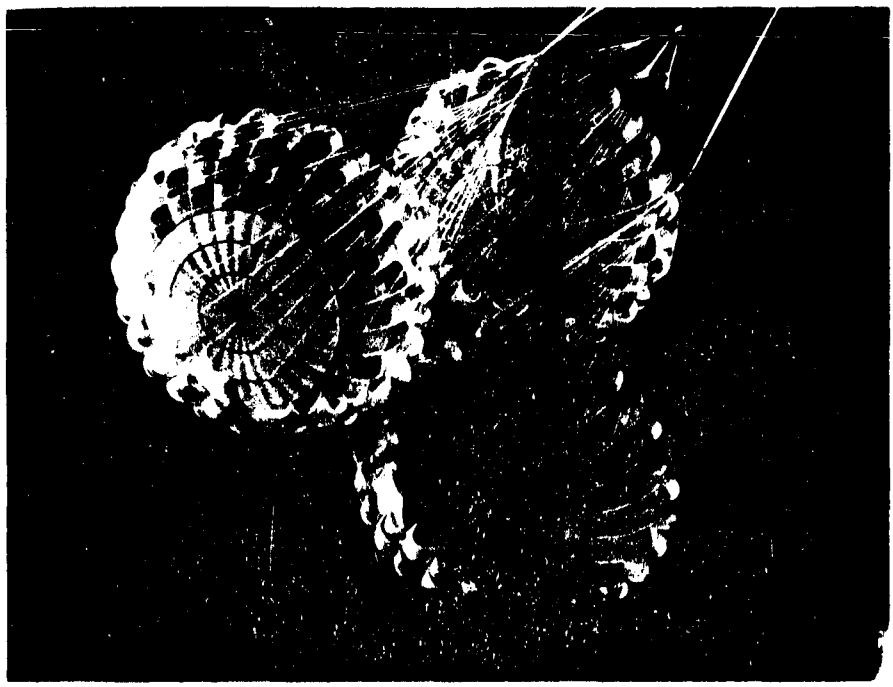

FIGURE 3.- DOUBLE PUSHER

A-29455-3

NATIONAL AERONAUTICS AND SPACE ADMINISTRATION
AMES RESEARCH CENTER, MOFFETT FIELD, CALIFORNIA

DEPLOYMENT AND GLIDE
PARAGLIDER

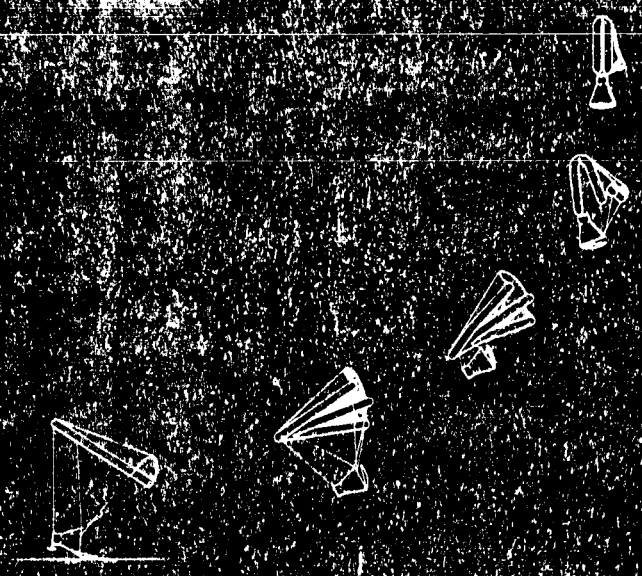

SLIDE 4 FIG

LANDING SYSTEMS

W. COOK
WASHINGTON, D.C.
JULY 10-11, 1962

INFLATABLE AFTERBODY

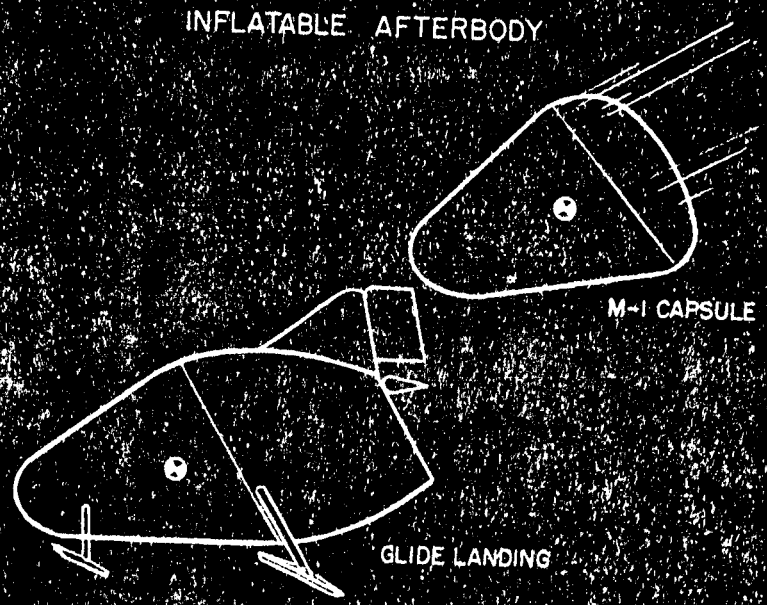

5 LANDING SYSTEMS

W. COOK
WASHINGTON, D.C.

ROTOR LANDING SYSTEM

SLIDE 6 FIG LANDING SYSTEMS

W. COOK
WASHINGTON, D.C.
JULY 10-11, 1962

LANDING MANEUVERS

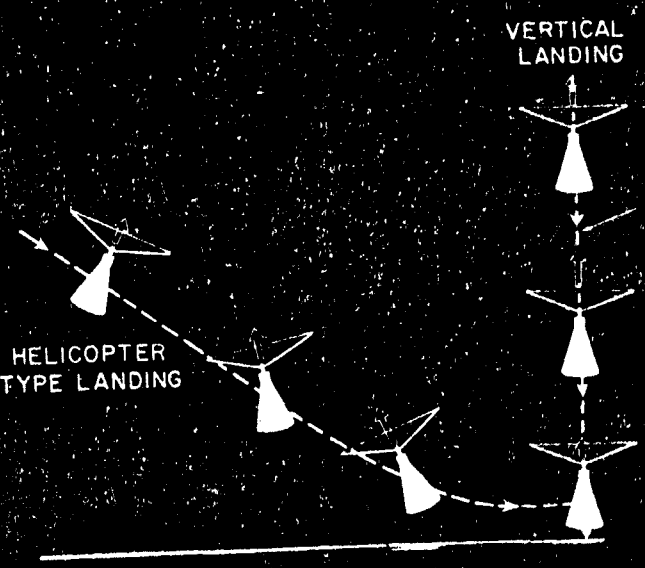

SLIDE 7 FIG LANDING SYSTEMS

W. COOK
WASHINGTON, D.C.
JULY 10-11, 1962

X65 84336

SURVEY OF FRC RECOVERY RESEARCH

By H. M. Drake

Recovery research at FRC has, as indicated in the first chart, been concentrated in the areas of conventional aircraft, drogue parachutes and paragliders. Planned work includes flight tests of lifting-body recovery vehicles and a lunar-landing simulator.

The FRC research on landing of conventional aircraft will not be discussed here since it has been adequate reported in references 1 through 7. This work is continuing.

The FRC has completed development and proof tests of two drogue chute systems, one for the Mercury capsule and the second for the B-58 escape capsule. Both programs utilized the F-104A airplane which is capable of launching up to 1500 pounds weight at Mach numbers up to 2 at altitudes between 30,000 and 50,000 feet. It can zoom, as shown in the second figure, to release the store at altitudes as high as 85,000 feet, but at lower speeds. The test conditions for the Mercury drogue are shown on the third chart and the test results are reported in reference 8. The B-58 escape capsule tests involved releases of a 630 pound capsule at a Mach number of 2.02 and altitudes of 45,000 and 31,000 feet. The maximum q for these tests was 1690 pounds per square foot. Tests were also performed at altitudes as low as 18,000 feet and a Mach number of 1.25. At present, no further drogue tests are planned.

Although not the subject of the meeting, a brief description might be given of the planned lifting-body program. The lifting-body program at FRC will be initiated by the construction of several lightweight, full-scale man-carrying glider vehicles. These vehicles will have configurations which high-speed tunnel tests have indicated to be attractive for reentry. Configurations such as the M2B, lanticular, and M-1-L are being considered. The low speed and landing characteristics of these lightweight (W/S 4-7 lb/sq ft) vehicles will be investigated in free flight following release from airplane tow. Later phases include the construction and tests of full-scale wing-loading vehicles of the more promising configurations. Tests at higher speeds with these heavyweight configurations may be performed.

A word might be said here regarding the capabilities of launch vehicles at the FRC. The capabilities of the F-104A have been mentioned. This airplane is also capble of launching rockets of up to 1500 pounds weight at up to 90° climb angle, see reference 9. Two B-52 aircraft are also available, which are used for launching X-15 aircraft. These B-52 aircraft are capable of launching stores of up to 35,000 pounds weight and approximately 10 feet in diameter. The launch-altitude capability extends to about 50,000 feet; the speed capability is about 0.8 Mach number. In addition to the F-104A and B-52 capability, an A3J has been requested for FRC for another program. This airplane could launch stores of up to 5,000 pounds at the same conditions as the F-104A.

Mr. Horton will discuss the current FRC paraglider program.

REFERENCES

1. Stillwell, W. H.: Results of Measurements Made During the Approach and Landing of Seven High-Speed Research Airplanes. NACA RM H54K24, 1955.

2. Matranga, G. J., and Armstrong, N. A.: Approach and Landing Investigation at Lift-Drag Ratios of 2 to 4 Utilizing a Straight-Wing Fighter Airplane. NASA TM X-31, 1959.

3. Matranga, G. J., and Menard, J. A.: Approach and Landing Investigation at Lift-Drag Ratios of 3 to 4 Utilizing a Delta-Wing Interceptor Airplane. NASA TM X-125, 1959.

4. Weil, J., and Matranga, G. J.: Review of Techniques Applicable to the Recovery of Lifting Hypervelocity Vehicle. NASA TM X-334, 1960.

5. Matranga, G. J.: Analysis of X-15 Landing Approach and Flare Characteristics Determined From the First 30 Flights. NASA TN D-1057, 1961.

6. White, R. M., Robinson, G. L., and Matranga, G. J.: Resume of Handling Qualities. NASA TM X-715, 1961.

7. Matranga, G. J., Dana, W. H., and Armstrong, N. A.: Flight-Simulated Off-The-Pad Escape and Landing Maneuvers for a Vertically-Launched Hypersonic Glider. NASA TM X-637, 1962.

8. Johnson, C. T.: Investigation of the Characteristics of 6-foot Drogue-Stabilization Ribbon Parachutes at High Altitudes and Low Supersonic Speeds. NASA TM X-448, 1960.

9. Horton, V. W., and Messing, W. E.: Some Operational Aspects of the use of Aircraft for Launching Solid-Fuel Sounding Rockets. Proposed NASA TN D-1279, 1962.

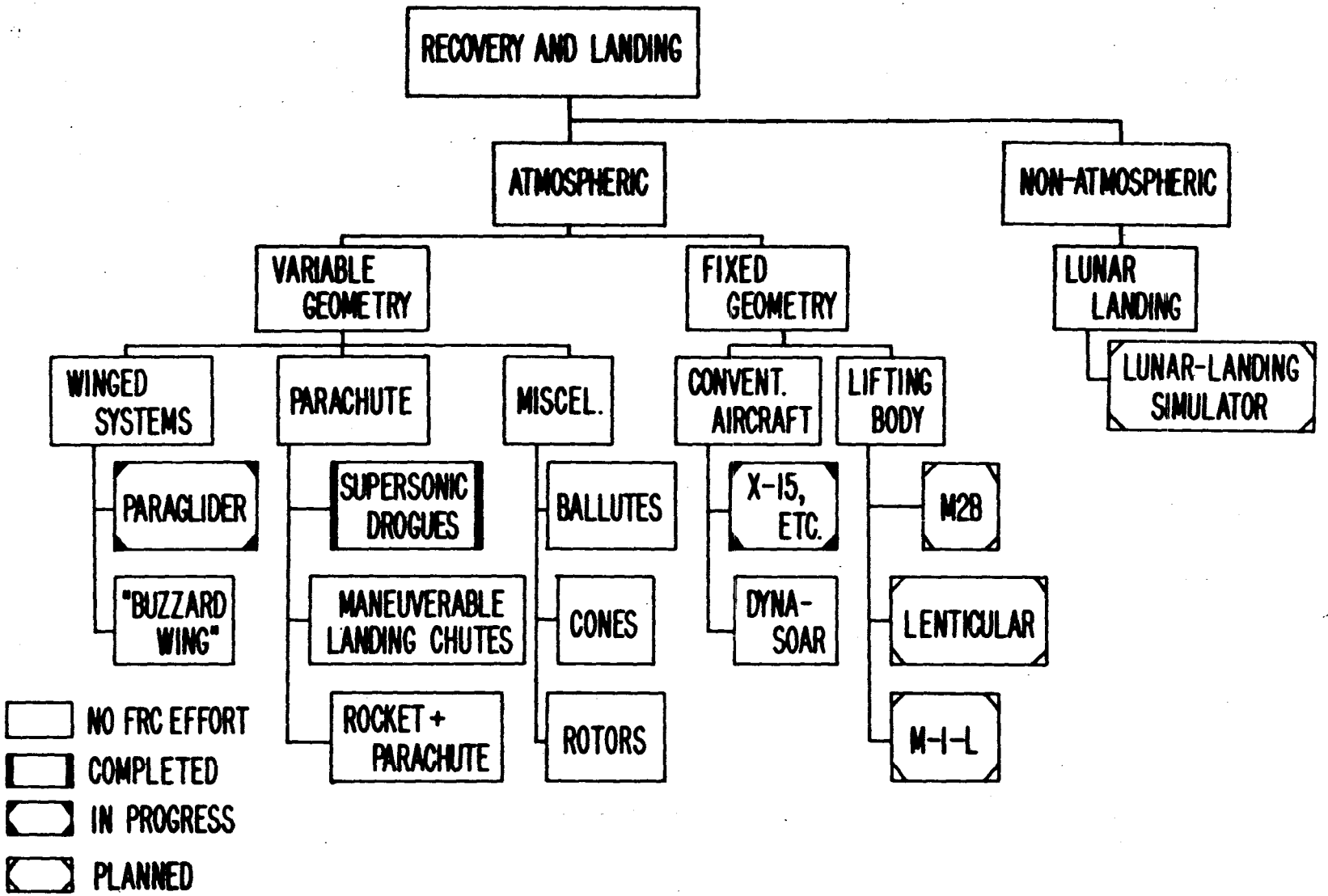
RECOVERY AND LANDING
ATMOSPHERIC
NON-ATMOSPHERIC
VARIABLE GEOMETRY
FIXED GEOMETRY
LUNAR LANDING
WINGED SYSTEMS
PARACHUTE
MISCEL.
CONVENT. AIRCRAFT
LIFTING BODY
LUNAR-LANDING SIMULATOR
PARAGLIDER
"BUZZARD WING"
SUPERSONIC DROGUES
MANEUVERABLE LANDING CHUTES
ROCKET + PARACHUTE
BALLUTES
CONES
ROTORS
X-15, ETC.
DYNA-SOAR
M2B
LENTICULAR
M-1-L
NO FRC EFFORT
COMPLETED
IN PROGRESS
PLANNED

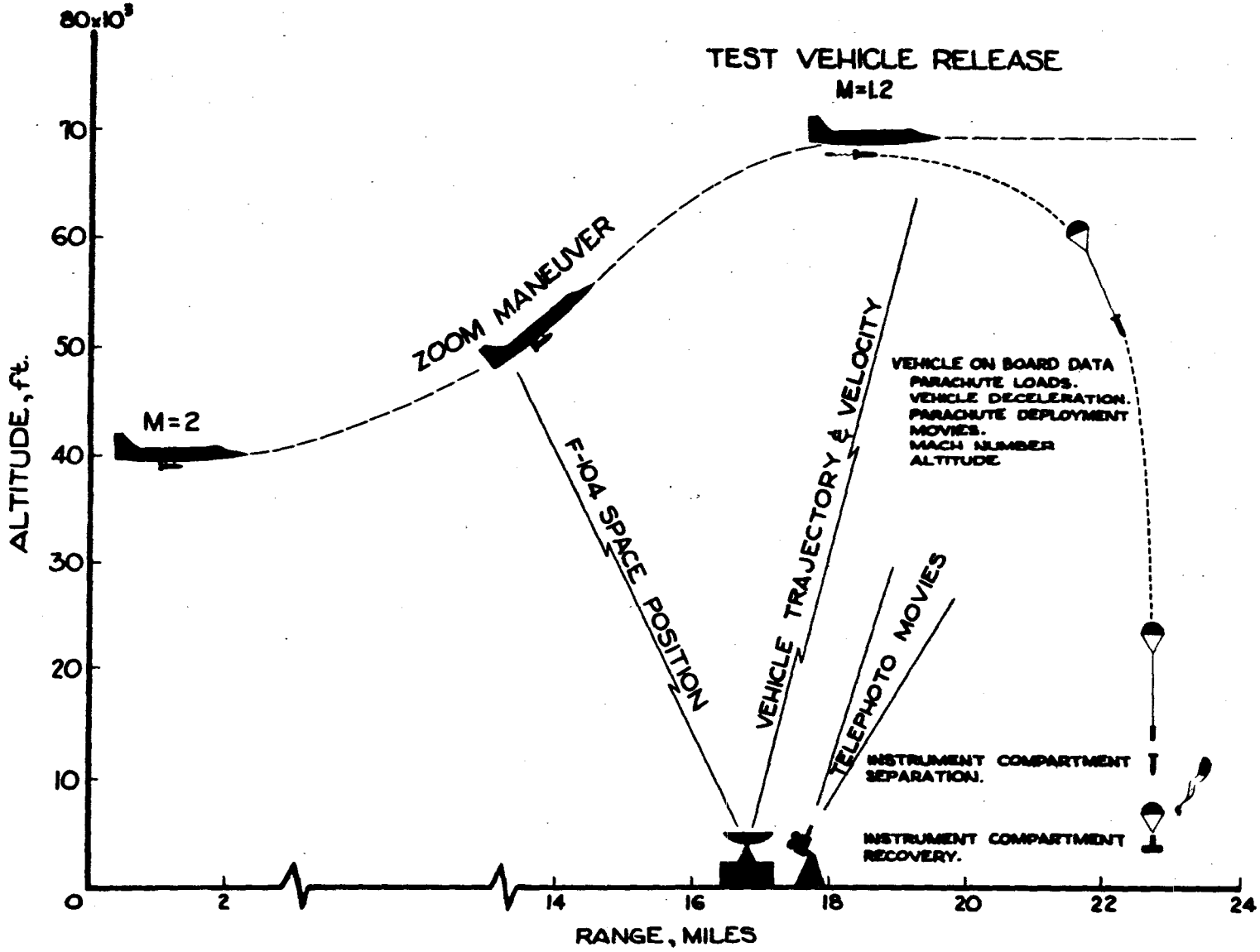
80x10³
70
60
50
40
30
20
10
0
ALTITUDE, ft.
TEST VEHICLE RELEASE
M=1.2
ZOOM MANEUVER
M=2
F-104 SPACE POSITION
VEHICLE TRAJECTORY & VELOCITY
TELEPHOTO MOVIES
VEHICLE ON BOARD DATA
PARACHUTE LOADS.
VEHICLE DECELERATION.
PARACHUTE DEPLOYMENT
MOVIES.
MACH NUMBER
ALTITUDE
INSTRUMENT COMPARTMENT
SEPARATION.
INSTRUMENT COMPARTMENT
RECOVERY.
2
14
16
18
20
22
24
RANGE, MILES

6 FT. DROGUE PARACHUTE TESTS

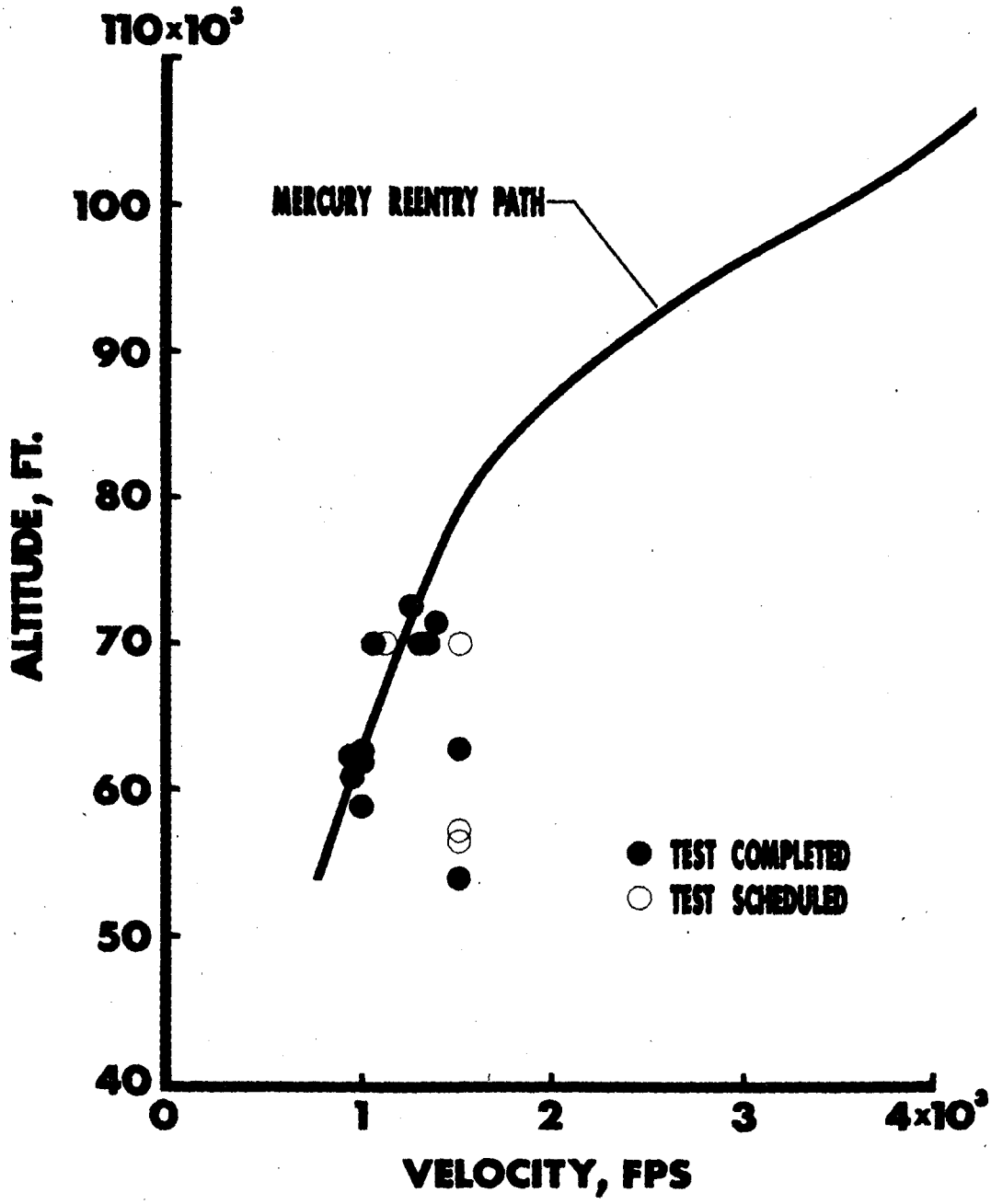

[redacted]

MANNED PARAGLIDER FLIGHT TESTS

By

Victor W. Horton

[redacted]

The current interest in utilizing the paraglider concept as a means of effecting a soft landing for the Gemini capsule prompted the Flight Research Center to design and construct a manned paraglider vehicle with which to conduct a limited, qualitative research program. This vehicle differs from paragliders that individuals, Langley Research Center and the Ryan Aircraft Company have flown in that it is manned, unpowered and towed aloft for release like the conventional glider.

The primary objective of the FRC flight test program is to demonstrate the approach, flare and landing capability of a paraglider vehicle with a high wing loading (W/S = 7 psf) and a low L/D (L/D = 2.5).

To meet this objective, the Paraglider Research Vehicle, PARESEV-1, was constructed in a manner to provide the maximum information in the shortest time. As you can see from the slide - (Slide of PARESEV-1) the design was simple and allowed for quick modifications if necessary.

Comments:
- Wing Sweep Angle 45°
- Fabric Plan Form 50°
- Area = 150 square feet
- Fabric -- Doped Irish Linen
- Battens -- 2/side
- Rigid control linkage
- W/S = 3.55
- Control available α 25° ± 10° lateral = ± 15°
- Two tow points -- high and low, no noticeable difference so chose low one
- Wing attach point -- 47.5% of keel aft of apex
- Communications -- FM radio
- Foot pedals for nose wheel steering only

Automobile powered tows up to heights of 200 feet and airplane powered tows to altitudes of 2500 feet were made with PARESEV-1. Satisfactory landings were made from free-flight with estimated sink rates of 2-4 fps at touchdown attained. The rod control system has its inadequacies,

however, due to flexibility in the system there was considerable response lag and some question as to whether or not the amount of stick displacement corresponded to the proper amount of input to the wing. This, plus the inherent problems of being towed, resulted in major damage to the vehicle during checkout of a new pilot. I might add that the pilot was not injured during this incident.

The craft was rebuilt and considerably modified to incorporate a cable and pulley control system and better shock attenuation in the landing gear as seen from the next slide. (Slide of PARESEV-1A).

Comments: Wing Sweep Angle 45°
Fabric Plan Form 50°
Area = 150 square feet
Fabric -- 6 oz. unsealed dacron
Battens -- 5/side
Cable and Pulley Control system
W/S = 4.25
Control available α 25° ± 10° lateral=± 7.5°
Pivot Point = 47.5% aft of apex
Communications -- VHF radio
Foot pedals for nose wheel steering only

This control system eliminated the slow response in that the response is now governed by the pilot's ability to overcome the inertia forces.

To date, PARESEV-1A has been flown numerous times by 4 different pilots of varying backgrounds and experience, and the general concensus is that the craft maneuvers and handles quite well at a W/S of 4.25 and a L/D maximum of 3.8.

At the present time, flight testing is being conducted at a W/S of 6.3 and an estimated L/D of 2.9. This change in W/S and L/D was accomplished by decreasing the wing area from 150 square feet to 100 square feet.

To obtain the end W/S value of 7.0, the present plans are that additional weight will be added to the undercarriage.

Flight data have been obtained on PARESEV-1A and is presented on the next slide. (Slide of Longitudinal Performance of PARESEV-1A).

Data points were obtained during stabilized glide by a relatively simple method. Altitude callouts were timed by stopwatch during descents of 2000' or more at constant airspeed. Angle of attack was obtained by measurement of wing incidence angle relative to fuselage and fuselage inclination (attitude). V_v with this wing varied from 16 to 33 fps with γ's of 14.5 to 21.5° in the IAS range investigated higher airspeeds were not investigated due to high stick force.

The next slide (slide of Predicted Longitudinal Performance of PARESEV-1B) shows the predicted performance of the PARESEV vehicle with a 100 square foot installed. Our designation for this vehicle is PARESEV-1B. Some preliminary results indicate an L/D of less than 3 between glide speeds of 50 and 60 KIAS.

The last slide (slide of Control-System Force Gradients) shows a non-dimensional stick force plot against IAS. As indicated, the forces increase rapidly with deviations from trim airspeed. The upper dotted line shows how the force curve can be shifted by moving the pivot point forward of the cp. This could be done in flight, however, our vehicle requires ground adjustment prior to flight. The curve can be shifted downward into the push force region by moving the pivot point behind the cp. Push forces, however, were not considered desirable due to an apparent reduction in longitudinal stability. Bolt rope can also be used to adjust the pivot point-cp relationship. Increase in percent of bolt rope used moves wing cp aft.

Stick position versus IAS is not shown, but is approximately linear and normal.

The wing appears in flight to be exceptionally stable and not appreciably effected by rapid control inputs or turbulence. The lower fuselage response, however, is noticeable to the pilot and similar to helicopters, in that lateral and longitudinal motions involve linear accelerations rather than angular accelerations. Because of this it would seem that some stability of the lower fuselage or payload about the a.c. of the vehicle would be desirable for our vehicle and could be included in the design, such as a membrane between forward and aft keel cables to improve zero damping.

Response to a control input is first noted by the undercarriage moving, followed by total vehicle motion.

The vehicle possesses longitudinal stick fixed static stability. Longitudinal motions are highly damped in this condition.

The vehicle does not possess longitudinal stick force stability, hence dynamic motions have not been investigated.

In the stick fixed case, the lateral and directional modes are statically stable and the dynamic motions are lightly damped.

Oscillations have only been encountered as a result of external stimuli (turbulence or tow rope) and result in coupled lateral-direct lower fuselage responses. Higher magnitude turbulence has induced coupled motions about all three axis.

More than 70 landings have been made from stabilized free flight conditions. About 40 were from release altitudes of 100 to 300' and 30 from releases above 1000'. Only one landing resulted in structural damage and this was due to flare being initiated at approximately the IAS for L/D maximum with the 100 foot wing. All other landings have been accomplished with less than 10 fps vertical velocity at touchdown and 75% of those are estimated at less than 5 fps by the pilot and observers. To achieve a satisfactory flare, about 10-12 kts. above the IAS for L/D maximum must be obtained prior to flare initiation. L/D maximum for large wing occurs at approximately 42KIAS and IAS used prior to flare initiation was 50 to 55 KIAS. For small wing, IAS for L/D maximum is estimated at 48 KIAS and successful flare have been accomplished starting from 60 to 65 KIAS. Excess energy is used to adjust flare rate during flare or to adjust altitude (second flare) after achieving zero vertical velocity. Approximately 3 seconds elapse from flare initiation to touchdown. Only visual perception of closing rate with labeled surface has been used to determine flare initiation point.

Towing the PARESEV is not a real problem but does require pilot familiarization with tow line dynamics.

Under the present plans, due to manpower requirements for other projects, the PARESEV program will be terminated after the flight data are obtained with the PARESEV-1B configuration. However, if problems arise in specific areas where the PARESEV could be of benefit, the project would be revived. I might add that the knowledge gained from short-term, relatively inexpensive test programs of this nature cannot be over-estimated.

LONGITUDINAL PERFORMANCE OF PARESEV IA

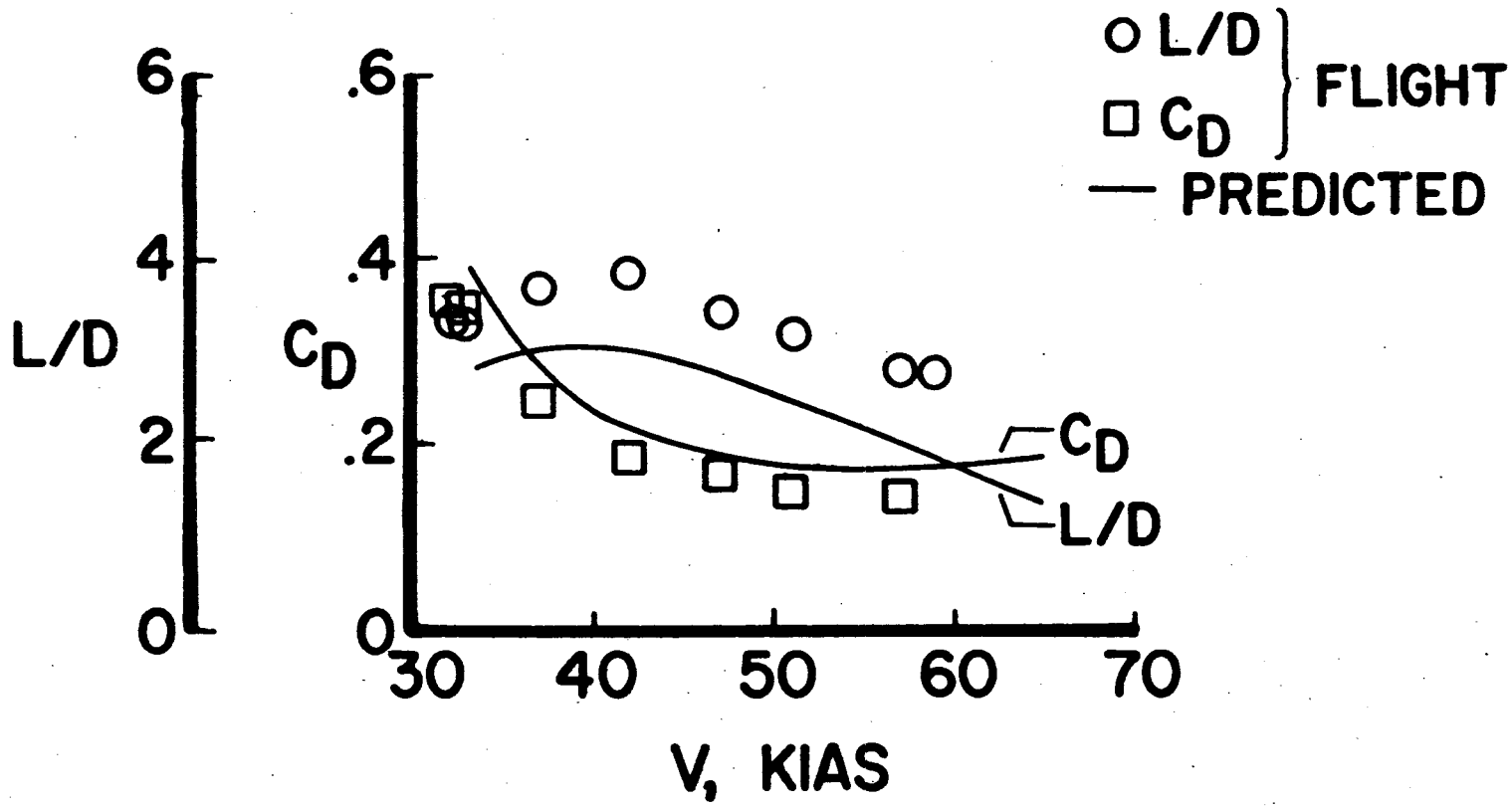

PREDICTED LONGITUDINAL PERFORMANCE OF PARESEV IB

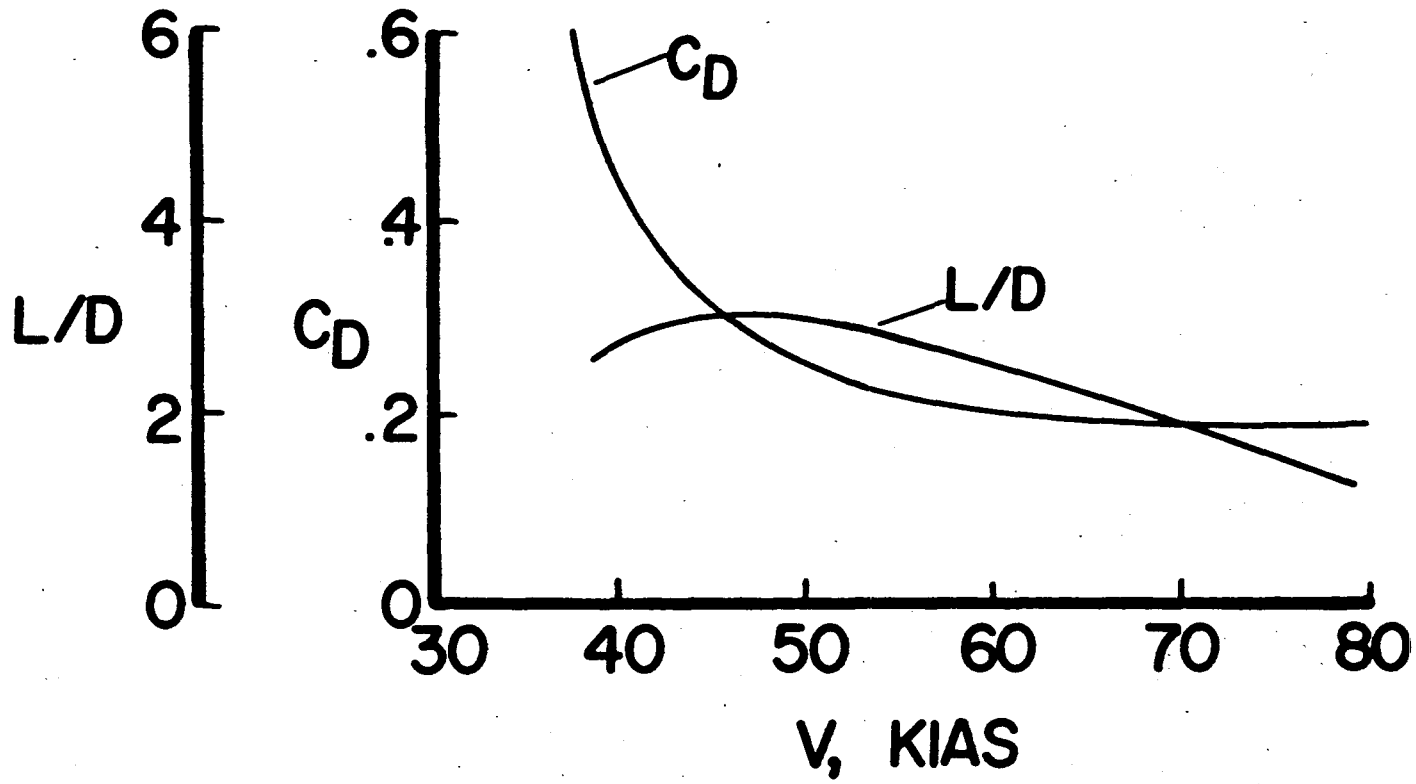

CONTROL-SYSTEM FORCE GRADIENTS

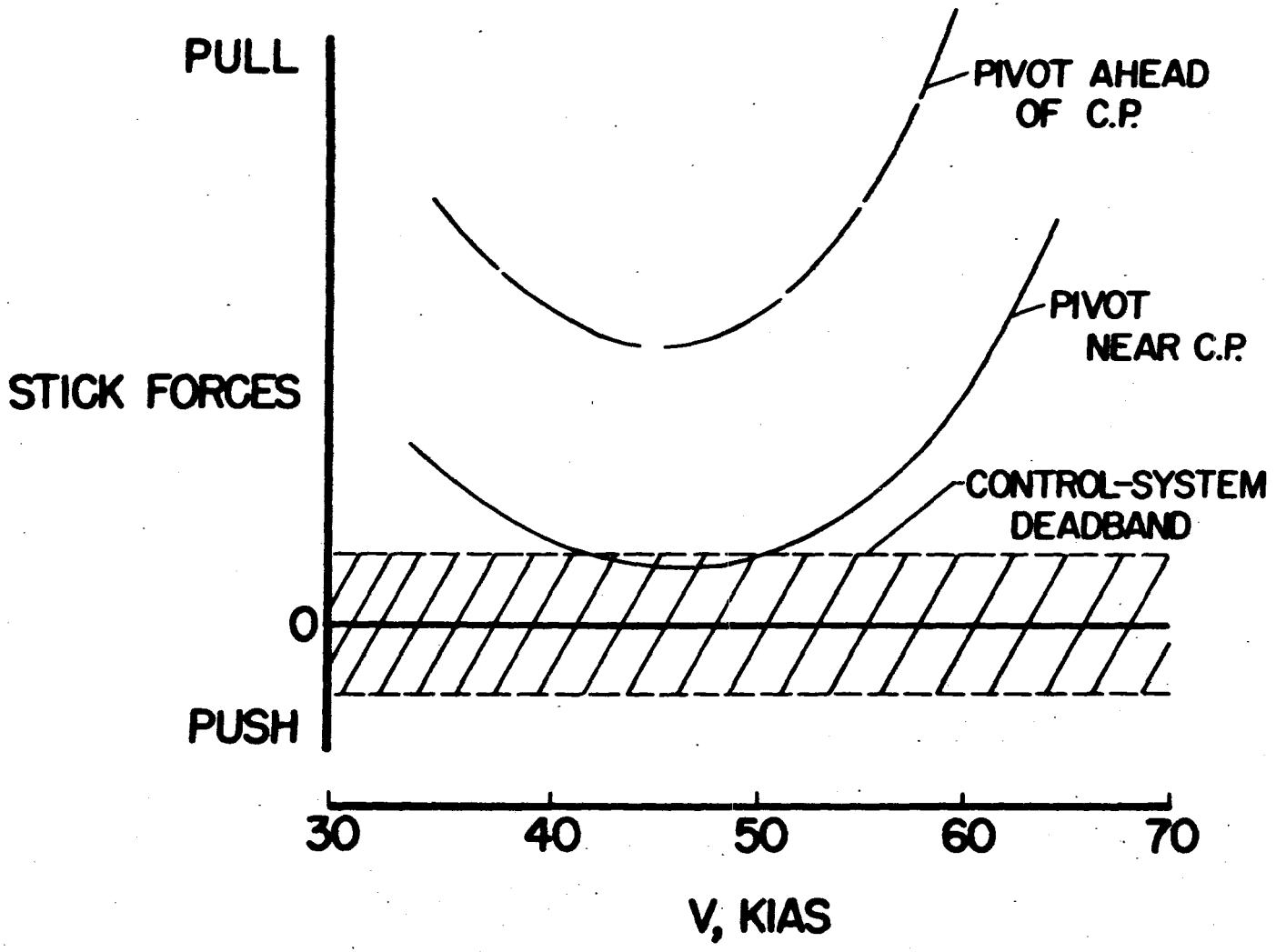

PARAGLIDER RESEARCH VEHICLE I

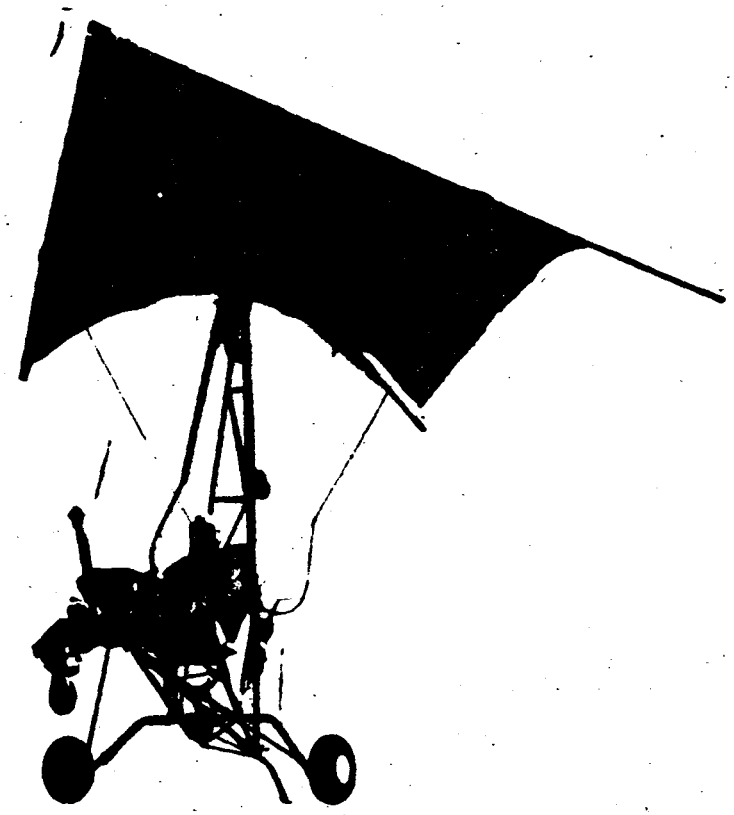

PARAGLIDER RESEARCH VEHICLE IA

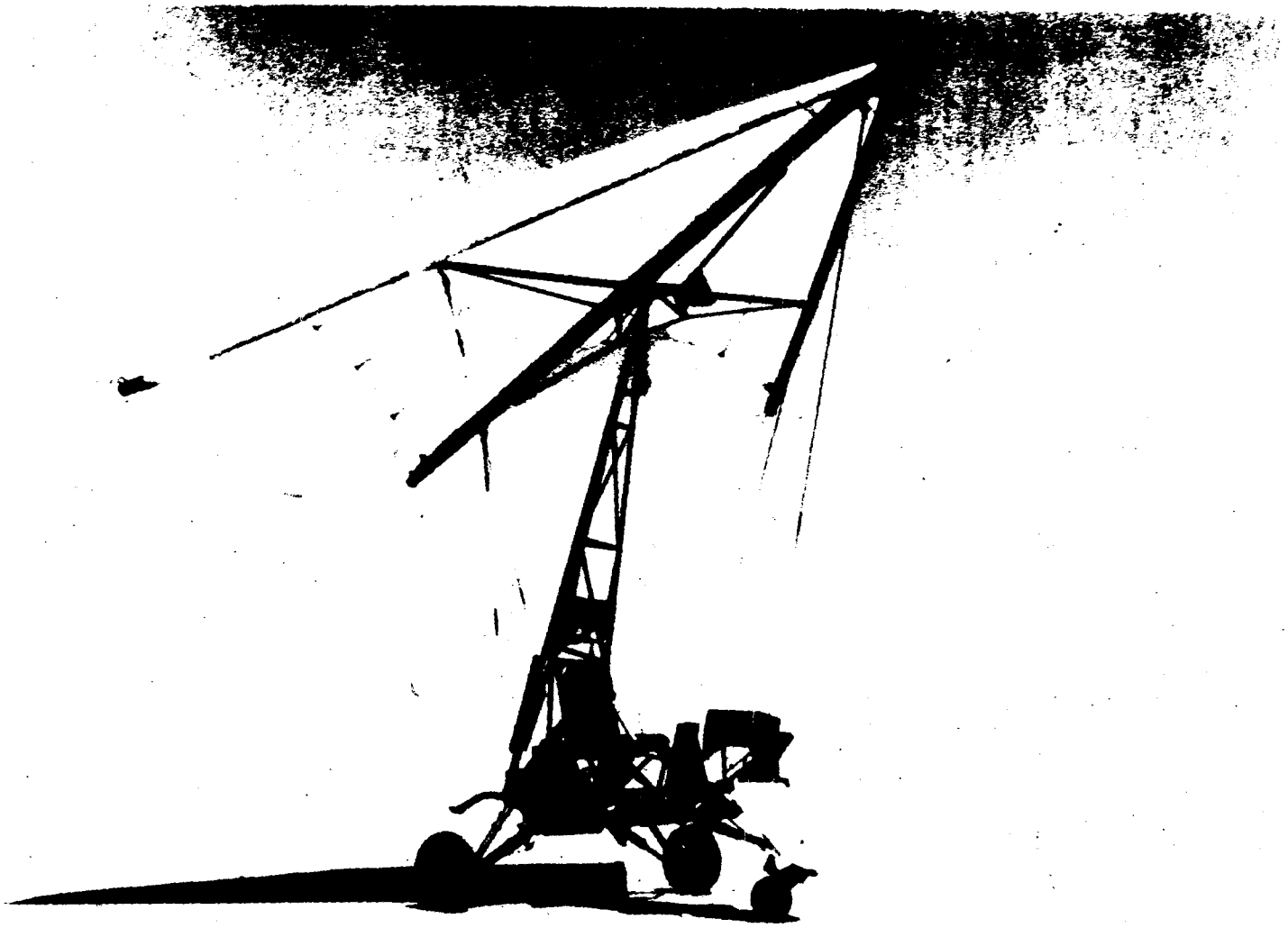

[redacted]

X65 84338

GEMINI LANDING AND RECOVERY SYSTEMS *

R. Rose
MSC

Mr. Rose indicated that the Gemini project has the following requirements for a landing system:

a) zero vertical velocity
b) controlled descent with up-wind capability
c) acceleration and forces at touch down in a known direction
d) minimum volume and light weight
e) water or land recovery capability
f) landing device (paraglider with parachute back-up) must not hold up Gemini schedule

Under the restraints noted above, the Gemini project office has concluded that the paraglider is the most feasible device for recovery.

Operation characteristics of the inflatable paraglider are as follows:

deployment at 55,000 ft with a q = 40 lbs/sq ft

a glide angle of -17.5° with a forward velocity of 68 fps and a sink rate of 21 fps

a pre-flare angle of attack of -1.5° with a forward velocity of 68 fps and a sink rate of 21 fps. Altitude for this maneuver is 390 feet.

At a flare altitude of 45 feet, the angle of attack is 8° with an increased forward velocity and sink rate of 96 fps and 35 fps respectively. Touch-down forward velocity is 68 fps with a vertical velocity ranging from 0 - 5 fps. Design studies indicate the 510-lb paraglider has a down-range capability of 21 NM and an up-range capability of 16 NM from 40,000 feet altitude in still air.

* Based on notes taken during presentation of paper.

PRESENTATION TO NASA HEADQUARTERS
LANDING AND IMPACT SYSTEMS

[redacted]

X65 84339

INTRODUCTION

Manned spacecraft with a blunt, lifting body configuration, such as the Mercury, Gemini, and Apollo spacecraft, require an auxiliary landing system for successful completion of the mission and safe return of the crew. Landing systems with widely varied performance characteristics are presently available or in various stages of development. The primary consideration in selection of a landing system for a particular space vehicle and mission is crew safety, or system reliability. Beyond reliability, the mission terminal flight plan will dictate the required landing system performance. For example, if the normal mission terminates with impact in water or an unprepared land surface, a near vertical terminal descent is preferable. Landing on a prepared land surface, on the other hand, leads itself to an aircraft type flared landing. A degree of gliding or range control then becomes necessary to insure landing on a prepared surface. (This does not necessarily mean that even with range capability the best method of landing is horizontally). The impact shock attenuation requirements are likewise predicated on the type landing system selected. Basically impact systems can be broken down into two required types; one for high vertical rate of descent with wind drift considerations, the other for lower vertical rate of descent with a horizontal velocity. Basic considerations such as weight, volume, deployment, stability, control, redundancy, and/or emergency escape, and complexity must also be evaluated in selecting a landing system for a particular vehicle.

APOLLO

1. The Apollo is one of the two Manned Spacecraft Center spacecraft presently under development. The Apollo landing system requirements are generally as follows:

a. A high degree of reliability, and a system that can be used under all flight conditions for earth landing requirements. This includes normal reentry, maximum dynamic pressure escape, and pad abort.

b. Stabilizes the Command Module during post-entry descent and reduces the vertical landing velocity to 30'/sec at 5000' altitude. Horizontal drift due to wind not to exceed 30 knots.

c. Reduces impact accelerations such that neither the Command Module structure or flotation is impared. Further attenuations to be by crew seat shock attenuation devices.

d. System to be compatible with the use of a moderate L/D terminal landing system such as a Parawing (this requirement was later deleted date May 16, 1962).

1. The system selection by MSC to most nearly fit the established requirements is as follows:

a. Descent System

(1) System selection criteria

The advantages and disadvantages for the selection of a cluster of three parachutes are shown in slide 1. The advantages of a parachute cluster are as follows: it is within the state-of-the-art, provides excellent pendulum stability, provides a high degree of reliability, very low weight and volume, is an easy way of obtaining redundancy, and it is a passive system. The only major disadvantages of a cluster is that it is nonmaneuverable. For Apollo, the use of a single parachute would have required that it have a diameter of approximately 127'. Present state-of-the-art in parachutes have determined test parachutes of this size are difficult to fabricate. Large parachutes also present a packing and installation problem. To provide redundancy, this would have also resulted in a heavier landing system and requiring more volume than the selected cluster arrangement.

(2) Deployment sequence

Slides 2 and 3 depict the deployment sequence for the Apollo earth landing system. The sequence of events are the aft section of the Command Module is jettisoned, a 13' diameter drogue chute is mortar deployed, the drogue chute is jettisoned at a predetermined altitude and the three main parachutes are deployed by mortar deploying pilot parachutes. The pilot parachutes then in turn pull the extraction chutes which deploy the main parachutes. The main parachutes are reefed for a period of six seconds prior to full inflation.

(3) Test program

The Apollo earth landing system will be tested at El Centro, California. The test will be conducted utilizing a B-66, C-130 and C-133A aircraft. The B-66 aircraft will be utilized in testing the drogue parachutes. The C-130 and 133A will be utilized in testing the single main parachute and the complete earth landing system. The present status of the Apollo test program is that 3 tests have been conducted on a single 88' diameter parachute to establish optimum parachute reefing parameters. It is anticipated that approximately 70 tests will be required for the development and qualification of the earth landing system. The parachute system flight envelope is probably best described at this point.

Graph No. 1 gives the drogue parachute design envelope and is self explanatory. Normal drogue parachute deployment is initiated at 25,000 feet. At a dynamic pressure of 140 psf, the Command Module is stabilized with the drogue chute descending to an altitude of 15,000 feet, where the main chute's deployment sequence is initiated at a dynamic pressure of 64 psf. The drogue parachute has been designed to be capable of deployment at a q of 210 psf and at any altitude from 3500 ft to 25,000 ft. In the case of "pad abort", the drogue chute can also be deployed through this same altitude range at a minimum dynamic pressure of 10 psf. Graph No. 2 shows the design envelope of the main parachutes. The main parachutes have been designed to be capable of being deployed at a maximum dynamic pressure of 96 psf at any altitude from 3500 to 15,000 ft and likewise, they are capable of being deployed at a minimum dynamic pressure of 10 psf. This low dynamic pressure could be encountered in the case of a "pad abort". There are some problem areas with this earth landing system which are anticipated although are not considered to be major obstacles to overcome. These problem areas are (1) the mortar deploying of all three main parachutes and (2) the effects of a malfunction of a single parachute on the other two parachutes.

b. Impact System

(1) System description

Slide 3 depicts the capsule impact attenuation system. This consists of 6 air oil struts for vertical attenuation and 8 aluminum honeycomb double acting struts for horizontal attenuation. The oil used in the air oil strut is Oranite 8515. The total stroke of the air oil strut is approximately 12". The aluminum honeycomb strut has a stroke of approximately 4".

Slide 4 shows the attenuation system used for the individual crew seats. This consists of 4 honeycomb shock struts for vertical loads, two honeycomb struts for horizontal loads and two honeycomb struts across the chest. The aluminum honeycomb struts are designed to control the "g" buildup.

(2) Design consideration

The known safe human tolerances are shown on graph no. 3. This impact attenuation system is designed for the following nominal conditions which are within the safe zone.

3 chutes out - vertical rate of descent 23 fps
horizontal rate of drift 30 fps
Max slope of 5° at impact
Allows 20 g's vertically; 10 g's horizontally at 250 g's/second.

Design emergency conditions:

2 chutes vertical rate of descent 30 fps
horizontal rate of drift 50 fps
Max slope of 15° at impact
Allows 40 g's vertically; 10 g's horizontally

(3) Test program

Present plans call for impact tests utilizing a full scale boilerplate Command Module. These tests will be conducted at NAA on a test rig presently under construction. This rig will not be available until probably January 1, 1963.

To reduce the number of boilerplate impact tests, a 1/4 elastically scaled model program will soon start at LRC. This model has a scale strength heat shield and strut attenuation system. This model will be tested on sand, hard surface, and water to determine the dynamics and acceleration loads.

The difficulty with an active system is the somewhat lower reliability because of the operation of additional mechanisms which have to be employed in releasing the heat shield.

Another problem would be the necessity to choose between having a deployed or nondeployed impact system when landing in water. For instance, with the proposed Apollo system, there is a great possibility that the heat shield, if deployed, may dig into the water causing severe capsule motions.

CURRENT ADVANCED LANDING SYSTEMS STUDIES

1. At this point some of the programs which are presently being conducted by Manned Spacecraft Center in support of both future spacecraft and Apollo should be described.

2. The first program is the development of a parachute known as the Glide-sail. This program is being accomplished by Northrop Ventura and has as a primary objective, the development of a gliding parachute having an L/D of approximately 0.7 to 1 and which can also be controlled directionally.

3. It is realized that the performance goals for a parachute of this nature would not provide a range capability but would allow avoidance of local obstacles and partially alleviate the impact attenuation problem by being able to overcome wind drift. The present status of this program is as follows: A wind tunnel test program has been completed by Ames Research Center using 18' diameter parachutes in the 40' x 80' wind tunnel; the results of the wind tunnel program have been verified by drop tests of both 63' diameter single and 3 chute

[illegible] El Centro, California; preliminary drop test data have verified the wind tunnel results which indicated a maximum L/D of approximately .5 to .7. This program is scheduled for completion in early October.

4. The second program consists of an in-house development of a similar glidesail parachute for descent and incorporating a landing rocket for attenuation. Air drop tests of the parachute, without the landing rocket, and static firings of the rocket motor have been completed. The results of these tests have shown the feasibility of a controllable parachute retro rocket earth landing system; therefore, air drop tests of the complete system utilizing a C-119 airplane will be conducted at Houston in the near future.

5. A third program is the development of a deployment technique for the Paraglider. A review of all the work being accomplished on Paragliders, indicated paraglider deployment was one of the major problems to be solved before it could be used as an earth landing system. A joint program with LRC has been initiated to investigate paraglider deployment. Langley will conduct the tests using the 19' transonic tunnel utilizing elastically and dynamicscale models. It is believed this program can contribute significantly to developing a satisfactory means of paraglider deployment.

FUTURE PROGRAMS

1. The Landing and Impact Systems Section have a number of future programs planned which cover various areas that are not presently being investigated. These programs are:

a. The development of a chute with an L/D greater than one.

b. The development of a landing rocket for attenuation of Apollo size spacecraft.

c. The development of large single parachutes capable of recovering spacecraft weighing 10,000 pounds.

d. Development of drogue parachutes in sizes approximately 14 to 16' in diameter which can be deployed at Mach numbers up to 2 at an altitude of 80,000 feet.

e. Investigate the feasibility of ejection seats for spacecraft.

f. The development of an altitude sensor to be used in conjunction with the landing rocket.

g. The study of soils as they apply to impact attenuation and its effect on the dynamics of the spacecraft.

h. The development of a rotor landing system.

4. The programs are readily understood, however, a few comments are pertinent relative to the last program pertaining to rotors.

5. LRC as well as the other NASA centers have programs investigating every facet of the parawing and the parachute. Little or nothing has been accomplished on rotors, however, theoretically, from a performance standpoint, the rotor system can provide a touchdown capability of near 0 vertical and horizontal velocity. It is intended that this program be accomplished as a joint effort with the Ames Research Center.

RECOMMENDATIONS

1. It is interesting to note the number of NASA centers which are represented and the general interest which is now being shown in landing systems. The problem of developing any earth landing system is a mammoth one and requires the complete cooperation of all the NASA organizations. It appears that a landing system committee should be established with a possible member from each center and headed by a representative from NASA Headquarters. In this manner, duplication of effort could be avoided. This, in turn, would reduce new landing system development time and cost.

2. I do not know what is the best landing system. It is certain that parachutes for the time being are the most reliable and probably the best known. There is considerable effort being expended in the development of the parawing, however, NASA needs to look toward the future and develop some other system that would overcome the deficiencies of the parawing and the parachute. The selection of such a system probably could best be accomplished by this proposed committee.

PARACHUTE SYSTEM

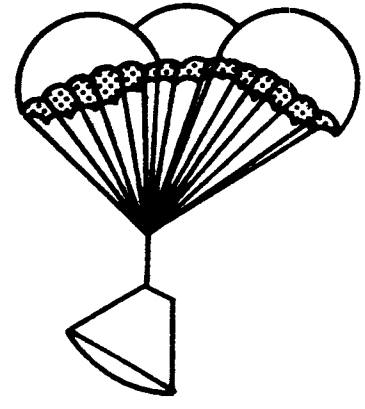

CLUSTER

PRO

STATE OF THE ART
PENDULUM STABILITY
RELIABILITY
LOW WEIGHT & VOLUMN
REDUNDANT
PASSIVE

CON

NON-MANEUVERABLE

NASA -MSC J. KIKER 6JULY62 S-150-7

APOLLO LANDING SYSTEM

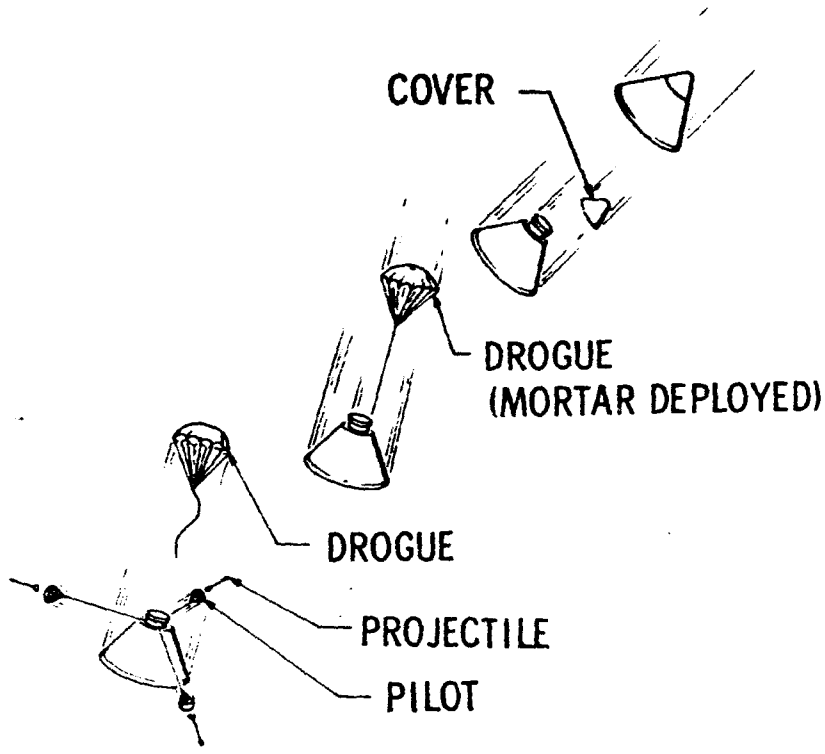

NASA -MSC J. KIKER 6JULY62 S-150-3

APOLLO LANDING SYSTEM

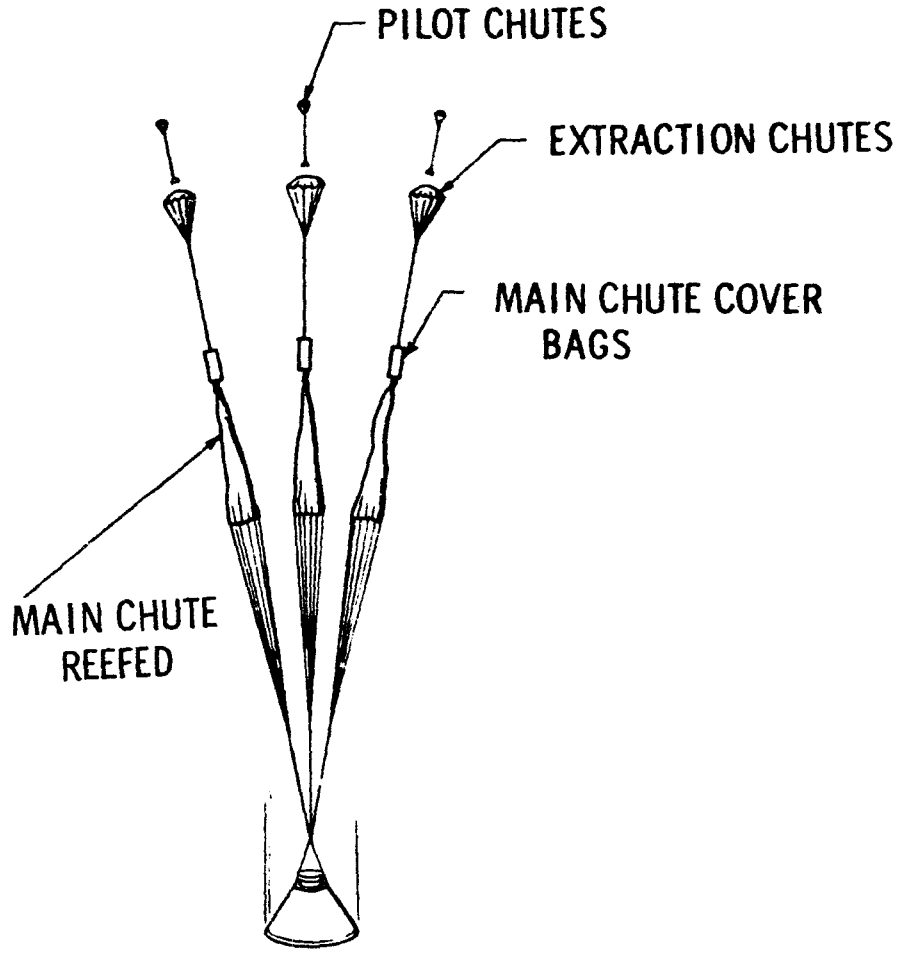

NASA -MSC J. KIKER 6JULY62 S-150-6

APOLLO CAPSULE IMPACT SYSTEM

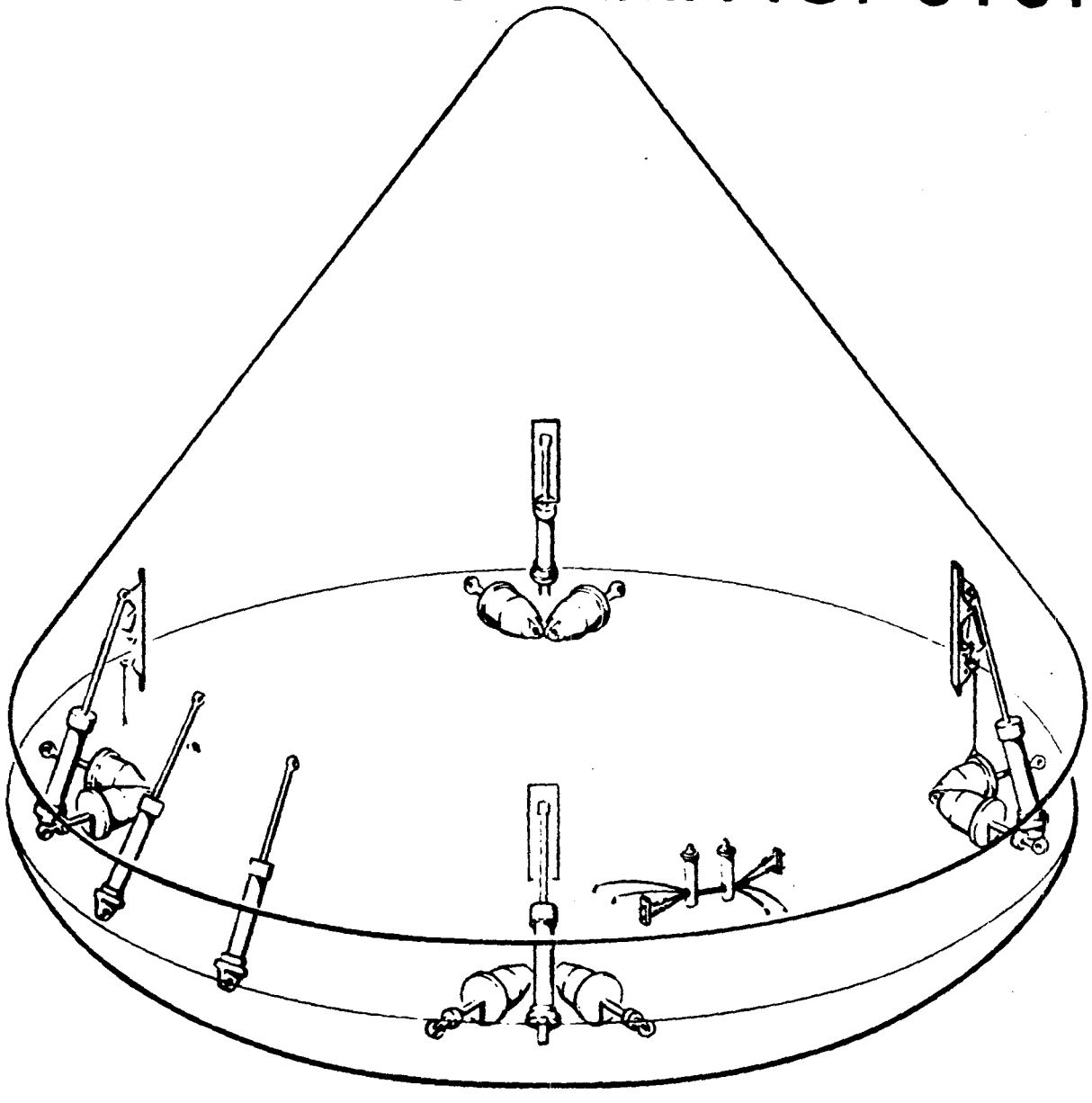

NASA - MSC J. KIKER 6JULY62 S-150-2

APOLLO CREW SEAT IMPACT SYSTEM

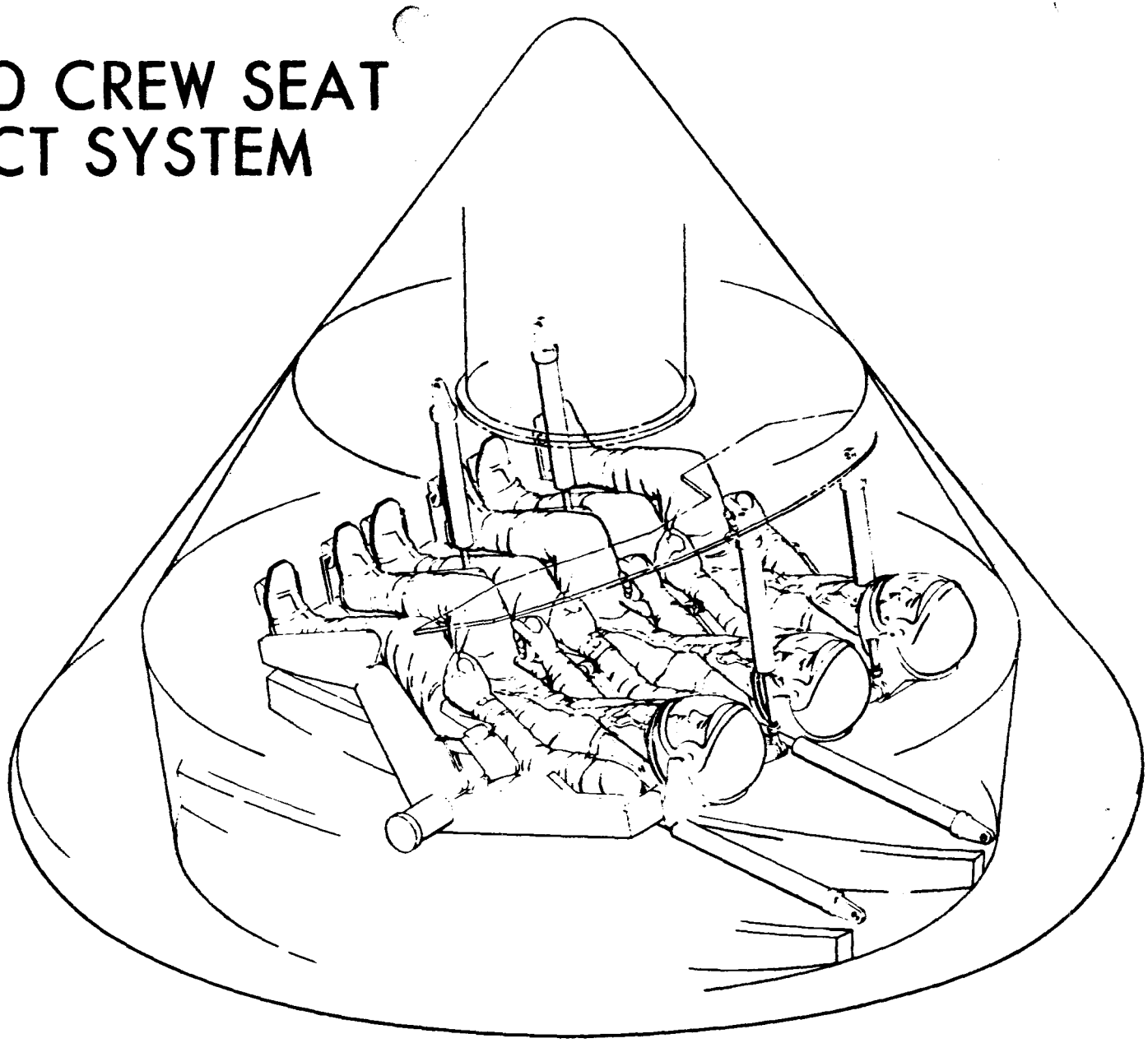

NASA-MSC J KIKER 6 JULY 62 S-150-1

APOLLO DROGUE PARACHUTE DESIGN ENVELOPE

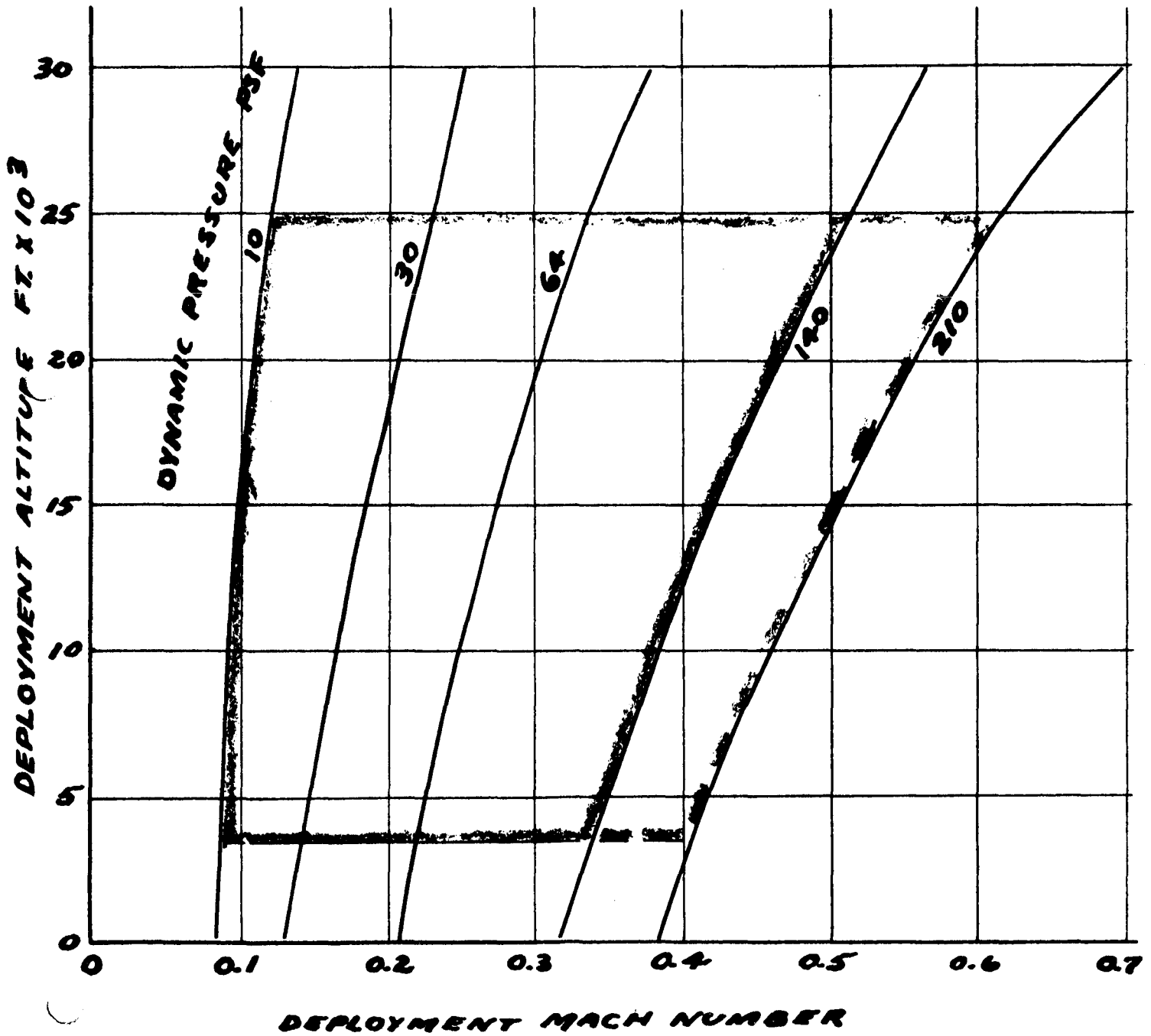

GRAPH #1

APOLLO MAIN LANDING PARACHUTE DESIGN ENVELOPE

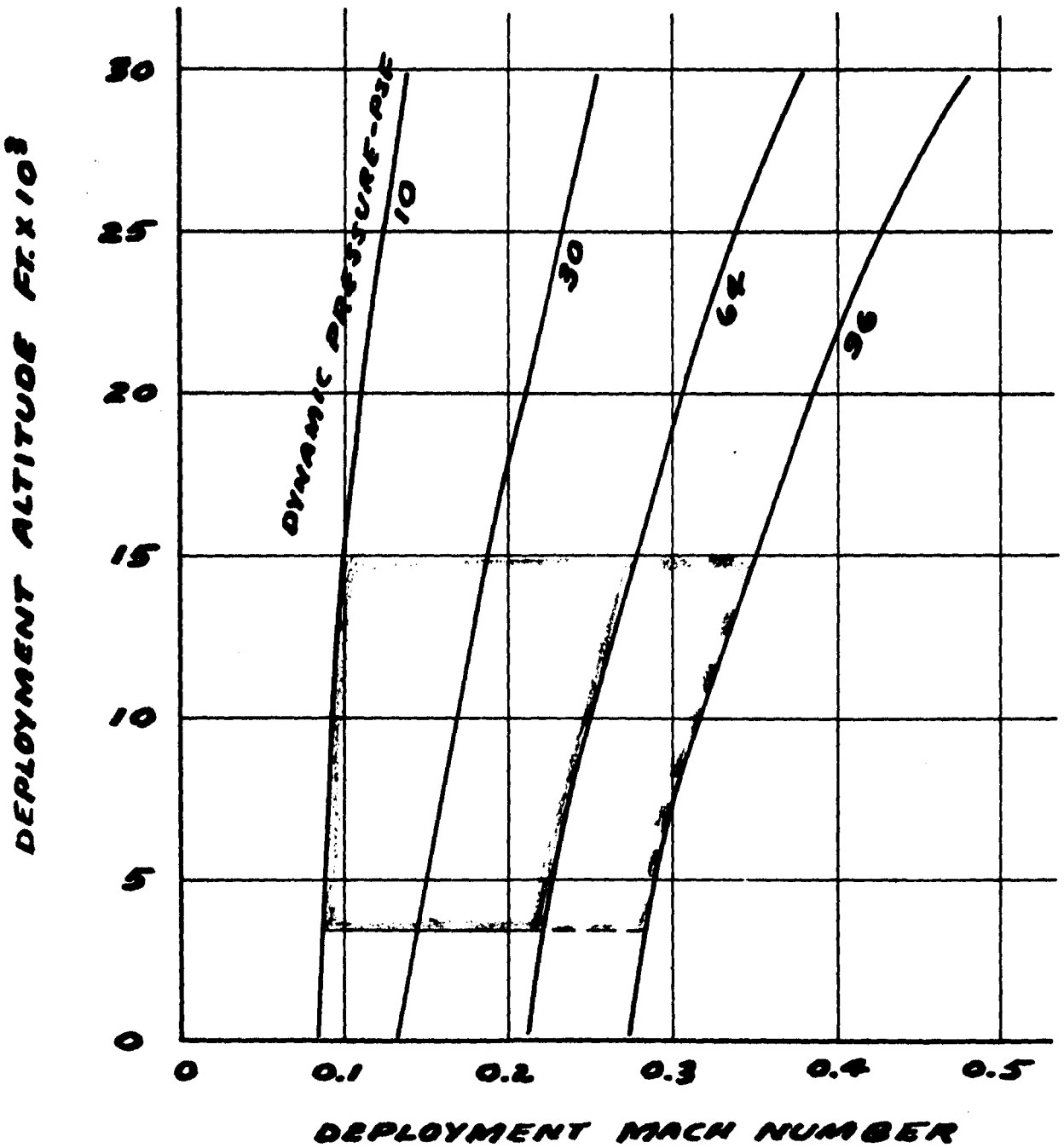

GRAPH # 2

KNOWN SAFE HUMAN TOLERANCES

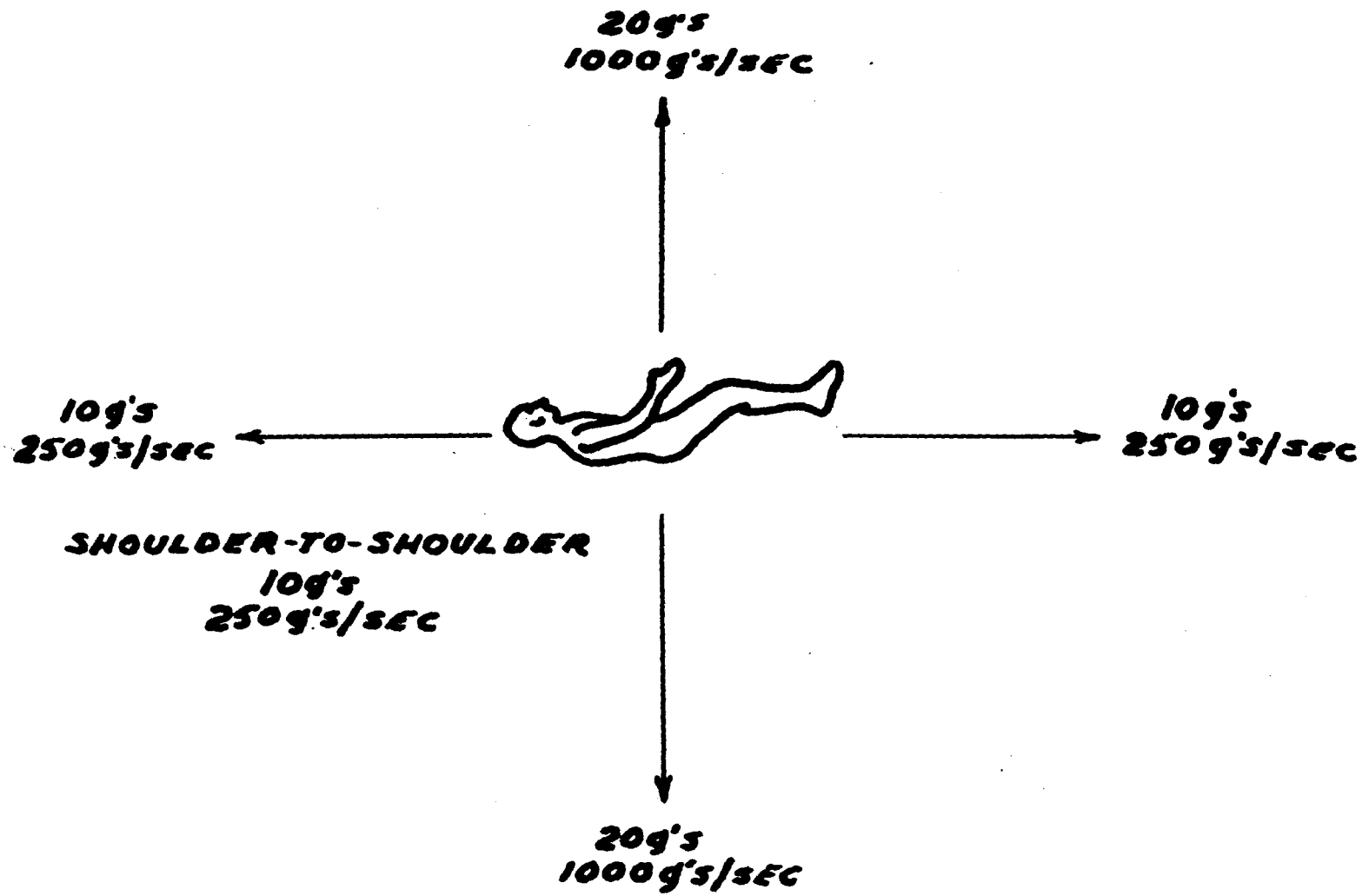

GRAPH #3

[redacted]

JPL Requirements for Spacecraft Landing and Recovery

Research and Technology
Notes for the OART Sponsored Meeting at NASA Headquarters
10-11 July 1962

Prepared by E. Pounder, E. Framan, J. Brayshaw

X65 84340

A. Introduction

The Jet Propulsion Laboratory is engaged in the design, manufacture, and operation of instrumented Spacecraft for NASA's Lunar and Planetary programs. In this capacity, the Laboratory has current interest in the landing and recovery field in two areas: 1) the return of small probes from the lunarsurface and, 2) the entry of instrumented probes into planetary atmospheres and operations using these probes near and on the planet surfaces.

At the present time there are no active projects for lunar return packages; however, some study work has been completed. It is clear that the search aspects of the problem are the only ones unique to the lunar return mission; the return guidance will require a search area of about 1000 x 2000 km, and the size of the capsule will preclude any but the most rudimentary on-board equipment.

The planetary program requires flights to Mars and Venus at each opportunity. The planning calls for entry attempts to be made as soon as adequate payload is available, and it is now believed that this will occur during the 1965-66 period.

The recovery and landing aspects of the designs are of utmost important, and are being considered in the studies. It is our opinion that the Laboratory will do very little in the in-house development of these systems, but will depend heavily on the other NASA centers and industry.

The following is a brief set of notes outlining the problem as we see it. The first section describes mission criteria, the second restraints, and the third lists major areas where R and D effort needs to be applied to obtain the best chances of success.

iii) If possible obtain data on planetary parameters - rotational rate, pole inclination, surface magnetic field, etc.

iv) Make near-planet particle and field measurement.

b) Mars

i) Do biology experiments on the surface.

ii) Investigate the atmosphere.

iii) Investigate physical surface properties. This might include local mapping, surface constituents seismology, etc.

iv) Near planet particles and fields.

C. Planetary Mission Restraints.

Many restraints can be written down for spacecraft design, but the ones listed here are prime for the planetary missions and must be carefully considered, both technically and economically.

1) Environment - In addition to the space environment considered for earth satellites, the change in heliocentric radius during a mission adds considerable complication to all systems. Also, the planetary environments contain many extremes and the models are based on a very small amount of information. The result is that the design problems are unique and difficult.

2) Infrequent Opportunities - 19 months for Venus, 25 months for Mars.

3) Dual Planet Capability - The general requirement for maintaining as much standardization in subsystems as possible is recognized as being most important. It is expected that the entry capsules will differ more than the spacecraft, but the Spacecraft-Capsule interfaces will certainly be as uniform as possible.

4) Reliability - The important items are:

a) Long lifetime - Mission durations of 120 days for Venus and 230 days for Mars are typical values. Subsystems which must work at the planets must also be "storable" in space for this period of time. Simplicity, redundancy, margins of safety, etc., must be carefully integrated into the effort.

b) The systems developed must be as "testable" as possible both in a development and qualification sense.

5) Sterilization - This will be a hard requirement for both planets, with most emphasis on Mars. Current JPL specs. call for heat sterilization (type approval) consisting

f three cycles, each 36 hours at 145°C. It is required hat this procedure be applied to the completely assembled ntry [illegible] ptions require a comprehensive demonstration of [illegible] ent capability.

D. R & D Requirements

In considering possible designs to meet the above requirements, certain areas for R and D effort have become apparent. Those pertinent to recovery and landing are listed.

1. Retardation systems for Planets.

   a) Maximum [illegible] ent Mach Numbers for retardation systems need to be increased to the highest possible value. This appears to be especially critical in the Mars situation because of the large scale height and low atmospheric density.

   b) Materials for high temperature operations (Venus, [illegible] sterilization compatibility need development. Ha[illegible] vacuum storage must also be understood.

   c) The entry environment imposes a high "g" [illegible] tradeoffs on the retardation system [illegible] this needs study. Typical values [illegible] and 500 g for Venus.

   d) The general scaling of retardation system[illegible] and Venus conditions needs considerable thought instance, some simple scaling [illegible] Mars parachute to carry a given mass [illegible] speed might be about twice the diameter and [illegible] weight of [illegible] earth equivalent. It is [illegible] [illegible] of parachute [illegible] that testing under simulated planet [illegible] S[illegible] gravity [illegible] tog[illegible] adec[illegible] quire careful thought and ingenuity.

2. Deployment Control Development.

   a) Systems to [illegible] deployment [illegible] planet e[illegible] [illegible] speed or [illegible] measure[illegible] [illegible] from [illegible] [illegible] nis [illegible] ssib[illegible] [illegible] syste[illegible] [illegible] measurement [illegible] [illegible] ymen[illegible]

maximum speed consistent with known (tested) decel[illegible] strength, stability, and heat resistance.

c) The above functions will certainly introduce complex[illegible] not suffered by the present simpler sensors such as acceleration and pressure sensors, but such complex[illegible] will undoubtedly be worth the performance gains. At Mars, for instance, altitude gain may be a factor of 2 over that realized by the simpler system's attempting provide safe deployment conditions over a wide spread in possible atmosphere properties.

3) Development of Balloon Systems. There are two major reasons for considering balloon systems.

a) To allow extended observation time under some specific set of conditions (constant altitude, for example).

b) To provide time for an Earth controlled landing site selector maneuver. The reaction time for the simplest form of Earth based selection is probably of the order of one hour.

Balloon schemes are most certainly considerations fo[illegible] (not Mariner), but in our opinion require extensive [illegible]ment. They appear to be heavy, fairly complex, an[illegible] the benefit of much real experience in terms of a[illegible] control flight deployment, vacuum storage, etc.

4) Landing Guidance and Control.

The landing problems are not unique to the planetar[illegible] missions, but the stakes may be higher than for an inst[illegible]ented probe in the earth's atmosphere. Problems inclu[illegible]

a) [illegible] site selection - This means detection of [illegible] [illegible]th suitable properties as opposed to [illegible] which would certainly depend on ast[illegible] [illegible]ital control. There are obvious [illegible] [illegible] unar problem. The main [illegible] [illegible]er communication times. [illegible] [illegible]res and the desire to land [illegible] [illegible] success of biology exper[illegible] [illegible] a parachute type [illegible] [illegible]ent velocity [illegible]

[illegible]

of a planet has many inherent problems. It is fortunate that in this process one can probably draw on the experience gained from the lunar programs. Techniques investigated for lunar missions include rocket landings (Surveyor) and crushable structures (Ranger). The vehicle should be designed on the basis of no site selection since a partial failure of site selection guidance should not cause mission failure. Other problems to be investigated include release of the retardation system after impact, accounting for both axial and transverse approach velocities, and the effects of any landing mechanisms on the entire system and its operation (i.e., communications, science).

6) Post Landing Orientation and Survival

a) Reorientation methods will be largely dependent on degree of landing guidance accuracy, i.e., minimization of drift and impact velocities.

i) For the case where these velocities are appreciable, the vehicle should be designed to tumble passively with minimum absorption of lateral momentum. When motion has ceased, orientation may be achieved a) wholely within the envelope of the vehicle, say by gravity or optics, in which case minimum expended energy and all orienting mechanisms are protected from the environment (heat, blowing sand, wind), or b) by actively altering the surface of the vehicle to produce torques tending to right the vehicle; however, these devices (legs, spring, draglines) have been exposed to impact injury and continue to be subject to environmental influence. Energy expended is greater since entire system may be lifted.

ii) For the case where precise landing control is available, orientation devices may be deployed before impact (legs, grapnels, attitude feelers, etc.) with lesser chance of damage.

b) Survival will require, in any case:

i) Thermal protection from solar or surface and atmospheric heating (cooling)

ii) Mechanical protection against winds, dirt, (humidity), attitude control with respect to local surface.

iii) Location of Earth Direction (communication to Earth) (omni-directional communication to an orbiter)

iv) Location of landing site on planet (astronomical observations). If an orbiter is available it may geographically locate the lander's radio signal.

In addition, it would be most helpful if efficient schemes for extracting electrical energy from the planetary

environment could be devised. Possible sources might be flight kinetic energy, surface winds, diurnal temperature cycles. Any useful developments in this area will probably have to await results from initial entry capsules.

7) Testing Techniques

One of the most significant tests which can be performed on planetary entry vehicles is a simulated entry on Earth of a complete system under controlled conditions. The objectives of such tests are to observe the operations of the system throughout the conditions of peak heating and loads, retardation, landing, etc., and to do this early enough before the flight to permit the addition of any reliability measures. Flight tests of this type involve a great deal of effort and dollars. It is therefore proposed that the following be studied:

a) How would tests of this type be performed? Can all factors be investigated in one flight or must they be broken down and performed on several flights.
b) How many flight tests per mission function and/or per mission would be necessary.
c) In performing such tests, how much of the actual flight mission is compromised by:
    i) Splitting up the test in functions.
    ii) Fitting the entry vehicle to a different booster.
    iii) Instrumentation.
    iv) Is the knowledge gained from the tests worth the cost and effort of performing them?

TP/EF/JB:pmm

JPL ACTIVITY IN RECOVERY FIELD

Part of the Mariner mission consists of the entry capsule, split off a flyby spacecraft, into a planetary atmosphere. This atmosphere-measuring probe was the first recovery problem faced by JPL. (Lunar landing by retro rocket has previously been studied here for Ranger.) Early work on recovery has been in the following categories:

1. Re-entry to Impact Trajectory Studies - Parametric study, assuming ballistic entry, translational motion only, and drag a function of Mach number. Parameters varied are:
    a. Entry conditions (path angle and velocity)
    b. Atmosphere density profile (since there is considerable tolerance in existing knowledge)
    c. Capsule ballistic coefficient
    d. Parachute deceleration with varying sequences opening at various flight conditions.

    It has been found that all the above effects influence the usefulness of a recovery system in meeting mission objectives, such as descent time and atmosphere depth to be sampled during this time.

2. Optimum Design of Parachute System for Planetary Missions - In order to determine a) the effects of (1) the general design and fabrication of parachute systems for the planets and b) the extent to which current parachute capabilities permit maximum utilization of available variations in entry parameters for

entrancing mission performance, a study contract has been let to a firm specializing in recovery technology.

3. Landing Impact and Reorientation Studies -

   a. Experimental and theoretical investigations into the properties of crushable materials for impact energy absorption.

   b. Preliminary studies on weight efficiencies of some orienting devices.

4. Recovery Study Based on Specific Hardware -

   As a part of a JPL-funded study to establish the overall suitability of the Discoverer vehicle for Mars atmospheric entry, General Electric MSVD made recommendations of a parachute system and deployment method.

References:

1. Mariner B Study Report, Technical Memorandum 33-34, Jet Propulsion Laboratory, Pasadena, Calif., March 1961 CONFIDENTIAL

2. Mariner B Capsule Study, Mars 1964 Mission, Engineering Planning Document 79, Jet Propulsion Laboratory, Pasadena, Calif., April 20, 1962

3. Parachute System Study, Statement of Work 2843, Jet Propulsion Laboratory, Pasadena, Calif., April 25, 1962

4. Suitability of Discoverer and Nerv Entry Vehicles for Mars Atmospheric Entry, JPL Contract 950226, General Electric Co., Philadelphia, Penna., April 30, 1962

5. Evaluation of Certain Crushable Materials, Technical Report 32-120, Jet Propulsion Laboratory, Pasadena, Calif., January 13, 1961.

JB:lk

NASA - Langley

[redacted]

LANGLEY RESEARCH EFFORTS ON RECOVERY SYSTEMS

by A. L. Neihouse

+65 84341

The only highly-developed recovery system available at present is a parachute system, such as for project Mercury. This may have to be used again, either as a primary or at least as a back-up system. However, an advanced recovery system capable of maneuverability is urgently needed and such a system should desirably provide near-zero vertical velocity and depending on trade-offs involved, low or near-zero horizontal velocity.

The first slide summarizes Langley's research efforts on recovery systems. Most of the effort to date has been on the parawing, which combines the stowability and light weight of a parachute with flight control and flared landing capability of a conventional wing. The results obtained in the various research areas will be discussed in five papers.

Some effort is now also being made on rotary-wing recovery systems. Performance and other characteristics are available from helicopter research; a current effort which will be discussed in a paper today deals primarily with deployment and dynamic stability.

Work has also been done at Langley on decelerators at both supersonic and subsonic speeds. Results of wind-tunnel investigations on decelerators at supersonic speeds will be summarized in a paper today. Although not discussed today, brief low-speed drop tests have also been made of inflatable devices which were dropped from a helicopter and successfully filled with foam in flight to provide drag in the air or to provide buoyancy after landing in the water.

A paper will also be presented on problems associated with energy dissipation upon ground impact in the recovery of space vehicles.

Some miscellaneous work which is not covered in the talks and which has been given only little effort deals with guided parachutes and with retro rockets in conjunction with a parachute. Use of these devices is depicted on the next slide.

Use of a flapped parachute, or of a cluster of parachutes with inflated rings gave an L/D of approsimately 0.5. The flapped parachute L/D was limited by collapsing of the forward edge of the chute skirt; the L/D of the clustered chutes appeared to be limited by the drag of the rings which were perhaps larger than necessary. Retro rockets in conjunction with a chute, although giving no glide capability, provided near-zero touch-down velocity in vertical descent.

LANGLEY RESEARCH CENTER EFFORTS ON RECOVERY SYSTEMS

Research Areas	Parawing	Rotary Devices	Aerodynamic Decelerators	Energy Dissipation	Guided Chutes	Retro Rockets
Static Aerodynamic Characteristics	✓	✓	✓	✓	✓	✓
Stability	✓		✓		✓	✓
Control	✓				✓	
Deployment	✓	✓				
Flared Landings	✓					
Loads Materials Aeroelasticity	✓			✓		

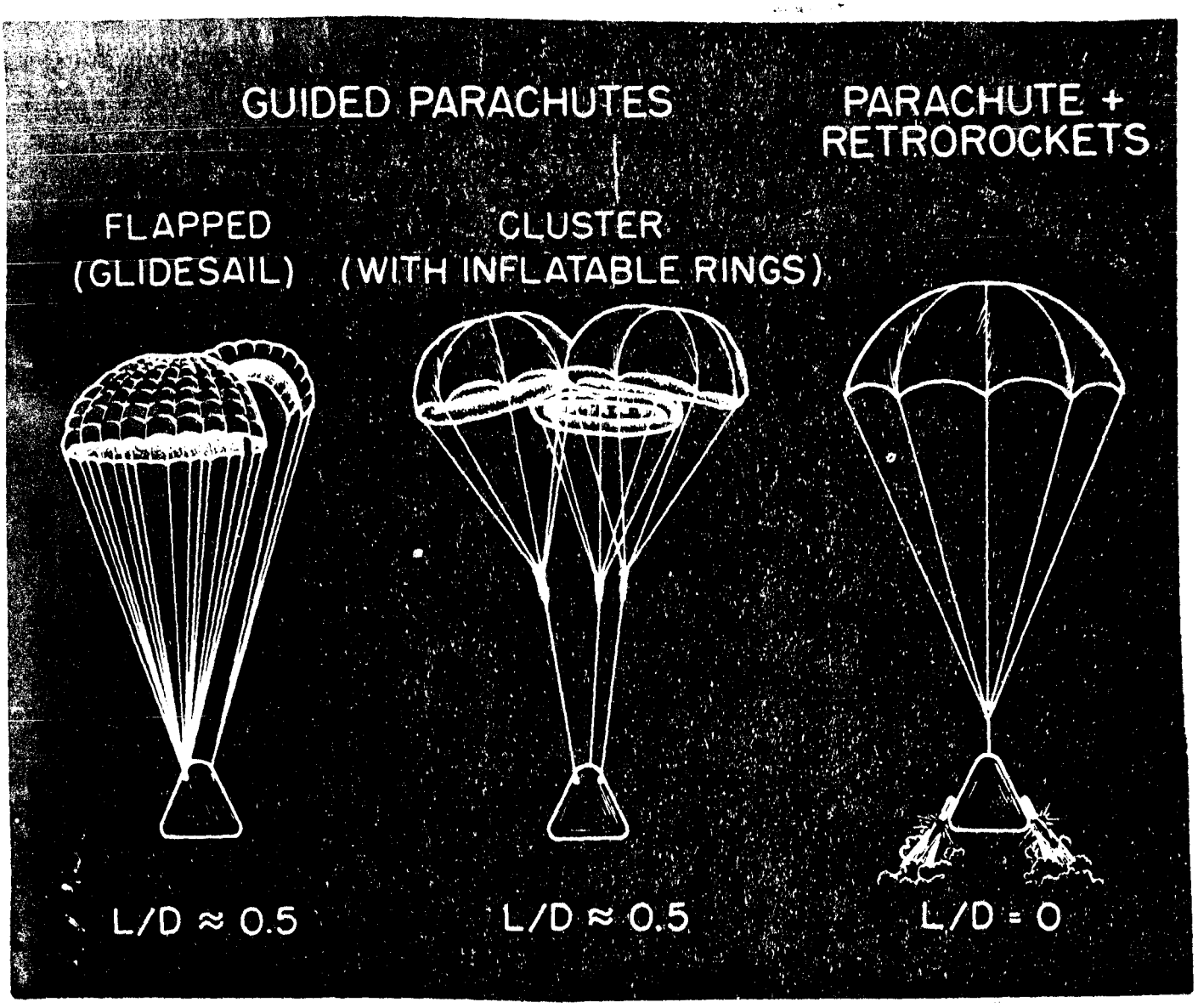
GUIDED PARACHUTES
PARACHUTE + RETROROCKETS
FLAPPED (GLIDESAIL)
CLUSTER (WITH INFLATABLE RINGS)
L/D ≈ 0.5
L/D ≈ 0.5
L/D = 0

NASA - Langley [redacted]

SUMMARY OF STATIC AERODYNAMIC CHARACTERISTICS OF PARAWINGS

By William C. Sleeman, Jr., Delwsin R. Croom
and Rodger L. Naeseth

X65 84342

This presentation will summarize some of our recent work on the static aerodynamic characteristics of parawings. It appears advisable to acquaint you with some of the terminology used in this presentation and several that will follow, so we will go to the first slide.

SLIDE 1

This slide shows a typical parawing with a conical shaped canopy. The leading edges and keel may be rigid or flexible members and the wing may or may not have a spreader bar to hold the wing sweep angle fixed. In this talk, and others, reference is made to the flat planform sweep and the dotted lines in the lower figure show the flat sweep. In constructing these wings, the fabric for the canopy is cut to the desired flat pattern sweep. When the sweep is increased to the flight sweep, two lobes are formed which have approximately conical shape in flight. The aerodynamic coefficients are based on the area of the flat planform and the keel length.

In some cases, flutter of the fabric at the trailing edge has necessitated the use of a bolt rope in the hem at the trailing edge as shown here.

SLIDE 2

The next slide summarizes some of the most important beometric parameters that we have investigated on parawings.

(Read from chart)

We are not going to talk about all of these items but we have selected several to illustrate the type of work that we are doing and to indicate the present state-of-the-art as regards maximum lift-drag ratios.

SLIDE 3

Let us now look at some familiar aerodynamic parameters. The next slide presents the lift-curve slope and $C_{L_{max}}$ as a function of flight sweep for a 45° flat pattern sweep. These results were obtained in a systematic planform study in which wing sweep was the primary variable on wings having rigid members. The little sketches show that as the sweep increased, the height of the lobes of the canopy increase.

The experimental and theoretical lift slopes are seen to be in very good agreement. The maximum lift coefficient for 50° sweep was about 1.1 and it decreased with increasing sweep. $C_{L_{max}}$ was not determined for the higher sweeps because C_L was still increasing with up to $\alpha = 55^{\circ}$, which was the limit of the test setup.

SLIDE 4

We go now to maximum lift-drag ratios obtained in the same planform study and the next slide presents the variation of L/D_{max} with sweep angle. Experimental results are shown by this curve and the dotted curve indicates an estimated upper bound, using theory for a conventional flat wing and an assumed skin friction drag of .013. We see that there is a considerable gap between the experiment for conical canopies and the theory for flat wings; and we will spend some time discussing why these differences are shown and how we might be able to raise the level of the experimental data.

We have not indicated a theoretical estimate for conical shaped wings because the lift-drag ratios are greatly influenced by several design factors other than the wing planform sweep and aspect ratio. Of course, as for conventional wings, the wing sweep and aspect ratio are among the most important factors, but for flexible wings, the canopy shape can be of equal importance to these primary variables. Other important factors affecting $(L/D)_{max}$ are the way the fabric is attached at the leading edge, the leading edge size and shape. We will discuss these effects briefly, but first I would like to point out that we are discussing wing-alone characteristics and the lift-drag ratios will be reduced by the addition of a payload and its connecting members. The amount of this reduction in L/D will, of course, be a function of the wing loading or relative size of the payload and wing.

SLIDE 5

The next slide shows the importance of the details of the leading-edge geometry for a 55° swept wing. Let's consider first, the effect of leading-edge diameter. This curve shows that reducing the diameter from 7-percent keel to 1.5-percent keel increased the L/D_{max} from 4.6 to 6.3. Next, let's look at the effect of how the fabric is attached to the leading edge. This is shown by the shaded symbols which show both the L/D_{max} and how the fabric was attached for a leading-edge diameter of 7-percent keel. Here we see that the L/D can be increased from about 3.5 to 4.6 by moving the fabric attachment from the bottom to the top of the leading edge.

These results indicate therefore that to get the best L/D_{max}, you want to minimize the leading-edge diameter and have the fabric attached at the top of the leading edge. Now, if you can't minimize the circular diameter for structural reasons, then, perhaps an airfoil shaped leading edge could be used. The plot on the right shows how L/D_{max} varies with airfoil thickness ratio on the leading edge. The value of t/c = 1.0 is the 3-percent circle shown on the left-hand plot. In these tests, the thickness remained constant (3-percent keel) and the chord was increased to obtain this variation of thickness ratio. These results show that the use of an airfoil section at the leading edge can provide gains in L/D_{max}.

SLIDE 6

Let's turn now to another facet of our systematic planform study in connection with lift-drag ratios. The next slide shows the effect of flat pattern sweep for a given flight sweep of 60°. We see that the lift-drag ratios show a consistent decrease as the canopy lobes become larger. One of the main reasons for this decrease in L/D is that as the wing surface becomes more and more conical, the wing has more twist across the span, and the twist may amount to as much as 40° or 50° washout. This very high twist can cause the tip sections to carry negative lift at low and moderate angles of attack, which would cause high induced drag. Here, we see that the wing having the highest L/D has the least twist and perhaps we could approach the ideal curve for L/D_{max} shown previously by making the wing flat. This would be fine, but we would be back to a conventional wing requiring a heavier structure. Some of our latest work has been

directed toward optimizing L/D on flexible wings by using wing canopies formed about a cylinder with its axis parallel to the keel.

SLIDE 7

This photograph shows one of these wings in the wind tunnel. The scimitar-shaped leading edge gives the same fabric height at the leading edge as at the trailing edge and the wing consequently has no twist or camber across the wing span. These members were used for expediency in the tests to hold the wing sweep fixed, in place of the more common spreader-bar installation. The forces on these members was substracted out of the data. Our next slide presents data for this wing, and others, and indicates the present state-of-the-art as regards L/D.

SLIDE 8

Here we have summarized measured lift-drag ratios for flexible parawings having both conical and cylindrical canopy shapes. This curve shows that an L/D of approximately 6 can be expected from an aspect-ratio 2.8 parawing having a conical canopy. The use of cylindrical canopy on this wing planform increases the maximum lift-drag ratio to a value of 10.

Now, a more obvious means for increasing L/D would be to increase the aspect ratio, and results are shown for an aspect-ratio-6 parawing with the two canopy shapes. Here we see that increasing the aspect ratio from 2.8 to 6 for the conical canopy produced an increase in $(L/D)_{max}$ from a value of 6 to a value of 8. And then, going from the conical to the cylindrical canopy with the aspect-ratio-6 wing gave a maximum value of lift-drag ratio of 14.

We would like to point out that no particular planform shown here should be considered the optimum parawing because for some applications, the L/D at high lift would be of greater importance than the maximum value of L/D. For example, the conical canopy provides higher L/D at high lift because the washout alleviates the tip stall. Our work on high performance parawings will be continuing in efforts to extend the L/D envelope in this direction (up and to the right).

In the selection of a wing configuration for a particular application, other factors such as structural weight trade-offs and complexity have to be evaluated in addition to the aerodynamic characteristics. Some of these structural loads considerations will be discussed by Mr. Taylor in one of the following talks.

SLIDE 9

Let's turn now from the subject of lift-drag ratios to other phases of our work on parawings. The next slide presents some typical lateral stability characteristics obtained in the wing planform studies. Inasmuch as the center of gravity for parawing applications is located a considerable distance below the wing, the moment reference for these stability parameters is positioned as shown.

These data are presented for the purpose of indicating the magnitude of these lateral derivatives throughout the sweep range. The importance of these derivatives will be discussed later in the presentation by Mr. Johnson.

SLIDE 10

Let's now consider a factor more akin to the sailmaker's art than wind-tunnel aerodynamics, but nevertheless of importance in the overall problem of obtaining a satisfactory canopy for a parawing. The next slide shows the effect of orientation of the fabric weave on the canopy shape.

These views were taken from a wind-tunnel study of identical wing planforms in which the only variable was fabric orientation. Straight-line grids were drawn on the flat pattern of each canopy and photographs were made at each test angle of attack. There was little difference in the aerodynamic characteristics but we see that the canopy in which the warp was parallel to the trailing edge had a smooth shape throughout most of the angle-of-attack range.

When the threads were run parallel to the keel, however, the canopy had an appreciable bulge in this area because the threads from the tip, rearward were not attached to a structural member. At low angles of attack this model had appreciable trailing-edge flutter and the first canopy was torn in shreads.

We have always made our canopies with the weave running parallel to the trailing edge and you may wonder why we have brought up the subject of fabric orientation. Well, most of the models we have received from contractors have had the fabric weave running parallel to the keel and we have encountered the same fabric distortion and trailing-edge flutter. Indications are that the fabric distortion can cause travelling waves in the canopy that start near the apex and move rearward. This could cause troublesome variations in control force at a given trim lift.

Our experience has been substantiated in work the Ryan people have done on the powered test vehicle. After installing their second canopy, which had the weave parallel to the keel, they had to install a boltrope and several batters in the rear part of the canopy to stabilize the fabric distortion.

SLIDE 11

Now, on some of our models, particularly those with flexible leading edges, we have found the use of a trailing-edge boltrope desirable. The next slide shows the effects of boltrope length on pitching moments and lift coefficients. For the 0-percent case, the boltrope length is equal to the length of the fabric trailing edge. The other curves are for the boltrope 2-percent and 4-percent shorter than the trailing-edge length.

Pitching-moments are presented about a moment reference on the wing keel 50-percent back from the apex, and we see that shortening the boltrope gives a fairly constant increment of C_m and C_L through most of the angle-of-attack range. These characteristics suggest that varying the boltrope length may be an effective means for longitudinal control.

SLIDE 12

Thus far, we have considered only the characteristics of the wing alone. The next slide shows some longitudinal characteristics in pitch of a complete configuration in which an inflated tube parawing is used in the recovery of the Gemini capsule. In these tests the capsule was mounted to a sting support through a six-component strain-gage balance. The wing was rigged for two different flight conditions, based on aerodynamic characteristics obtained from our general parawing research program. For these tests, the wing was in flight, and its attitude and position were determined by the aerodynamic forces on the wing and the restraint of the cable rigging.

The glide configuration was selected to trim the configuration near L/D_{max} with the capsule at an angle of attack of 18° and the wing at 20°. In the rigging for the landing configuration the front cable was lengthened and the wing rotated to an angle of attack of 45°. The capsule angle for the landing is 0° to enable the capsule to touch down on skids.

We see that the estimated rigging for these conditions produced approximately the desired trim angle of attack. The lift-drag ratios are low, mainly because of the large diameter inflated tube leading edges used. $(L/D)_{max}$ for the wing alone was about 3.4.

We would like to point out that these results are applicable only at the trim conditions because, in order to change the lift coefficient a different rigging would be required. We are not certain of the significance of these results, such as the break-in pitching moments below trim. If these moments are indicative of the flight vehicle, then we may have cause for concern; however, our flight tests of inflated tube models have not indicated difficulties in this area.

We believe that there are limitations in static wind-tunnel tests of this nature and more work is needed to establish proper testing techniques to provide static data that can be properly interpreted.

SLIDE 13

In the design of the Gemini recovery system, estimates had to be made of cable tension loads in order to size the cables properly. It would appear desirable to rig the wing so that the cable loads were more or less equally distributed. Now, these estimates involve assumptions and uncertainties and it was desirable to get an experimental check on these cable loads.

The next slide presents some cable tension loads in terms of the percent of total load for each cable. Data are shown for the landing configuration where the loads were the highest. We see that the loads in the cables going to the center keel were about the same at the design capsule angle of 0° with the lines going to the leading edges carrying a somewhat higher percent of the load.

For angles below the design point the diagonal line tends to go slack and for angles above 0°, the diagonal loads up rapidly and the front line tends to go slack.

These data are believed to be subject to the same limitations mentioned in connection with the previous slide with regard to tunnel test technique. We believe, however, that these results are useful in evaluation cable loads for the design point and furnish a valuable reference for assessing the estimated loads. I would also like to mention that when we resolved these loads into lift and drag components and computed the summation of pitching-moment contributions, we got excellent agreement with the results presented in the preceeding slide.

CONCLUDING REMARKS

I believe that we should bring this presentation to a close now with a brief recall of some of the salient points covered. First with regard to lift-drag ratios:

(a) In addition to the expected effects of wing aspect ratio and sweep on $(L/D)_{max}$, the canopy shape was found to have a first order effect on this parameter, also.

(b) The details of the fabric attachment and leading-edge size and shape have an important effect on $(L/D)_{max}$.

(c) Lift-drag ratios for a low-aspect-ratio parawing can approach closely those of a flat wing of the same aspect ratio if an untwisted cylindrical canopy shape is used. $(L/D)_{max} = 10$ for aspect ratio 2.8.

(d) A value of $(L/D)_{max}$ of 14 was obtained with an aspect-ratio-6 parawing having a cylindrical canopy.

Next, the fabric orientation was shown to be important; for a smooth canopy contour, the weave should be parallel to the trailing edge.

And finally we discussed some model tests results of the Gemini configuration and pointed out some limitations of static wind-tunnel tests for this type of cable-supported configuration.

TYPICAL PARAWING

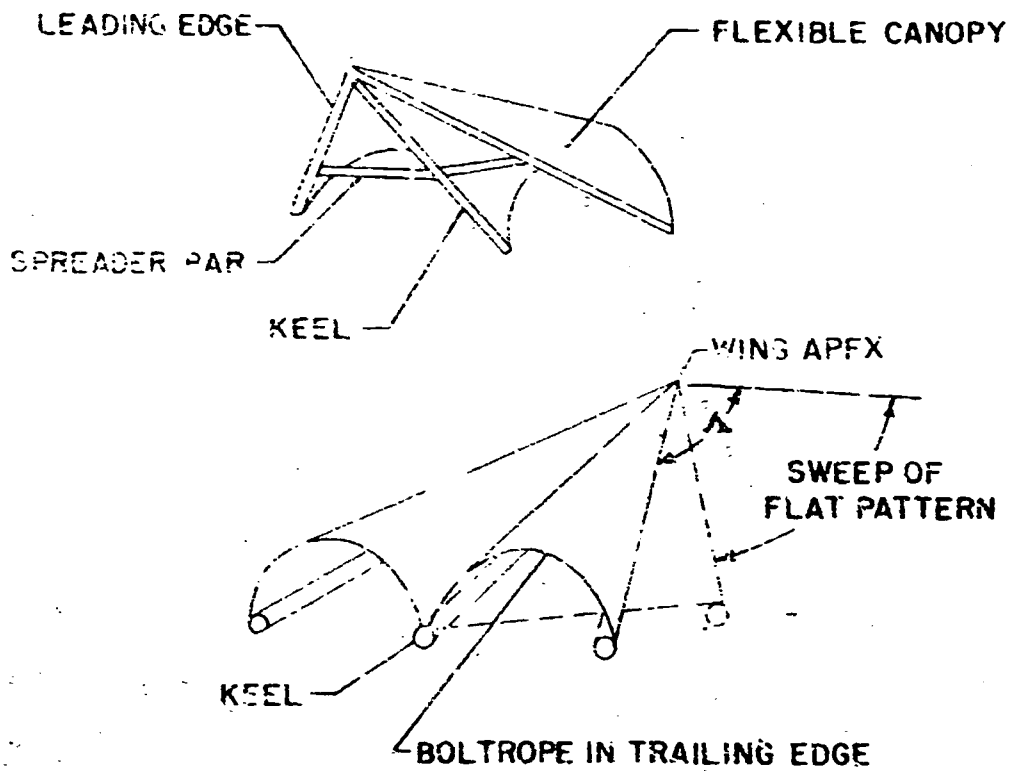

SUMMARY OF GEOMETRIC PARAMETERS STUDIED IN STATIC WIND TUNNEL TESTS OF PARAWINGS

A. WING PLANFORM

- SWEEP 40° TO 75°
- ASPECT RATIO 1.0 TO 6.0
- TAPER RATIO 0

B. WING LEADING EDGE

- SECTION: C AND ⬭
- DIAMETER: 1.5% TO 7.0% l_K
- FABRIC ATTACHMENT

C. CANOPY SHAPE

- CONICAL TWIST & CAMBER
- CYLINDRICAL ZERO TWIST AND CAMBER

D. SPREADER BAR

- NO BAR
- SIZE & SHAPE
- LOCATION

E. CONTROLS

- WING SHIFT (C.G. MOVEMENT)
- WING TIP DEFLECTION
- BOLTROPE
- LEADING EDGE DEFLECTION

F. CANOPY FABRIC ORIENTATION

FABRIC WEAVE PARALLEL TO:

1. KEEL
2. TRAILING EDGE

G. COMPLETE CONFIGURATIONS

1. RYAN POWERED VEHICLE
2. MICROMETEOROID EXPERIMENT
3. SATURN BOOSTER
4. GEMINI RECOVERY
5. AUXILIARY WING FOR AIRCRAFT

AERODYNAMIC CHARACTERISTICS OBTAINED

C_L, C_D, C_m, L/D, C_{L_α}, $C_{L_{MAX.}}$, C_{l_β}, C_{n_β}, C_{Y_β}, PRESS. DIST., CABLE TENSION, CONTROL EFFECTIVENESS

NASA-LANGLEY

EFFECT OF PARAWING LEADING EDGE SWEEP ON
C_{L_α} AND $C_{L,MAX.}$
45° FLAT PLANFORM SWEEP

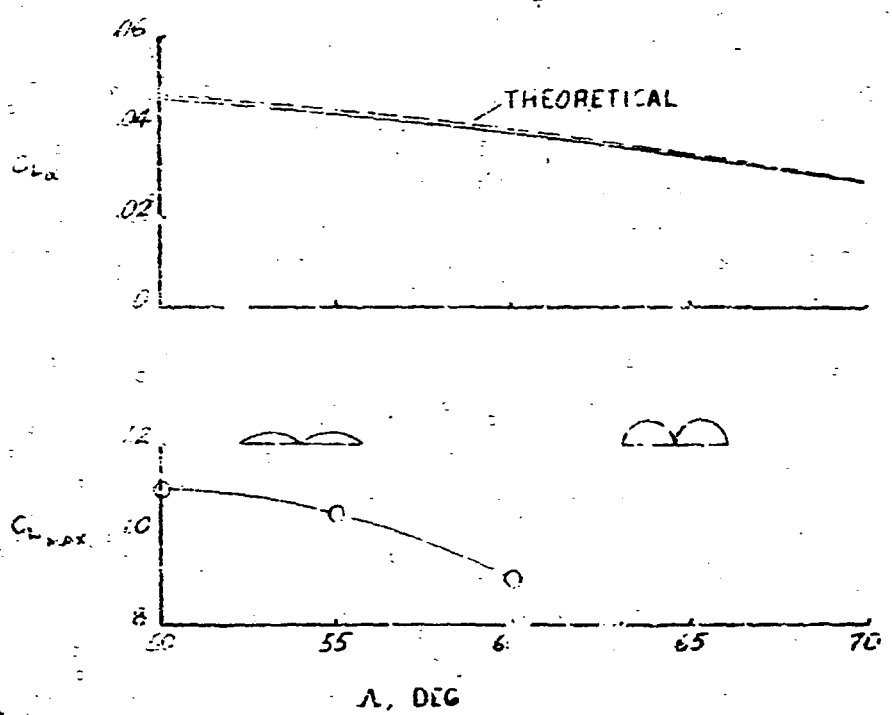

NASA LANGLEY

EFFECT OF PARAWING LEADING EDGE SWEEP ON $(L/D)_{MAX}$ 45° FLAT PLANFORM SWEEP

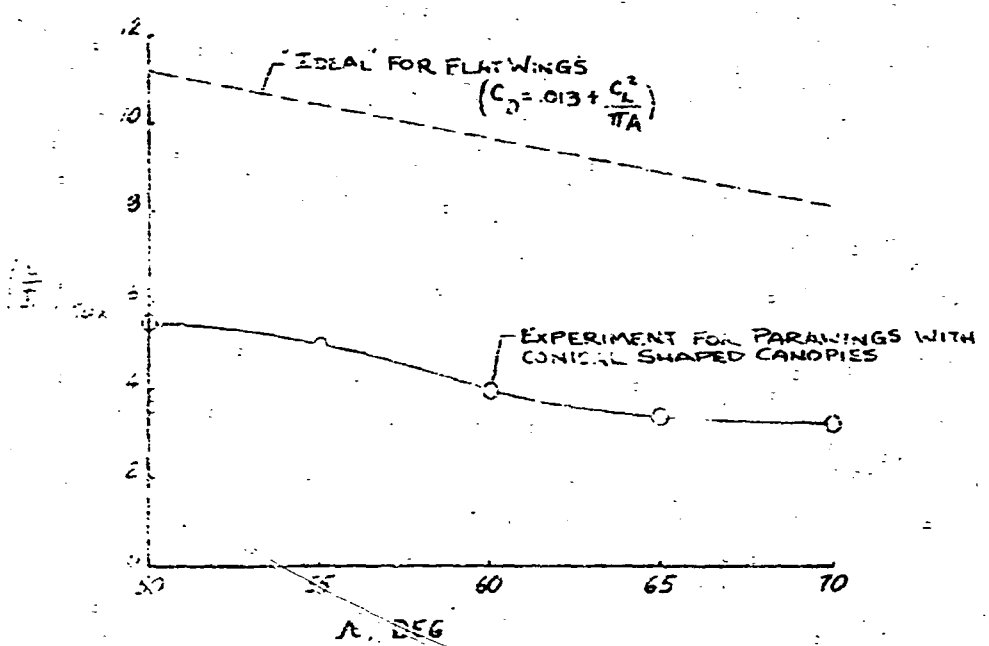

4

NASA-LANGLEY

EFFECT OF LEADING EDGE DIA., FABRIC ATTACHMENT, AND L.E. THICKNESS RATIO ON $(L/D)_{MAX}$.

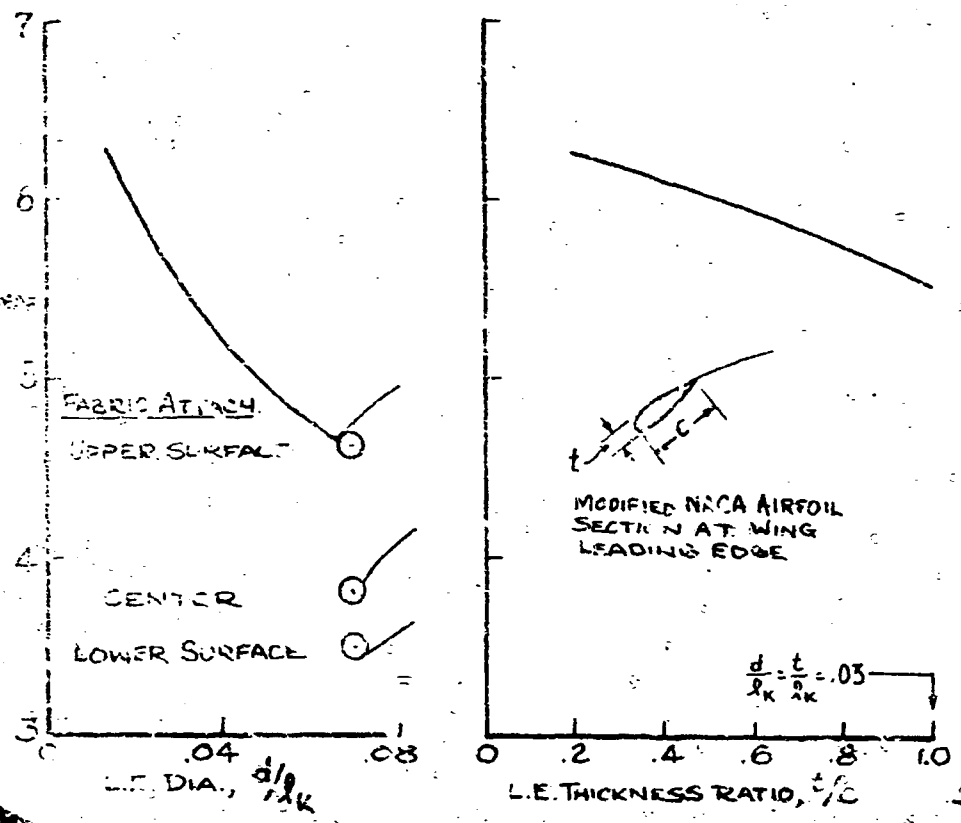

EFFECT OF CANOPY SIZE
IDENTICAL PROJECTED PLANFORM

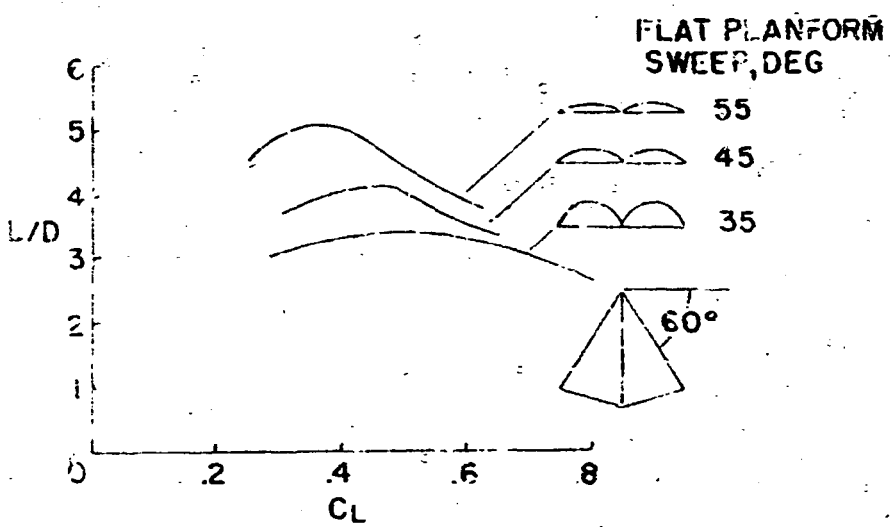

NASA-LANGLEY

L/D VALUES FOR PARAWINGS WITH CONICAL AND CYLINDRICAL SURFACES

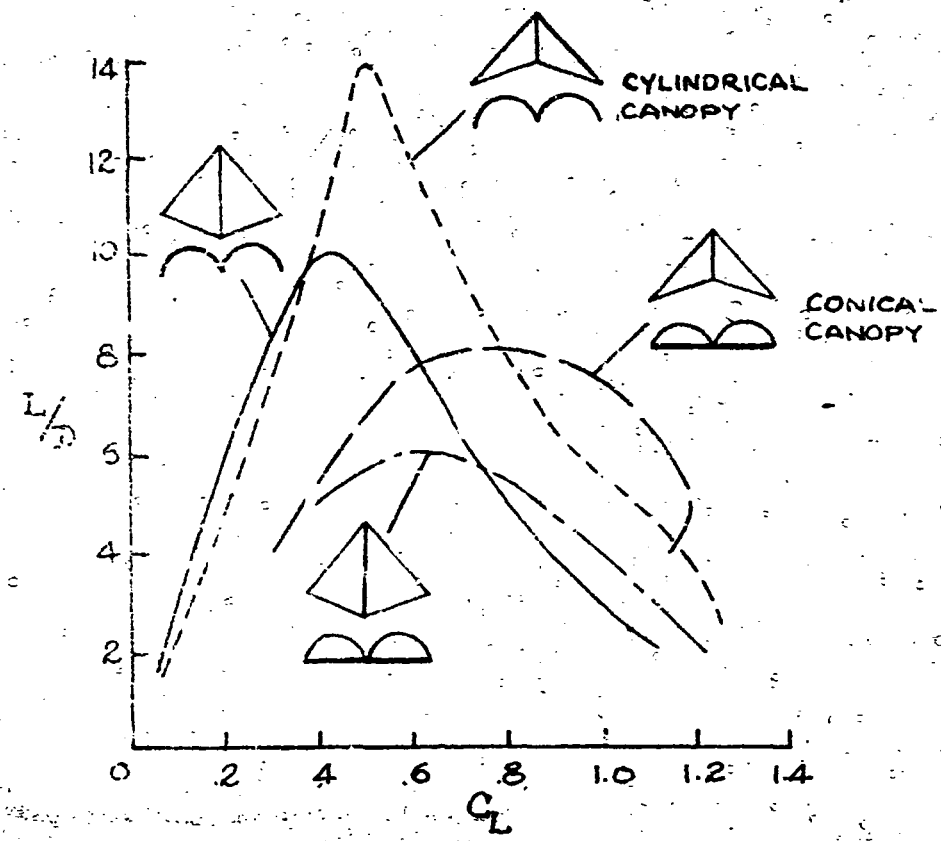

NASA-LANGLEY

EFFECT OF SWEEP ON WING-ALONE LATERAL-STABILITY PARAMETERS

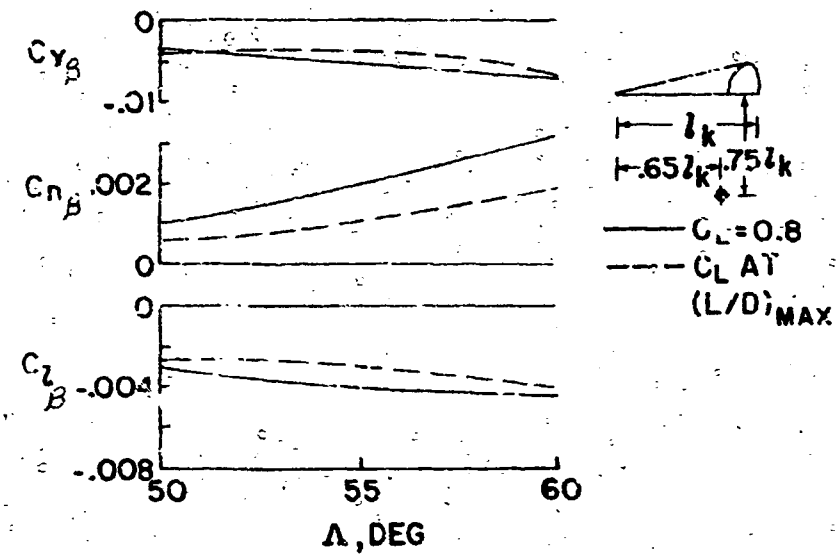

NASA-LANGLEY

EFFECT OF FABRIC ORIENTATION
ON CANOPY SHAPE

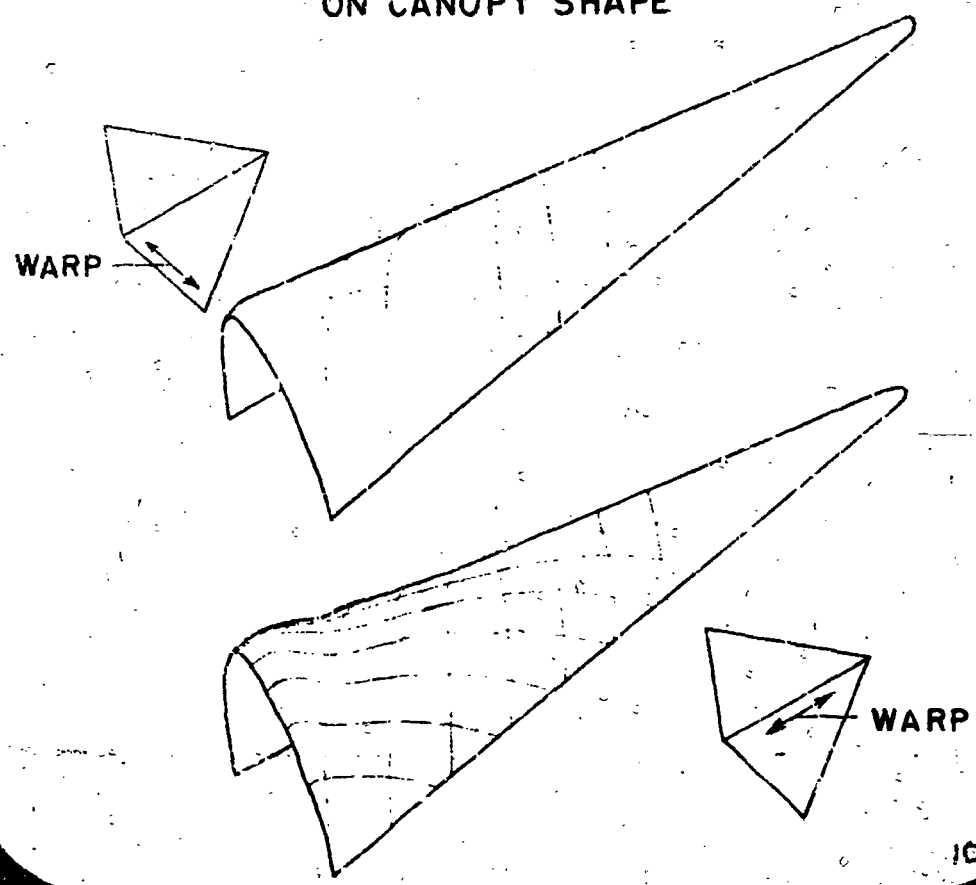

EFFECTS of BOLTROPE SHORTENING

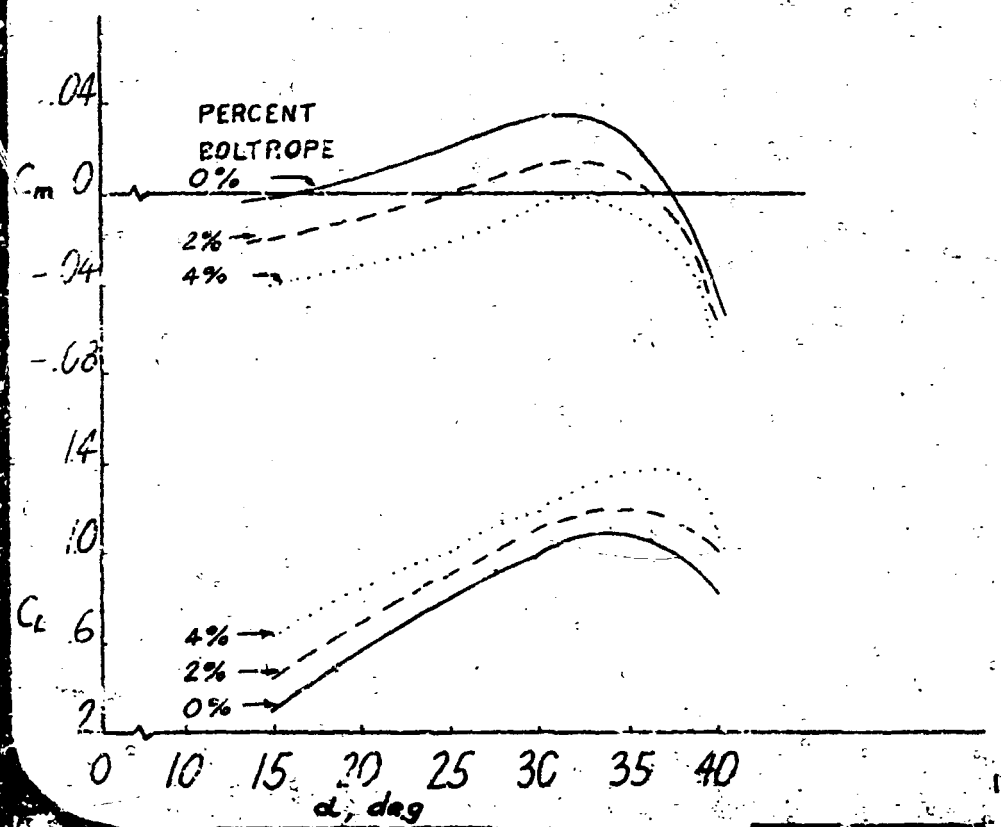

GEMINI-PARAGLIDER CHARACTERISTICS

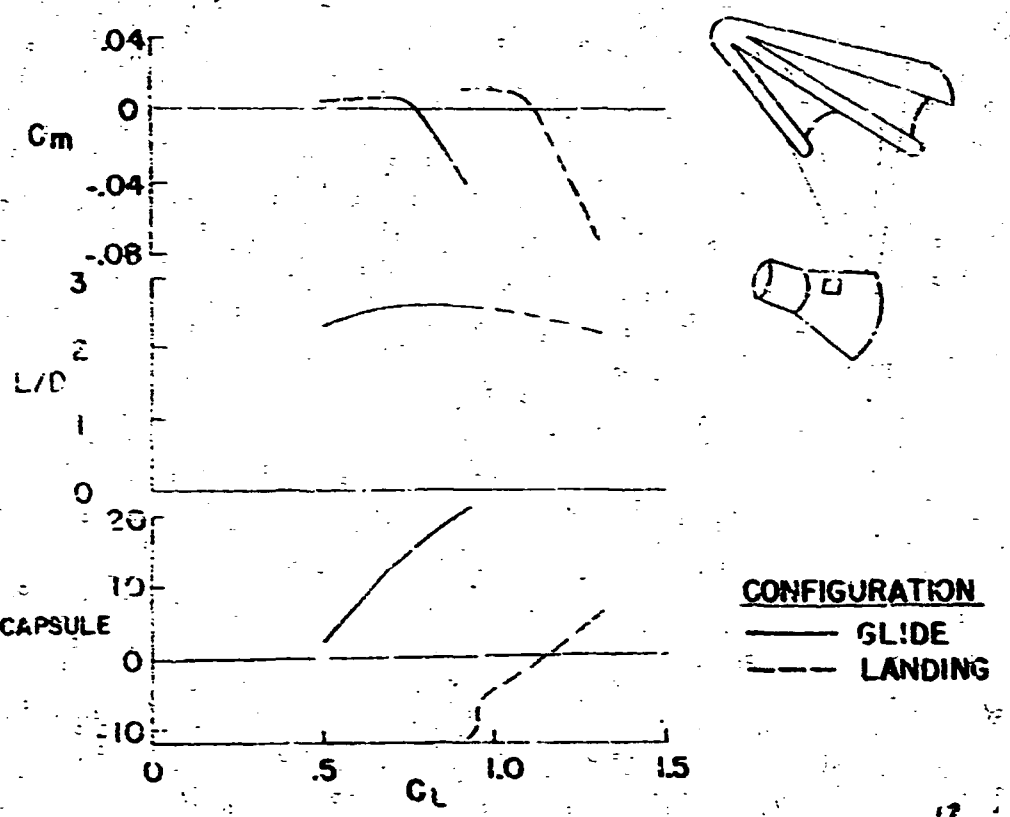

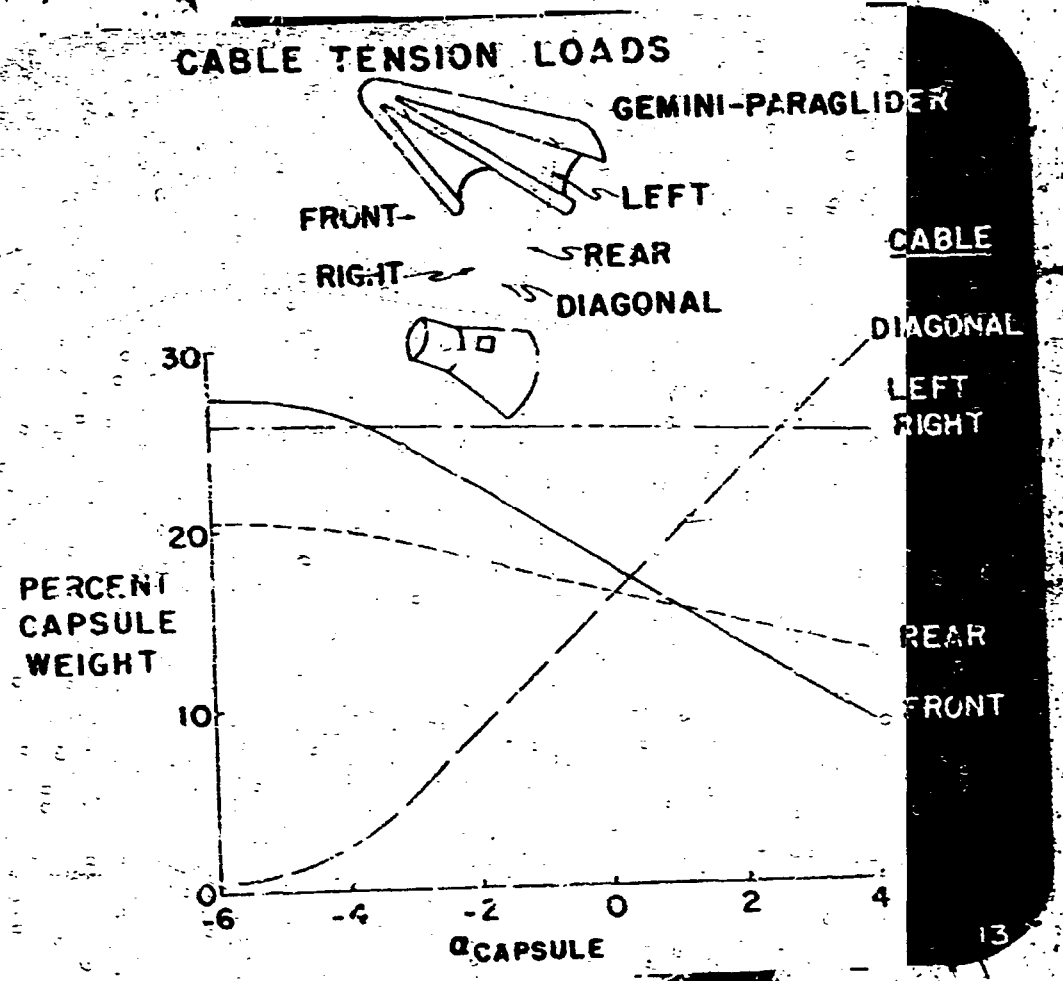

NASA-LANGLEY

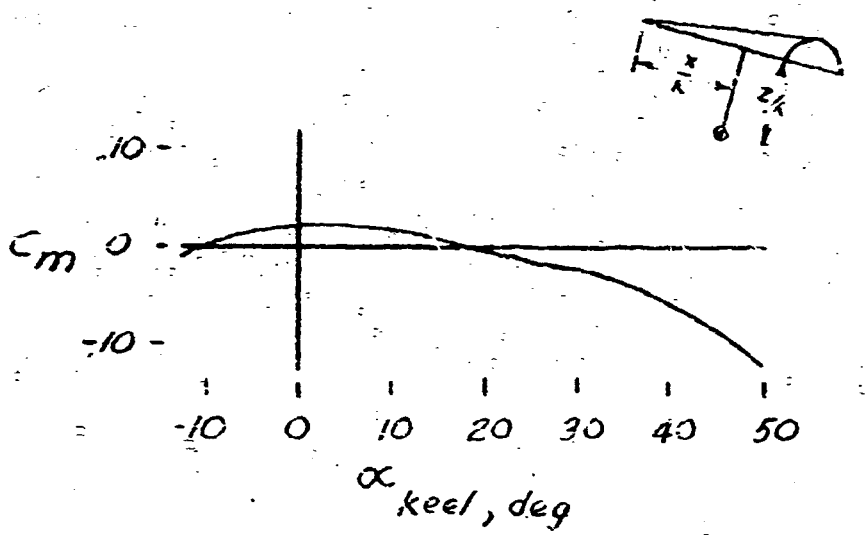

Fig. 1

NASA-LANGLEY

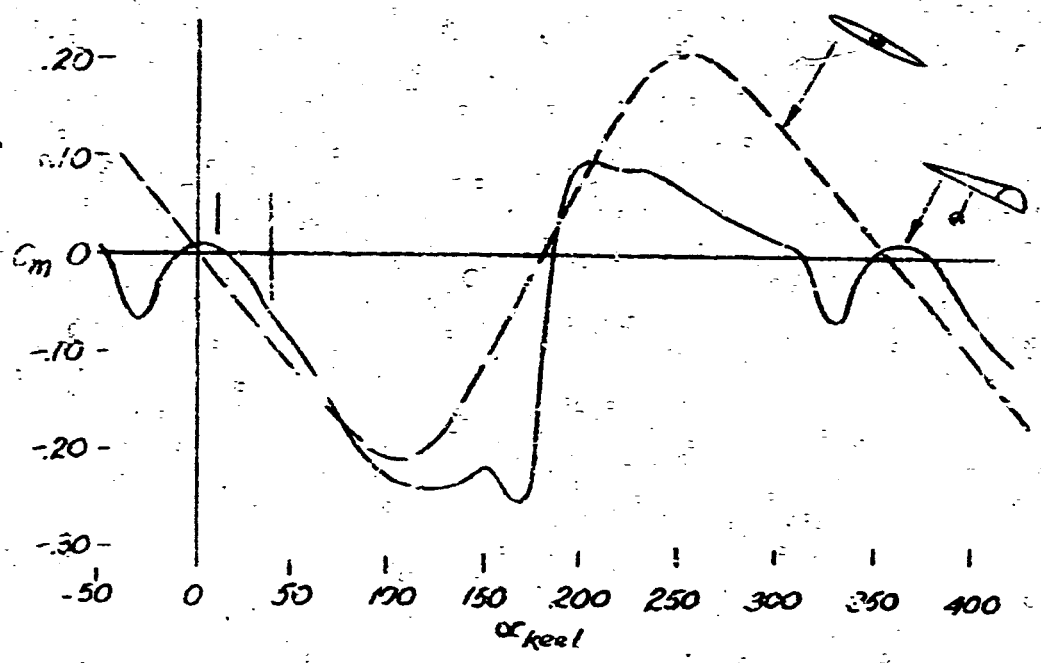

Pitching moment characteristics

NASA - Langley Field, Va.

Fig. 2

NASA-LANGLEY

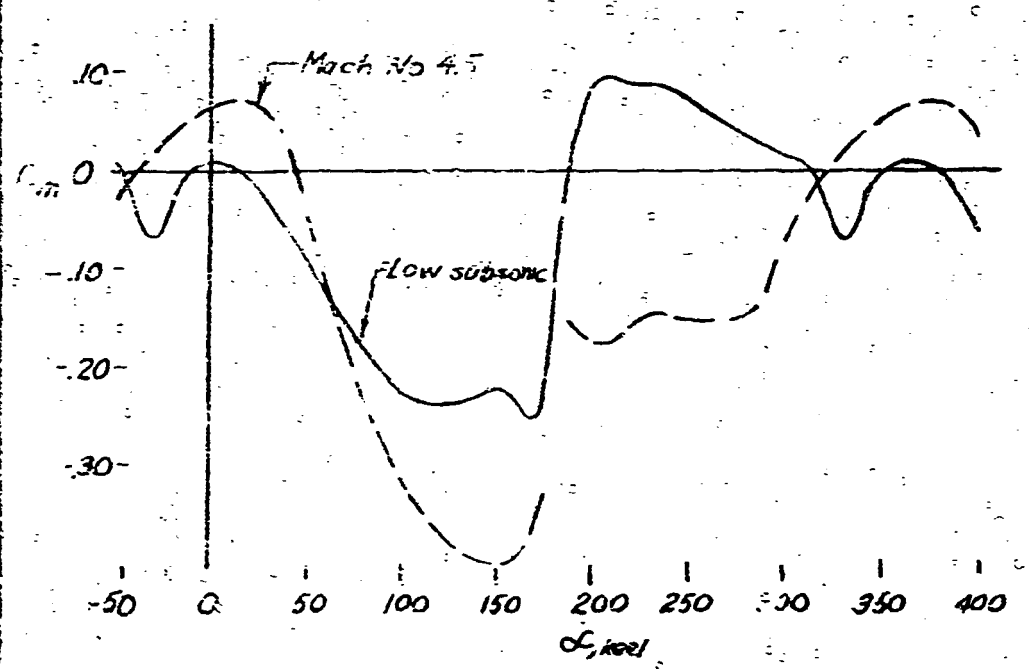

Pitching moment characteristics

Fig. 3

NASA-LANGLEY

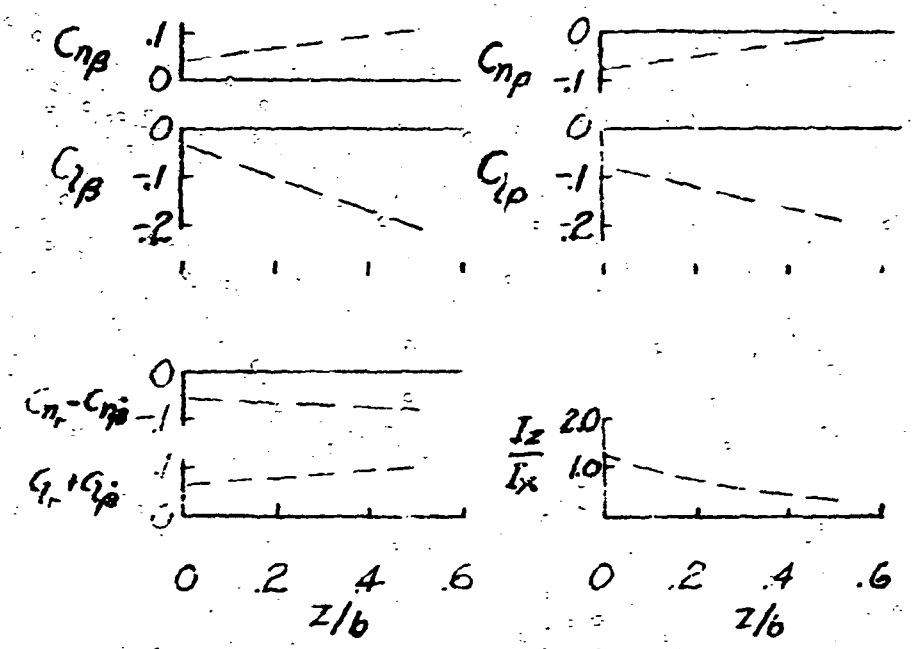

LATERAL STABILITY PARAMETERS

NASA-LANGLEY

Fig. 4

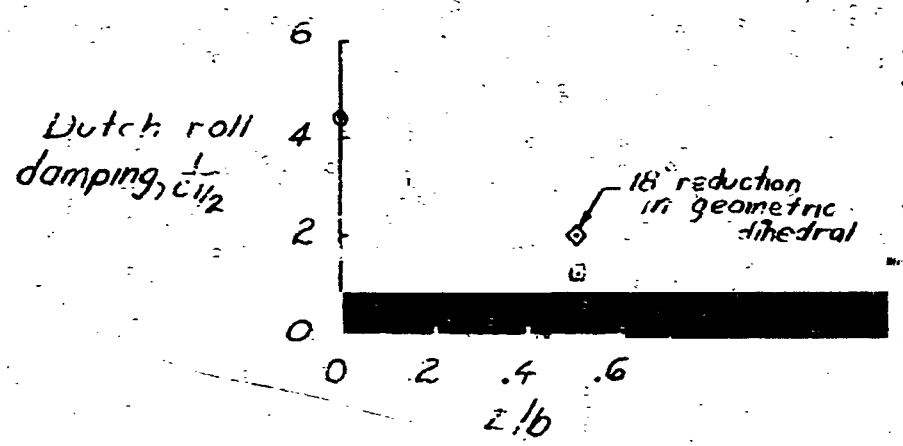

CALCULATED DUTCH ROLL DAMPING

Fig. 5

NASA-LANGLEY

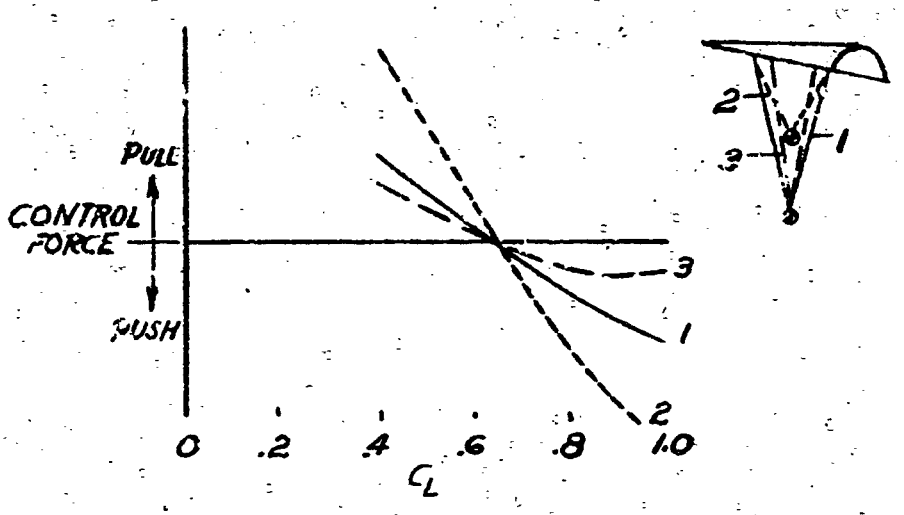

Longitudinal control force characteristics

Fig. 6

NASA-LANGLEY

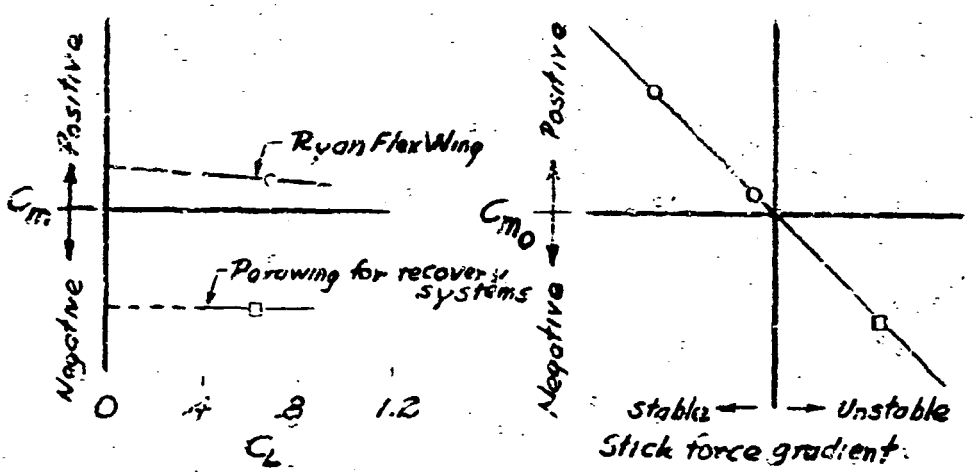

Effect of C_{m_0} on longitudinal stick force gradient

Fig. 7

NASA-LANGLEY

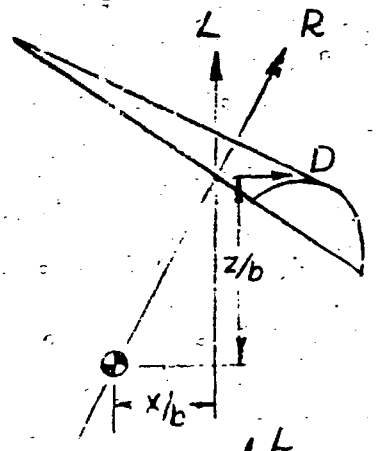

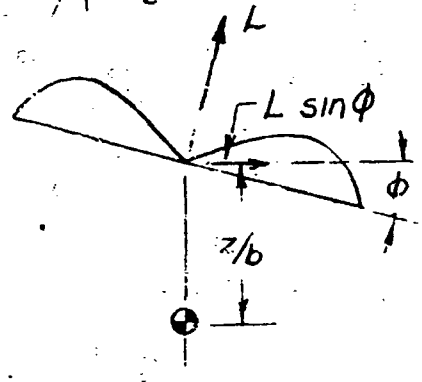

$C_l = C_L \sin\phi \, z/b$

$C_n = C_L \sin\phi \, x/b$

$$C_{l_{net}} = C_L \sin\phi \, z/b \left(1 - \frac{-C_{l_\beta}}{C_{n_\beta} \cdot b/D}\right)$$

LATERAL CONTROL EQUATION

Fig. 8

NASA-LANGLEY

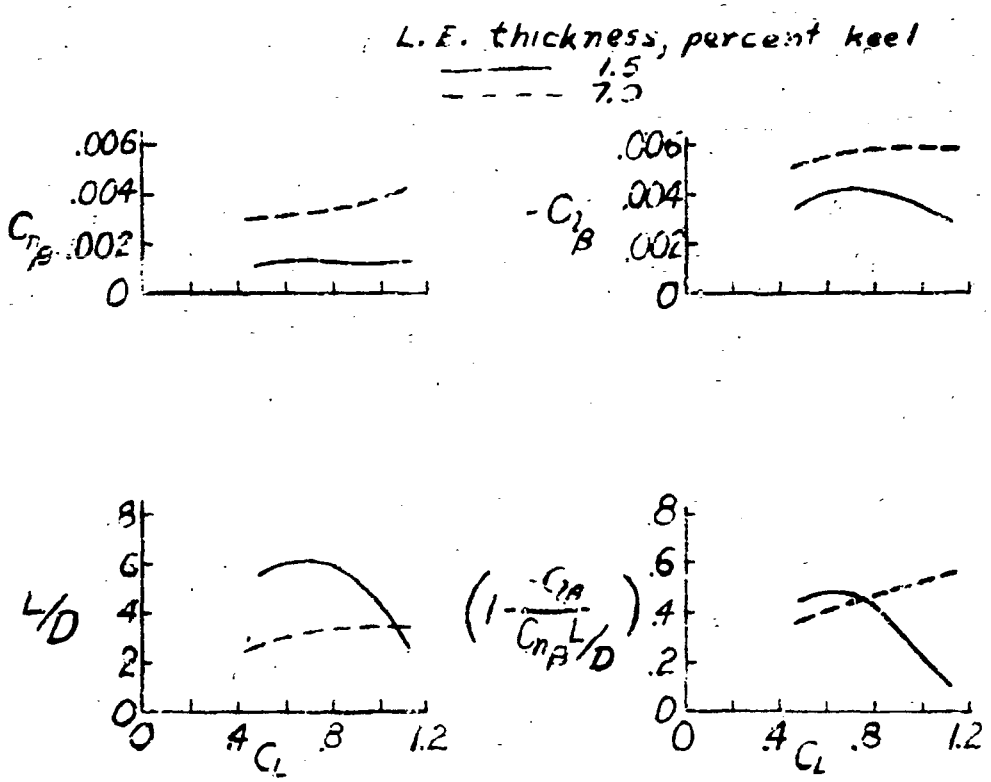

LATERAL CONTROL FACTORS

Fig. 9

NASA-LANGLEY

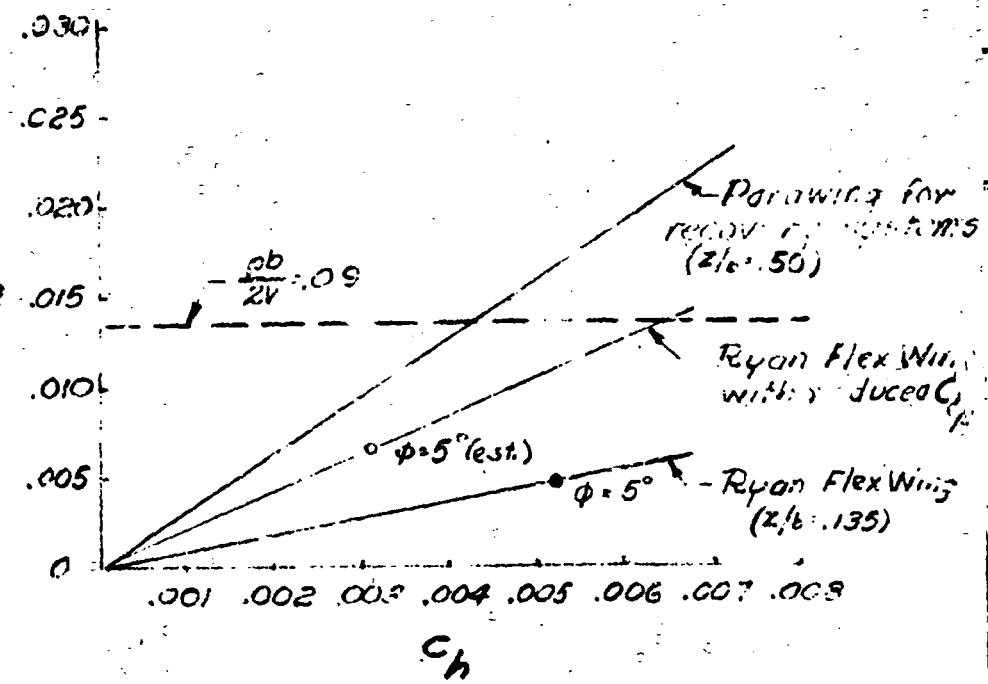

ROLLING MOMENT AND HINGE MOMENT RELATIONSHIP

Fig. 10

NASA-LANGLEY

ALTERNATIVE CONTROL METHODS

1. Trailing edge bolt rope
2. Trailing edge risers
3. Hinged leading-edge and keel members
4. Auxiliary surfaces

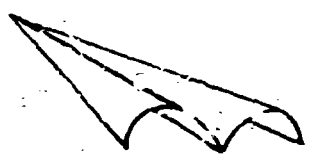

NASA-LANGLEY

Fig. 11

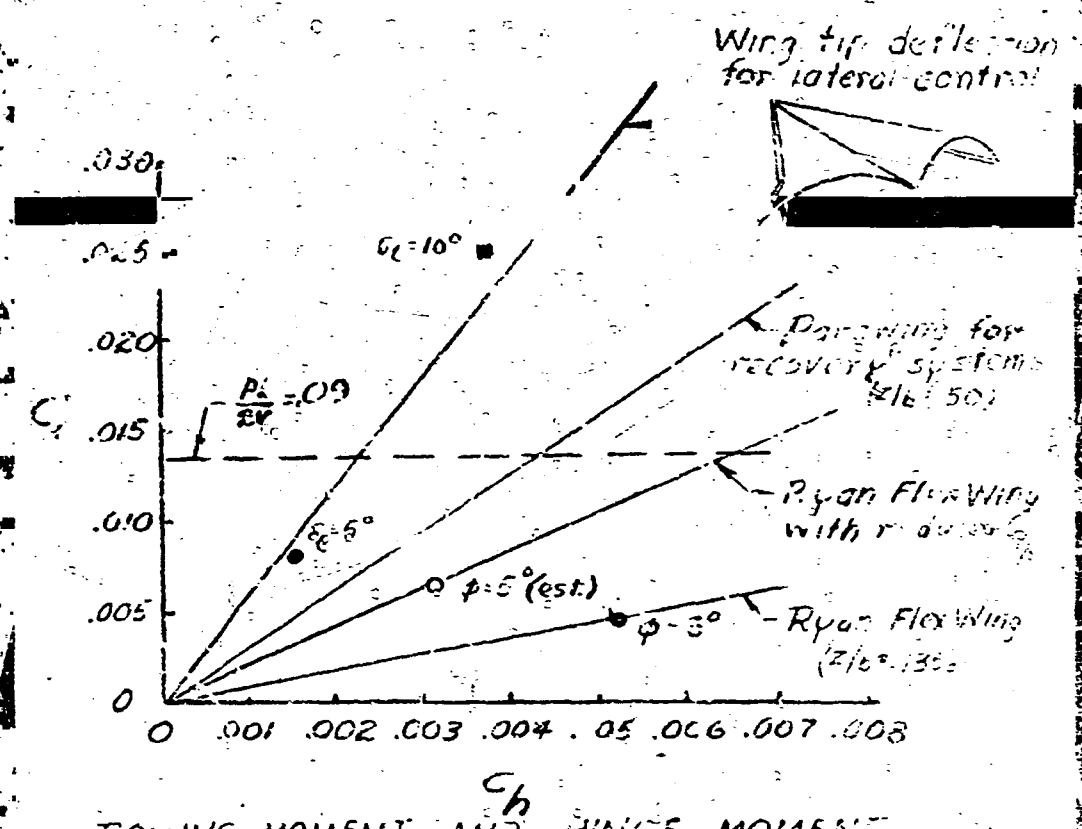

ROLLING MOMENT AND HINGE MOMENT RELATIONSHIP

Fig 12

NASA-LANGLEY

NASA - Langley X64-35843

DYNAMIC STABILITY AND CONTROL CHARACTERISTICS OF PARAWINGS

By Joseph L. Johnson, Jr. and James L. Hassell, Jr.

INTRODUCTION

Recently, the Langley Research Center has conducted several investigations to determine the dynamic stability and control characteristics of models employing the parawing concept. These investigations have consisted of free-flight model tests conducted in the Langley full-scale tunnel and outdoors using the drop-model technique with uncontrolled and radio-controlled models.

The models used in the dynamic stability studies have varied from small-scale, simple research configurations to large-scale, inflatable configurations similar to those currently being considered for recovery system applications. Control for most of the model flight tests was obtained from the center-of-gravity-shift control system but a few tests were made in which other methods of control were evaluated. This paper presents a brief summary of the dynamic stability and control information obtained in these tests and includes the results of related analytical studies and force test investigations.

LONGITUDINAL STABILITY CHARACTERISTICS

Some static longitudinal stability information obtained in recent force test investigations of parawings are presented in figures 1 to 3. Basic pitching moment data for a parawing configuration having a low center of gravity position is presented in figure 1 for an angle-of-attack range of the keel from -10° to 50°. These data show static longitudinal stability

over most of the positive angle-of-attack range with an increase in static stability above the stall. For some parawings, longitudinal instability or pitch-up has occurred near the stall. In the low positive angle-of-attack range, parawing configurations have been found to have very low static stability and instability at low negative angles of attack. This static instability, either at low or high angles of attack can lead to dynamic stability problems. One problem of this type is a tendency toward an end over end tumbling motion which may occur under some conditions of flight. Some static force test information related to the tumbling problem is presented in figure 2.

The data of figure 2 show static pitching moment characteristics over a 360° angle-of-attack range for a parawing configuration with low center of gravity together with similar data for a conventional delta wing configuration with the center of gravity in the plane of the wing. Notice the near 0° and, of course, 360° angle of attack (which also corresponds to 0°) both configurations have a stable trim point. In the case of the conventional wing, a disturbance which pitches the wing away from its trim point is opposed by large restoring moments which are symmetrical at positive or negative angles of attack. In the case of the parawing, however, there is a region of static longitudinal instability at low negative angles of attack and large differences in the magnitude of the positive and negative pitching moments over the angle-of-attack range. The static instability at low negative angles of attack is related to the reversal in the fabric as the wing pitches through zero angle of attack. The large asymmetry in the positive and negative pitching moments is related to the

low center-of-gravity offset. A parawing configuration which pitches downward through its trim point to low negative angles of attack will encounter the region of static longitudinal instability and will therefore tend to pitch downward to even higher negative angles of attack. If the pitching motion is great enough to overcome the restoring moments in the first half of the cycle, then the pitching motion will continue with energy being fed into the system as the configuration seeks its stable trim point near 0° angle of attack. This energy acts as a driving force which tends to pitch the configuration through its stable trim point and into the region of static instability. From these results it can be seen how a steady nose-down tumbling motion could be established for a configuration of this type. It should be pointed out, however, that predictions of a tumbling motion cannot be made based on static data alone. There are other factors, such as damping in pitch and mass and inertia characteristics which must be considered in determining stable and unstable boundaries in a dynamic stability problem of this type. It should also be pointed out that the data presented in figure 2 apply to configurations having rigid connections between the center of gravity or payload and the parawing and therefore are not directly applicable to recovery systems where flexible risers are involved unless the risers are in tension.

Presented in figure 3 is the low subsonic parawing data from the previous figure together with data at a Mach number of 4.5 for the micrometeoroid parawing configuration. It is interesting to note the general similarity in the static pitching characteristics for the two cases in that the Mach number 4.5 data show static instability at low negative angles of

attack and unsymmetrical pitching moment variations over the angle-of-attack range. Based on these data it would appear that the micrometeoroid configuration may have tumbling problems similar to those encountered with the low subsonic models. Analysis made by the 7 x 10-foot tunnels branch has indicated that the build-up in dynamic pressure which occurs when this configuration enters the atmosphere acts to prevent tumbling but there are critical conditions in this speed range where tumbling may occur.

LATERAL STABILITY CHARACTERISTICS

To date, the dynamic lateral stability characteristics of parawings have been found to be generally satisfactory. Presented in figure 4 are some static and dynamic lateral stability derivatives which were measured for a parawing configuration at various center of gravity locations below the parawing keel. Presented in this figure are the static lateral stability derivatives C_{n_β} and C_{l_β}, the yawing derivatives $C_{n_r} - C_{n_{\dot\beta}}$ and $C_{l_r} + C_{l_{\dot\beta}}$, the rolling derivatives C_{n_p} and C_{l_p}, and the ratio of yawing inertia to rolling inertia I_Z/I_X. Some significant changes in these derivatives as the center of gravity was lowered (that is, increasing Z/b) are the increases in directional stability and positive dihedral effect, the increase in damping in roll, and the decrease in the radio of I_Z/I_X. The effect of the changes in these derivatives on the calculated Dutch roll damping is presented in figure 5. Plotted in figure 5 is the calculated Dutch roll damping, $1/c_{1/2}$ (one over cycles to damp to one-half amplitude), against Z/b. Although the data show that the damping for the configuration with the low center of gravity (Z/b = .5) is only about one-fourth of the value for the configuration with the center of gravity on the keel (Z/b = 0),

the damping is still considered good for the low center-of-gravity condition. Reducing the geometric dihedral by 18°, which has been suggested as a possible means of improving lateral control (as will be discussed later), increased the damping for this condition. It should be pointed out that the values of damping shown here do not take into account the effects of bodies beneath the parawing. In cases where large destabilizing bodies are used, the Dutch roll damping could possibly be reduced down into the unstable region.

CONTROL CHARACTERISTICS

As was pointed out in the INTRODUCTION, control for most parawing flight tests to date was obtained from the center-of-gravity-shift control system. Longitudinally, this control system has been found to be generally effective but in some cases large stick forces and unstable stick force gradients have been encountered. Presented in figure 6 are calculated data which show the variation in longitudinal stick force with lift coefficient for a control system of this type using several different riser arrangements. These results, which were presented by Hewes at the Apollo Conference last year, show unstable stick force gradients and indicate that the gradients can be altered appreciably by changing the riser lengths and attachment points. Analysis indicates that the stick force gradients could have been made stable in these cases by proper arrangement of the risers. It is, of course, desirable to have the stick force gradient stable from handling qualities considerations and to keep the gradients low from control power requirements.

In the analysis of this type of control system it was found that the significant factor involved in determing the stick force characteristics was the C_{m_o} of the wing. Some information to illustrate this point is presented in figure 7. On the left side of this figure is a plot of the pitching moment coefficient (referred to the parawing keel) against lift coefficient and, on the right side, is a plot of C_{m_o} against stick force gradient. The data presented are for the Ryan Flex-Wing configuration and for an inflatable parawing of the type being considered for recovery system applications. In the case of the Ryan Flex-Wing, it was found that at moderate lift coefficients this configuration had positive values of C_{m_o} which produced a high stable stick force gradient. In order to reduce the stick forces in this case, the gradient was lowered by reducing C_{m_o} through trailing-edge modifications to the wing so that in the final arrangement the stick forces were in a more tolerable region. Based on these data, it appears that parawings for recovery systems, which have been found to have negative values of C_{m_o}, will have high unstable stick force gradients unless some means is used to reduce these values of C_{m_o}, either by changes in the wing itself or by changes in the rigging as mentioned earlier.

From the lateral control standpoint, there has been some indication of possible problems in the use of the center-of-gravity-shift control system. An equation for calculating the net rolling moment produced by this type of control system is presented in figure 8. This equation is $C_{l_{net}} = C_L \sin \phi \, Z/b \, (1 - -C_{l_\beta} / C_{n_\beta} \, L/D)$. The $C_L \sin \phi \, Z/b$ term in this equation is derived from the fact that when the wing is banked, the lift vector is tilted and has a component which produces a rolling moment about

the center of gravity through the moment arm Z/b. The term $(1 - -C_{l_\beta}/C_{n_\beta} L/D)$ is called the rolling effectiveness factor and is derived from the fact that the lift component which produces roll is rearward of the center of gravity and also produces an adverse yawing moment through the arm X/b. When the sideslip angle resulting from this adverse yawing moment is taken into account, it can be shown that the favorable rolling moment produced by the lift vector is reduced through the effective dihedral parameter C . For configurations having high ratios of $-C_{l_\beta}/C_{n_\beta}$ and low values of L/D, the rolling effectiveness term becomes small and therefore the net rolling moment produced in such ases is reduced. Presented in figure 9 are some data showing the effect of leading-edge thickness on these parameters. Plotted in this figure are values of C_{n_β}, $-C_{l_\beta}$, L/D and the rolling effectiveness factor $(1 - -C_{l_\beta}/C_{n_\beta} L/D)$ for a parawing with a leading edge thickness of 1.5 percent of the keel and another having a leading edge thickness of 7 percent of the keel. These results indicate that the rolling moment produced by banking the wing is reduced by about 50 percent at moderate lift coefficients for either wing and that the rolling effectiveness for the wing with the thin leading edges decreases rapidly with increasing lift coefficient and approaches zero near maximum lift coefficient. It is significant to note that for the thick leading-edge configuration, which is representative of inflatable parawings now being considered for recovery systems, there is an increase in effectiveness with increasing lift coefficient.

In discussing lateral control characteristics, another factor which must be considered is that of lateral hinge moments. Some indication of the lateral hinge moment characteristics involved in the center-of-gravity-

shift control system was obtained in the force test investigation of the Ryan Flex-Wing airplane. Some of the results obtained in this investigation are presented in figure 10. Plotted in this figure is rolling moment coefficient against roll hinge moment coefficient. The horizontal dashed line plotted in this figure represents the value of C_l required to produce a pb/2V of 0.09 based on a value of damping in roll of -.15. This value of pb/2V is the minimum value specified in the handling qualities requirements for a light liaison airplane. It is presented here merely to establish a reference for purposes of comparison and is not intended to imply that this value of pb/2V is a valid specification for parawing applications. For recovery system applications, a smaller value may well prove to be acceptable. Considerably more research and flight experience will be required to establish the proper criterion for this case. The solid circle at the lower right, which represents measured data, shows that 5° of wing bank produces only about one-third of the rolling effectiveness required by the pb/2V = .09 criterion. The stick force corresponding to the hinge moment for this condition was about 70 pounds. Analysis indicated that reducing C_{l_β} by using 18° negative geometric dihedral angle of the wing would improve the rolling effectiveness and reduce the hinge moments. It was also estimated that increasing Z/b up to 0.5, which is a value representative of parawing recovery systems, would substantially increase the rolling moments without increasing the hinge moments.

Because of the problems that have been encountered with the center-of-gravity-shift control system, some attention has recently been given to other methods of control for parawings. Presented in figure 11 are some of the alternative control methods that have been proposed. These methods are:

1. Trailing edge bolt rope. In this control system the tension is increased or decreased in a cable in the parawing trailing edge to provide pitch or roll control.

2. Trailing edge risers. In this control system risers are attached to the parawing trailing edge and pulled down or released to provide control.

3. Hinged leading-edge or keel members. In this control system hinges are placed in the wing leading edges or keel and the aft portion of these members deflected for control.

4. Auxiliary surfaces. This control system is concerned primarily with surfaces placed at the rear of the wing to provide directional control.

Some promising results have been obtained with a wing-tip control system in tests in the Langley full-scale tunnel with the Ryan Flex-Wing airplane. In order to show how these results compare with those for the center-of-gravity-shift control system, data for both types of control are presented in figure 12. Plotted in this figure are the data for the wing bank control system from figure 10 for comparison purposes. Also plotted are measured data for 5° and 10° deflection of the aft 25-percent of the wing leading edges for control. These results show that with about 7° deflection of the wing tips a $pb/2V$ of .09 could be produced with a hinge moment coefficient considerably less than that produced by banking the wing. The stick force corresponding to the hinge moment for 7° deflection of the wing tip was about 30 pounds on the Ryan Flex-Wing airplane.

SUMMARY

1. Parawing configurations generally have satisfactory dynamic longitudinal stability characteristics in the normal operational angle-of-attack range but there may be problems at extreme angles of attack (either high or low) because of static longitudinal instability.

2. Laterally, parawing configurations generally have satisfactory dynamic stability characteristics.

3. From the control standpoint, the use of the center-of-gravity-shift control system may be generally satisfactory for recovery systems applications but this type of control system may introduce some stick-force problems and may become inadequate for configurations having high ratios of dihedral effect to directional stability and low values of L/D.

STATIC AERODYNAMIC CHARACTERISTICS
OF PARAWING (BASIC Λ=45°, DEPLOYED Λ=55°)

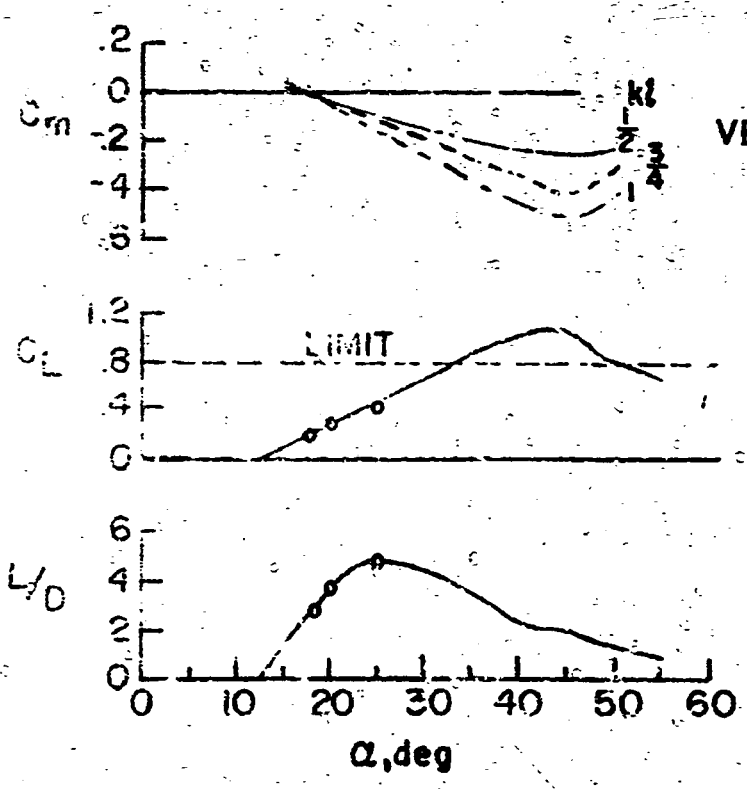

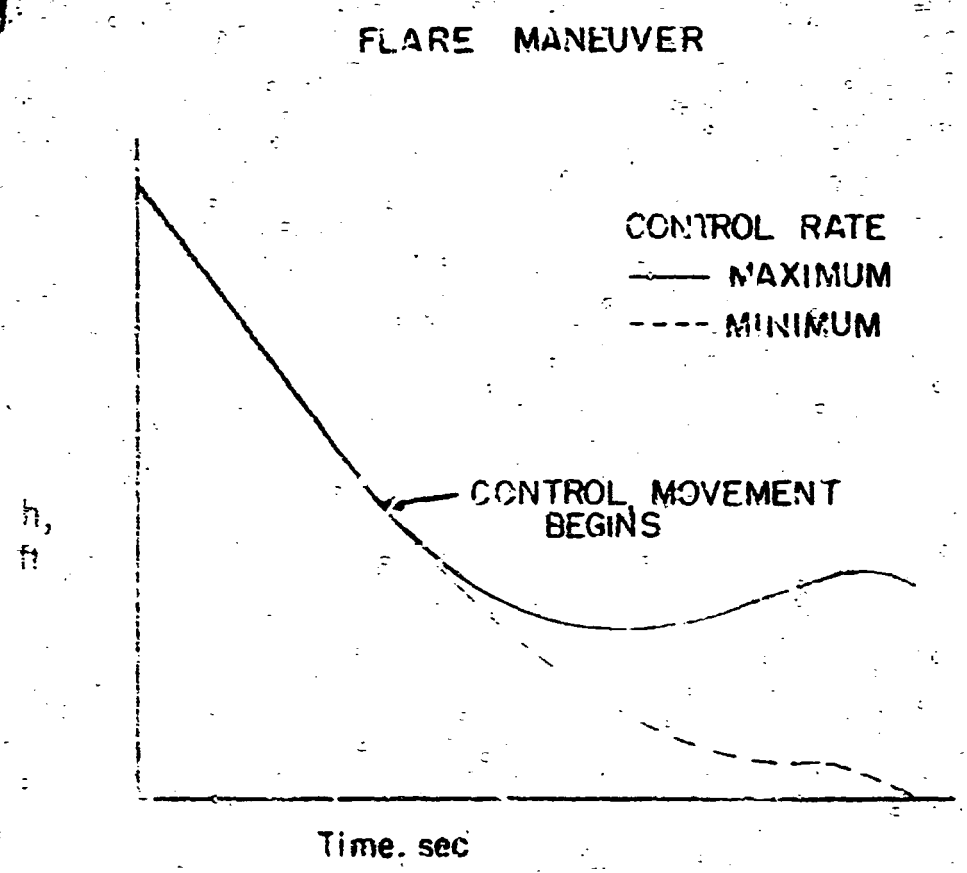

2

NASA-LANGLEY

ALTITUDE USED DURING FLARE

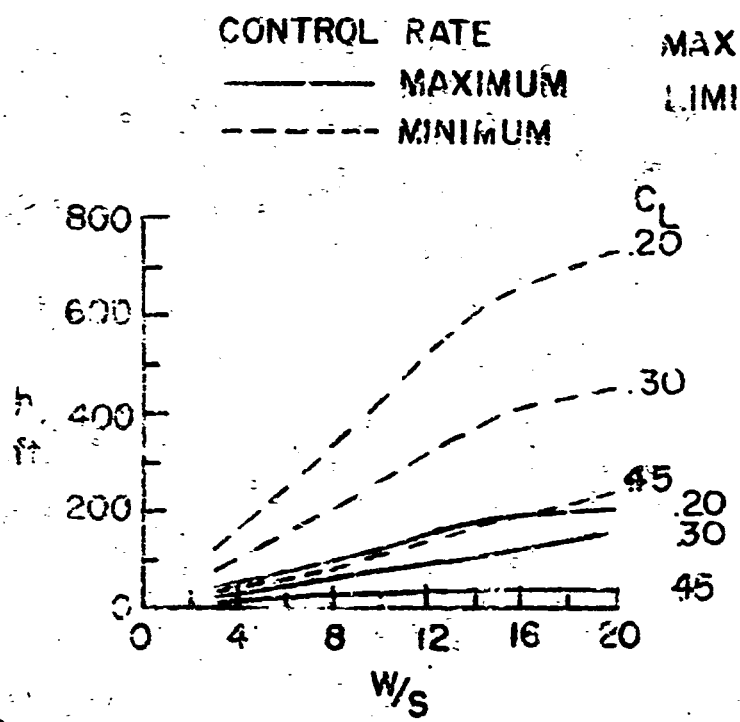

3

DESCENT RATES FOR TRIMMED GLIDE CONDITIONS

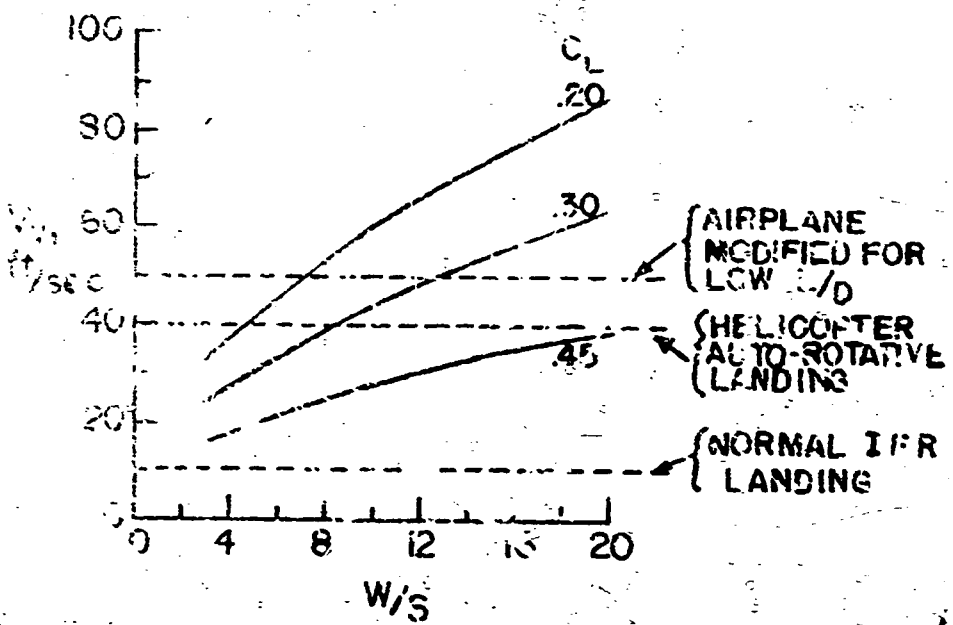

NASA - Langley

X64-35844

DEPLOYMENT TECHNIQUES OF A PARAWING
USED AS A RECOVERY DEVICE FOR MANNED REENTRY
VEHICLES AND LARGE BOOSTERS

by Sanger M. Burk Jr.

One of the problems associated with recovery of manned reentry vehicles and large boosters is deployment of the recovery device, and studies of this problem at Langley to date have been primarily on parawings. A slide has been prepared showing the status of parawing-deployment investigations at Langley.

SLIDE NO. 1, PLEASE

The majority of the investigations were made at low subsonic speeds utilizing dynamic models in free flight. For the investigations made to date, the results obtained are primarily in the form of movie film which shows the deployment process. As the chart indicates, most of the deployment tests have been on parawings having rigid leading edge and keel members. I would like to discuss very briefly these tests. The drop tests consisted, in general, of releasing dynamic models at low speeds ($q \approx 5^{\#}/ft^2$) from a hovering helicopter; most of the deployments were successful. Results from rocket launch tests indicated successful deployments could be obtained at Mach numbers between 2.0 and 3.0 and at altitudes ranging up to 180,000 feet. On the landing loads track models were deployed at a dynamic pressure of about $13^{\#}/ft^2$. The wind tunnel tests consisted of deploying the model at a dynamic pressure of $13^{\#}/ft^2$ and also at Mach numbers between 2.5 and 4.5. Currently planned investigations include drop tests of a full scale model of a parawing which will be used in the micrometeoroid experiments. This model will be released at low speeds from a helicopter. Finally, for the wind tunnel tests two aeroelastically scale models are being constructed. Tests will include the

determination of the loads during deployment and also its proper deployment sequence. A third parawing configuration is under study which would have curved leading edges or a cylindrical canopy shape so as to obtain larger L/D's. (Slide off)

My talk today will deal with the results of an investigation involving complete deployment of a parawing when stowed as a recovery device on a 1/5-scale model of a manned reentry vehicle and on a 1/12-scale model of a large booster. These models were radio-controlled and released from a helicopter for flight testing at an approximate altitude of 3500 feet. The next slide shows the full-scale characteristics and schematic drawings of the booster-parawing combination and of the manned reentry vehicle-parawing combination.

SLIDE NO. 2, PLEASE

The results of the investigation will be shown in motion pictures and will illustrate some of the problem areas encountered and how a satisfactory deployment technique was developed. However, because some of the details of the deployment technique may be hard to follow in the motion picture film, the sequence for satisfactory deployment is shown on slides. First, a deployment is shown utilizing a folded parawing for compact stowage on the booster, and then a deployment is shown utilizing a telescoped parawing on the reentry vehicle. The next slide shows the satisfactory deployment technique for the booster.

SLIDE NO. 3, PLEASE

The next slide shows the satisfactory deployment technique for the reentry vehicle.

SLIDE NO. 4, PLEASE

The movie film I am going to show you depicts some of the highlights of the investigation, including, as previously mentioned, some of the problems encountered and the satisfactory technique developed.

MOVIE FILM PLEASE

In conclusion, on the basis of the ensuing motions obtained in this investigation it appears that deployment problems, not considering loads, associated with parawings as a recovery device at low speeds can be satisfactorily solved within the present state of the art.

RESEARCH ON PARAWING DEPLOYMENT AT LANGLEY

Status	Type of Parawing	Free Flight			Wind Tunnel
		Drop tests	Rocket launch	Landing loads track	
Investigated	Rigid	Yes	Yes	Yes	Yes
	Inflatable	Yes	No	No	No
Currently planned	Rigid	No	No	No	No
	Inflatable	Yes	No	No	Yes

1.

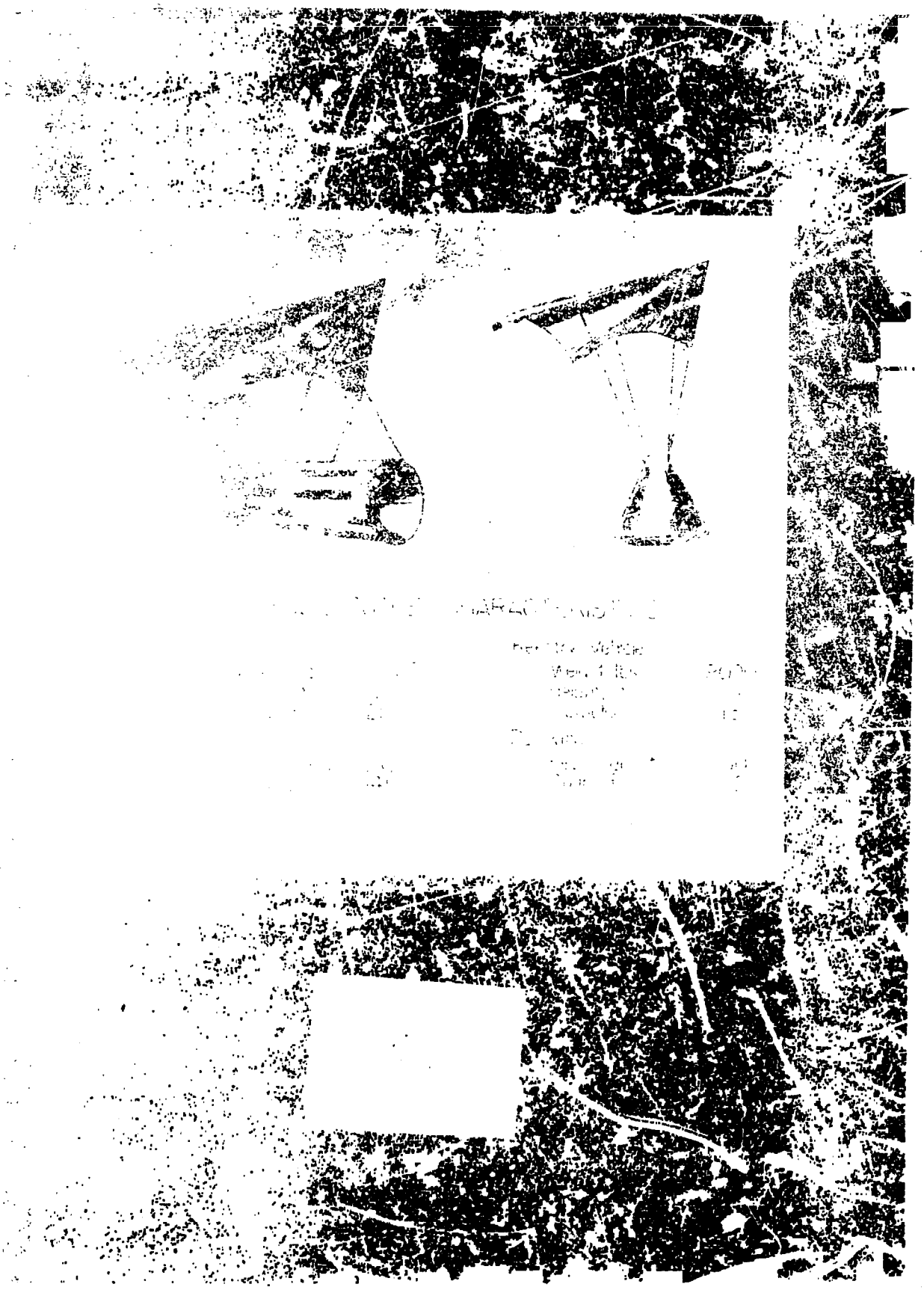

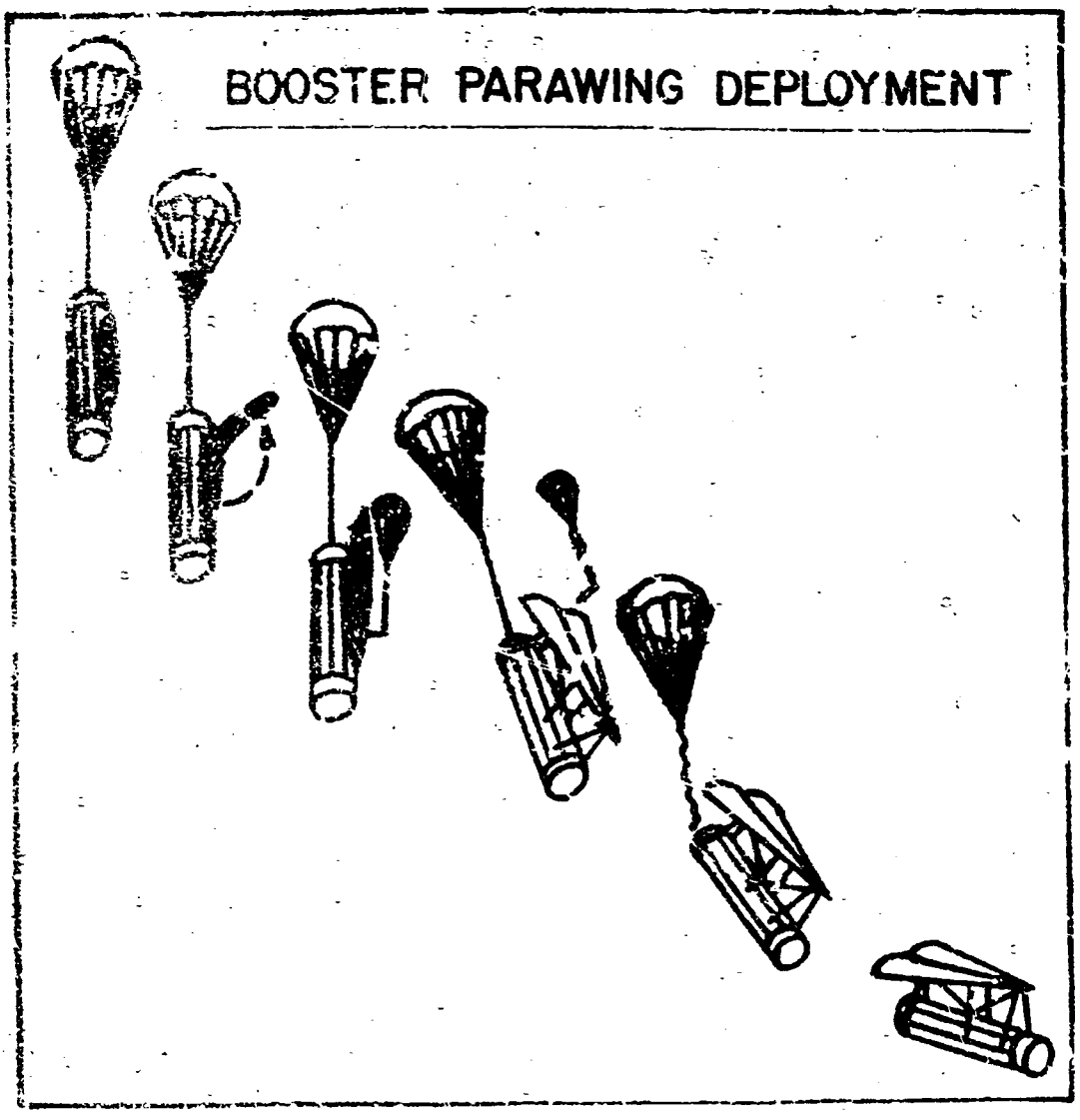
BOOSTER PARAWING DEPLOYMENT

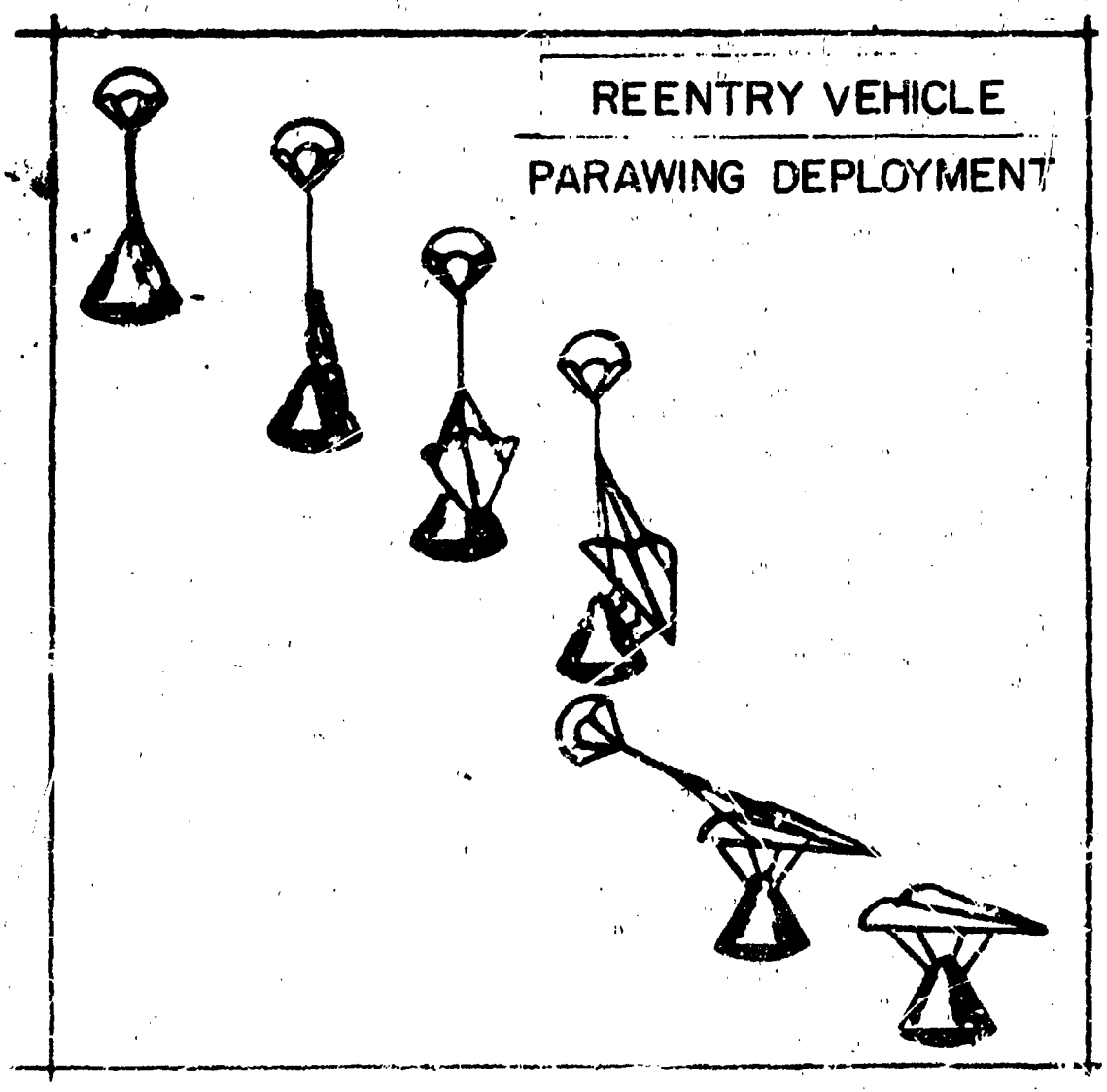

4

X64-35845

NASA - Langley

AN ANALYTICAL INVESTIGATION OF LANDING FLARE MANEUVERS OF A PARAWING-CAPSULE CONFIGURATION

By Ernie L. Anglin

Presented To
Space Vehicle Landing and Recovery Research
and Technology Meeting
NASA Headquarters, Wash., D. C.
July 10-11, 1962

An analytical study is being made to determine the capabilities of various parawing configurations for executing satisfactory flared landing maneuvers, and to investigate the factors which influence this capability. This study was initiated because doubt existed as to whether a parawing could perform a flare from trimmed glide conditions at max L/D, especially at low wing loadings.

For this study, a cone-shaped capsule having a weight of 5000 pounds is used for a payload. Control is achieved by varying the position of the payload with respect to the wing. A time history of the motion during the flare is obtained by utilizing three-degree-of-freedom equations of motion and a high-speed digital computer.

SLIDE NO. 1

The static aerodynamic characteristics of the wing used are shown as a function of angle of attack. This data is for a wing having rigid keel and leading edge members and a conical shape when deployed. This wing had a basic sweep angle of 45 degrees laid out flat, and a deployed sweep angle

of 55 degrees. The aerodynamic data shown is pitching moment coefficient, lift coefficient, and L/D. The pitching moment coefficients are for the three vertical payload positions investigated; 1/2, 3/4, and 1 keel length below the wing. For each of these vertical payload positions, you will note that a stable pitching moment curve exists. The maximum lift-coefficient is approximately 1.0; the maximum L/D is 4.7. The symbols on the C_L and L/D curves indicate the trimmed glide conditions from which flares were attempted. These trimmed glide conditions are for lift coefficients of .2, .3 and .45. The .45 condition is where the maximum L/D occurrs. For all motions encountered during the flare attempts, the lift coefficient was never allowed to exceed a value of .8.

SLIDE NO. 2

From each trimmed glide contion, flares were attempted as follows: At some position along the flight path, indicated here by the arrow, the control movement for the flare was begun. The control movement used was a single shift of the payload longitudinally, made at a constant rate. As shown by the solid and dotted lines, respectively, a maximum and a minimum control rate were determined which would give a satisfactory flare without exceeding the C_L limit of .8. A flare initiated below the altitude used for the maximum control rate cannot, of course, be completed before ground contact. Flares initiated above the altitude used for the minimum control rate can be satisfactorily completed, but the completion will occur somewhere above ground level. The altitude range between these two limits is the range available to the pilot during which he must decide when he is at the proper altitude and begin his control movement. The pilots' decision time will be a function of this altitude range and the rate of descent.

SLIDE NO. 3

The altitude used during the flare is presented as a function of wing loading and trimmed glide lift coefficient. A wing loading range of 3 to 20 pounds per square foot was investigated. The maximum L/D and the C_L limit are listed. Again, the solid lines are for the maximum control rare, and the dotted lines are for the minimum control rare. For this particular wing, it was found that a satisfactory flare maneuver could be obtained from all combinations of wing loadings, vertical payload positions, and trimmed glide lift coefficients investigated. Larger pilot decision times come with the higher wing loadings and lower C_L's. At the same time, flares made in this region must be initiated at relatively high altitudes, which may become difficult for the pilot to judge accurately. Conditions with low wing loadings and higher C_L's can be flared from altitudes which are closer to the ground and which are therefore easier for the pilot to judge, but the decision time is greatly reduced. The decision times encountered herein varied from 6 seconds to 1 second. The time from the flare initiation to the flare completion at touch-down varied from 2 seconds (for ____ $w/s=3$ $C_L=.45$) to 21 seconds (---- $w/s=20$ $C_L=.2$). G-loads encountered by the pilots are normally less than 1 1/2-g's. It was found that all the flares shown here were made without exceeding this value, so the g-loads encountered are well within the range of the pilot's present experience.

SLIDE NO. 4

The rates of descent for the trimmed glide conditions used are presented as a function of wing loading and trimmed glide C_L. These rates of descent are compared with the rates presently encountered by pilots. The first dotted line is at 10 feet per second, a rate normally used by aircraft

making an IFR type landing. The next dotted line, at 40 feet per second, represents the rates encountered by helicopter pilots making auto-rotative landings. The last dotted line, at 50 feet per second, indicates a descent rate encountered when a T-28 airplane was modified for low L/D landings. (NASA Memo 3-12-59L). The X-15 (NASA TM X-195) has a descent rate of 120 feet per second, but it also has a wing loading of 66, so it cannot be directly compared with the parawing values shown. The rates of descent for the parawing configuration are therefore within the range of present pilot experience. However, the pilots are not used to encountering these rates at the relatively low wing loadings shown here.

The landing flare parameters just presented have been discussed with several Langley pilots. It is felt that additional pilot experience is necessary due to the relatively high descent rates and the small pilot decision times associated with the lower wing loadings. It should be mentioned that one of the Langley pilots has recently made some flared landings in an aircraft with an L/D of 3 and a wing loading of 11. The flare portion of the landings was accomplished successfully, but some difficulty was encountered in making the touch-down at a predetermined spot on the runway.

Among the factors which should receive additional study are the capabilities of different wing shapes, the effects of flexibility in the leading edge sweep angle when no spreader bar is present, control rigging set-ups and their corresponding power requirements, and pilot capabilities.

X64-35846

NASA - Langley

PARACHUTE LOADS, AEROELASTICITY AND MATERIALS

By Robert T. Taylor and James F. McNulty

INTRODUCTION

Improvements in paraglider aerodynamic performance characteristics indicated by recent wind-tunnel tests have prompted the Langley Research Center to investigate paraglider loads as a function of the aerodynamic parameters involved in the performance increases. An effort is also underway to attempt to calculate both the aerodynamic loads and performance associated with these configuration changes, to allow the evaluation of parametric changes without the need for extensive tunnel testing.

Structural analyses have been continuing which point up some interesting results as regards the problems of weight and materials.

It is the purpose of the present paper to present some of the highlights of recent research concerning loads, structures and materials, and to indicate by implication, the type of data which are available for use in the design of paragliders.

DISCUSSION

Uncertainties in the exact shape of the cloth membrane of the paraglider have been the biggest obstacle in calculating the air-load distribution over a representative canopy. Some early pressure data obtained on rigid conical models has suffered in application because of the aforementioned shape uncertainties. Recent force test measurements have been made on a semispan glider model with a cloth wing, which is shown in the first slide.

SLIDE I

The model shown here was mounted on two balances, one semispan balance which allowed the measurement of total load and another six-component balance which measured the load on the leading edge.

The variables covered were aspect ratio 2.5, 4.0, 6.0 and twist distribution indicated below by the values of washout at the .80 span station. Loads carried in the paraglider structure can be divided into two classes: (1) loads normal to the plane formed by the wing tip and keel. and (2) loads parallel to the plane of the wing tip and keel. These loads may be treated separately and added vectorially to arrive at a final loading, on which the design of the structure may be based.

SLIDE II

The next slide shows a comparison of the measured spanwise lift distribution obtained from pressure surveys on a rigid conical model, and calculated values using the twist distribution of the models. As might be expected the calculated values agree well with the measurements when the twist is known.

Spanwise lift centers are also shown on the slide. Here we have the lift center given by pressure tests, the calculated lift center, and spotted on for comparison is the lift center obtained from the semispan force test model. While only one point is shown here, good agreement with both theory and pressure tests was obtained throughout the "linear" angle-of-attack range and agreement is shown with the pressure measurements past the stall.

The lower part of the figure shows the extreme loading due to twist at a lift coefficient of zero.

Not much more can be said about the normal or lift distribution of load in the paraglider members without knowing the placement and number of the shroud lines, so let us look at the moments about the apex, in the plane of the leading edge and keel.

SLIDE III

Here we have plotted apex hinge moment as a function of angle of attack for an aspect ratio-2.5 glider with canopies having different values of washout. The sketches show the relative degree of flatness of the canopies under load. The darkened symbols indicate the angles of attack at which $(C_L)_{max}$ occurred.

These data serve to illustrate a number of points: (1) increases in washout are associated with decreasing in-plane apex moment, and decreasing lift-drag ratio if the leading-edge sweep or wing span is held fixed. (2) the design of the glider frame for strength is fixed by the maximum lift-coefficient point. The data were taken through an angle of attack of 90°, and while not shown here the level of apex moment at $C_{L_{max}}$ or stall is not exceeded.

Below the stall you will notice that the slope of C_L with α is negative for the full canopy and positive for the flat canopy. In the case where the wing is flexible (e.g. can change sweep or span with changes in angle of attack) the slope of this line may effect the gust response of the glider. Note that with this full canopy a positive change in α reduces the tendency to close which might increase the span somewhat making the glider more sensitive to gusts while with the flat canopy positive angle-of-attack changes reduce span possibly alleviating the gust response.

Paraglider wings with flexible frames have been tested at Langley in connection with government sponsored programs for (1) the recovery of the Saturn booster in which the Marshall Space Flight Center is interested and (2) in connection with the recovery and launching of the Gemini spacecraft, which is of interest to the Manned Spacecraft Center.

Generally speaking the introduction of flexibility into the structure results in some saving in weight. The next slide (slide IV) shows some curves which indicate paraglider structural efficiency. Here is plotted the ratio of paraglider weight to gross weight for rigid and flexible systems. The scale on the right represents the volume required to stow the paraglider system, and is obtained by assuming a stowed density of 23 pounds per cubic foot.

Decreases in weight can be achieved if structural flexibility is allowed in the paraglider frame as shown here. It should be noted, however, that flexible gliders are much more difficult to analyze both aerodynamically and structurally because of the interdependence of aerodynamic load and configuration.

Elastically and dynamically-scaled inflatable models of both relatively rigid and flexible paragliders are being fabricated under contract with G. A. C. These models will be used to study the paraglider deployment characteristics along with the effects of aeroelasticity. In addition these models reproduce the buckling in the inflated structural tubes which is important in defining aerodynamics.

These data should be available to evaluate the trade-offs between weight and performance previously mentioned.

The last curve on the slide shows further improvement in the weight picture through the use of different gas tight materials, in this case a film-fabric construction of dacron and mylar similar to the sample I have here. Should such a material prove feasible and allow the omission of the elastomer which weighs as much as the fabric, significant weight savings would result.

We will discuss more about materials later.

In addition to being more difficult to analyze, flexible paragliders usually suffer some degradation in performance. The next slide shows a plot of L/D against C_L for the Gemini-paraglider configuration. The three curves represent the aerodynamics of gliders having three stiffnesses. The degradation in $(L/D)_{max}$ is obvious but note that at higher C_L the curves tend to merge, so that if touchdown conditions are more important in a particular application than range considerations the requirement for stiffness in the glider frame may be relaxed to yield a somewhat lighter weight and more readily stowable recovery system.

High temperature materials are also under investigation by Langley Research Center in connection with the micrometeoroid paraglider experiment which will have to survive reentry temperatures (1000° F). For the inflated members of the paraglider, Langley Research Center is investigating the feasibility of a fiberglas-silicone combination. Since silicone is difficult to "work", seams and junctures represent a considerable problem which is being studied. Firings from White Sands Missile Range are scheduled for next summer.

In conjunction with the aerodynamic and materials studies, Langley Research Center continues investigations in structural analysis. While structural design analysis procedures have been developed for paragliders with co-planar leading edges and keel (these procedures have been used for free-flight models, wind-tunnel models and the micrometeoroid paraglider), the recent incvation of the utilization of helical leading edges, discussed by Mr. Sleeman, represents a new structural problem. Langley Research Center has a program underway to define its structural problem areas; it is hoped that the material and geometric

coefficients being developed by testing by Goodyear and North American under a MSC contract will suffice to allow an evaluation of the problem. Should a favorable solution to this problem be indicated, it is anticipated that scaled models will be used for test purposes since it has been found that designs can be scaled without use of "exotic" materials.

EFFECT OF STIFFNESS ON L/D

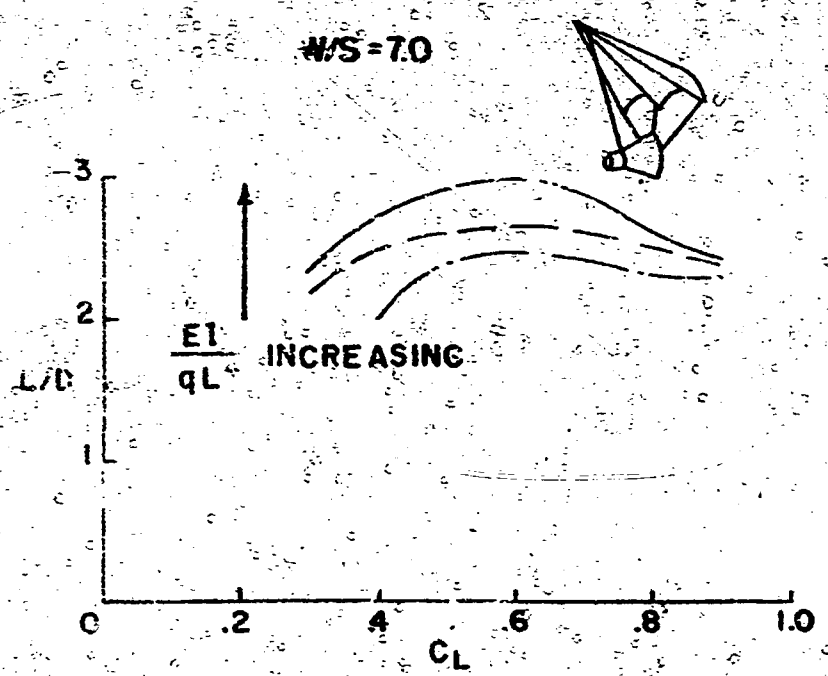

PARAGLIDER STRUCTURAL EFFICIENCY

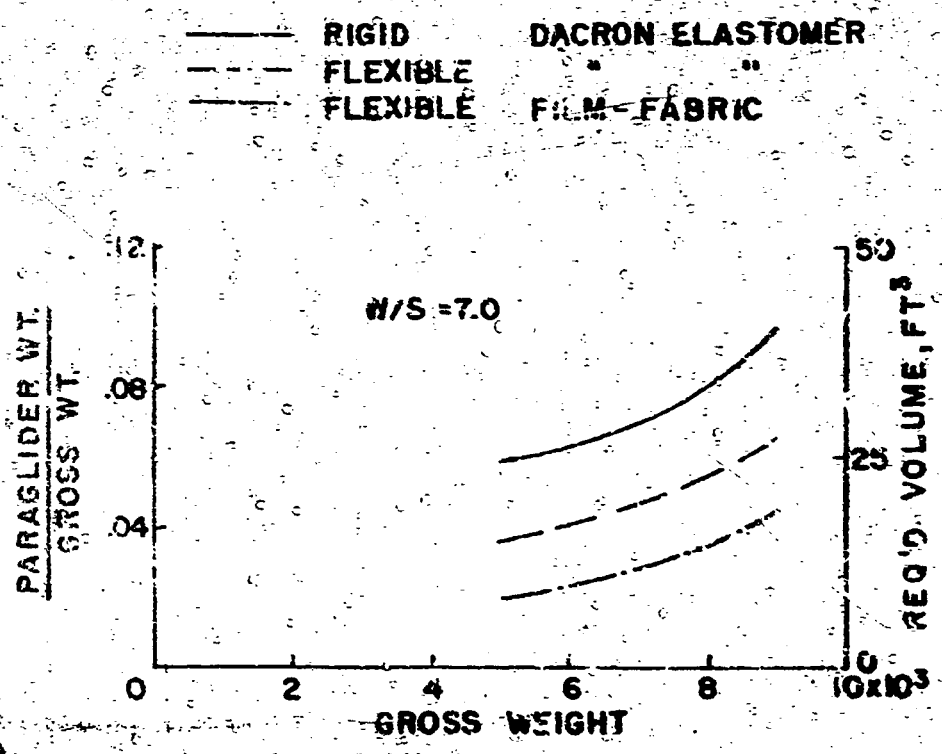

EFFECT OF TWIST ON APEX HINGE-MOMENT (IN PLANE)

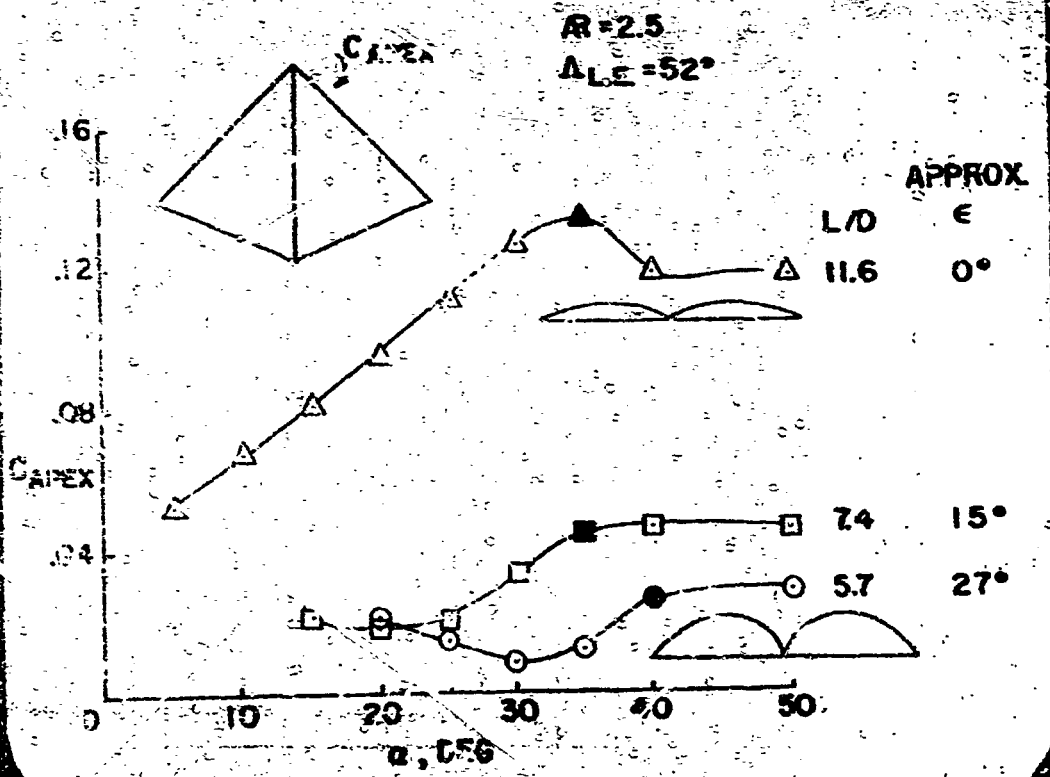

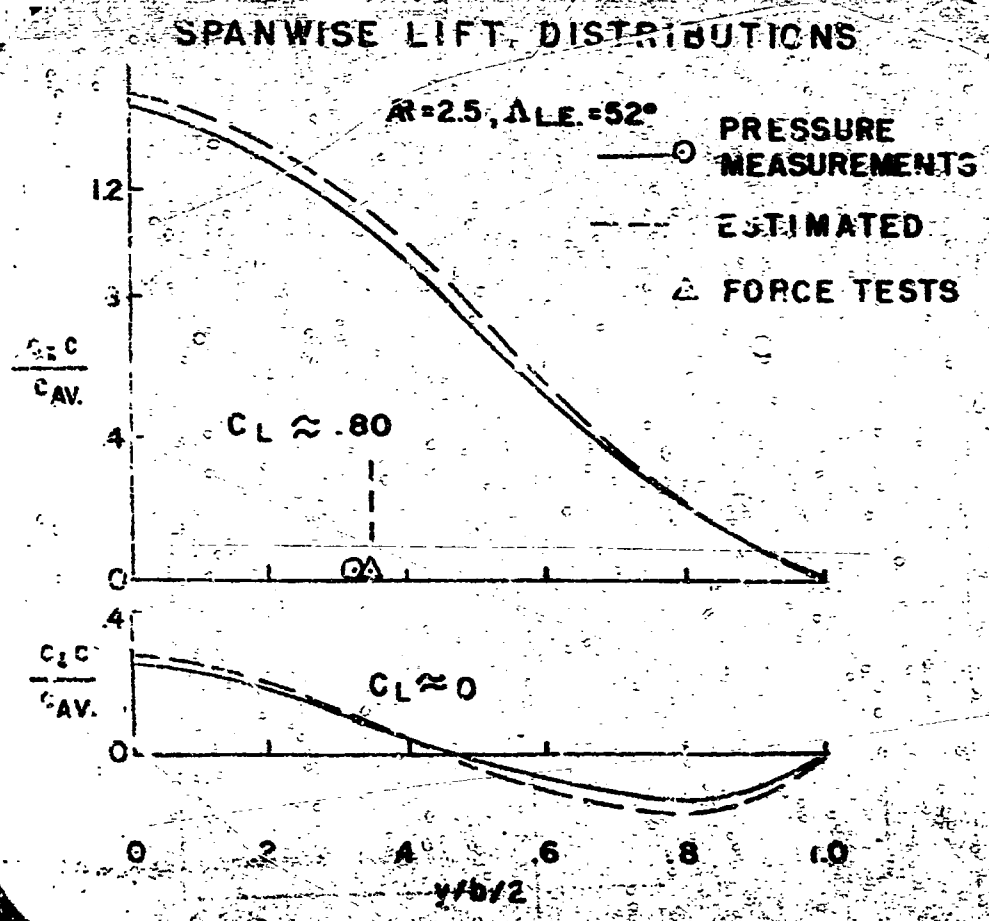
SPANWISE LIFT DISTRIBUTIONS
AR=2.5, Λ L.E.=52°
PRESSURE MEASUREMENTS
ESTIMATED
FORCE TESTS
1.2
.8
.4
0
$\frac{C_l c}{c_{AV.}}$
$C_L \approx .80$
.4
0
$\frac{C_l c}{c_{AV.}}$
$C_L \approx 0$
0
.2
.4
.6
.8
1.0
y/b/2

SEMI-SPAN WIND TUNNEL MODEL

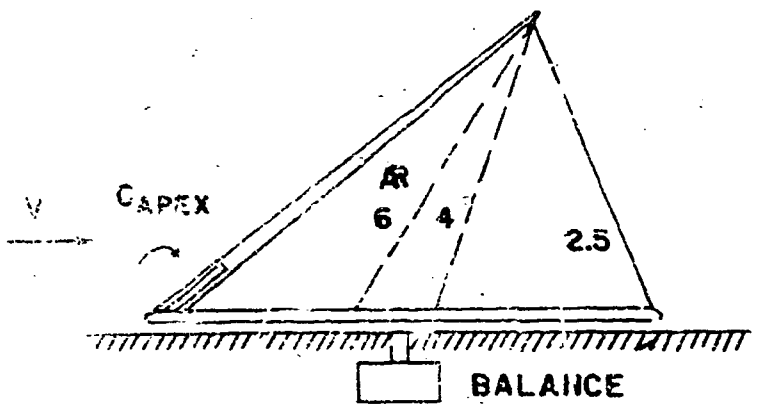

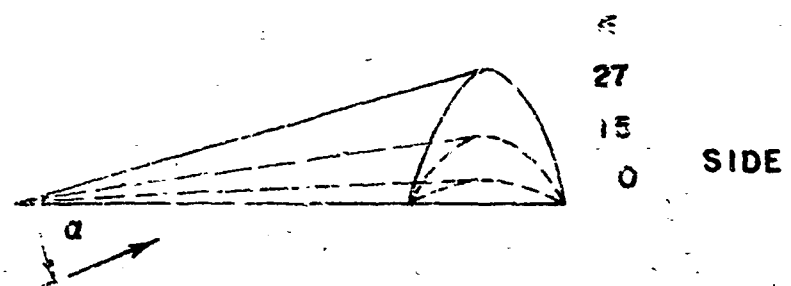

X64-35847

NASA - Langley

ROTARY-TYPE RECOVERY SYSTEMS

by Charles E. Libbey

The Langley Research Center has tested, or is currently testing, several types of rotary devices with applications for recovery systems. The first slide is a chart of these systems showing the areas where data are presently available and the areas where research is still required. (Slide.)

The vortex ring parachute resembles a Maltese cross when viewed from above. Deployment, stability, and performance tests have been completed. A report containing this data is in the review stage now and will be available soon. This system is not intended to glide, however as for most parachutes, it can be forced to produce a small amount of L/D.

The flexable rotary wing consists of strong cables at the leading and trailing edges with parachute type material stretched between them. A weight at the tip provides centrifugal force to maintain all components in tension while rotating. Some preliminary deployment tests have been conducted using a 4 bladed 6 foot diameter model. The cloth rotor blades were attached to a 32 inch diameter vortex ring parachute which was used to provide the initial rotation for the system. After the deployments, the rate of rotation increased, indicating that the blades were autorotating and were not being driven by the rotating parachute. Performance data have been obtained for a 2 bladed 4 foot diameter rotor, most of it for the vertical autorotative descent condition. For these tests, the blades were attached to a short wooden paddle wheel type of hub arrangement. A few tests at lower angles of attack have indicated that this system does have gliding capabilities although how well it will glide is not known.

The conventional rotary wing is the helicopter type system. This is the configuration for which a vast amount of performance data are available, including data for gliding flight and flared landings. This is the configuration for which most of the tests on stability in vertical autorotation descent have been conducted. No deployment tests have been conducted, and none are planned.

The folding and the telescoping rotary wings are essentially the same as the conventional rotary wings, but they are intended for a more compact stowage of the system. Deployment tests are planned for both of these systems. The effects, if any, of the telescoping joints or the folding hinges on the performance is not known. A few stability tests have been conducted using 4 foot diameter models with telescoping and folding type construction. (Slide off.)

I would now like to discuss some of the areas of this chart for which data are available. A short film will be presented next which shows a vortex ring parachute being deployed while in free fall and rotating. (Film.)

As you have seen in the movie, the parachute is very stable with oscillations of less than 1°. The next slide shows the variation of the coeficient of drag with the incedence setting of the individual blades (canopy segments). (Slide.) The drag coefficient is based on the total cloth area of the parachute. The high drag (C_D=2.1) obtained with this particular parachute would mean that for a given payload the rate of descent would only be 60 percent of what it would be if a conventional parachute of the same cloth area were used. (Slide off.)

A few preliminary deployment tests of flexable fabric blades have been conducted and have pointed out some of the problem areas which will

have to be studied and corrected. A short film showing one of these problem areas will be shown. This film was taken at approximately 1500 frames per second and will be projected at 24 frames per second. Therefore, the motions seen are approximately 63 times slower than they actually occurred. The deployment of the blades takes place in about one quarter of a second. The steady state motion seen after the deployment, was taken approximately 6 seconds later. It is part of the same test. (Film.) It is believed that the problem illustrated in this film can be solved with a controlled slower deployment of the blades.

Experience in the Recovery Systems Branch has indicated that use of a rotary wing recovery system may involve problems of dynamic stability. Parametric tests are being conducted at Langley to determine how much effect the various parameters have on the stability of a rotary wing in free vertical autorotation descent. Some of the parameters which have been very briefly examined and have been shown to have an effect on the stability of this system are listed in the following slide. (Slide.) There are other variables which quite likely effect the stability also, such as, solidity ratio, number of blades, blade weight, blade incidence angle, and payload configuration.

The next film will illustrate a rigid rotary wing on an apollo type capsule in vertical autorotative descent. The first sequence is an unstable configuration. By varying one of the parameters (in this case hub inertia), the stability was increased as seen in the second sequence, however, it was still only marginally stable. A further modefication produced a completely stable configuration. (Film.)

A few tests have been conducted with a 48 inch diameter rotor, considering only two variables, hub inertia and disk loading. The results are presented in the next slide. (Slide.)

As can be seen from this slide, as the hub inertia is increased, the disk loading must also be increased to maintain stability. If some of the other parameters are changed, this curve will be shifted. For instance, decreasing the blade hinge angle will shift the curve downward.

In conclusion, it can be said that rotary type recovery systems can be made inherently stable, can produce high drag, fair gliding capability, and near zero vertical and horizontal speeds at landing.

ROTARY-TYPE RECOVERY SYSTEMS

	DATA AVAILABLE			GLIDING CAPABILITY
	DEPLOYMENT	STABILITY	PERFORMANCE	
VORTEX RING PARACHUTE	YES	YES	YES	NO
FLEXIBLE ROTARY WING	SOME	NO	SOME	YES
CONVENTIONAL ROTARY WING	NO	SOME	YES	YES
FOLDING ROTARY WING	NO	SOME	NO	YES
TELESCOPING ROTARY WING	NO	SOME	NO	YES

VARIATION OF C_D WITH BLADE PITCH SETTING FOR 64" DIA VORTEX RING PARACHUTE

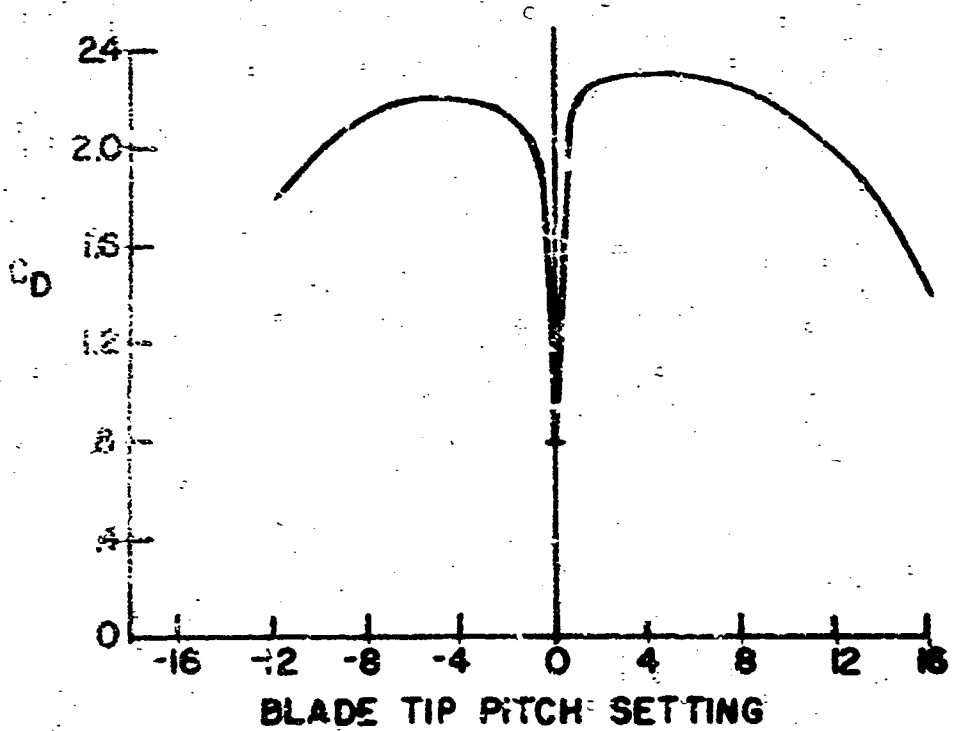

PARAMETERS WHICH EFFECT THE STABILITY OF ROTARY WING RECOVERY SYSTEMS

1. DISK LOADING
2. HUB INERTIA
3. BLADE HINGE ANGLE
4. DISTANCE BETWEEN BLADE HINGE AND AXIS OF ROTATION
5. VERTICAL LOCATION OF CENTER OF GRAVITY

STABILITY BOUNDARY FOR A 48" DIA ROTOR IN FREE VERTICAL AUTOROTATIVE DESCENT

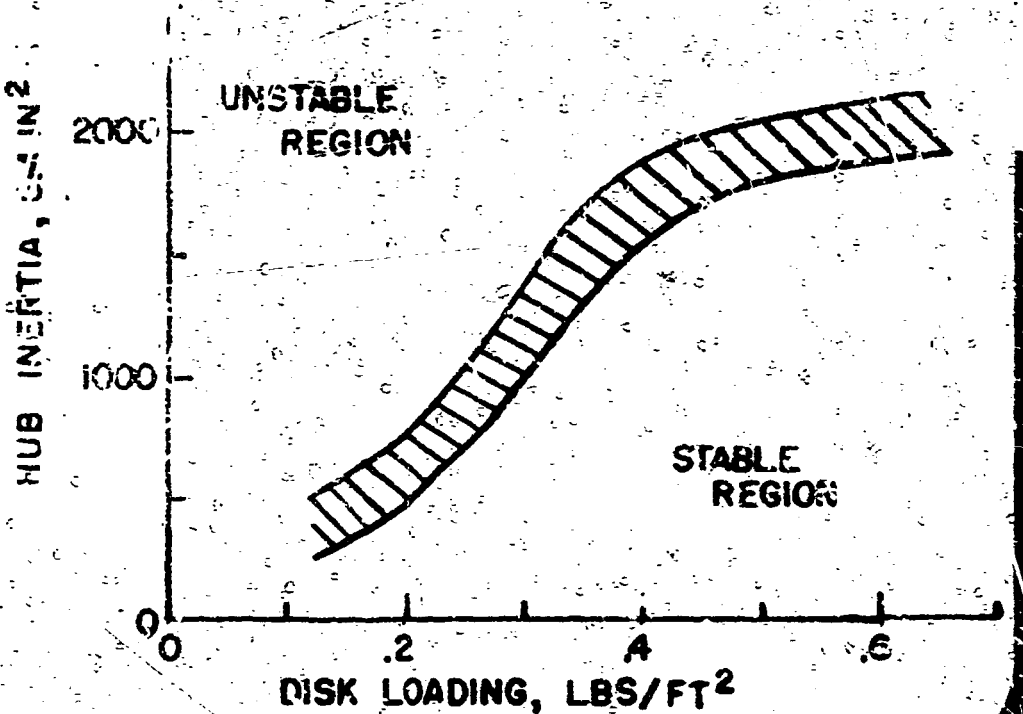

NASA - Langley

PARACHUTE PERFORMANCE AT SUPERSONIC SPEEDS

X64-35848

By Nickolai Charczenko

The recovery of high speed vehicles created a new requirement in recovery operations, decelerators have to perform at very high altitudes and supersonic speeds. Although the requirements have changed, the basic considerations in the selections of drag devices essentially remain the same for the supersonic speed range as they were for subsonic. The following slide shows these basic requirements, they are:

Slide I

Based on these requirements, conventional parachutes appear to be well suited for this job, in view of the fact that they have been proven to be highly reliable in subsonic operations. They have an apparent weight advantage over other nonlifting types of decelerators and we were more familiar with parachutes than any other drag devices. For these reasons, they were a natural choice for supersonic speed range. However, tests at supersonic speeds revealed some problem areas of parachute performance. The three major problem areas are:

Slide II

We were primarily concerned with the first two of these problem areas at supersonic speeds, which we will consider at this time. The third one can be anticipated in the future.

Slide III

The experimental results of flexible ribbon-type parachutes indicate two major areas of parachute instability: oscillatory motion of the parachute about the point of attachment and shock pattern fluctuations accompanied by a violent canopy breathing along with reduced inflation and drag characteristics. The latter which is referred to as inflation

instability has been the subject of considerable investigation. The basic problems involved in the inflation instability are high rates at which the shock is alternately swallowed and expelled (somewhat analogous to the inlet buzz phenomenon) and the interaction between the boundary layer on the individual shroud lines and the shock wave in front of the parachute canopy. This type of instability causes large variations in drag with frequencies exceeding 100 cps.

Slide IV

The next slide shows some parachutes employed in supersonic speeds. The bottom one is a typical ribbon parachute used in most of the investigations. Various means have been tried with this type of parachute to eliminate inflation instability such as varying porosity, varying number of shroud lines, extending the skirt, attaching an inflated tube to the skirt and others, but only limited success was achieved by these means. It was evident by now that the best we can hope for, in light of the fact that the fluctuations in shock pattern exist even for the rigid parachute models in the free stream as far as shock fluctutations are concerned, is to reduce their influence on the breathing of a parachute. I believe this has been achieved to a large degree with the parachute designed by Cook Research Laboratory, under an Air Force contract. These parachutes are radically different from most parachute designs. Their main features being low porosity conical inlet canopies and high porosity flat roofs. Both of these designs have performed satisfactorily in the Mach number range of 2.30 to 4.65. A high speed schlieren movies showing stability of these parachutes will be shown later.

Slide V

As far as the drag of parachutes is concerned, we would like to have a drag coefficient of 0.5 or better for parachutes at supersonic speeds. The next slide shows a drag level for various drag devices. Here the drag coefficient is plotted versus Mach number at ten base diameters downstream for parachutes and rigid types of drag devices. Drag coefficient for most ribbon type parachutes falls in this region. The conical inlet canopy has improved the drag coefficient of parachutes as shown in this slide. Even though considerable improvement in drag coefficient and stability was achieved with the conical inlet parachutes, the variations in drag still existed, though to a lesser degree than with ribbon type parachutes. Due to the problem areas encountered with parachutes operations at supersonic speeds, other drag devices were being developed concurrently and a comparison in drag coefficient between them and parachutes is made in this slide. It can be seen that the drag coefficient of parachutes can be exceeded by a factor of two to three by some rigid type decelerators. Thus there is a wide margin of drag coefficient that can be used as a tradeoff for weight. Rigid and inflatable types of decelerators will be discussed in more detail in the following paper.

In this investigation, no effort was made to establish regions of optimum performance; however, from visual observations of these and other tests and from high speed schlieren movies, it was evident that the performance of the parachutes was wake-dependent. A wake study for various bodies to about 15 base diameters downstream of the vehicle would be most helpful in analyzing and possibly explaining the variation instability and, at some Mach numbers, decrease in drag coefficient with increase in trailing distance. I think our biggest problem in the development of stable

parachutes for the supersonic speed range has been the lack of adequate theory to guide the investigations. Consequently, most of the work has been done on a trial and error basis.

The wind tunnels are well suited for the research of decelerators because the parametric study under a wide variety of test conditions can be easily simulated. However, after a workable design has been evolved in the wind-tunnel testing, this should be augmented by free flight tests to check out the system under the actual test conditions. Free flight tests are being considered to check out parachutes that had satisfactory performance in the wind-tunnel tests.

NONCONVENTIONAL PARACHUTES

Some exploratory work has been performed on the nonconventional type parachutes in the wind tunnel at supersonic speeds. These are parachutes with high rotational speeds, typical representation of which are vortex ring parachute and rotafoil. Both of the above mentioned models were tested at supersonic speeds, but they failed before any significant drag measurements could be obtained. However a visual check of drag indicator before failure occurred showed high drag values in some cases. Further research along these lines would be warranted.

High speed movies that were obtained in a few seconds of their operation will be presented at this time along with schlieren movies of the previously discussed parachute models.

BASIC CONSIDERATIONS IN SELECTION OF DECELERATOR DEVICES

1. Good stability
2. Effectiveness in producing drag
3. Minimum bulk and weight
4. Stowage or packageability
5. Capability of withstanding high temperature

NASA-LANGLEY

PROBLEM AREAS FOR PARACHUTES AT SUPERSONIC SPEEDS

1. Stability

2. Drag

3. Aerodynamic heating

TWO MAJOR TYPES OF PARACHUTE INSTABILITY AT SUPERSONIC SPEEDS

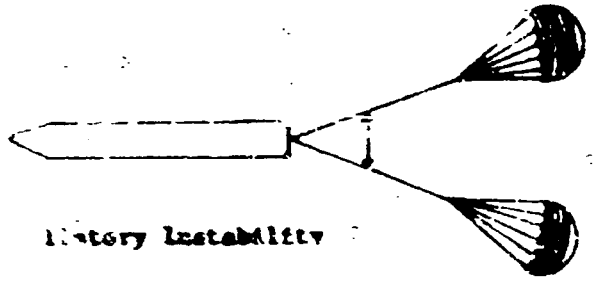

Oscillatory Instability

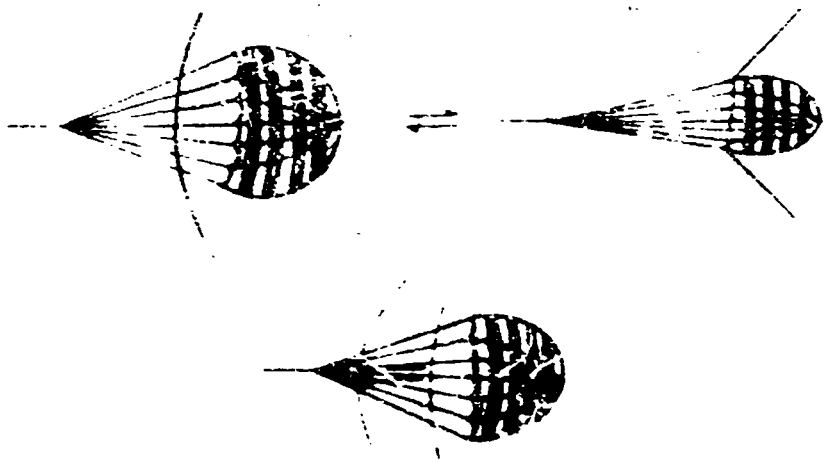

Inflationary Instability

NASA-LANGLEY

N64-35849

NASA - Langley

AERODYNAMIC DRAG AND STABILITY CHARACTERISTICS OF SOLID AND INFLATABLE DECELERATOR DEVICES AT SUPERSONIC SPEEDS

By John T. McShera Jr.

ABSTRACT

Experimental drag and stability characteristics of towed decelerators at supersonic speeds are presented in this paper. The decelerators discussed include towed spheres, towed cones (both solid and inflatable), and inflatable towed cone-balloons (both closed pressure and ram-air type devices).

INTRODUCTION

If conventional methods of recovery are to be utilized in the final stage, it is particularly important that the velocity of the payload be gradually reduced as the payload reenters the atmosphere from high-speed high-altitude flight. Investigations have indicated that conventional parachutes are not satisfactory for this first stage deceleration because the parachutes are unable to withstand aerodynamic heating, inflate satisfactorily, and maintain stability under supersonic flow conditions. An initial deceleration system which will reduce the velocity of the payload by substantially decreasing its ballistic coefficient will lessen the initial shock on the payload and on final recovery devices such as parachutes. Spherical balloons and cone devices have been considered as possible decelerators because of their stability and relatively high drag coefficients. Both solid and inflatable decelerators have been investigated and will be discussed in this paper.

Slide 1

This slide shows typical examples of the solid and closed pressure vessel inflatable decelerators that were tested.

The 80° cone and sphere shown here were tested both solid and inflatable with very little difference in drag and stability between them. The separation fence shown on some of these configurations is needed for stability at subsonic speeds. The solid models shown here are typical of rigid decelerators at supersonic speeds. They are simple in construction, inherently stable at these speeds, and produce high drag coefficients. The 70° cone balloon (called a tailute) has drag values between the 60° and 80° solid cones. Therefore it would appear that the cone balloon and the cone give similar if not identical results for a given cone angle.

It has been established that the stability of cones decrease with increasing cone angle while drag increases with increasing cone angle in the supersonic speed range and cones with 90° angles were intermittently unstable at these Mach numbers. Although it hasn't been tested it would appear that an 80° cone balloon would be optimum from this investigation from the point of view of drag and stability.

At this stage, a decelerator that had better drag and stability characteristics than a parachute and yet the same storage capability had been developed. However, the problem of having to carry heavy inflation equipment aboard the payload to be recovered still existed. This is where the need for a self-inflating configuration was realized.

Slide 11

This slide shows the development of the ram air ballute from the front inlet to the present side inlet type.

This front inlet configuration was one of the first tries at using the ram air (dynamic pressure) to inflate the decelerator. Many different means of inflating the ballute employing front inlet type configurations were tried; however, there was a mass flow pulsation phenomena in the supersonic speed range which resulted in adverse vibratory fabric loading and subsequent failure of the models. This pulsation problem was solved by placing different percent screens over the inlet; however, this lowered the drag compared to the closed pressure 70° cone balloon or ballute shown in this slide. The side inlet configuration of the 70° cone balloon or ballute was developed as a result of testing at a Mach number of 10. The wake from the forebody did not tend to collapse or recover at any distance aft of the payload that was capable of testing within the

tunnel. The core of this wake existed over and outside the ram air inlet diameter; therefore the side inlets were used to feed the ram air into the ballute. This method of extended ram air inlets worked very well.

Essentially what is being developed here is an improved type of high speed parachute that will retain the parachutes weight and packaging features and yet overcome its short comings with respect to supersonic stability and aerodynamic heating resistance.

Slide III

This slide shows a typical plot of drag coefficient versus Mach number. The configurations represented by this figure is the 70° ballute with side inlets and one of the better parachute configurations at a length of tow cable to diameter of forebody ratio of 10. The forebody used in all these tests is shown at the top of the slide. These side inlets fully inflate the model to the same shape as the inflatable closed pressure 70° cone balloon giving approximately the same drag and stability.

Ballutes made of dacron and nylon neoprene have a maximum performance limit of approximately M = 5. Ballutes made of metal fabric (Rene' 41) coated with a special silicon ceramic elastomer have proved satisfactory at M = 10.

Ballutes have built in "reefing" at all speeds and since parachutes have not been successfully reefed during deployment at high supersonic speeds, it is clear that opening shock loads are higher in parachutes and the result is a heavier cloth structure and subsequent weight penalty. A ballute is a more rigid inflatable structure than a parachute which results in improved stability (less coning).

Slide IV

This slide shows the research areas in which I believe work still needs to be done.

1. reduce internal pressure -

Tests just completed on the 70° ballute with side inlets showed that internal pressures as high as 4 times dynamic pressure were measured. Previous tests showed a pressure equal to dynamic pressure was all that was needed to fully inflate the decelerator. Therefore there still needs to be some development in inflation procedures to reduce the amount of pressure inside the decelerator.

2. maintain inflation throughout trajectory -

Various techniques for inflating the optimum drag shape should be investigated and should also include a determination for maintaining inflation procedures throughout the descent trajectory down to sea level in order to possibly eliminate the requirement for deployment of a final stage parachute.

3. correlate tunnel results with flight -

To establish more complete data, consideration should be given to perform free flight tests to achieve flight test deployment conditions that can be duplicated in the wind tunnel.

A parametric performance study should be then made in the wind tunnel to ascertain if stability can accurately be determined in wind tunnel testing using an infinite mass relationship.

4. extend results to subsonic and hypersonic speed -

Additional wind tunnel testing is also required in the subsonic and hypersonic speed ranges on the basic shapes discussed in this presentation in order to investigate the capabilities of these decelerator systems at speeds up to Mach numbers of 10 and a wide range of dynamic pressures and temperatures that will be encountered in recovery.

MOVIE

1. This 1st shot shows the 70° cone balloon or bailute with side inlets at a Mach number of 2.5 q = 250 psf. Its drag coefficient of 0.9 was the same as the 70° cone balloon closed pressure inflatable model.

2. This picture shows the towed 80° ram air bailute at a Mach number of 2.75, q = 250 psf This model never fully inflated and it points out the mass flow pulsation phenomena which causes the adverse fabric loading and subsequent failure that existed in many of the front inlet ram air ballutes.

DECELERATOR SHAPES TESTED

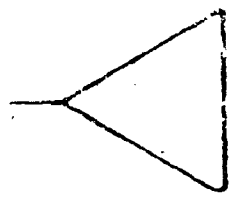

60° Cone

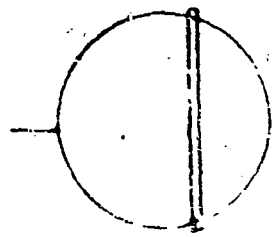

Sphere

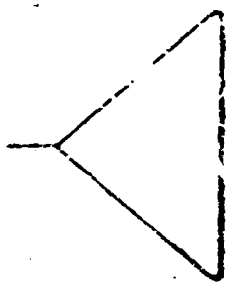

80° Cone

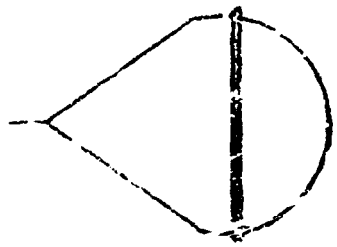

70° Cone Balloon (Bullute)

SLIDE I

DEVELOPMENT OF THE BALLOON

75" Gum Balloon

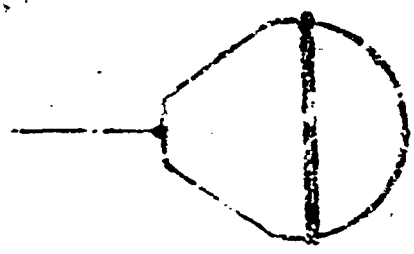

70" Front Inlet Balloon

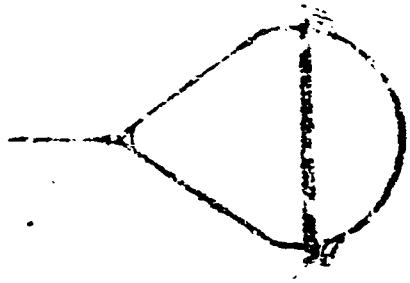

70" Side Inlet Balloon

SLIDE II

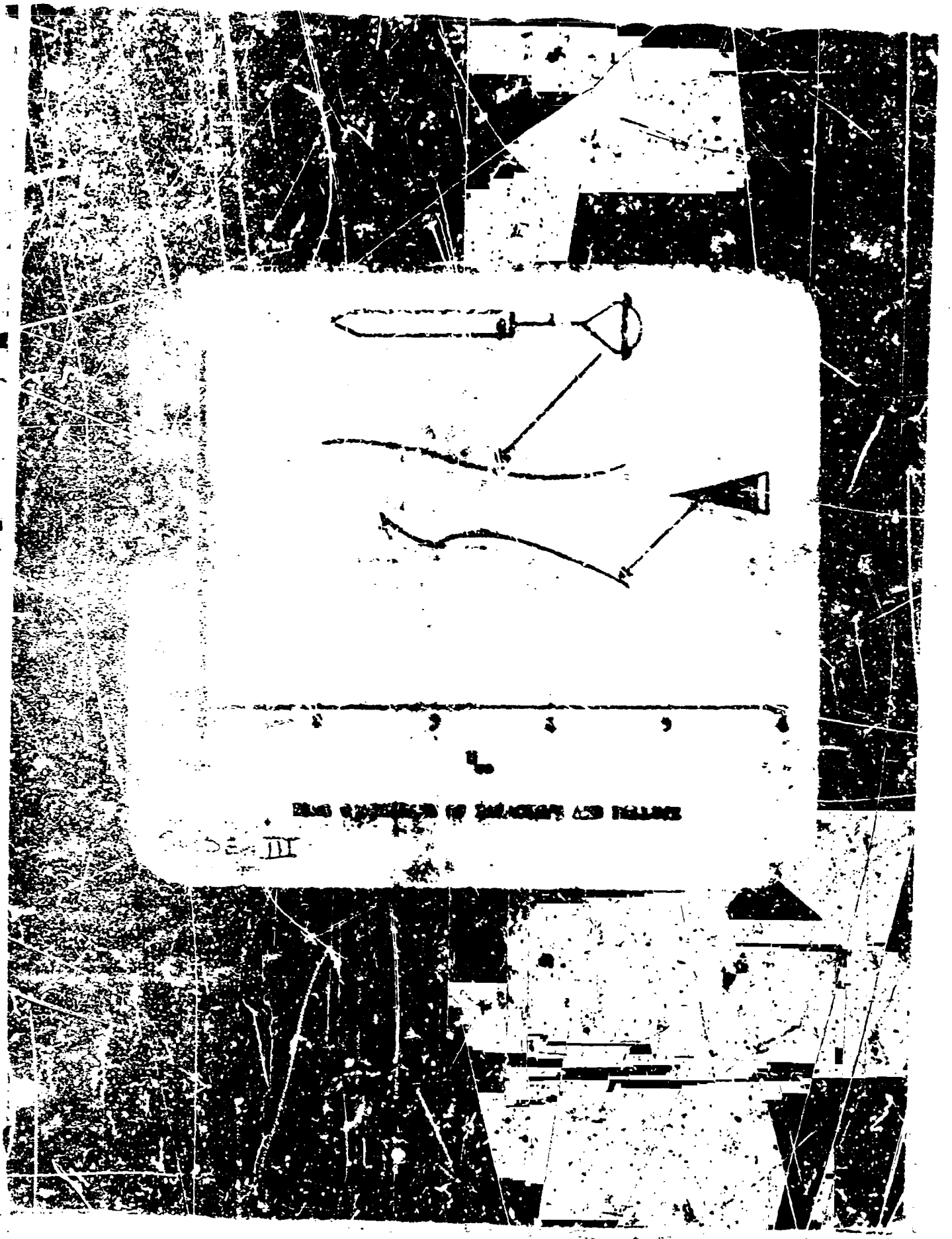

RESEARCH AREAS

1. Reduce internal pressure

2. Maintain inflation throughout trajectory

3. Correlate tunnel results with flight

4. Extend results to subsonic and hypersonic speed

Slide IV

NASA - Langley

X64-35850

HEADQUARTERS MEETING July 10-11, 1962

THE PROBLEMS OF THE ENERGY DISSIPATION SYSTEMS IN SPACECRAFT RECOVERY

By Lloyd J. Fisher

Several aspects of earth landing requirements for manned space vehicles are being investigated by Langley Research Center. The character of research undertaken consists of experimental and analytical studies of the fundamental energy dissipation capabilities of materials and methods and of the landing characteristics of space vehicles having various landing systems. The requirements generally placed on the energy dissipation system are that the landing accelerations and landing motions resulting from contact with the landing surface, be kept within tolerable limits both for occupants of the vehicle and for the vehicle structure. For man in space flight the non-emergency limit has been placed somewhere near 20g's maximum acceleration and 250g's/sec. onset rate of acceleration. The spacecraft has been permitted to sustain some small damage. Mercury vehicles were not intended for reuse but some of the other vehicles such as Gemini, will be reused. In any case, both from the standpoint of safety for the astronaut and for maintaining the integrity of the spacecraft, violet behavior on landing should be avoided.

We are currently investigating landing impact energy dissipation systems for the Apollo earth landing module simulating a parachute type landing. We are studying the

completion of a brief model investigation of the landing loads and stability characteristics of a Saturn booster recovered on a hard surface runway -- simulating a paraglider type landing. Investigation will be started soon on the ditching characteristics of the Gemini vehicle, which will also simulate a paraglider landing. A limited program is underway on the use of certain materials as energy dissipators. Our current emphasis in the materials program is on materials for the frangible metal tube dissipator, and we are planning some work on foamed metals as energy dissipators. Since the fragmenting tube process is probably not familiar to everyone, the first slide illustrates the essential components of this system. An example of a frangible-tube installation could be a hard aluminum-alloy tube such as this attached to a vehicle, and a die such as this attached to a landing skid or foot. The tube presses over the die during impact and fails in fragments as shown here. This is a system for working metal to its ultimate strength and through a large percent of its length.

The next slide 2 shows the energy dissipation capabilities of several materials that have been used or considered for use in landing systems. Some of the less efficient but readily adaptable dissipators, such as the fabric air bag and aluminum honeycomb, which absorb about 4000 and 6000 ft-lbs of energy per pound of material, have received considerable attention to date. This is to be expected because of the ease of

application and availability of these materials. Honeycomb has been one of the most often suggested energy dissipators taking many forms, shapes, and sizes and has been proposed in one application or another for most spacecraft. Its main disadvantages are bulk and the fact that it can take relatively little side load. The air bag has also been proposed in many forms as a solution for spacecraft landing problems. The fabric air bag lends itself extremely well to storage, as on a capsule type spacecraft where volume is at a premium, and it is being used on Mercury. Susceptibility to puncture and to side-load failure are its major disadvantages. The strain strap, which absorbs about the same energy per pound of material as does aluminum honeycomb, has also found ready application; one case in point being the strut-type leading gear of Dyna-Soar. The pressurized metal cylinder and balsa wood have fairly high efficiencies, absorbing about 14000 and 24000 ft-lb per pound of material. These systems are bulky to store, although no more so than honeycomb. Balsa, however, has an undesirable rebound characteristic. The frangible metal tube has high efficiency absorbing about 31,000 ft-lb per pound of 2024-T3 aluminum alloy but loads must be applied along the axis of the tube, and the tube must be kept snug against its working die. As mentioned earlier work is continuing at Langley on the fragmenting tube process. Alignment is a problem with all of the systems and when appreciable velocity components are involved, either horizontal

or vertical or both, some positive means of positioning the energy dissipation element is required.

The following slide shows a sketch of a practical installation of a strain strap in combination with landing skids. The strain strap is a replaceable element which fails by plastic yielding and the skid moves aft and up while alignment is maintained by the strut. Such a gear when used on Dyna-Soar would be retracted and stored through doors in the lower surface of the wing which serves as the heat shield. However, on the Gemini configuration a somewhat similar gear has been kept separate from the heat shield. Slide 4, please. The Gemini vehicle has been rotated over on its side for landing and the tri-skid landing gear is positioned accordingly. Here the heat shield is undisturbed by the landing gear. Currently, hydraulic shocks are being considered for Gemini although at least one "McDonnell" man says they will be heavier than strain-strap dissipators.

The strut arrangements shown are very suitable for systems having positively controlled forward landing directions. Energy due to vertical velocity is dissipated principally by the strain strap or hydraulic shock absorber and most of that due to horizontal velocity is dissipated by friction during the landing runout. Fairly good runways, or at least selected sites, are required for stability in such landings.

Methods of integrating the energy dissipation system with configurations that land on the heat shield are shown in the

next slides. This slide illustrates a passive system that has received strong consideration for Apollo earth landing. Aluminum honeycomb or some such material would be used between the heat shield, which is expected to "ball-can" during impact, and the astronauts' pressure compartment. There is a very short stroke available in this system resulting in accelerations of about 40 to 50g's on the capsule structure, so couch support systems must further attenuate the landing impact loads. The passive system is of interest primarily because no malfunction in operation can occur prior to usage since no extension or deployment of parts is required. The following slide shows another approach taken with Apollo toward integrating the landing gear with the components of the spacecraft. The heat shield is extended in this case and shock absorbers are installed between the heat shield and the upper capsule. One set of absorbers shown here in an approximately upright position is used to dissipate vertical loads and another set of absorbers shown here at an appreciable angle us used to dissipate horizontal loads. Both of the Apollo versions shown are expected to land on the ground on the heat shield at a nose down attitude and skid and rock on the heat shield during runout. Slide off.

In general, there are several ways of dealing with vertical energy dissipation. Some systems are more efficient than others, some package better than others, but a variety of promising systems are available. Horizontal energy dissipation

is, in a way, simpler to deal with than vertical energy dissipation since translational friction is all that is involved; however, runout becomes a factor. The right or wrong combination of landing surface and landing speed is critical during runout and vehicle configuration also enters the picture. The results of inadequately dealing with these parameters are high accelerations, instability, and turnover. Parachute let-down systems have more trouble with horizontal velocity than do most of the other systems because they aren't designed for horizontal velocity. This is just as true of cargo drops as it is of spacecraft landings and it is easy to appreciate the problem. The parachute landings of manned vehicles, for example, have been planned at velocities of about 30 feet per second vertical with expectations of from 0 to about 50 or 60 feet per second horizontal. The horizontal velocity is due to the wind and so is unpredictable making design difficult since a wide speed range must be accounted for by the energy dissipation system. Also, direction of landing with the parachute is unknown, consequently, it is desirable that the energy dissipation system be omnidirectional in behavior and this too is hard to achieve. Let down systems that have a more or less fixed horizontal velocity such as the paraglider also have positively controlled forward landing directions and even braking rockets, since they do not drift as easily with the wind (as do parachutes) have more exactly defined design loads, speeds, directions, etc.

The following movies show some conditions at which models of various spacecraft tend to turn over or have undesirable behavior.

The first movie shows a model of the Mercury vehicle landing on water at simulated velocities of 30 feet per second vertical and 60 feet per second horizontal. This is a repeat run. The turn-over is primarily the result of too high a velocity.

The next movie shows an Apollo type model landing at velocities simulating 30 feet per second vertical and 30 feet per second horizontal. First a landing on sand, then a landing on a hard surface runway. The turn-over is caused by the "oil canning" of the model heat shield.

Now a model having a four strut landing gear landing at relatively low speeds, 10 feet per second vertical and 10 feet per second horizontal. Here is a landing on a hard surface, then a landing on a soft powdered material. Penetration and pile-up of the surface material caused tip-up.

The next sequence of movies show turn-overs that are not caused by horizontal velocity or landing surface, but by vehicle shape and landing attitude. Here is a skid-rocker landing of a vehicle with a c.g. height to base diameter ratio of 0.3 Now a vehicle with a ratio of 0.2. The landing attitude and speed were the same in both bases. Vehicle shape or proportions caused turn-over.

The next movie sequence shows model landings of a Saturn booster simulating paraglider let-down on a smooth, hard-surface runway. The landing gear is a four strut tail-skid gear. The landing speeds are relatively low considering the size of the vehicle, simulating 80 knots horizontal and 10 feet per second vertical. The following movie shows a tri-cycle landing gear employing a wheeled nose gear and skids on the main gear. There is little to choose from in behavior between these gears although we did find some wheel problems due to model design that could cause ground loops as shown here. Movie off.

The next slide (7) shows maximum normal and longitudinal accelerations for the passive system Apollo configuration during landings on sand at a vertical velocity of 30 feet per second and horizontal velocities of 0 to 50 feet per second. Horizontal velocity had little effect on the maximum acceleration, either normal or longitudinal as shown by the scatter of the velocity points. Landing attitude had little effect on normal acceleration due to the degree of penetration into the sand. The solid points indicate test model turn-over during impact.

The last slide (8) gives computed limits of stability for a skid-rocker landing gear. Computed limits for a friction coefficient of 0.4 and a c.g. height to base diameter ratio of 0.24 are shown. The stable region is below the curves.

Turn-over would be expected at conditions above the curves. The equations of motion show that turn-over for a skid-rocker configuration is independent of change in horizontal velocity and this has been substantiated by model tests for a range of touchdown speeds. This pilot shows the effect of vertical velocity. The range is well outside that of the model investigation which simulated paraglider landings at vertical velocities of about 10 feet per second and less. The skid-rocker landing method is most suited to horizontal type landing and these data show this. For example, at 10 feet per second there is a stable range of some 45° in landing attitude. In a vertical type landing at say 30 feet per second this stable range is reduced to only 12°. The curves approach asymptotically the friction angle. (The friction angle is about 42° for this configuration, and is the angle that the resultant of the friction force and the normal force makes with the normal axis of the vehicle. It is also the angle at which the vehicle would slide during landing without oscillation in trim.) Slide off.

There are several problem areas in the landing energy dissipation systems being used for spacecraft recovery. There are also regions, or areas, for most systems presently being considered that result in satisfactory landing impact and runout. This is a natural situation because every vehicle whether it be helicopter, airplane, or spacecraft can be expected to be limited somewhat in landing attitude and speed.

FRAGMENTING TUBE SYSTEM

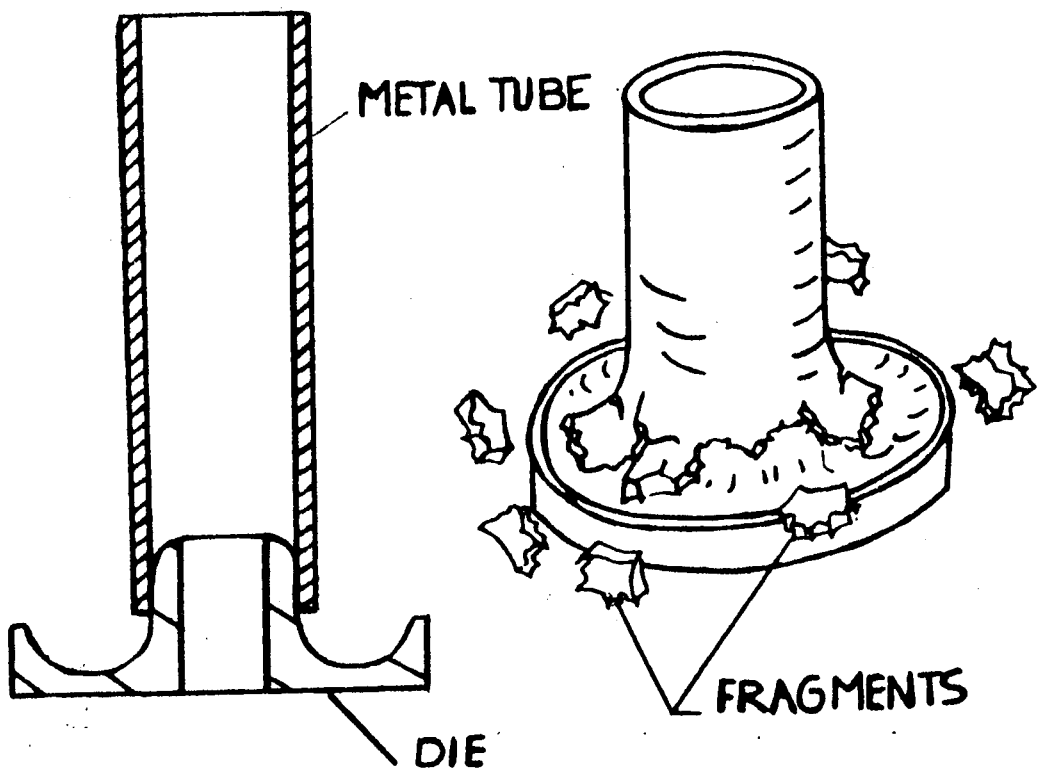

NASA

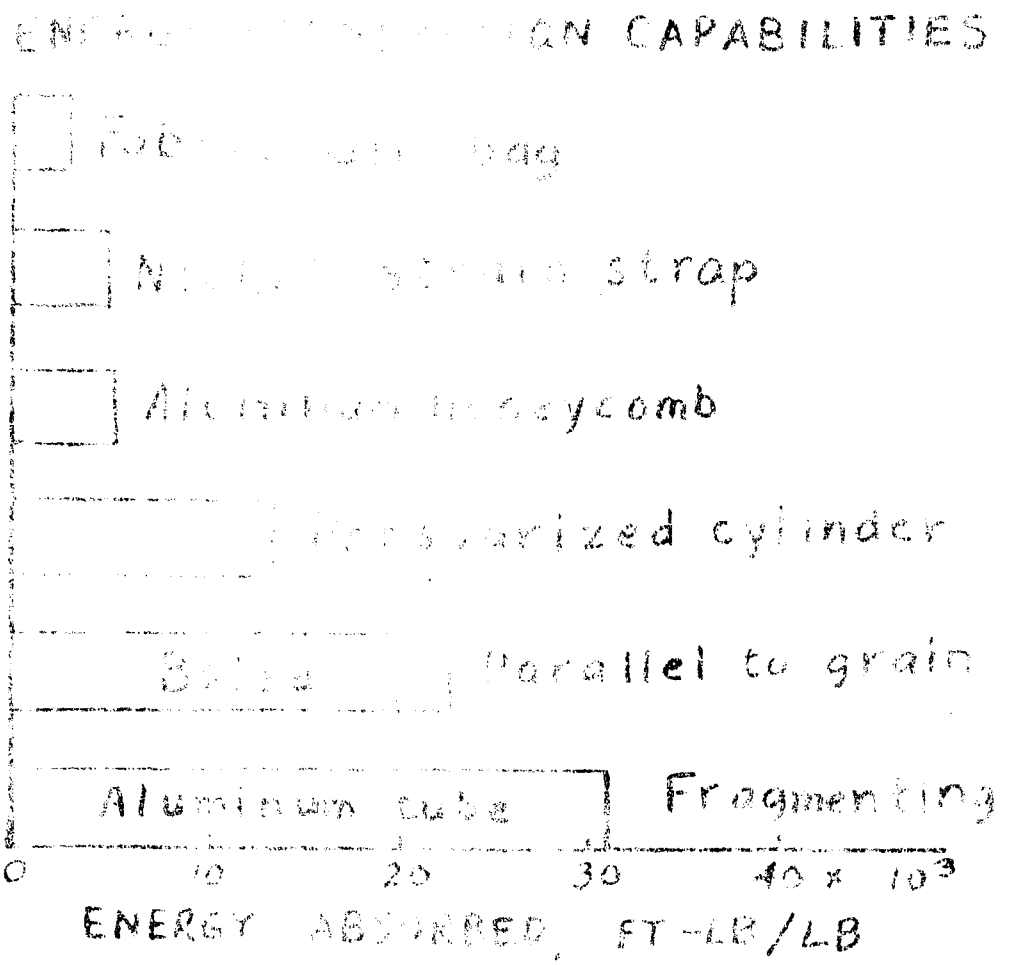
CAPABILITIES
strap
cylinder
Parallel to grain
Aluminum tube
Fragmenting
0
10
20
30
40 x 10³
ENERGY ABSORBED, FT-LB/LB

LANDING GEAR COMPONENTS

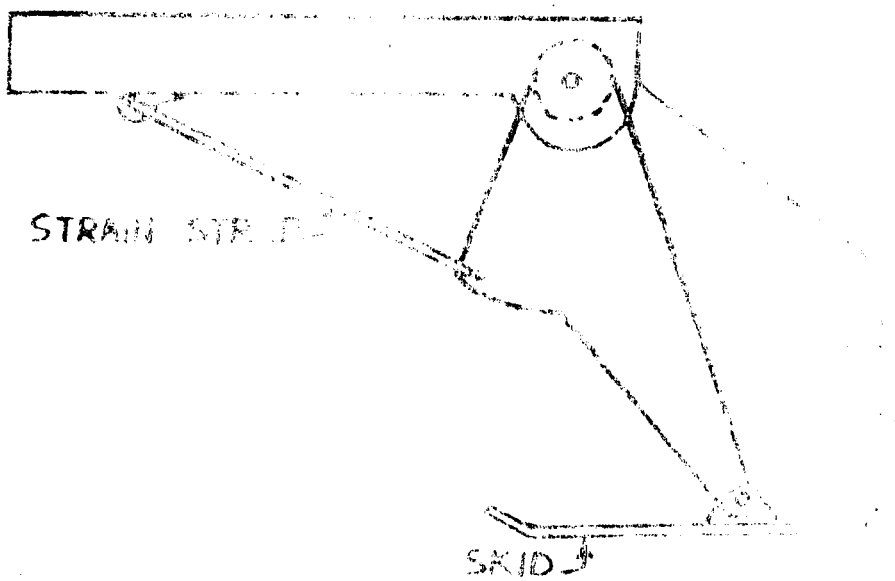

PASSIVE LANDING SYSTEM

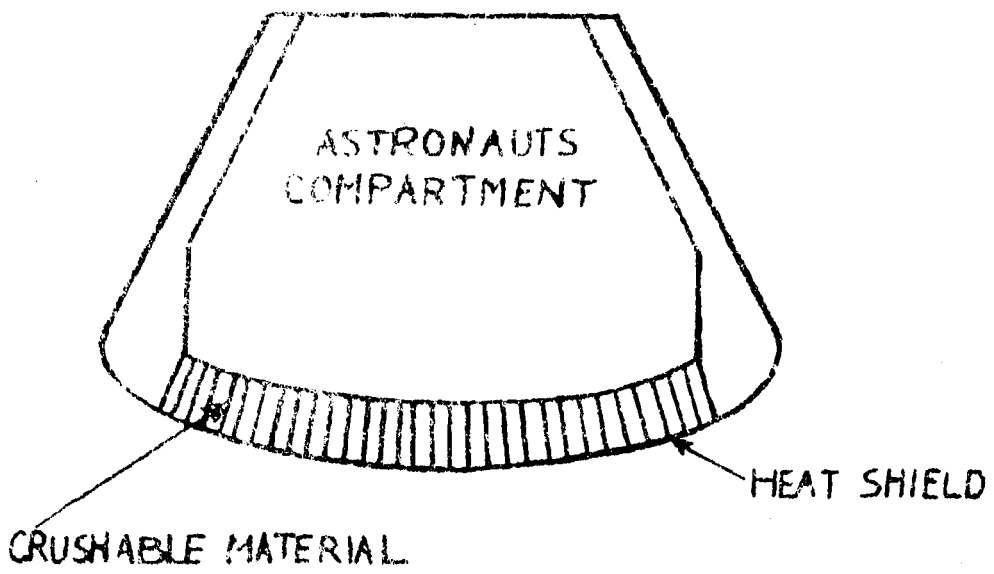

MULTI-ABSORBER SYSTEM

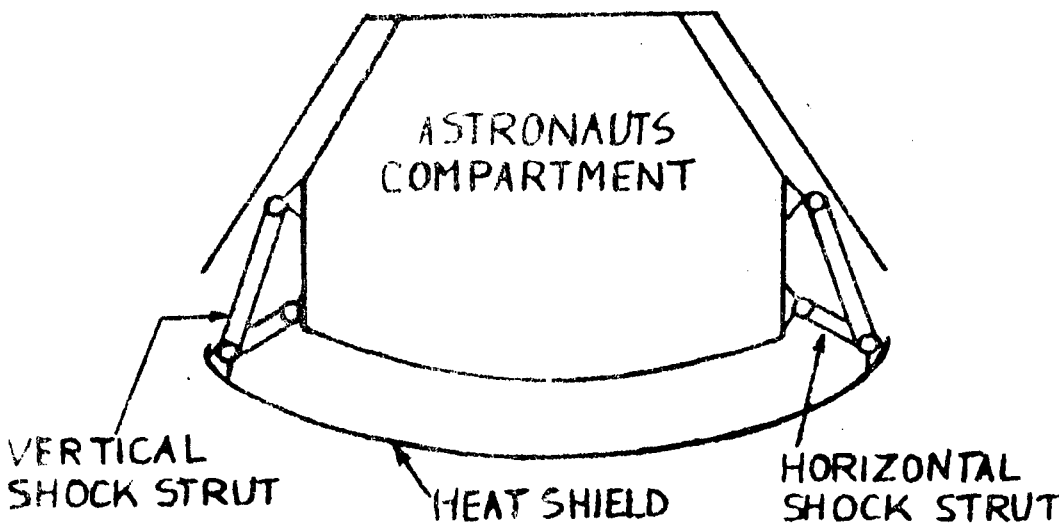

NASA - Langley Field, Va.

LANDING ACCELERATIONS

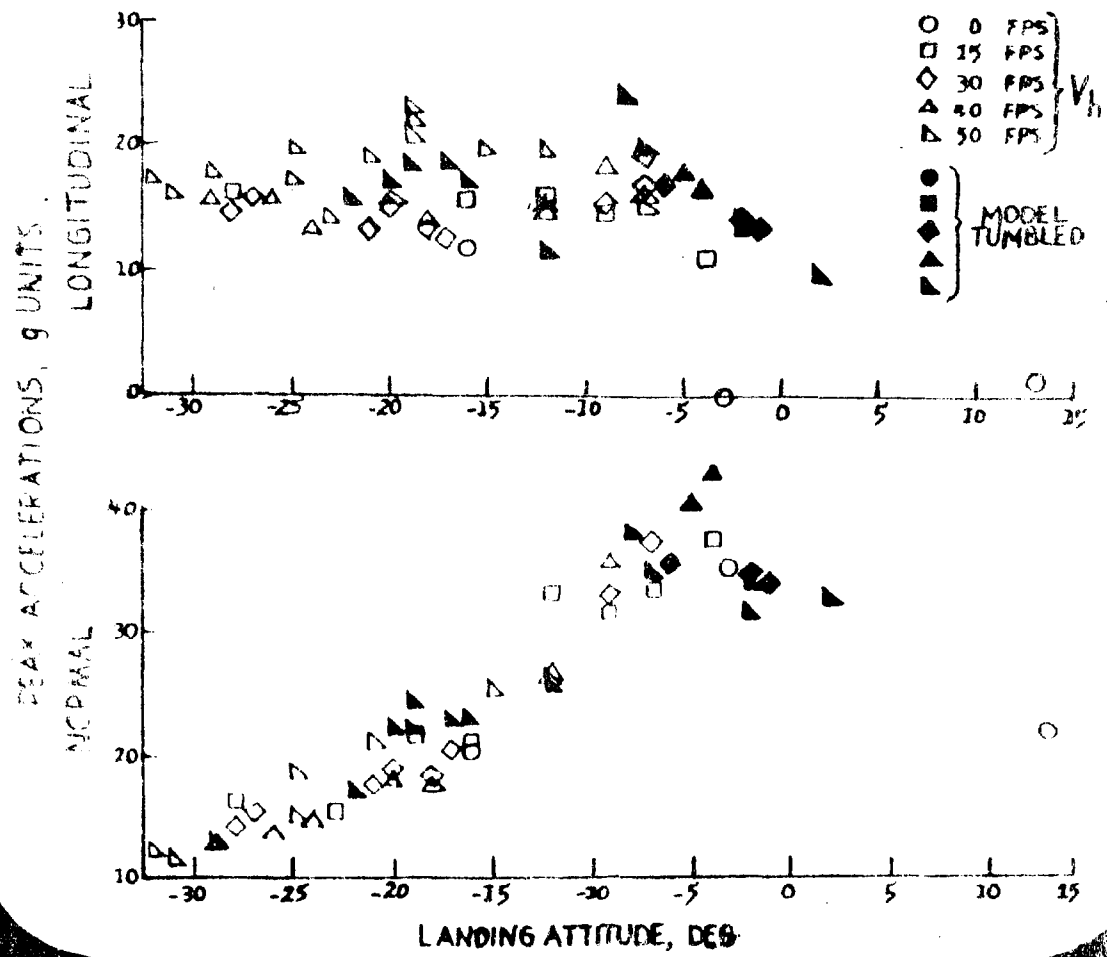

NASA Langley Field, Va.

AGENDA

MEETING ON SPACE VEHICLE LANDING AND RECOVERY

RESEARCH AND TECHNOLOGY

NASA Headquarters
July 10-11, 1962
9:00 A.M. EDT

I. July 10, 1962 - Opening Remarks - J. E. Greene- Headquarters

II. Presentation of Program Summaries from the Centers

Parachute Recovery Systems Design and Development Efforts Expended on MERCURY-REDSTONE Booster and SATURN S-1 Stage - Barraza, R. M. - MSFC

Application of Paragliders to S-1 Booster Recovery for C-1 and C-2 Class Vehicles - Mc Nair, L. L. - MSFC

Recovery of Orbital Stages - Fellenz, D. W. - MSFC

A Review of Launch Vehicle Recovery Studies - Spears, L. T.- MSFC

A Review of the Space Vehicle Landing and Recovery Research at Ames - Cook, W. L. - ARC

Survey of FRC Recovery Research - Drake, H. M. - FRC

Manned Paraglider Flight Tests - Horton, V. W. - FRC

Gemini Landing and Recovery Systems - Rose, R. - MSC

Apollo and Future Spacecraft Requirements and Landing Systems Concepts - Kiker, J. W. - MSC

[redacted]

III. July 11, 1962 - Continuation of Program Summaries

JPL Requirements for Spacecraft Landing and Recovery - Pounder, T., Framan, E., and Brayshaw, J. - JPL

Langley Research Efforts on Recovery Systems - Neihouse, A. I. - LRC

Summary of Static Aerodynamic Characteristics of Parawings - Sleeman, W. C., Croom, D. R., and Naeseth, R. L. - LRC

Dynamic Stability and Control Characteristics of Parawings - Johnson, J. L., and Hassell, Jr., J. L. - LRC

Deployment Techniques of a Parawing Used as a Recovery Device for Manned Reentry Vehicles and Large Boosters - Burk, S. M. - LRC

An Analytical Investigation of Landing Flare Maneuvers of a Parawing-Capsule Configuration - Anglin, E. L. - LRC

Paraglider Loads, Aeroelasticity and Materials - Taylor, R.T. and Mc Nulty, J. F. - LRC

Rotary-Type Recovery Systems - Libbey, C. E. - LRC

Parachute Performance at Supersonic Speeds - Charczenko, N.- LRC

Aerodynamic Drag and Stability Characteristics of Solid and Inflatable Decelerator Devices at Supersonic Speeds - Mc Shera, J. T. - LRC

The Problems of the Energy Dissipation Systems in Spacecraft Recovery - Fisher, L. J. - LRC

[redacted]